

UNDERSTANDING HUMAN-SPACE SUIT INTERACTION TO PREVENT INJURY DURING EXTRAVEHICULAR ACTIVITY

by

ALLISON ANDERSON

B.S. Astronautics Engineering
University of Southern California, 2007

M.S. Aeronautics and Astronautics
Massachusetts Institute of Technology, 2011

M.S. Technology and Policy
Massachusetts Institute of Technology, 2011

Submitted to the Department of Aeronautics and Astronautics
in Partial Fulfillment of the Requirements for the Degree of

DOCTOR OF PHILOSOPHY IN AEROSPACE BIOMEDICAL ENGINEERING

at the

MASSACHUSETTS INSTITUTE OF TECHNOLOGY

June 2014

© 2014 Massachusetts Institute of Technology. All rights reserved.

Author

Department of Aeronautics and Astronautics
May 22, 2014

Accepted by

Paulo C. Lozano, Associate Professor of Aeronautics and Astronautics
Department of Aeronautics and Astronautics
Chair, Graduate Program Committee

UNDERSTANDING HUMAN-SPACE SUIT INTERACTION TO PREVENT INJURY DURING
EXTRAVEHICULAR ACTIVITY

by

ALLISON ANDERSON

DOCTOR OF PHILOSOPHY IN AEROSPACE BIOMEDICAL ENGINEERING

at the

MASSACHUSETTS INSTITUTE OF TECHNOLOGY

Certified by.....
Prof. Dava J. Newman
Professor of Aeronautics and Astronautics and Engineering Systems
MacVicar Faculty Fellow, Director Technology Policy Program, Director MIT-Portugal Program
Massachusetts Institute of Technology
Committee Chair, Thesis Co-Advisor

Certified by.....
Dr. Brian Corner
Three-Dimensional Data Acquisition and Analysis Laboratory
US Army Natick Soldier Research, Development & Engineering Center
Thesis Committee Member

Certified by.....
Prof. Jeffrey Hoffman
Professor of the Practice, Department of Aeronautics and Astronautics
Massachusetts Institute of Technology
Thesis Co-Advisor

Certified by.....
Prof. Robert J. Wood
Charles River Professor of Engineering and Applied Sciences, Director Microrobotics Lab
Harvard School of Engineering and Applied Sciences
Thesis Committee Member

UNDERSTANDING HUMAN-SPACE SUIT INTERACTION TO PREVENT INJURY DURING EXTRAVEHICULAR ACTIVITY

by

Allison Anderson

Submitted to the Department of Aeronautics and Astronautics on
May 22, 2014 in Partial Fulfillment of the Requirements for the Degree of
Doctor of Philosophy in Aerospace Biomedical Engineering

ABSTRACT

Extravehicular Activity (EVA) is a critical component of human spaceflight. Working in gas-pressurized space suits, however, causes fatigue, unnecessary energy expenditure, and injury. The problem of injury is particularly acute and is exacerbated with the additional hours astronauts spend training inside the suit, especially underwater in NASA's Neutral Buoyancy Laboratory (NBL). Although space suit performance and improved system designs have been investigated, relatively little is known about how the astronaut moves and interacts with the space suit, what factors lead to injury, and how to prevent injury. At the outset of this research effort there were no technologies suitable to evaluate human movement and contact within the space suit during dynamic movements.

The objective of this thesis is to help understand human-space suit interaction and design hardware to assess and ultimately mitigate injury. This is accomplished through two specific aims.

The first specific aim is to use data mining techniques to uncover trends in space suit configuration, training environment, and anthropometry, which may lead to injury. Two groups of subjects were analyzed: those whose reported shoulder injury incidence is specifically attributable to the NBL or working in the space suit, and those whose shoulder problems began in active duty, meaning working in the suit could have been a contributing factor. The first statistical model correctly identifies 39% of injured subjects, while the second model correctly identifies 68% of injured subjects. For both models, percent of training incidence in the space suit planar hard upper torso (HUT) was the most important predictor variable. Frequency of training and recovery between training were also identified as significant metrics. These variables can be monitored and modified operationally to reduce the impacts on the astronaut's health. Several anthropometric dimensions were also found to have explanatory power for injury. Expanded chest depth was included in both models, while bi-deltoid breadth was relevant for identifying injured NBL subjects and shoulder circumference was relevant for identifying injured Active subjects. These dimensions may be targeted as particularly important to accommodate in future designs of the HUT or any advanced concept space

suits. Finally, for the NBL subjects, previous record of injury was found to be an important factor. Further descriptive analysis implies that analyzing the HUT style and size together may be critical for future detailed studies on fit and accommodation. These results quantitatively elucidate the underlying mechanisms of shoulder injuries for astronauts working inside the space suit.

The second specific aim is to develop a wearable pressure sensing capability to quantitatively measure areas on the body's surface that the space suit impacts during normal EVA movement. A low-pressure sensing system was designed and constructed for the upper body during dynamic movements inside the space suit environment. Sensors were designed to measure between 5-60 kPa with approximately 1 kPa resolution. The sensors are constructed from hyper-elastic silicone imbedded with a microfluidic channel. The channel is filled with liquid conductive metal, galinstan, such that an applied pressure corresponds to a change in resistance of the liquid metal. The system of 12 pressure sensors accommodates anthropometry from a 50th percentile female to a 95th percentile male upper body dimensions with near shirt-sleeve mobility. The wiring was intentionally designed to achieve the best trade between flexibility, resistance, and stretch ability, but ultimately was the greatest limitation in system durability. The electronics architecture utilizes onboard data storage with more than 4 hours of use. The entire system was designed with extreme environments in mind, where considerations of shock, battery hazards, and material properties in mixed gas, pressurized atmosphere were minimized to ensure user safety.

The pressure sensing system was used in a human subject experiment to characterize human-suit interaction. Three experienced subjects were asked to perform a series of 3 isolated joint movements and 2 functional tasks, all focused on upper body movement. Movements were repeated 12 times each and pressure responses were evaluated both by quantifying peak pressure and full profile responses. Comparing subjective feedback to the quantitative pressure data allows a sense of the variability of movement and minor changes in loading on the body while performing suited motions. Users generally felt they were consistent for all movements. However, using a nonparametric H-test, 53% of movements were found to be biomechanically inconsistent ($p < 0.05$). This experiment provided the first "window" inside the suit to evaluate contact pressures and sequential indexing of the person inside the suit for realistic EVA movement. It cannot be extrapolated how changes in contact pressure would affect a subject's propensity for injury as injuries accumulate over long time scales. However, changes in pressure may be due to alterations in biomechanical strategies or fatigue, both of which could be precursors for injury and discomfort.

This work focuses on the upper body, but the methods may be extended to the full body as future work. It provides solutions that could be applied beyond the field of aerospace to assess human-garment interactions and recommending armor protection for defense applications to alleviate fall impacts for medical applications. The contributions to the field include the development of a protection system that assesses and prevents injury inside gas-pressurized space suits.

ACKNOWLEDGEMENTS

“Smooth-On: It will change your life!”

- Smooth-On, Inc.

A bold claim. When I first saw this proclamation stamped on the outside of an industrial sized box of silicon elastomer, typically used by crafters and hobbyists to make trinkets, now used in my new Wyss lab to make sensors, I burst out laughing. How could a vat of stretchy plastic promise so much? Much to my surprise, no one else I told this joke to seemed to find it remotely amusing. Perhaps they realized, more so than I at the time, just how prophetic this claim would be. This elastomer, my sensors, have in fact changed my life. The struggles and triumphs of the past 6 years have redefined who I am completely. Of course, it's not just the sensors, the research, the work that has caused the transformation. It's the people I've encountered that has made the real impact.

I cannot possibly begin my acknowledgements without starting with my advisor, Prof. Dava Newman. She has been my most avid supporter and her insight has been critical to accomplishing this thesis. Additionally, she has given me room to fail and learn how to identify the research questions that interest me most, a passion without which you can never be successful. One of her most profound contribution in advising her students is to teach them to live their lives to the fullest extent possible. She does this both through support of all my crazy endeavors and through the example of her own adventures. I've been blessed to have her as my advisor and am grateful for her positive influence.

I would also like to thank my incredible thesis committee. Other graduate students should be so lucky. Despite your protestations that I would never make my graduation timeline (yes you were right, it was tough), you always encouraged me forward. Dr. Corner, your critical insight and perspective from outside academia challenged me to approach the problem in new, interesting ways. Prof. Hoffman, your first-hand knowledge of the space suit environment gave me much needed direction. I've always been impressed by your ability to stare at any problem and understand the fundamental principles governing it. This is a quality of yours I constantly try to emulate. Prof. Wood, I'm so grateful you took me as a space-crazed graduate student into your lab and provided me the technical insight to actually solve this pressure-sensing problem. Thank you all for your constant corrections toward the path that I ultimately traveled.

I would also like to thank all my research collaborators. Your work is here in this thesis, shared with me. You can't comprehend my gratitude for all your efforts and your ideas. The list is, to me, astounding. Prof. Roy Welsch basically thought I was a crazy student who constantly pestered him about statistics until he realized that this project, was in fact, pretty cool. Shane McFarland put forth so much effort to guide me through the NASA approval process and feedback on the experimental design itself. Then of course there are the student and post-doc collaborators who really rolled back their sleeves: Yigit for teaching me how to build sensors and for iterating on their design with me. Pierre and

Alexandra for being blindsided in their first semester with research, but always doing it with a smile, awkward mixed CD, and BBQ. Ana and Michal for helping me get through those dark early days when it was time to hit the reset button. Finally, to the many professional colleagues who constantly provided support, information, and a collaborative spirit: Gui Trotti, Dr. Rick Scheuring, the folks at the LSAH, Jason Norcross, Amy Ross, Shane Jacobs, Nick Lesniewski-Laas, Daniel Vogt. To my friends and colleagues at Dainese, especially Stefano, Andrea, and Marcello. Grazie mille per tutto il vostro meraviglioso lavoro creativo. Ancor più, grazie per tutte le avventure, per le gite in bicicletta, per il cibo delizioso, e per le lezioni di italiano. Finalmente ho imparato come si pronuncia la parola ciliegia!

Next, to my dear friends. My labmates, the MVL-ers. Every working environment I have from now on will be but a shadow of your awesomeness. In particular the oldies Aaron, Brad, Justin, Torin were a part of my every day at MIT and some of my closest friends. So happy none of you are girls so I have the sole claim on lab grandma. I would like to give a particular shout-out to each of my former officemates (especially Roedolph, Andie, and Becky), for never once, not even ONCE telling me to clean up my half of the office or to move all my crap and sports equipment out of their way. May we forever have the best Astronaut Hall of Fame with the most duplicated photos possible. To my TPP-ers, whose friendships are the outlet I needed, in particular Cory, Phil, Ruth, and Avi. I have no doubt you will continue to be an integral part of my life. To Paul and Rita, the two people with whom I felt the most companionship over the reality of graduate school, but for different reasons. Paul, I'm so grateful you were my thesis writing buddy. You deserve to be insanely happy with Natasha in Chicago. Rita: (insert tune) I'm sorry I don't understand where all this is coming from. I thought we weren't doing fine (but now we're graduating). You're a constant pillar of support and I knew no matter what, you were right there with me. I will always cheer for Benfica if you always cheer for the Bruins. Berivan, thank you for listening to me and being persistent in our friendship. I promise someday I'll tell you my thoughts and feelings... ok maybe not. To my friends on the tri-team for providing a fun environment to cultivate my new favorite hobby, particularly Bryce and Mitch for always giving me something to chase. To Claire for teaching me about rocks. To Hall for your millions of delicious meals. To Brandon and Dan for witty banter that makes my head explode. To Sabrina for being my pen pal. Above and beyond all, Kate formerly-Crandall-now-Pickering, my surrogate sister. No one could be more different from me, nor know me so completely. I'm never lacking anything when we spend time together. Thanks for being my friend, even though you got our relay disqualified when we were 5 years old. You know breaststroke was my jam.

Finally, I would like to thank my family. No matter what I say, it will be insufficient. To my siblings for inspiring me with your incredible talents. You gave me my imagination with all our games, which I like to believe has turned into professional creativity. To my nephews. I had no idea I could ever love anyone so instantly and completely until I met each of you. To my grandparents: Grandma Anderson for teaching me how to be strong. Papa Anderson for teaching me to "just keep doin' what you're doin'". Grandma Whiteneck for teaching me how to give to others. Grandpa Whiteneck for teaching me how to work hard. To my parents, this work is dedicated. I love you all with all my heart.

TABLE OF CONTENTS

Abstract.....	5
Acknowledgements.....	7
List of Acronyms.....	11
List of Figures.....	13
List of Tables.....	15
1. Introduction.....	17
1.1. Motivation.....	17
1.2. Objective.....	19
1.2.1. Specific Aim 1.....	19
1.2.2. Specific Aim 2.....	19
1.3. Thesis Summary.....	20
2. Literature Review.....	22
2.1. Extravehicular Activity (EVA).....	22
2.1.1. U.S. Space Suits.....	22
2.1.2. Orbital EVA.....	25
2.1.3. Training.....	26
2.1.4. Future EVA Tasks.....	28
2.2. EVA Related Injury.....	28
2.3. Suit Performance Characterization.....	32
2.4. Pressure Sensing Technology.....	35
2.5. Applications Beyond Space Missions.....	39
2.6. Conclusion.....	40
3. Statistical Evaluation of Shoulder Injury.....	41
3.1. Database.....	41
3.1.1. Anthropometric Data.....	42
3.1.2. Training History Data.....	42
3.1.3. Injury Record Data.....	43
3.2. Methods.....	46
3.3. Data Mining Results.....	47
3.4. Discussion.....	49
3.5. Conclusion.....	55
4. Wearable Pressure Sensing System.....	58
4.1. System Requirements.....	58
4.2. Sensor Utility.....	59
4.2.1. Design and Fabrication.....	59
4.2.2. Sensor Performance.....	63
4.2.3. Remaining Utility Requirements.....	69

4.3.	Sensor System Wearability	70
4.3.1.	Human Accommodation	71
4.3.2.	Wiring Mobility	71
4.3.3.	Electronics and Data Transfer	75
4.3.4.	Novel Sensor Integration	77
4.3.5.	Environment	78
4.4.	Discussion	78
4.5.	Conclusion	81
5.	Pressure Interface Experiment	83
5.1.	Experimental Methods	83
5.1.1.	Sensor Systems	83
5.1.2.	Experimental Design	85
5.1.3.	Subject Selection	86
5.1.4.	Polipo sensor Calibration	88
5.1.5.	Data Processing	88
5.1.6.	Pilot Study	89
5.2.	Results	90
5.2.1.	Data Integrity	90
5.2.2.	Neutral Posture Pressure Loads	90
5.2.3.	Maximum Pressure Profiles	92
5.2.4.	Temporal Analysis	101
5.3.	Discussion	101
5.4.	Conclusion	105
6.	Conclusion	107
	References	115
	Appendices	123

LIST OF ACRONYMS

ABF – Anthropometry and Biomechanics Facility
DCCI – David Clark Company, Incorporated
DCM – Display and control module
EMU – Extravehicular mobility unit
EVA – Extravehicular activity
FSR – Force sensing resistors
HUT – Hard upper torso
IMU – Inertial measurement unit
ISS – International Space Station
JSC – Johnson Space Center
LCVG – Liquid cooling ventilation garment
LSAH – Longitudinal Study on Astronaut Health
MAD – Median absolute deviation
MIT – Massachusetts Institute of Technology
NASA – National Aeronautics and Space Administration
NBL – Neutral Buoyancy Lab
PLSS – Personal life support system
SAFER – Simplified aid for EVA rescue
SSA – Space suit assembly
SOP – Secondary oxygen pack
WETF – Water Emersion Training Facility

LIST OF FIGURES

Figure 2.1. EMU spacesuit pieces and comfort garments.	23
Figure 2.2. Pivoted and planar hard upper torso (HUT) styles.	24
Figure 2.3. Advanced concept space suits for technology demonstration.	25
Figure 2.4. EVA as performed on orbit and in the training environment of the NBL	26
Figure 2.5. The wall of EVA.	27
Figure 2.6. Shoulder anatomy.	29
Figure 2.7. Shoulder movement during abduction.	30
Figure 2.8. Neck and torso injuries post NBL training session.	31
Figure 2.9. Upper body injuries occurring in EVA.	33
Figure 2.10. Example work envelope modeling and experimental suit testing.	34
Figure 3.1. Receiver operating characteristic curve.	48
Figure 3.2. Correlation matrix and histogram of variables included in the NBL injury model.	50
Figure 3.3. Comparison of anthropometric variables included in the NBL and Active models for injured subjects.	51
Figure 3.4. Plot of median and median average distance for injured and uninjured subjects.	53
Figure 3.5. Histogram of NBL subjects by injury and chosen size HUT.	54
Figure 4.1. Each step in the sensor construction process.	61
Figure 4.2. Sensor molds components and features.	61
Figure 4.3. Channel filling and completed sensor.	62
Figure 4.4. Flex circuit components and improvement features over previous designs.	62
Figure 4.5. Calibration apparatus.	63
Figure 4.6 Simulated calibration data.	64
Figure 4.7. Variation on curve fit.	65
Figure 4.8. Hysteresis effect of loading and unloading.	66
Figure 4.9, Sensor creep demonstrated.	67
Figure 4.10. Drift associated with a constant load.	68
Figure 4.11. Dynamic response of the sensor to known loading.	69
Figure 4.12. Components of the pressure sensing system.	70
Figure 4.13. Wiring design and construction of the Polipo.	72
Figure 4.14. Components of the “chele”.	73
Figure 4.15. Wiring and implementation.	74
Figure 4.16. Electronics housing and configuration.	75
Figure 4.17. Design and fabrication of the base layer garment.	77
Figure 4.18. Final design of the Polipo pressure sensing system.	78
Figure 5.1. In-suit sensor systems.	84
Figure 5.2. In-suit sensor systems.	85
Figure 5.3. Experimental test protocol for a single subject.	86
Figure 5.4. Movement tasks performed by each subject.	87

Figure 5.5. Advanced concept space suits for technology demonstration used in this experiment.	88
Figure 5.6: Polipo sensor locations	91
Figure 5.7. Offloading pressure response profiles from Sensor 10.	92
Figure 5.8. Sensor placement over the arm.	92
Figure 5.9. Temporal activation of sensors for Cross Body Reach.	102
Figure 6.1. Dynamic response of the sensor to known loading.....	110
Figure 6.2. Each component of the Polipo pressure sensing system	111
Figure 6.3. Temporal activation of sensors for Cross Body Reach.	112

LIST OF TABLES

Table 2.1. Taxonomy describing EVA injury categories.....	32
Table 3.1. Common subjects between three components of database.....	42
Table 3.2. Anthropometric dimensions included in the database.....	43
Table 3.3. Aggregated training information used as proxy variables for statistical analysis.....	44
Table 3.4. Model fit to subjects whose incident was reported as a result of working in the NBL.....	48
Table 3.5. Model fit to subjects whose incident was reported during active duty and while working in the NBL.....	49
Table 3.6. Comparison of preference of planar and pivoted HUT sizes for both NBL and Active groups.....	55
Table 3.7. Comparison of total training incidence in planar and pivoted HUT sizes for both NBL and Active groups.....	56
Table 4.1A. Detailed Utility and Wearability design requirements.....	60
Table 4.2. Discrimination of sensors.....	66
Table 4.3. ANSUR database body dimensions for 50 th percentile female and 95 percentile male.....	71
Table 4.4A. Detailed Utility and Wearability design requirements revisited.....	80
Table 5.1: Useful movement profiles.....	91
Table 5.2. Subject 1, Sensor 2 maximum pressure (kPa).....	93
Table 5.3. Subject 1, Sensor 11 maximum pressure (kPa).....	95
Table 5.4. Subject 2, Sensor 6 maximum pressure (kPa).....	98
Table 5.5. Subject 3, Sensor 5 maximum pressure (kPa).....	100
Table 6.1. Model fit to subjects whose incident was reported as a result of working in the NBL.....	108
Table 6.2. Model fit to subjects whose incident was reported during active duty and while working in the NBL.....	109

1. INTRODUCTION

1.1. Motivation

Extravehicular activity (EVA) is critical for human spaceflight to achieve tasks such as habitat construction, hardware repair, and planetary exploration. These activities are complex, requiring substantial preparation to be executed safely and successfully. EVA has enabled us to accomplish some of the greatest feats of the space program, such as the Apollo moonwalks and Hubble Space Telescope repair missions. Despite its many advantages, these activities are not without cost to the astronauts who perform EVA.

Gas pressurized space suits cause injuries and increase metabolic expenditure (Morgan, Wilmington et al. 1996, Williams and Johnson 2003, Longnecker 2004, Strauss 2004, Viegas, Jones et al. 2004, Carr 2005, Hochstein 2008, Jones, Hoffman et al. 2008, Scheuring, Mathers et al. 2009, Opperman 2010). During the first spacewalk performed, Alexi Leonov was nearly unable to reenter his spacecraft due to his immobile suit and inability to see through his fogged visor. Apollo astronauts sustained hand, joint, and skin irritation injuries (Scheuring, Jones et al. 2008). The current U.S. space suit, the extravehicular mobility unit (EMU), causes a variety of musculoskeletal injuries. The EMU is pressurized with gas to 29.6 kPa (4.3 psi), forcing the astronaut to expend energy to deform the suit and limiting his or her mobility. Each space suit has a geometrically defined work envelope in which these costs are minimized, but may not always be adhered to by astronauts (Morgan, Wilmington et al. 1996, Newman, Schmidt et al. 2000, Schmidt 2001, Jaramillo, Angermiller et al. 2008, Gernhardt, Jones et al. 2009, Norcross 2010).

The most common types of injuries are to the hands, feet, and shoulders (Strauss 2004, Scheuring, Mathers et al. 2009). Most of the remaining injuries and areas of discomfort occur at joints or on the skin's surface, where astronauts impact and rub against the suit as they bend the garment. Although most inflight injuries have been minor and have adversely affected mission success, injury incidence during EVA is much higher than injury that occurs elsewhere on-orbit (Viegas, Jones et al. 2004, Scheuring, Mathers et

al. 2009, Opperman 2010). EVA-associated injuries have been exacerbated with the increased number of EVAs and training sessions for the construction of the International Space Station (ISS) in the neutral buoyancy lab (NBL) training pool (Gernhardt, Jones et al. 2009). Astronauts and tools are made neutrally buoyant to simulate the weightlessness of microgravity, allowing for realistic mission preparation with mockups of the ISS, robotic arms, and other pieces of space hardware. Astronauts spend approximately 12 hours in training for each hour spent in flight for EVA preparation (Strauss 2004). Additionally, they go through skills and maintenance training to become familiar with working in the suit even before being assigned to a mission. An astronaut may spend their entire career intermittently working inside the space suit in the training environment. As a result of this accumulated time in the suit on Earth, injuries seen on-orbit are magnified and new injuries have been introduced. For example, in the presence of gravity some training positions in the NBL may invert the astronaut, causing his or her body weight to rest on the shoulders and hard space suit components. This induces discomfort and injury, in some instances requiring surgical intervention (Williams and Johnson 2003, Strauss 2004, Strauss, Krog et al. 2005, Opperman, Waldie et al. 2009).

Relatively little is known about how an astronaut moves inside the space suit to move the suit itself. Hypothesized causes of injuries are suit fit, shifting, improper use of protective garments, and repetitive motion working against the suit (Williams and Johnson 2003, Strauss 2004, Benson and Rajulu 2009). Suit fit is a critical element in preventing astronaut injury. Achieving the best fit is extremely individualized and discomfort “hot spots” on the body may exist in an area for one crewmember but not for another. Even between training sessions minor adjustments need to be made to a suit to achieve the best fit (Gast and Moore 2010). Additionally, an astronaut’s body dimensions, for example, height or thorax, change as they enter the microgravity environment (NASA 2011). The neutral body posture in the weightless environment may necessitate further suit adjustment. No matter which environment the astronaut is working in, movement in the suit is limited and unnatural due to each space suit’s inherent programming, or planes through which the suit can move due to the angle of rotational bearings (Cowley, Margerum et al. 2012). Astronauts must learn to change their biomechanical movement strategies, rather than attempting to move as they do naturally, or unsuited (Gast and Moore 2010). The difference between how a person moves relative to the suit has not been quantified. Previous studies used a variety of techniques, such as photogrammetry, motion capture, and ergonomic strength measurement to evaluate suited performance (Parry, L. Curry et al. 1966, Greenisen 1986, Reinhardt and Magistad 1990, Morgan, Wilmington et al. 1996, Schmidt 2001, Holschuh, Waldie et al. 2009, Matty and Aitchison 2009, Meyen, Holschuh et al. 2011, Valish and Eversley 2012). Results, however, are difficult to compare because their methodologies and measurements are inherently different. Additionally, studies are limited because they have only measure performance from the outside of the suit, thereby characterizing the human and space suit as a whole. For injury prevention, however, human–suit interaction is the area of inquiry that has not been studied.

Future gas pressurized space suit designs will be governed by mobility requirements as we look to explore on other bodies in the solar system. Surface exploration will require

significantly greater ranges of motion and more frequent sorties, leading to more total time spent in EVA. This could potentially lead to higher injury incidence if the space suit system is not enhanced to find long-term, healthy solutions to EVA injury (Newman 2005, Gernhardt, Jones et al. 2009, Norcross, Lee et al. 2009).

1.2. Objective

The objective of this research is to understand human-space suit interaction and design hardware to assess and mitigate injury and discomfort inside the space suit. This will be achieved through two specific aims.

1.2.1. *Specific Aim 1: Analyze data for correlations between anthropometry, space suit components, and shoulder injury.*

Shoulder injuries are some of the most serious and debilitating injuries associated with EVA training. Using a database compiled by NASA personnel on subject anthropometry, training time in different space suit components, and reported shoulder incidents, the following hypotheses will be evaluated:

Hypothesis 1: Anthropometric dimensions will be a predictive factor in identifying astronauts with a reported shoulder incident.

Hypothesis 2: Suit training variables in the planar hard upper torso (HUT), rather than training in the pivoted HUT, will be a predictive factor in identifying astronauts with a reported shoulder incident. Suit training variables are defined by aggregating training information, such number of or percentage of training incidences in the planar or pivoted HUT.

Hypothesis 3: Operational training variables will be predictive factor in identifying astronauts with a reported shoulder incident. Operational training variables are defined by aggregating training information, such as frequency of training, accumulation of days between training incidences, or career duration of active duty training.

Hypothesis 4: Record of previous injury will be a predictive factor in identifying astronauts with an additional shoulder incident.

Each of these hypotheses investigates a specific causal mechanism found in the literature associated with EVA shoulder injuries and relates it to a reported shoulder incident. Hypothesis 4 will only be evaluated for those subjects with injury incidents directly attributable to the space suit.

1.2.2. *Specific Aim 2: Quantify and evaluate human-space suit interaction with a pressure sensing tool.*

There is currently no method by which to measure how the person moves inside the space suit. Focusing on the upper body, a pressure sensing tool will be created to quantify human-space suit interaction under different loading regimes. The following

design requirements will be evaluated to determine the success or failure in designing a wearable pressure sensing garment for the space suit environment:

Design Requirement 1: A pressure sensing tool will achieve both high wearability and high utility in a space suit environment. Wearability is defined by mobility, comfort, and safety of the user. Utility is defined by range, accuracy, resolution, and coverage of the sensor system.

Design Requirement 2: Human and space suit interaction characterized by interface pressures will show trends consistent with expected loading regimes. Trends are defined by sensor pressure profiles over isolated or functional tasks. Expected loading regimes are defined by subjective feedback or inferred loading based on anticipated contact.

Design Requirement 1 evaluates the performance of the pressure sensing system to ensure it is properly scoped for its intended use. Design Requirement 2 investigates the system's ability to function properly in the environment of the space suit so its results may be interpreted with confidence.

The pressure sensing tool will be used to evaluate human-space suit interaction to assess consistency of movement. Consistency of movement is an important metric revealing fatigue or changes in biomechanical strategies, both of which could be precursors to EVA injury. The following hypothesis will be evaluated in a human subject experiment inside the space suit:

Hypothesis 5: Subjects with experience working in the space suit will perform motion tasks with consistent movement strategies. Movement strategies are defined by peak pressures averaged over trials or full time averaged pressure profiles.

1.3. Thesis Summary

This thesis evaluates human-space suit interaction to understand how the person works and moves inside the suit. The intent is to use this information to better understand and mitigate EVA injury. Chapter 2 presents a review of the relevant literature on astronaut injury, injury mechanics, methods by which researchers assess human-space suit performance, pressure sensing tools, and wearable electronics. It demonstrates our gap in knowledge regarding the relevant factors associated with space suit injury and lack of understanding of how an astronaut moves inside the suit. Chapter 3 presents the statistical methods used to evaluate the relation between astronaut anthropometry, space suit components, training factors, and injury. Statistical models to predict propensity for injury will be discussed to evaluate Hypotheses 1 through 4. Chapter 4 describes the design and construction of a pressure sensing garment used to measure the pressure interface over the arm between a person and the space suit. The characterization and evaluation of the pressure sensing device is used to evaluate the system's ability to achieve Design Requirement 1. Chapter 5 presents the results of a

human subject test characterizing space suit interaction using the novel pressure sensing system. The results of the experiment demonstrate the value of pressure sensing as a “window” inside the suit. Design Requirement 2 is evaluated to ensure the sensor system functions for the environment in which it was designed. Hypotheses 5 is evaluated using the data collected in the experiment. Finally, Chapter 6 summarizes the major findings of my work and proposes further follow-on studies, and discusses the implications of the statistical analysis for space suit design and the training procedures. Design of the pressure sensing system, advantages, and how the system may be improved to gain additional utility are discussed. Finally, further in-suit studies are identified that will improve our understanding of human-space suit interaction.

There are three primary contributions of this research:

- 1) To quantitatively evaluate the hypothesized mechanisms of space suit shoulder injury.
- 2) To design a novel, wearable pressure sensing device geared toward low-pressure sensing regimes in extreme environments.
- 3) To perform the first documented experiment with instrumentation inside the space suit to characterize the pressure interface associated with an astronaut’s movement.

Each of these contributions addresses a specific gap in our knowledge of human-space suit interaction, space suit and subject performance, and astronaut EVA injury.

2. LITERATURE REVIEW

Despite many years of experience designing, building, and testing gas-pressurized space suits, relatively little is known about how an astronaut moves inside the suit. The causal mechanisms of injuries incurred as a result of working in the suit can only be hypothesized, rather than directly measured. This research addresses this gap in our ability to evaluate space suit design and understand injury. The following is a review of the literature on space suit design and EVA working environments. The types of injuries and the hypothesized reasons for injury are reviewed, with particular focus on the shoulder and upper body. The methods of characterizing space suit performance are demonstrated as insufficient for understanding human-suit interaction. Novel techniques such as wearable pressure sensing are a promising area for investigation. However, a review of the state-of-the-art shows there is currently no viable solution for measurement inside the space suit due to limitations of mobility, materials, or hardware. Finally, research in fields beyond space suit design are highlighted as possible contributors to bridge this gap. This work could extend into other arenas of injury prevention such as for the elderly during falls and military personnel encumbrance such as heavy packs and personal protection.

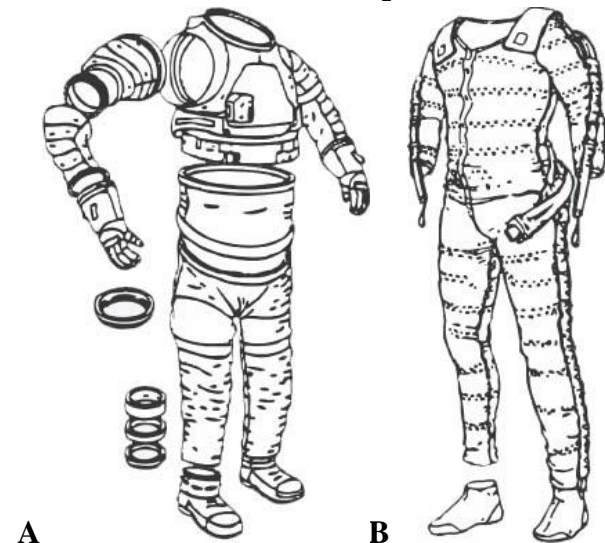
2.1. Extravehicular Activity (EVA)

Since Ed White's first EVA in 1964, the fundamental challenges faced by U.S. space suit designers have not changed. Providing pressure, oxygen, waste removal, communication, food, water, thermal control, mobility, slight radiation protection, and a safe working environment are the primary needs that must be addressed (Thomas and McMann 2006). Although suits have drastically improved, resulting in the engineering feat found in the current extravehicular mobility unit (EMU), these issues have yet to be overcome to achieve a work environment that is both natural and comfortable for its wearer.

2.1.1. U.S. Space suits

U.S. astronauts currently fly and train in the EMU. This system includes the space suit assembly (SSA), protective and comfort pieces, and the life support system. A comprehensive description of these systems can be found in (Harris 2001) and (Thomas and McMann 2006).

Many components of the SSA, shown in Figure 2.1A, are available in multiple sizes to allow astronauts to mix pieces and provide a better fit. This philosophy allows the system to be reusable with the minimal number of components while attempting to cover the entire astronaut population (Kozloski 1994). The hard upper torso (HUT) is a hard fiberglass shell forming the central structural component of the EMU on which other suit pieces are mounted. In training, there are two HUT styles astronauts may select from: pivoted and planar, both shown in Figure 2.2. The pivoted HUT has a bellows at the scye shoulder bearing, giving it greater mobility over the planar HUT, whose rotating bearing attaches directly to the upper arm piece. The pivoted HUT is no longer used on orbit since a rupture in the bellows would be a catastrophic failure of suit integrity (Williams and Johnson 2003). The arm pieces are made of fabric and use a convolute pattern to help minimize the effects of suit volume change and improve mobility. They have restraint ribbons along the longitudinal, neutral axis of the limb, rather than over the back of the elbow since this would restrict movement. They are designed with a slight bend in their neutral, inflated posture, giving the piece an inherent axis of rotation during movement. Hard sizing rings are added to change the length of the arm and shift the designed elbow joint center proximally or distally. The glove attaches to the soft arm pieces through the wrist bearing. There are many glove sizes, some of which are custom made for astronauts. The lower torso assembly covers the trunk from the waist, pants, and boots, connecting to the HUT at the waist bearing



and to the leg pieces through another bearing. Like the arm piece, the knee joint uses a convolute pattern. Mobility in the hips is limited, but is typically not required for microgravity operations. The boots come in two sizes and are fabric with minimal structure built into them, other than the flat sole (2002, Thomas and McMann 2006).

Protective comfort pieces are worn to mitigate some of the negative effects of wearing the SSA, seen in Figure 2.1B. The primary component is the liquid cooling ventilation garment (LCVG), which regulates body temperature by circulating water through Tygon tubing for flow over the body and heat absorption from the skin. Additionally, the LCVG circulates air in the suit by moving air from the extremities returning it to the primary life support

Figure 2.1. EMU spacesuit pieces and comfort garments. A) The EMU in an exploded view so the hard upper torso, soft pieces, sizing rings, and boots may be seen. Courtesy of Hamilton Sunstrand. B) Each of the comfort pieces, including the LCVG with padding, ventilation tubes, and boot inserts. Photo credit "Human Spaceflight".

system (PLSS). The EMU LCVG covers the body from the wrists to the ankles and neck (2002, Thomas and McMann 2006, Jones, Graziosi et al. 2007). Optional suit elements used to protect the hands are comfort gloves, meant to prevent rubbing and absorb moisture (Strauss 2004, Opperman, Waldie et al. 2010). A wrist cuff (essentially the upper part of an athletic sock) is also a comfort option. The boots are modified to accommodate multiple users with sizing inserts. These inserts partially fill the boot volume, but are not optimized for protection. An optional internal toe cover may be used to protect against impact (Strauss 2004). Current injury countermeasures include thin strips of padding sewn to the LCVG in areas where astronauts may feel hot spots of discomfort; however, this padding is not designed for long-term injury prevention (Strauss 2004, Opperman 2010). The HUT has a built-in harness system with restraint straps to prevent shifting during neutral buoyancy training. The harness system is optional but encouraged to prevent shoulder injury (2002, Williams and Johnson 2003).



Figure 2.2. Pivoted and planar hard upper torso (HUT) styles. *There are two HUT styles with their primary difference being the shoulder scye bearing to which the arm components attach. The pivoted HUT, shown on the left, has a pivoting bellows to allow for greater shoulder mobility than the planar HUT, shown on the right. Photo credit NASA.*

The life support system includes the PLSS, secondary oxygen pack (SOP), and display and control module (DCM), and the simplified aid for EVA rescue (SAFER). It is a backpack housing the consumables, electric, and communications components. The PLSS pumps water and air to the LCVG for circulation. The PLSS also regulates the suit environment by supplying new oxygen, regulating pressure, and removing waste such as carbon dioxide and humidity. The SOP provides additional oxygen and pressurization should the PLSS fail, and is only meant for contingency situations. The DCM is mounted to the front of the HUT providing information about the state of suit consumables and allows the astronaut to regulate suit properties, such as temperature. The SAFER system attaches to the PLSS and is meant for contingency situations should an astronaut become untethered and need to return to the spacecraft. It has never been used on orbit (Thomas and McMann 2006).

In addition to the EMU, there are several prototype suits geared toward improving capabilities for planetary and deep space exploration. The Mark III (Figure 2.3B), originally built in 1987 by NASA and ILC Dover, is the most well characterized prototype suit. It incorporates some hard components and rotating bearings (rather than soft fabric pieces) over the torso and hips to improve mobility and mitigate the effects of volume change. The concept was originally designed with planetary exploration in mind, hence the focus on mobility. The suit has seen several iterations and improvements since its original design. Although the bearings reduce the joint torques required to

move the suit by creating a plain of rotation, this programming alters normal biomechanical strategies and forces the astronaut to work in a manner different from unsuited motion. This effect was also seen in the AX-5, a full body hard suit designed at NASA Ames (Reinhardt and Magistad 1990). Soft suits, such as the Modified ACES, Demonstrator Suit, and the Mobility Mockup, are designed by the David Clark Company, Incorporated (DCCI). The Demonstrator Suit (Figure 2.3A) was designed to address launch and entry requirements and contingency EVA situations where high suit mobility is desirable. Their Mobility Mockup allows these concepts



Figure 2.3. Advanced concept space suits for technology demonstration. A) *The David Clark Demonstrator suit. Photo credit (Jacobs 2011)* B) *The Mark III designed for planetary exploration and mobility.*

to be implemented rapidly on a full pressure suit to determine relative success or failure of components design (Jacobs 2011). Additional prototype suits include the REI-Suit and the Z-1 suit designed by ILC Dover for NASA. Finally, there are a few space suit concepts being developed in academia, such as the University of Maryland's MX-2, the University of North Dakota's NDX-2, and MIT's mechanical counter-pressure BioSuit™, which are test-beds for advanced space suit design and operations research (Braden and Akin 2002, Newman 2005, Judnick 2007, Anderson 2011, de Leon and Harris 2011).

2.1.2. Orbital EVA

EVA is one of most critical tasks humans perform in space. It is extremely important that EVA is performed correctly, efficiently, and safely. An astronaut in orbital EVA is shown in Figure 2.4. The EMU is not an easy environment in which to work. The suit is pressurized with gas to 29.6 kPa (4.3 psi) making it stiff in the vacuum of space. Additional rigidity comes both from changes in suit volume and fabric stiffness as the joints bend (Parry, L. Curry et al. 1966, Abramov, A. Stoklitsky et al. 1994, Schmidt 2001, Holschuh, Waldie et al. 2009). This makes it difficult for the astronaut to move within the garment. Even within the work envelope, some tasks require reach, while others require the astronaut to bend his or her arms at the elbows to work close to the body. There is a trade that must be made when sizing the suit to the work envelope: to optimize suit fit either with arms fully extended or near to the body. Sizing determines where the elbow axis of rotation is placed, affecting where the person contacts the suit and the torque required to bend. In addition to discomfort from joint mismatches, the lower body is often used to produce a counter-torque against lateral forces created by the astronaut to perform his or her tasks. Astronauts stabilize themselves using handholds, foot restraints, and tethers on the robotic manipulator arm (Strauss 2004). Maintaining this posture within the suit causes increased metabolic expenditure and fatigue. Although no EVA-related injury has prevented successful completion of a mission objective, there have been several instances when the EVA was nearly

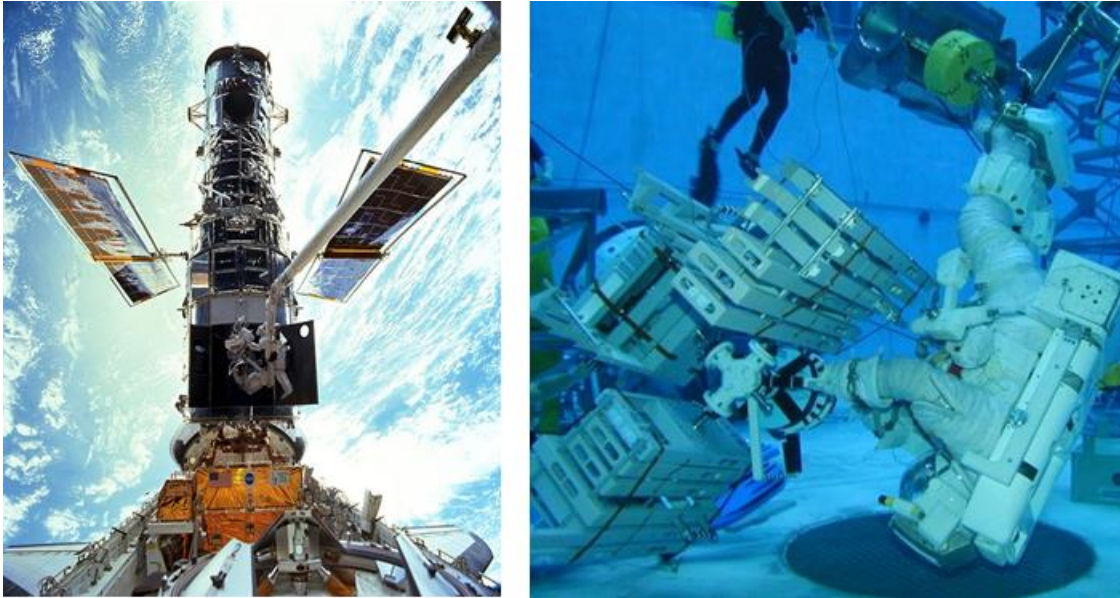


Figure 2.4. EVA as performed on orbit and in the training environment of the NBL. A) An astronaut on the robotic arm repairing the Hubble Space Telescope. B) An astronaut training in the inverted position inside the NBL. Photo credit NASA.

terminated due to suit discomfort (Scheuring, Jones et al. 2008, Scheuring, Mathers et al. 2009). Injury incidence rates are greater than those reported elsewhere in flight. Scheuring et al. reported 0.26 injuries per EVA, a dramatic increase over spacecraft based activities (Scheuring, Mathers et al. 2009). EVA is physically demanding, mentally challenging, and requires a great level of skill.

Prior to each EVA on orbit, astronauts go through a laborious routine to prepare for their sortie. A major aspect of preparation is to ready the suit and ensure it is sized properly and structurally sound. On the ground, astronauts work with suit technicians and sizing specialists to ensure their suit is optimal. In space, however, technicians have estimated sizes based on anticipated body changes. Adjustments may need to be made based on both personal preference and shifts in body characteristics (Benson and Rajulu 2009, NASA 2011). For example, spinal elongation of approximately 3% stature and variation in chest circumference by several centimeters was seen during Skylab and is now used as the NASA design standard (NASA 2011). These variations could cause changes in suit sizing leading to unintended discomfort.

2.1.3. Training

All astronauts must go through many hours of training, including preparation for EVA. Astronauts prepare in the space suit by training in analog environments, with the majority of training time spent in the neutral buoyancy lab (NBL), seen in Figure 2.4 (Gast and Moore 2010). The neutral buoyancy lab is a large swimming pool facility at NASA Johnson Space Center used to simulate the weightlessness of microgravity. The pool is capable of housing several full-scale mock-up modules of the International Space Station (ISS) and many other flight hardware elements. The NBL facility allows high

fidelity training so astronauts may practice complete sorties (Williams and Johnson 2003).

Every astronaut trains in the NBL during their career. For some, this may mean basic training to become suit qualified, which is a total of approximately 12 hours in the NBL. For EVA specialists, however, many additional hours are required to develop the necessary skills to perform EVA during a mission: up to 88 hours of training before even being assigned to a mission (Strauss 2004). Once assigned to a mission, astronauts will begin practicing their mission’s specific sorties. The number of hours varies depending on the flight and the technical details of the EVA. For ISS construction, the average number of hours spent in training was 11.6 hours for each hour of on-orbit EVA (Strauss 2004). The average astronaut spends between 200-400 hours in training over the course of their career (Rubins 2014). The increased time spent in EVA on-orbit to complete ISS construction is called the “wall of EVA”. Figure 2.5 shows the increase in hours spent on-orbit in EVA (Gernhardt). The resulting increase in time spent training for each EVA in the suit is cited as a contributing factor for the increase in injury incidence rate (Williams and Johnson 2003, Strauss 2004, Scheuring, McCullouch et al. 2012).

The NBL is an impressive facility that provides a high fidelity simulation of the EVA environment for the full operational timeframe of an EVA sortie in a relatively cost-effective manner. However, like every analog, it has its limitations. Gravity acting on the person inside the neutrally buoyant space suit causes shifting within the suit not seen on orbit. The astronaut inside the suit can shift as the body’s orientation changes during training. This can cause discomfort and injury. Additionally, the viscosity of water adds

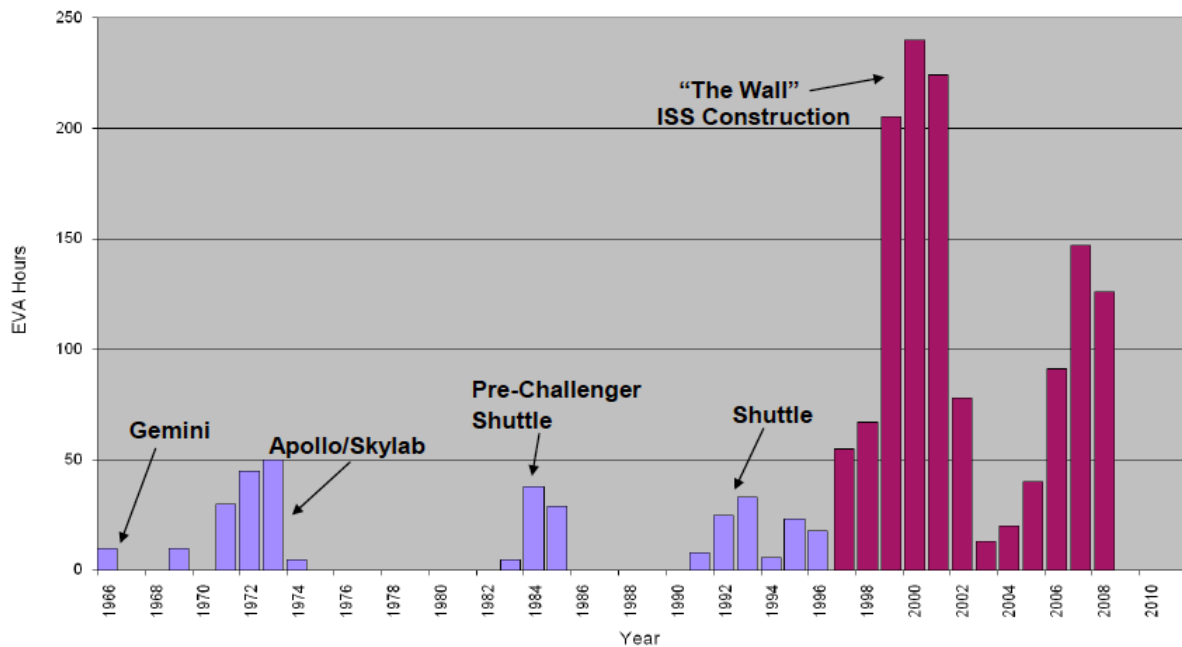


Figure 2.5. The wall of EVA. Depicts the number of hours spent in EVA over the duration of the US spaceflight program. The construction of the ISS represents a significant increase in EVA experience and training. Image credit (Gernhardt).

resistance to astronaut movement, causing astronauts to produce different movement than would be required otherwise and incur additional metabolic associated with overcoming the viscous drag with motion (Newman 1992, Newman and Alexander 1993). Also, although made neutrally buoyant, the tools used by astronauts are often quite heavy, requiring a great deal of force to change their momentum and move them from site to site. Heavy tools can cause musculoskeletal stress and may require torques that can exacerbate injuries. Time constraints in preparing for a mission may also prevent astronauts from fully recovering before performing another session in the NBL (Williams and Johnson 2003, Strauss 2004, Strauss, Krog et al. 2005)

2.1.4. Future EVA tasks

EVA in the immediate future will continue to be performed in microgravity. However, the next generation space suit will need to accommodate both microgravity and planetary environments. This will lead to modifications in space suit requirements and performance, with new considerations for astronaut injury protection (Griffin, Howard et al. 2009). Even with our limited planetary EVA experience, it is clear that crew comfort during EVA is essential (Carson, M. Rouen et al. 1975, Waligora and Horrigan 1975, Scheuring, Jones et al. 2008). We will need better design and injury mitigation strategies in order to predict and prevent astronaut injury beyond what can currently be tested on the Earth's surface.

2.2. EVA Related Injury

Hand and finger injuries are the most common injuries both during training and in-flight. Injuries include onycholysis, or fingernail delamination, blisters, contusions, and abrasions (Strauss 2004, Viegas, Jones et al. 2004, Strauss, Krog et al. 2005, Ansari, Jones et al. 2009, Scheuring, Mathers et al. 2009, Opperman, Waldie et al. 2010). Astronauts size their suits based on personal preference, optimizing whether they prefer to work in a tighter or looser fitting suit (i.e., nearer to or further from suit contact). Resolving hand injury is one of the most difficult challenges space suit designers face, but is not addressed in this research effort, nor reported on herein.

Shoulder injuries typically occur during training and are the most severe injuries astronauts face. These injuries were extensively covered by Williams and Johnson through year 2003 and is known as the Tiger Team Report (Williams and Johnson 2003). In a study by Strauss on training injuries, thirteen of the twenty-two participants were followed for shoulder-related injuries, and two required surgical interventions (Strauss, Krog et al. 2005). More recent reports show that the number of surgical interventions has increased dramatically, with 40 shoulder injuries and 11 surgical interventions in total (Scheuring, McCullouch et al. 2012). Two of the main hypothesized causes for EVA-related shoulder injury are restriction of normal shoulder movement by the HUT and supporting body weight against the HUT. The 2003 Tiger Team Report called for substantive operational changes to the training protocol to limit time in inverted positions where the body rests on the shoulder bearings of the HUT (Williams and Johnson 2003). Since shoulder injuries persist despite these changes,

evidence is mounting that HUT design and shoulder movement are the dominant factors in injury (Scheuring, McCullouch et al. 2012).

A full description of provocative shoulder motion for EVA shoulder injury is found in (Williams and Johnson 2003), and is summarized below. Figure 2.6 shows the anatomy of the shoulder. Normal shoulder movement is achieved by motion of the clavicle at the sternum, the acromion at the scapula, and the humerus against the glenoid capsule which deepens the shoulder socket joint. Additionally, the scapula slides against the thorax. Glenohumeral motion accounts for approximately two thirds of the movement from zero up to 120 degrees of arm abduction, with the remaining third attributable to scapulothoracic motion. However, beyond 120 degrees, motion is almost entirely scapulothoracic since the humerus is restricted by the acromion. The muscles that comprise the rotator cuff are among those recruited to produce this motion. The rotator cuff is most relevant group of muscles for the discussion of EVA injury. These muscles maintain stable contact between the humerus and glenoid cavity and connect the scapula to the humerus (Williams and Johnson 2003, 2012).

It is theorized when scapulothoracic motion is restricted, normal shoulder movement is prevented. To compensate, astronauts rely more heavily on the rotator cuff muscles. This causes overuse of the rotator cuff, leading to injury. Impingement of the shoulder also causes inflammation of the bursa and tendons below the clavicle (Williams and Johnson 2003). Scapulothoracic motion can be restricted both by limited clearance within a HUT which fits tightly on an astronaut, or by lateral shifting of the shoulder bearing when the HUT is too loose.

Figure 2.7 shows the changes in shoulder muscle movement as a result of HUT restriction of scapulothoracic movement. Sub-figures i.-iv. for unimpeded motion show glenohumeral motion up to 120 degrees, with scapulothoracic motion up to full range of motion in sub-figures v.-vi. The corresponding HUT restricted motion shows the absence of normal scapulothoracic motion. Motion is achieved through the glenohumeral joint. Impingement of the muscles may occur as astronauts shift within the suit during training and rest their body weight upon their shoulders against the HUT. This is particularly true when the astronaut is in an inverted position. Resting body weight on the shoulder impinges on the rotator cuff muscles, causing tears, pinched nerves, and uncomfortable pressure contacts



Figure 2.6. Shoulder anatomy. Shoulder motion is produced by four joints and one articulation. The rotator cuff is the primary group of muscles associated with EVA shoulder injuries. Image credit (Stanford, 2012)

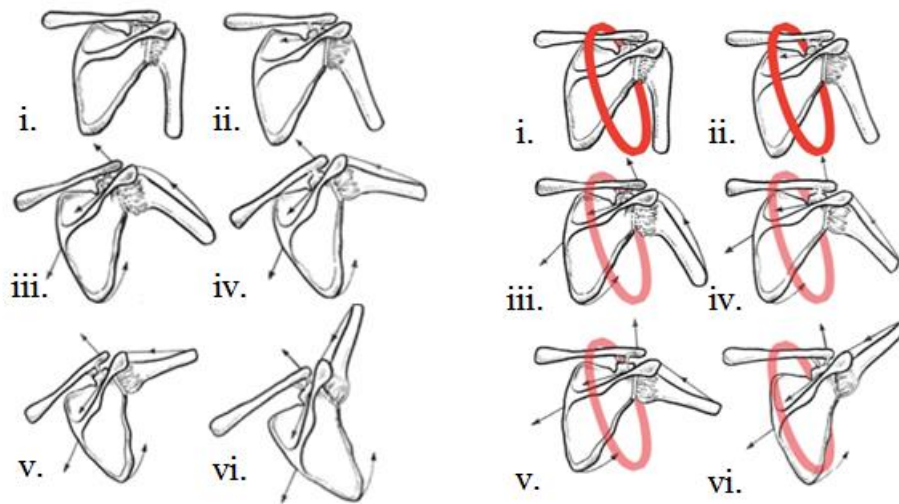


Figure 2.7. Shoulder movement during abduction. A) Normal shoulder abduction. Initially, two thirds of the movement is achieved through both scapulothoracic movement and glenohumeral movement. Then, movement shifts to entirely scapulothoracic movement. B) Shoulder movement impeded by the ring representing the HUT shoulder bearing. The ring prevents scapulothoracic movement, causing the person to rely on glenohumeral movement and producing unnatural movement and over recruitment of the rotator cuff. Photo credit Williams and Johnson, 2003.

(Williams and Johnson 2003, Strauss 2004). Currently, inverted NBL training is still performed, but in limited duration.

Previous work at NASA JSC on analyzing shoulder injury has focused on both orbital and training injuries in conjunction with the Longitudinal Study on Astronaut Health, the Injury Tracking System, and the Astronaut Strength Conditioning and Rehabilitation personnel (Longnecker 2004, Hochstein 2008, Scheuring, Mathers et al. 2009). Recently, shoulder injury information was matched with the crewmember's HUT selection to look for statistical correlations between HUT style (planar vs. pivoted) and frequency of suited activity. This work found the planar HUT to be the most provocative for injury, there is huge individual variability between those who do and do not get injured (Scheuring, McCullouch et al. 2012). Other information, such as subject anthropometry and training history may provide additional insight into shoulder injury but has not been explored and remains an important knowledge gap.

Beyond shoulder injuries, the primary injuries occurring at the limb joints (wrist, arms, knees, and ankles) are abrasions and contusions as a result of rubbing and impact against the soft suit components to move the garment. It has been suggested that when the convolute suit joint is not aligned well with the body joint, the propensity for injury is increased (Strauss 2004, Benson and Rajulu 2009). Abrasions and contusions are soft tissue and skin injuries forming under a variety of conditions. There is huge variability in an individual's propensity for injury, and targeting specific causal factors is challenging (Kawchuk and Elliott 1998, Xing, Pan et al. 2007, Desmoulin and Anderson 2011). Factors influencing the likelihood of injury include normal force, shear and friction force, frequency of impact/rubbing, presence of moisture, and previous



Figure 2.8. Neck and torso injuries post NBL training session. *Skin irritation and redness on the neck near the HUT, on the arm due to the upper arm bearing, and on the back from resting on the LCVG tubing. Photo credit Strauss, 2004*

exposure to injury (Mailler and Adams 2004, Carlson 2006). In the space suit environment, this interaction is caused by bending the soft goods, compression against the pressure bladder (which may wrinkle as the suit is pressurized), or through shifting in the suit. In training, additional injuries are seen in both the face-up and face-down positions, since the astronaut is now laying on the suit in a way not done in space, and the weight of the astronaut is supported by the HUT and the ventilation tubes of the LCVG. This pressure can lead to skin indentation and reddening, as seen in Figure 2.8 (Strauss, Krog et al. 2005, Scheuring, Mathers et al. 2009).

Hip, trunk, and feet injuries on orbit are fairly benign. They are primarily caused by impact and rubbing with the HUT, waist bearings, and soft elements resulting in injuries to those described previously for the upper body. Many EVA tasks are performed in footholds as the primary restraint. Although the EMU is designed with limited lower body mobility, astronauts must produce a counter torque by flexing leg and ankle muscles to maintain proper orientation while they work. Poor fitting boots and boot inserts allow the astronaut to rotate backward, causing the foot and toes to impact the top surface and rub (Strauss 2004). Additional discomfort is caused by the pressure bladder wrinkles, which cause blisters, contusions, abrasions and loss of feeling. On one EVA, this almost led to early termination of the EVA (Scheuring, Mathers et al. 2009). In training and during experiments to evaluate planetary locomotion and exploration procedures, the shifting body also causes the tops of the foot and distal toes to impact the boot (Strauss 2004, Norcross, Lee et al. 2009).

The following taxonomy is proposed to categorize injuries, shown in Table 2.1. The first category is “Dynamic Motion Injuries” which occur at the joints and are caused by movement leading to rubbing and impact with the suit. The second category of injuries is “Alignment Injuries”. These include trunk and neck, where injury occurs because the person is not properly placed within the suit during training. The third and final category is “Hybrid Injuries” which occur with both improper placement and movement, but would not occur when only one of those conditions is met. Shoulder and feet injuries fall into this category. A summary of EVA injuries and the category in which they lie is seen in Table 1. Defining the problem in this way allows protection devices to be implemented within a category and makes designing solutions a more tractable problem. Figure 2.9 summarizes the suit related upper body injuries, which are the focus of this work.

Table 2.1. Taxonomy describing EVA injury categories.

Injury Category	Anatomical Location	Description
Dynamic Movement	Arms and Wrists	Contusions and abrasions from rubbing at joint. Discomfort from impact with the soft goods, bearings, and sizing rings to produce movement
	Legs and Ankle	Contusions and abrasions from rubbing at joint. Discomfort from impact with the soft goods, bearings, and sizing rings to produce movement
Alignment	Neck	Impact with the HUT, specifically while inverted in training
	Hips and Trunk	Discomfort and skin irritation in supine and prone positions. Impact with the bearings, LCVG ventilation tubes, and inner contours of the HUT
Hybrid	Shoulder	Nerve impingement, rotator cuff pinching and tearing from impeded motion with body shifting and pressure on HUT
	Feet	Hard impact, loss of feeling, blisters, contusions, and abrasions while trying to maintain position with poorly fitting boot inserts and socks

In addition to the causal mechanisms of shoulder injury, general reasons for injury are hypothesized to include improper suit fit, shifting or improper use of protective garments, and repetitive motion working against the suit (Williams and Johnson 2003, Strauss 2004, Benson and Rajulu 2009). Current injury prevention is achieved by workaround modifications to the suit environment and individual physical training, rather than by implementing substantive design changes. Although acceptable for short-term prevention, the system must be modified to find long-term solutions. A greater understanding of human-suit interaction will help future suit designs minimize injury.

2.3. Suit Performance Characterization

The performance and movement of the space suit have been studied both experimentally and theoretically. However, evaluating how the astronaut interacts with the space suit is not possible with current measurement techniques. Performance is usually measured for the astronaut-space suit system. Additionally, few studies have focused on resolving issues associated with EVA injury.

There have been many experiments to characterize range of motion, work envelope, reach envelope, and the suited strength required to move inside a variety of suits. Example data from work envelope and reach tests is seen Figure 2.10A. Although none of these types of tests are specific to EVA injury, they offer the best understanding of human-suit interaction we are currently able to achieve. One of the most commonly studied metrics is joint torque required to move the suit. There are three test methodologies: unsuited externally applied torque (Parry, L. Curry et al. 1966, Reinhardt and Magstad 1990, Schmidt 2001, Holschuh, Waldie et al. 2009, Matty and Aitchison 2009, Valish and Eversley 2012), robotically applied internal torque (Parry, L. Curry et al. 1966, Schmidt 2001, Meyen, Holschuh et al. 2011), and suited internally

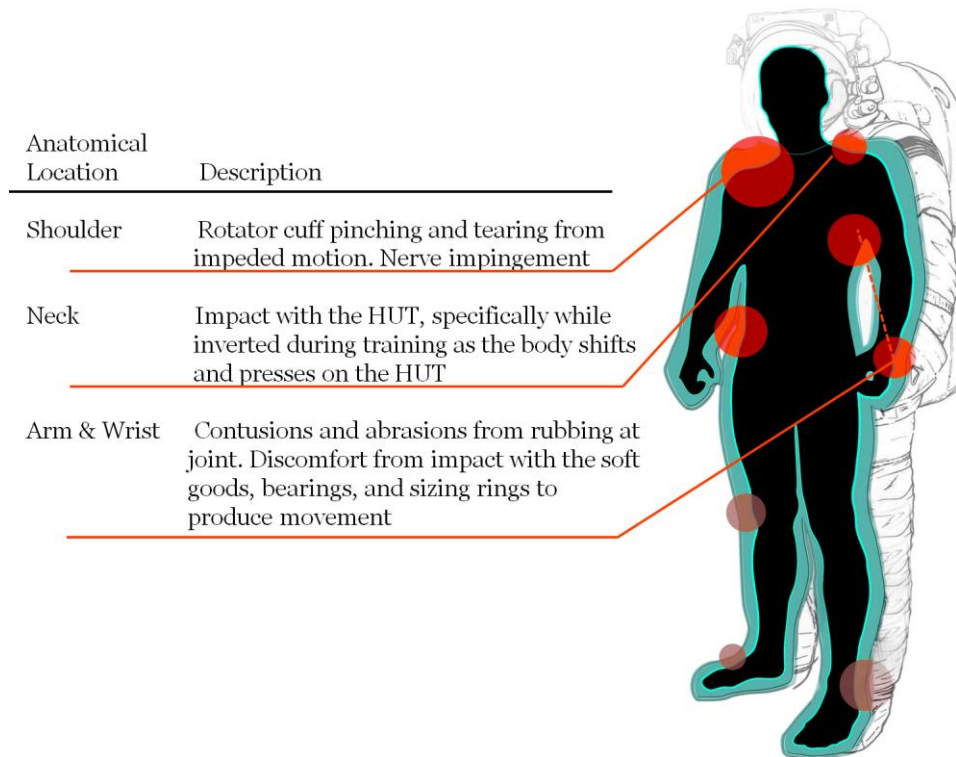


Figure 2.9. Upper body injuries occurring in EVA. *These injuries are the focus of this research effort.*

applied torque (Parry, L. Curry et al. 1966, Greenisen 1986, Morgan, Wilmington et al. 1996, Matty and Aitchison 2009). Unsuiting, externally applied torques are perhaps the easiest to measure, but do not account for the additional volume taken by the human. It is not possible to achieve accurate torque data from human suited testing, due to high variability per subject, off axis torques, and errors induced in the protocol (Parry, L. Curry et al. 1966, Gilkey 2012). Robotic testing has the advantage of being repeatable while still accounting for the way the space suit geometry changes when articulated internally, but only partially represents the volume of a person and is driven by preprogrammed movements. Data among these three testing methodologies is highly variable and dependent on testing methodologies (Gilkey 2012). Unfortunately, data cannot be compared across methodologies.

There has been a recent increase in the testing of newer space suits, such as the Mark III, Demonstrator Suit, and I-Suit, including metabolic measurements, operational feasibility (Norcross, Lee et al. 2009, Norcross 2010), and range of motion data (Jaramillo, Angermiller et al. 2008, England, Benson et al. 2010, Ripps, Garcia et al. 2011, Aitchison 2012). Testing on newer suit configurations is ongoing. Experimental evaluation of the human-space suit system gives gross metrics of performance and the upper bound of human capabilities within the environment. There is currently no way to evaluate human movement from within the suit, although recent work has focused on determining body joint angles within the suit (Di Capua and Akin 2012, Kobrick, C. Carr et al. 2012, Bertrand, Anderson et al. 2014). Knowing joint angles or where the body

impacts the suit would improve performance data collection techniques through precise torque measurements, human range of motion inside the suit, and greater insight into metabolic cost data.

Experimental studies are limited by their generalizability between suits, test subjects, and diversity in test conditions. EVA modeling helps to bridge the knowledge gap between experimental data and future space suit design recommendations and concepts (Parry, L. Curry et al. 1966). An example of modeled EVA work envelope is seen in Figure 2.10B. Work envelope has been the primary human-space suit performance metric that has been modeled, which is then compared to experimental subject testing (Schmidt 2001, Jaramillo, Angermiller et al. 2008, Griffin, Howard et al. 2009). Schmidt and Newman also derived physics-based models for space suit joint torques (Newman, Schmidt et al. 2000, Schmidt 2001), which can be related to physiology metabolic cost models. These models are typically used to establish suit thermal and life support design requirements (Kuznetz 1969, Waligora and Horrigan 1975, Carr 2005). Additionally, scenario-based EVA modeling helps give a greater understanding of how the astronaut interacts with the environment (Newman and Schaffner 1998, Anderson 1999). In the future, planetary human-suit performance may be based more so on modeling than experimental data, given our limited experience on the lunar surface (Waligora and Horrigan 1975, Griffin, Howard et al. 2009, Cowley, Margerum et al. 2012). These modeling efforts have not focused on how the suit impacts and constrains the wearer and where contact between the human and the suit occurs, which is critical information to reduce EVA injury. A model of that nature would require complicated dynamic simulations and a means by which to validate results, a technology not currently available.

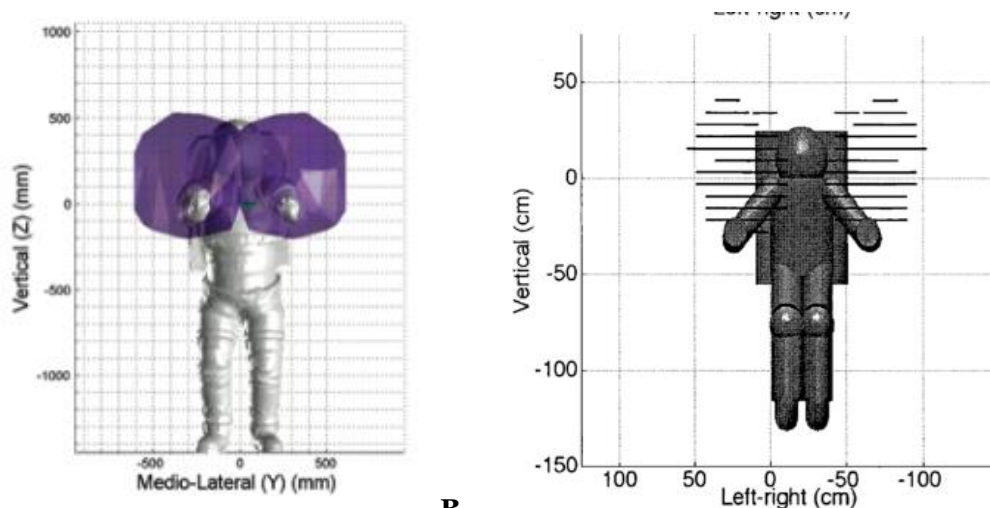


Figure 2.10. Example work envelope modeling and experimental suit testing. A) Experimental data shown for male crew member with arm length between 57 and 60cm. Image credit Jaramillo and Rajulu, 2008. B) Modeled data shown for female of size 50th percentile with 95% strength. Image credit Schmidt 2001.

2.4. Pressure Sensing Technology

To fill our gap in knowledge regarding how astronauts move inside the space suit and how movement relates to injury, it is desirable to explore new technologies such as pressure sensing. Pressure sensing between the human and space suit would measure the interaction directly, rather than being inferred as with other methods. With knowledge on sensor placement, the information could be used to assess biomechanics, space suit movement modeling, and even suit performance.

To the author's knowledge, only three pressure-sensing systems have previously been used for space suited applications. The first is the Tekscan system (Boston, MA) used in the Man Vehicle Laboratory for mechanical counterpressure space suit design and biomedical applications (Newman 2005, Judnick 2007, Anderson 2011). TekScan uses electrically conductive dye to detect changes in pressure (Brimacomb, D. Wilson et al. 2009). There are a wide variety of sensor configurations and pressure ranges. Despite the advantage of familiarity and adaptability, the system becomes unreliable at low pressures and is prone to calibration error, especially over a deformable body (Brimacomb, D. Wilson et al. 2009, Anderson 2011). The second system previously used for space suit design is Xsensor. Xsensor is a pressure-sensing mat using capacitors separated by a deformable elastomer (Cork 2007). The system was used in a shoulder injury study to evaluate the effectiveness of the HUT shoulder harness and its ability to distribute pressure. It was used in both pressurized and unpressurized EMUs. The system, however, uses custom made mats and is not easily integrated into an LCVG. Additionally, it had similar issues quantifying absolute values of pressure accurately (Witt and Jones 2007). The third is the Novel pressure sensor mat (Novel, GmbH, Munich, Germany) and was used suited and pressurized in unpublished work from researchers at the Anthropometry and Biomechanics Facility at NASA JSC. Novel sensors also use capacitance for pressure sensing, and are considered the best commercially available pressure sensing option. The mat was placed over the shoulder to measure pressure caused by the EMU. Each of these sensor systems are mat configurations and have limitations in experiments requiring a high degree of mobility. In their design, any folding of the sensor mat induces an artificial pressure into the reading. Additionally, it may inhibit mobility as subjects move through full range of motion.

A review was conducted to determine promising technologies to satisfy the need for pressure sensing inside the space suit without the same wearability issues mentioned previously. There are many types of pressure sensing technologies available. Traditionally, pressure sensors have been developed for biomedical applications such as gait analysis and to measure pressure distribution for bed and wheelchair bound patients. Recently, there has been a boom in technology developed for robotic applications such as human-robotic interaction, robotic environment sensing, and industrial monitoring. Many robotic applications focus on developing a skin-like touch sensor. Tactile sensing is very complex and requires integration of a great deal of information such as surface features, friction, or compressibility. Differentiation occurs through touch that is not easily taken into account given current technology (Lee and

Nicholls 1999). Regardless, research to produce tactile sensors has led to a huge increase in pressure and force sensing technologies.

There are many commercially available systems designed for biomedical and industrial applications. A review of 14 technologies was performed to assess their suitability for human applications and integration into a wearable device for the space suit environment. Commercially available sensors are advantageous in that they have low development overhead and are well characterized. However, these systems are more costly and offer less flexibility to be customized to this specific application. Of all identified commercially available technologies, those developed by Tekscan (Boston, MA) and Novel (Munich, Germany) are the most promising. Due to the previously mentioned limitations of these systems, research and developmental technologies were investigated.

Sensors designed for research purposes are promising since they may be inexpensive and can be highly customizable. Given the many applications in the literature, however, the solution space is extremely broad. One way to categorize sensor types differentiates between extrinsic and intrinsic sensors. Extrinsic sensors detect contact locations and pressure/force, giving information about the specific area of contact. These systems may become complicated in design. An example of such a sensor would be a synthetic skin (Alirezai, Nagakubo et al. 2007). Intrinsic sensors collect information regarding resultant forces on the entire system, without being able to resolve exactly where contact occurs. An example of this type of sensor would be a synthetic finger with the pressure/force-sensing element at the center of the design with synthetic tissue surrounding it (Wettels, Santos et al. 2008). Intrinsic sensors may give the same pressure/force reading with different contact locations, due to the potential ambiguity as you sense through elastic mediums (Lee and Nicholls 1999, Tegin and Wikander 2005). For the purposes of this work, since contact location is important, only extrinsic concepts are considered.

Extrinsic sensors will be further categorized on their underlying physical principle for detection, the most common of which are resistive, capacitive, piezoresistive, and force.

The most common and well-explored type of pressure sensor is based on the resistance and conductance of various materials. Many sensor designs use fluids as the conductive variable. Researchers at the Wyss Institute use microfluidic channels with conductive liquid metals in various configurations to distinguish between mechanical strain and normal pressure (Park, Majidi et al. 2010, Park, Chen et al. 2012). Noda et al. have used similar fluids in larger channels to resolve the same ambiguity. However, their design requires recalibration at each level of strain (Noda, Iwase et al. 2010). Composite carbon particles may be added to elastic materials in varying quantities to alter the resistivity of the sensor. As the particles shift with mechanical strain or applied pressure, the resistance changes. The mechanism for conductance is not well understood, making interpreting the output curve complicated (Ventrelli, L. Beccia et al. 2009, Lacasse, Dushaine et al. 2010). Another technique is to use a conductive fiber and measure resistance changes with strain. This has been used successfully to create foams for medical monitoring of movement and breathing. Using foam, however, causes

hysteresis in measurements (Brady, D. Diamond et al. 2005, Dunne, S. Brady et al. 2005). Yoshikai et al. showed how conductive yarn could be used for applications requiring high elasticity, however with high error and low response time. This team employed a novel method, electrical impedance tomography, to resolve pressure distributions over complicated geometries (Alirezai, Nagakubo et al. 2007, Yoshikai, Fukushima et al. 2009). Wang et al. used saw-toothed layers to sandwich a conductive fabric and create fabric strain with normal force (Wang, T. Hua et al. 2011). Finally, conductance can be used as pressure increases output from (Takei, T. Takahashi et al. 2010) or completes an electric circuit (Inaba, Hoshino et al. 1996, Duchaine, Lauzier et al. 2009) when rows and columns of conductive material meet the juncture of contact.

Using capacitance as a means to detect pressure is a very simple and commonly studied type of sensor. Many designs, consist of compressible foam sandwiched between conductive fabric whose capacitance varies as the material gets closer or further apart with changes in pressure (Sergio, Manaresi et al. 2002, Meyer, Lukowicz et al. 2006, Cork 2007, Metzger, E. Fleisch et al. 2008, Meyer 2008). Capacitive systems trade off simplicity in design for greater variability in the response profile. They have greater hysteresis and creep than other sensor types (Tegin and Wikander 2005). Additionally, there is a limit to their effective size, since capacitance must change over an area (Meyer 2008). Some researchers, however, have used capacitance to distinguish between complex sensing scenarios. The system developed by Cotton et al. can distinguish between normal force and strain by detecting electric fields at the edges of the sensors (Cotton, Graz et al. 2009). Another group at the University of Tokyo layered capacitors with different foam compliance to give a sense of “sharpness” of the object detected (Hoshi and Shinoda 2006). When sampled in an array, capacitive sensors provide a simple and robust solution to pressure sensing over an area.

Systems using piezoresistive fabrics are not as common in the literature, since many researchers favor simpler designs, such as capacitance. However, some applications, such as musical instrument interface, requiring higher resolution (Roh, Mann et al. 2011) detection used a grid of columns and rows, as seen in other designs. Voltages are measured at the junction with conductive thread and correlated to the pressure applied (Kolesar and Dyson 1995, Roh, Mann et al. 2011)

Another simple tool that may be implemented in my system is a force sensor. An example of a commercially available force sensor is Force Sensing Resistors (FSR) by Interlink (Camarillo, CA). These sensors must be mounted on hard, flat surfaces and do not work well for precision measurements (Interlink, 2013), making them undesirable for human applications. Multi-axis force sensors are more appropriate for this work. There have been many efforts to miniaturize force sensors so they may be placed on discrete locations of the body without substantial interference of movement. One of the major challenges to these designs is finding materials strong enough not to break under biomechanically induced loads (Beccai, S. Roccela et al. 2005). Most multi-axis force sensors use piezoresistance or capacitance to detect force. A summary of available sensors and their performance may be found in (Valdastri, S. Roccela et al. 2005). There is a trade-off between the sensor’s simplicity and the need to have multiple sensors to

achieve the same level of areal resolution of other technologies. Increasing the number of sensors complicates the system design.

There are several other solutions that do not fall into the previously mentioned sensing categories. Both Tseng and Lee used fluid filled reservoirs to detect pressure, with Tseng measuring impedance and Lee measuring deflection of a diaphragm (Lee, R. Goonetilleke et al. 2001, Tseng, Fisher et al. 2009). Alterations in fluid wave propagation was used in 2D fabrics, but the system is too complicated for our purposes (Chigusa, Makino et al. 2007). There are many more unique solutions to measuring pressure/force. However, given the application, the most promising technologies to pursue for further study use resistance since they have less hysteresis, greater accuracy, and can accommodate the range of pressures anticipated at the contact between the person and space suit. Additionally, some sensors, such as those developed by the Wyss Institute for Biologically Inspired Engineering at Harvard, may be used for dual application to determine joint angles, which would be highly desirable (Park, Majidi et al. 2010, Park, Chen et al. 2012).

Beyond the sensor itself, there are challenges in achieving a wearable electronic system suitable for the space suit environment. Currently, the only in-suit monitoring U.S. astronauts wear the operational bioinstrumentation system (OBS) to provide electrocardiogram signals for EVA, launch, and entry (Dismukes 2002, Dismukes 2002). However, future concept space suits may incorporate additional electronics to provide information to astronauts and ground crew. As electronics and sensor systems get smaller and more efficient, a great deal of research has been done on their applications for wearable human use. For space applications, requirements focus on safety, comfort, ease of use, operational simplicity, cost, electrical design, thermal, space environment, controls and displays, and operational life of systems (Carr 2001). Requirements for space suit electronics have been explored for advanced concept space suits, such as the BioLife system envisioned for the BioSuit™, where sensor integration is one of the primary concepts behind the technology (Canina 2006). Wearable electronics for the space suit has focused primarily in two areas: biomedical monitoring and information display.

For biomedical monitoring, efforts focus on monitoring biological systems with insight into the astronaut's effort, consumables, and health (Carr 2000). Research from biomedical device development outside of space applications has developed similarly, such as monitoring electrocardiogram, respiration, or stress for at-risk patients (Carr 2000, Catrysse 2004, Canina 2006, Tang 2007). Recent NASA work has also evaluated both unsuited and suited data collection to evaluate astronaut performance. An internal research group at NASA JSC focuses on electronic system design for a variety of sensor applications integrated to wearable garments (Simon 2013). Work at Kansas State University investigates wireless data transfer between different sensor systems in a simulated space suit to create a wireless body area network (Taj-Eldin 2013). Pressure sensing was not considered in these applications since it is not a traditional physiologic measure, but rather is a parameter specific to monitoring human-suit interaction.

Display and information design focuses primarily on display and control technologies, such as command and control of rovers (Graziosi 2005, van Erp 2005), the use of tactile feedback for information display (Rochlis 2000) and head mounted displays (Graziosi 2006). None of these systems were tested inside actual space suits but were evaluated in analog environments. Carr et. al developed a heads-up display evaluated in a suited EVA experiment, where data was transferred wirelessly to and from the subject (Carr 2001, Carr 2002). Although interesting from an EVA efficiency perspective, this work does not provide insight into distributed sensor architectures implemented in the space suit.

From this review there is currently no solution for measuring the pressure interface between the human and space suit in dynamic movement over a large area of the body in the desired pressure range. Additionally, in-suit sensing is a relatively unexplored area, and few systems have been implemented in the pressurized suit environment.

2.5. Application Beyond Space Missions: Divers to the Elderly

The need to mitigate injury and discomfort is not exclusive to the space suit environment. The contributions from this work have the potential to be used in other extreme working environments, such as for high altitude pilots wearing gas-pressurized suits with similar rigidity. Additionally, designs of soldier packs and armor would benefit from a similar analysis of encumbrance and pressure/force distribution over the body to optimize comfort and prevent injury (Knapik, J. Staab et al. 1990, Martin and Hooper 2001).

The envisioned system capability may also be used in biomedical applications. Hip fractures in the elderly is increasingly becoming a problem, with approximately a third of patients dying within a year of a fracture and another third having lasting disabilities (Villar, P. Hill et al. 1998). Falls resulting in hip fractures place a disproportionate burden on healthcare costs, recovery, and death (Hayes, Myers et al. 1996). Hip fractures in the elderly primarily occur due to side falls where the greater trochanter, the thin neck connecting the main shaft of the femur to the femoral head, is most vulnerable to impact. Hip protection devices have obvious advantage in preventing lateral impact from falls (Kannus, J. Parkkari et al. 2000). Unfortunately, effectiveness is contingent upon patient compliance to wear the device, which is typically low. In a study where effectiveness and the design were well vetted, 31% of subjects still did not wear the hip protector despite its proven effectiveness (Kannus, J. Parkkari et al. 2000). In another, only 50% of subjects were willing to wear hip padding daily, with compliance dropping to 30% over the study period. The main reason cited for not using the protection were discomfort and poor fit (Villar, P. Hill et al. 1998). Developing successful, comfortable protective devices may improve compliance, decreasing mortality and morbidity rates of hip injuries. Fit and comfort could be improved with measurements provided by wearable pressure sensing system.

Injury prevention both in extreme work environments and against fall impacts for the elderly are promising crossover applications. The transferability to each of these environments warrants further study.

2.6. Conclusion

The US space suit is a complicated and well-engineered machine (Harris 2001, Thomas and McMann 2006), but is a difficult environment in which to work due to its stiffness and rigidity (Parry, L. Curry et al. 1966, Schmidt 2001, Holschuh, Waldie et al. 2009). Space suit injuries caused as a result of training for EVA in the NBL are some of the most serious and debilitating injuries astronauts face (Longnecker 2004, Strauss 2004, Jones, Hoffman et al. 2008, Scheuring, Jones et al. 2008, Gernhardt, Jones et al. 2009, Scheuring, Mathers et al. 2009). The causal mechanisms of injury have been hypothesized but little quantitative study has been done, primarily due to the lack of tools to assess injury (Williams and Johnson 2003, Scheuring, McCullouch et al. 2012). Current methods of evaluation treat the space suit and person as one system and measure gross metrics of performance (Morgan, Wilmington et al. 1996, Jaramillo, Angermiller et al. 2008, Matty and Aitchison 2009, Norcross, Lee et al. 2009, Norcross 2010, Aitchison 2012, Valish and Eversley 2012). Information regarding shoulder injury, anthropometry, and training in the NBL environment is spread among many different groups each with variable reporting criteria. Investigating how these factors contribute to shoulder injury is critical to understand and mitigate the problem. In-suit sensing on human-suit interaction would allow the biomechanics of comfort and injury to be assessed, but there is no sensor system currently viable for this application (Cork 2007, Judnick 2007, Witt and Jones 2007, Brimacombe, D. Wilson et al. 2009, Anderson 2011). This is particularly true when considering the harsh environmental requirements of working inside the suit (Carr 2000, Carr 2001, Canina 2006, NASA 2011). This work fills these gaps both through statistical analysis to understand the underlying mechanisms of injury, and through experimental evaluation of human-suit interaction using a pressure-sensing system specifically designed for dynamic movement inside the environment of the space suit.

3. STATISTICAL EVALUATION OF SHOULDER INJURY

Shoulder injuries are some of the most serious and debilitating injuries associated with EVA training. Recent studies have documented that 23 astronauts have required shoulder surgeries, many 11 of which are directly attributable to working in the space suit (Scheuring, McCullouch et al. 2012). There are several hypothesized reasons for the increase in shoulder injuries in the training environment of the NBL. The first is the design of the space suit hard upper torso, or HUT, and its restriction of shoulder movement. Secondly, operational implementation of training, such as the frequency and orientation of the astronaut's body during training, may contribute to injury. Finally, individual variability due to body morphology or propensity of shoulder injury of each person may be contributing factors (Williams and Johnson 2003, Strauss 2004, Scheuring, McCullouch et al. 2012). The causal mechanisms of injury have not been quantitatively investigated.

The objective of this statistical analysis investigating astronaut injury is to explore the relationship between anthropometry, space suit HUT design, and training data to shoulder injury. Hypotheses 1 through 4 will be evaluated by statistical regression to determine which variables contribute to increased propensity for astronaut injury.

3.1. Database

An extensive, new database was compiled by NASA personnel at the Longitudinal Study on Astronaut Health (LSAH) and is the most comprehensive of its nature. The database includes 3 major components: Anthropometric measurements, Training record, and Injury record.

Each astronaut in the database was given a unique identifier and all data was made non-attributable. Due to the many resources compiled to create this comprehensive database, there is some variation in which subjects can be found in each of the three sections. There are a total of 278 astronauts with information in at least one of the three sections.

However, only 119 of the astronauts are common to all three. The remaining astronauts have data in at least one of the remaining sections, summarized in Table 3.1.

3.1.1. Anthropometric Data

There are 16 anthropometric dimensions included in the database. The measurements and the method by which data are taken is described in Table 3.2. Measurements are focused on the upper body and were identified by subject matter experts as potentially the most relevant dimensions for susceptibility to shoulder injury. The data was collected during the process of fitting the astronaut for their EMU components, but not all astronauts have complete data sets. There are 180 astronauts with reported anthropometry dimensions.

Table 3.1. Common subjects between three components of database. Each database was compiled from a different resource, and therefore has some variability in the subjects presented. There are 278 subjects, 118 of which are common to all three databases.

Database	Anthro.	Training	Injury
Anthro.	180		
Training	180	224	
Injury	119	142	196
Total	278		
Common	119		

Anthropometric information is known to be normally distributed within a population (Proctor 2008). However, this assumption may not be met with small sample sizes. Additionally, gender was excluded from the analyzed NASA database to keep the information non-attributable, meaning it is possible for the data to be bimodally distributed. The degree of normality will influence the regression techniques used to analyze the data. Therefore, a Kruskal-Wallis test for normality was conducted. None of the 16 dimensions were statistically significant ($p > 0.05$); therefore, anthropometric data was treated as normally distributed, as expected. Each dimension was checked for outliers and 7 data points were removed for being more than 4 standard deviations from the mean. These dimensions were attributable to errors in entering the data, as confirmed by NASA personnel.

Additionally, many anthropometric measures are strongly correlated. In some instances, measures may be collinear since they may be inclusive of one another, for example the dimensions for total arm length versus forearm length. The degree of correlation influences the regression techniques used to analyze the data. Of the possible 78 correlation coefficients, 74 had $p < 0.05$. Therefore, the anthropometric data was treated as highly correlated, as expected.

3.1.2. Astronaut Training History Data

The astronaut training record section contains 5 different sets of information: training day, either the actual or estimated time in the space suit, whether the subject was wearing either the planar or pivoted HUT, and the size of his or her HUT on a given training day. The training day variable begins with the subjects first time in the pool, and continues sequentially over the duration of his or her career. For some subjects, HUT size and training time was not estimated or recorded. Each training injury incident, however, includes the HUT type worn by the astronaut.

Table 3.2. Anthropometric dimensions included in the Anthropometry database. *There are 16 anthropometric dimensions included in the database, most of which focus on the upper body. Descriptions provided by the LSAH of how the measurements were taken is presented.*

Anthropometric Dimension	Description
Height (Stature)	Subject stands erect, head facing forward, heels together, and weight distributed equally on both feet. Measure the vertical distance from the standing surface to the top of the head with the arm of the anthropometer firmly touching the scalp.
Cervical Height	Subject stands erect, head facing forward, heels together, and the weight distributed equally on both feet. Measure the vertical distance from the standing surface to the cervical landmark (protruding bone where the bottom of the neck meets the torso of the body).
Mid-Shoulder Height (Left and Right)	Subject stands erect looking straight ahead, heels together and weight distributed equally on both feet. Measure the vertical distance from the standing surface to the mid-shoulder landmark (mid-point between the neck and the outward edge of the shoulder).
Acromion Height	Subject stands erect, head facing forward, heels together, and the weight distributed equally on both feet. Measure the vertical distance from the standing surface to the acromion landmark (outward edge of the shoulder).
Arm Reach Measurement (Left and Right)	Subject stands with their back against the wall with the arms extended to the front and parallel to the floor while maintaining shoulder contact with the wall. Measure from the middle
Expanded Chest Depth	Subject stands erect looking straight ahead, arms relaxed at sides, heels together, and weight distributed equally on both feet. Measure the horizontal distance across the trunk at the level of the widest area of the bust point while the subject is holding a full breath.
Inter-Acromion Distance	Subject stands erect, head facing forward, and the weight distributed equally on both feet. Measure the distance between acromion landmarks (outward edges of the shoulders) with the arms relaxed at the side.
Chest Breadth	Subject stands erect, looking straight ahead with the arms slightly abducted. Measure the horizontal distance across the trunk at the level of the widest area of the bust point.
Bi-Deltoid Breadth	Subject stands erect looking straight ahead, with the upper arms hanging relaxed. Measure the horizontal distance across the body at the level of the widest point of the shoulders (deltoids).
Acromion Radiale Length (Left and Right)	Subject stands erect with the arm extended and slightly forward. Measure the distance from the acromion landmark (outward edge of the shoulder) to the radiale landmark (crease of the inner side of the elbow).
Lower Arm Length Measurement (Left and Right)	Subject bends the arm 90 degrees at the elbow with the fingers extended. Measure the distance from the middle fingertip to the elbow tip landmark (protruding bone found when the elbow is bent).
Shoulder Circumference	Subject stands erect looking straight ahead, arms relaxed at sides and weight distributed equally on both feet. Measure the horizontal circumference of the body widest point of shoulders.

There are 223 astronauts in the training record. These astronauts span active duty from 1981 to 2012. There are 12,170 training events recorded. For each of these, training day and HUT type information is complete. There are 151 subjects missing the actual or estimated minutes during training for at least one run, and 117 subjects are missing at least one recorded HUT size.

The training record data was aggregated into five different dimensions. These dimensions are summarized in Table 3.3. Each dimension is a proxy variable to capture a specific aspect of the training history which may or may not play a role in shoulder injuries. None of the dimensions are normally distributed. Due to incomplete information for HUT size and minutes in the suit, proxy variables using this information were not included in the regression models. However, sizing and training minute information was used for descriptive statistics on injured and uninjured subjects presented in section 3.3.

3.1.3. Injury Record Data

Table 3.3. Aggregated training information used as proxy variables for statistical analysis. Five variables were created by aggregating the training data for each subject. Variables are not normally distributed.

Predictor Variable	Description	Formula	Variables
Total Incidence	Total number of training events	$\sum_{i=1}^n k_i$	i : observation n : total observations k : training event
Percent Incidence, Planar	Percent of training events performed in the Planar HUT	$\sum_{i=1}^n k(p)_i / \sum_{i=1}^n k_i$	p : planar event
Longevity	Total number of active duty days	$s_n - s_1$	s : training day
Frequency	Average number of active duty days per training event	$(s_n - s_1) / \sum_{i=1}^n k_i$	
Recovery	Measure of how much recovery subjects received between training runs. Sum of the inverse of days between training	$\sum_{i=1}^{n-1} \frac{1}{s_{i+1} - s_i}$	

The injury record includes every shoulder incident reported by an astronaut, whether it occurred pre-selection, in active duty, or during retirement. Shoulder incidents are recorded by the date of the report (although this may not correspond to the date of the injury), date of surgery if one occurred, whether relation to training in the water emersion training facility (WETF) or NBL was noted, precursory events, diagnosis, and the subsequent treatment.

Although there are 196 astronauts with reported shoulder incidents, only a small subset is relevant to the research questions explored here. Incidents were evaluated to divide subjects into 4 groups based on their reported shoulder incident, relation to the suit or training environment, precursor events, and diagnostic of the injury. Additionally, the phase of duty in which the injury occurred, whether it was pre-selection to the astronaut corps, during active duty, or retirement was included. Note that although referred to as an “injury”, not all shoulder incidents categorized from the database are considered a medical injury. However, any reported incident may be relevant and is considered in these models. In some instances, injuries were reported as directly caused by a traumatic event, and are categorized below as an “attributable” injury. The four groups are 1. those whose injuries are known not to be result of working in the suit or training environment, 2. those whose injuries are known to be caused by the suit or training environment, 3. those who began shoulder pathologies during active duty so suit or training environment may be a contributing factor, and 4. those with shoulder pathologies either prior to selection or after retirement, indicating shoulder injuries may be a result of normal shoulder degeneration with the suit/training environment as a potentially contributing factor. Each astronaut’s unique identifier and the category into which they fall is found in Appendix A.

There were 59 subjects for which it was clear the suit or NBL training were not related to their injuries. Subjects with the following exclusion criteria are:

- Pre-existing injury only with no subsequent injury
- Attributable to Launch and Entry Suit
- Active duty injury attributable to traumatic event
- Recorded injury was not shoulder related
- Active prior to EMU
- Retirement injury attributable to traumatic event

There were 35 subjects whose injuries were directly attributable to the suit and training environment as specified in the injury record. Reasons for inclusion are:

- Pre-existing injury with Suit or NBL identified as active duty injury
- Active duty injury only, NBL attributable
- Active duty injury only, Suit attributable
- Active duty NBL attributable injury, followed by related retirement injury

There were 62 subjects for whom it was not clear if the injuries were related to training or suit activity. If repetitive shoulder activities were cited as the cause of the injury, the subject's injuries were not categorized as traumatic events (which would put them into the first category). Rather the subject was included here since suit injuries may accumulate over time. For example, a bicycle accident is a trauma induced injury, as opposed to a softball injury which is due to repetitive use. The former is a single event leading to injury, whereas the latter could be compounded both by the activity and by training in the suit. Subjects with active duty shoulder injuries were:

- Active duty reported injury only
- Active and Retirement injuries reported

Subjects whose injuries may be related to shoulder degeneration were included under the following circumstances. There were 40 subjects in this group. Note that any sequential events occurred on the same shoulder or the subject was moved to other categories:

- Pre-selection and retirement injuries
- Pre-selection and active duty injuries
- All 3 career phases, attributable to an event
- All 3 career phases, unspecified cause of injury
- Retirement injury only

These four categories form the subject pools against which the predictor variables were regressed to determine the statistical relation to reporting a shoulder incident. The first group of subjects evaluated are those whose injuries are directly attributable to the suit or training environment, henceforth referred to as the NBL group. The second group of subjects are those whose pathologies began in active duty and are combined with the

NBL subjects for a second statistical analysis. This group is referred to henceforth as the Active group.

There is a great deal of variability to recording shoulder incidents. Historically, there was a tendency to under-report or delay reporting, so as not to affect the astronaut's flight status and career. Additionally, there was no standard method by which information was recorded, so details vary with each report. With the recent attention to shoulder injuries, many of these issues are being resolved and future data will be recorded more systematically. However, when dealing with historical information, this is an important limitation to note.

3.2. Methods

A logistic regression was chosen to analyze the relationship between training data, anthropometry, space suit components, and shoulder incidents. Logistic regression does not require any underlying assumptions of the predictor variable distribution. Finally, it is used to regress against binomial response, in this case either injured or uninjured. The equation for logistic regression is:

$$Y_i = 1/(1 - e^{X\beta}) \quad (3.1)$$

where Y_i is the logistic response function, X is the matrix of observations for each explanatory variable, and β is the matrix of fit coefficients. When expanded for each explanatory variable:

$$X\beta = \beta_0 + \beta_1 X_1 + \dots + \beta_n X_n \quad (3.2)$$

To determine the proper variables included in the regression models, the following method was used. This analysis was performed using Matlab (Natick, MA) and all code to analyze and process the data can be found in the Appendix B.

The data used for the regression was compiled from the information in the previously described database. There are relatively few data points and a large number of potential predictor variables. Because this study focuses on shoulder injury, lower arm dimensions were excluded. There were 61 subjects both with anthropometry and training information in the database, but never reported a shoulder incident. These subjects were included in the model as uninjured, bringing the total number of subjects evaluated to 180 astronauts.

Anthropometric data was centered about the mean and normalized by standard deviation (σ). The training data was also scaled and centered, but since the variables are not normally distributed, the median and median absolute deviation (MAD) were used. Three variables, the total number of incidences, training frequency, and recovery, were exponential in nature and were log-transformed to improve the fit of the model. For the NBL injured subjects, an additional predictor variable was included for whether or not the subject had been previously injured.

Given the large number of predictor variables, bootstrapping was used to identify the most relevant factors (Rice 2007). A model fit to the entire data set may lose some of the subtly relevant predictor variables in favor of a more parsimonious model. This is particularly true for the NBL injured group of subjects where an injury is an infrequent occurrence. A 500 iteration bootstrap was fit to 50-50 data split where every injured subject was used for each model, but the uninjured subjects were randomly selected using resampling. Forward stepwise logistic regression was used to fit the model with the decision criteria for inclusion being to minimize the AIC statistic. For each of the 500 models built, the relevant predictor variables were logged. For the NBL subjects, variables appearing in 10% of the models were considered for inclusion in the final model. For the Active subjects, variables appearing in 30% of the models were considered for inclusion.

Using the variables identified in the bootstrap, a model was fit to the entire dataset. The variables were checked for correlations, and if necessary additional variables were removed. A stratified 5-fold cross validation was performed using the final predictor variables to determine the model's fit to "unseen" data. The 180 subjects were randomly divided into 5 equal sections, preserving the global incidence rate of injured and uninjured subjects. A model was built on 80% of the data and tested using the remaining 20%. Nominally the model was fit with the cut off value of 0.5, above which a subject is categorized as injured. The cut off value was shifted to improve prediction rates, trading off correctly identifying injured subjects as more important than miscategorizing uninjured subjects given the costs associated with misclassification. The percent of correct predictions, percent of correct negative predictions, and percent of correct positive predictions were logged for each of the 5 models. To reduce the effects of randomness, cross validation was performed 50 times and mean and standard deviation of predictive capability were calculated over all 250 trials.

3.3. Data Mining Results

The final model fit to all uninjured and injured subjects that fall into the NBL identified category is shown in Table 3.4. There were 35 astronauts considered injured in this model, and 145 considered uninjured. There were three relevant predictor variables related to training: the percent time in the planar HUT, training frequency, and recovery. Two anthropometric dimensions were found to be important predictors for injury: expanded chest depth, and bi-deltoid breadth. Finally, history of a previous injury was found to be a relevant predictor. This model has a log-likelihood overall model fit p - value = 0.003. The area under the ROC curve is 0.73, shown in Figure 3.1, and the Hosmer-Lemeshow test for fit is not significant ($p = 0.84$). Each of these metrics indicates the model fits the data well. When evaluated in cross-validation, using a cut-off value of 0.3, the model had a 69% overall accuracy rate and correctly identified 39% of injured subjects as injured (standard deviation, $\sigma = 9\%$).

Table 3.4. Model fit to subjects whose incident was reported as a result of working in the NBL. Six predictor variables were found to be important for identifying injury: three related to training, two anthropometric dimensions, and record of previous injury.

	Coef.	Variable	Wald	p-value
β_0	-1.79	Constant	-6.59	-
β_1	1.06	Percent in planar HUT	3.44	.0006*
β_2	0.073	Training frequency	0.47	0.64
β_3	0.42	Recovery metric	2.09	.037*
β_4	-0.33	Expanded chest depth	-1.15	0.25
β_5	0.19	Bi-beltoid breadth	0.7	0.48
β_6	0.98	Previous injury	1.66	0.1

The same methodology was used subjects in the Active category combined with the NBL subjects. There were 75 astronauts considered injured in this model and 105 considered uninjured. The record of previous injury was not included in this analysis since it is a confounding variable with the way Active injured subjects were categorized. The final model is shown in Table 3.5. A total of 5 predictor variables were found to be important for identifying subjects as injured. There are 3 variables related to training: percent incidences in planar HUT, frequency of training, and recovery. There are two relevant anthropometric predictor variables identified: expanded chest depth and shoulder circumference. This model has a log-likelihood overall model fit with p-value = 0.003. The area under the ROC curve is 0.67, shown in Figure 3.1, and the Hosmer-Lemeshow test was not significant (p = 0.89), also indicating this model is a good fit to the data.

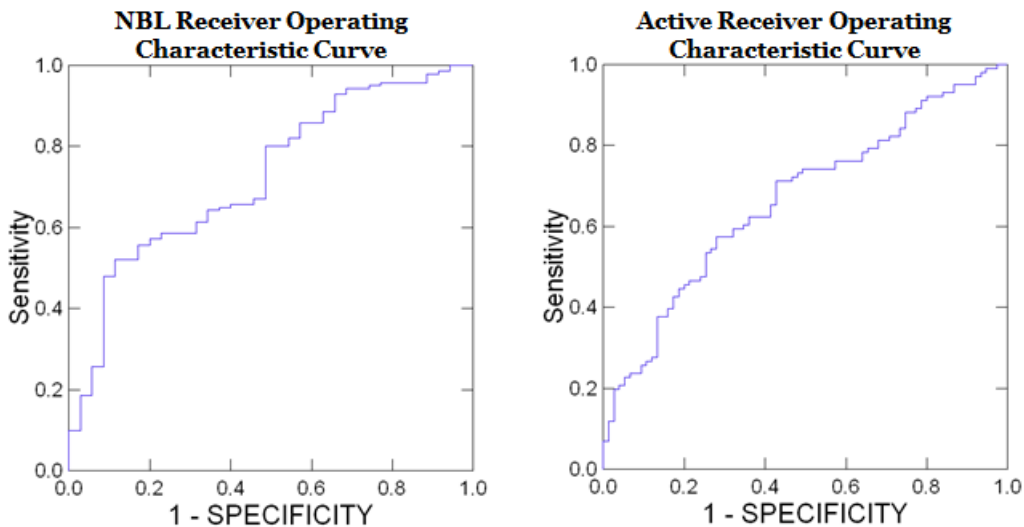


Figure 3.1. Receiver operating characteristic curve. A) For the NBL model. The area under the curve is 0.73. B) For the Active model. The area under the curve is 0.67

Table 3.5. Model fit to subjects whose incident was reported during active duty and while working in the NBL. Five predictor variables were found to be important for identifying injury: three related to training and two anthropometric dimensions.

	Coef.	Variable	Wald	p-value
β_0	-0.37	Constant	-2.2	-
β_1	0.55	Percent in planar HUT	3	.003*
β_2	0.23	Training frequency	1.89	0.06
β_3	0.37	Recovery metric	2.36	.02*
β_4	-0.31	Expanded chest depth	-1.36	0.17
β_5	0.5	Shoulder circumference	2.34	.02*

The cross-validated correct prediction rate is 57% with a cut-off value of 0.4. The correct prediction of injured subjects is 68% ($\sigma = 10\%$).

In addition to the models presented here, models were evaluated using only anthropometric information and only training information for both groups. For both groups, models built with only training information were found to be significant. However, anthropometry alone did not produce a significant result. For all cases, cross-validated performance was poor, therefore only models using anthropometry in conjunction with training information and record of previous injury (NBL subjects only) were considered. This achieved a better overall model fit and improved predictive performance.

3.4. Discussion

For both groups of injured subjects, the NBL and Active groups, a logistic regression model was calculated with a statistically a good fit to the data. The two models use similar predictor variables.

For both models percent of training incidences in the planar HUT is a highly significant factor. It was consistently the best predictor of injury and was the most frequent identified variable in bootstrapping. This confirms Hypothesis 2, *“Suit training variables in the planar hard upper torso (HUT), rather than training in the pivoted HUT, will be a predictive factor in identifying astronauts with a reported shoulder incident.”* It has long been asserted that training in the planar HUT is the most relevant factor, and these results support this assertion for both groups of injured subjects.

The same training variables, frequency and recovery, were included in both models. Although frequency was not significant in the NBL model by the Wald criteria, which evaluates whether the factor contributes significantly to the model, it was included to improve predictive power. Note that the recovery metric is strongly correlated (value of 0.93 as shown in Figure 3.2) with total number of training incidence. Recovery was chosen over total training incidence because it improved the correct prediction of injured subjects as compared to the former. However, total training incidence should be

considered as an important variable for future modeling work as more data is collected. These variables confirm Hypothesis 3, “Operational training variables will be predictive factors in identifying astronauts with a reported shoulder incident.” The importance of including these factors shows that an astronaut who trains frequently will have a higher propensity for injury, in addition to whether or not those training runs are over a concentrated time period. Although these may seem like confounding factors, as seen in Figure 3.2, the correlation between these variables is low, 0.22.

Additionally, anthropometric variables were found to be relevant for both models, confirming Hypothesis 1, “Anthropometric dimensions will be a predictive factor in identifying astronauts with a reported shoulder incident.” Expanded chest depth was shown to be relevant for both models to provide explanatory power for both groups of subjects. As a variable with a negative coefficient, a decrease in expanded chest depth will increase the odds of being injured. It has been proposed that smaller subjects who must work inside the HUT too large for them may have additional problems articulating the suit due to the lateral shifting of the scye bearing, potentially leading to injury (Williams and Johnson 2003). Although this work cannot support nor refute this claim, it does support that smaller expanded chest depth increases propensity for injury.

One additional anthropometric dimension was chosen as a factor for each model, but the variable is different for each group of subjects. For NBL subjects, bi-deltoid breadth

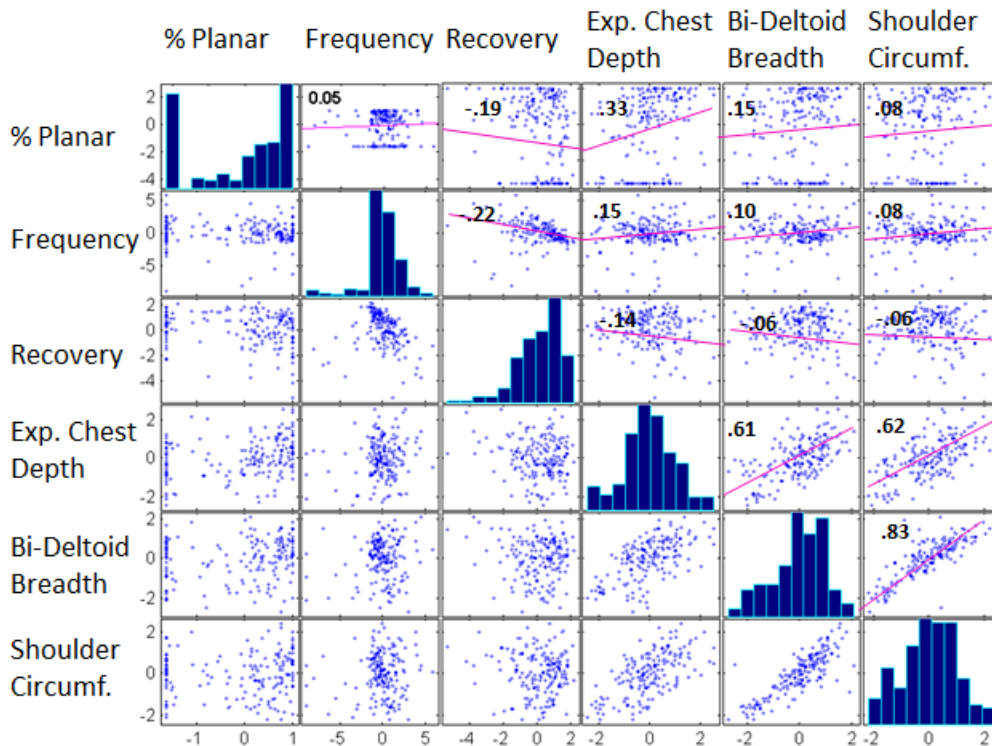


Figure 3.2. Correlation matrix and histogram of variables included in the NBL injury model. Histogram of each variable is given on the diagonal axis. The pairwise correlation is given in each row/column pair with the correlation coefficient. The highest correlation is between anthropometry with a value of .6. Categorical variable of previous injury not shown.

was an important predictor, whereas for the Active subjects, shoulder circumference was a strong predictor and was statistically significant. Although, as seen in Figure 3.2, these variables are correlated with one another, they were poor predictors when used in the opposite model (i.e. replacing bi-deltoid breadth for shoulder circumference in the NBL model does not give a well fit model). The histograms for injured subjects in each of these variables are shown in Figure 3.3. The dimensions included for each model are highlighted in red boxes. Expanded chest depth for both groups of injured subjects, there may be an apparent skew right, although it's not definitive from the histogram. This corresponds to the weaker p-values for this variable while still providing predictive power. However, for bi-deltoid breadth, there is a clear left skew for the NBL injured subjects. The skew may also be apparent for Active subjects, but it is not as obvious. When evaluating shoulder circumference, the NBL subjects are centered about the mean, while there is a left skew for the Active subjects. Visually, it is apparent why each dimension was selected for the models, while being excluded from other. For each model respectively, if the bi-deltoid breadth or shoulder circumference increases, the odds of getting injured also increases, as opposed to the smaller expanded chest depth. This variable seems to be identifying injured subjects on the larger spectrum who are potentially fitting more tightly into their HUT, not allowing for normal movement. As described in Chapter 2, subjects with less clearance for scapular thoracic motion may not be able to move as unsuited, leading to shoulder injuries. Although this work cannot confirm nor support this claim, it does indicate it is an interesting area for future inquiry.

Finally, Hypothesis 4 is confirmed, *“Record of previous injury will be a predictive factor in identifying astronauts with an additional shoulder incident.”* Although there are many astronauts with previous shoulder injuries without subsequent problems, and

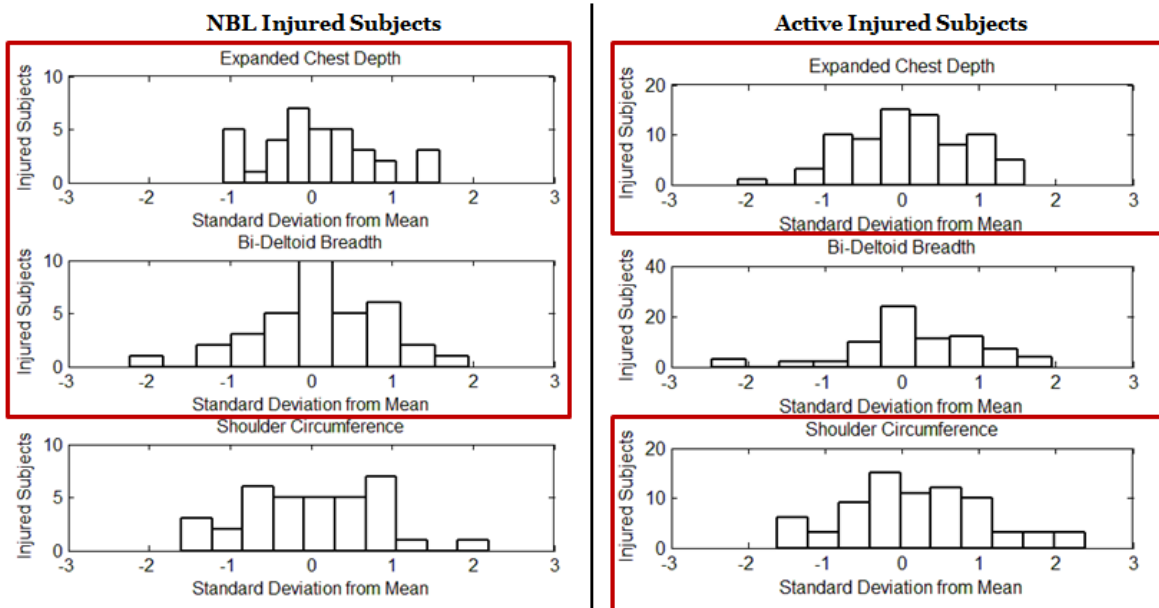


Figure 3.3. Comparison of anthropometric variables included in the NBL and Active models for injured subjects. Histograms of each variable are given while the variables included for each model are highlighted with the red box. The histograms allow a visual inspection of how the data is skewed and corresponds to correct inclusion of the variables in the model.

many without previous injury as evidenced by the Active group of subjects, it was shown here that for NBL subjects it was a strong predictor variable. This may be due to normal shoulder deterioration, and personnel at JSC are currently working an age-matched incident rate against which to compare astronaut shoulder injury incidence rates.

Although these models fit the data by objective measures, there is an inherent optimism in that their performance is evaluated against the data from which it was fit. Cross-validation allows us to understand how the model performs on “new” data which was not seen when the model was built. Ideally, the model would separate the injured from the uninjured with no type I (false positive) or type II (false negative) error. For the purposes of predicting astronaut shoulder injury, type I error is favored due to the consequences of misidentifying a subject who will be injured at the cost of crew health and safety and mission success. The NBL model with a cut off value of 0.3 has a reasonably high overall accuracy rate of 69%. However, it only correctly identified 39% of injured subjects. Although predicting any injured subject correctly is an improvement over the current state, it is desirable for this rate to be higher. The overall prediction rate was sacrificed to increase the subjects who could be identified as injured by shifting the cut-off value. Only 19% of the subjects in the NBL data are injured and it therefore has a tendency to predict subjects as uninjured. However, for the Active model, the incident rate is higher, 42% or 75 injured astronauts. Here, the overall prediction is 57% with a cut-off value of 0.4, but the correct prediction of injured subjects is 68%. The ability to identify injured subjects is greatly improved in this model, at the cost of misclassifying subjects who were uninjured in reality. Note that shifting the classification cut-off value back to the original 0.5 does not improve the overall prediction rate, but rather moves subjects from type I to type II error, which is undesirable. Both the NBL and Active models are able to identify some subjects as injured, but their performance is not as strong as desired. The models cannot fully separate subjects, but rather pushes injured subjects closer to the surface. This is similarly reflected when the residuals are evaluated. For the NBL model, large deviation from normality for the injured subjects and deviation at both tails for the Active model is seen. This indicates the models are missing critical information to better identify injured and uninjured subjects properly. However, given the current data set, these models provide the most utility.

Although HUT size information was excluded from the regression model, it is instructive to analyze this data with descriptive statistics. Any statistical comparisons between injured and uninjured groups were performed with a two-tailed Wilcoxon Rank Sum (nonparametric equivalent to a Z-test) because the sizing and training data is not normally distributed. For NBL subjects, the injured subjects performed a total of 2,861 training runs, with a median of 62 and median absolute deviation (MAD) of 39 training incidents per subject. This is statistically different ($p = 0.02$) from uninjured subjects who performed 8,716 training runs, a smaller median of 50 (MAD = 35). The main effects plot is shown in Figure 3.4. Of these training incidents, the injured group of subjects is missing 3% of HUT size data, while the uninjured is missing 12% of data. This must be considered when evaluating the sizing differences between the two groups. Similarly Active injured astronauts performed 5,519 total runs, with a median of 62 (MAD = 39) runs per subject. Uninjured subjects performed 6,058 runs or a smaller median of 49 (MAD = 36) runs per subject. There is a statistical difference between

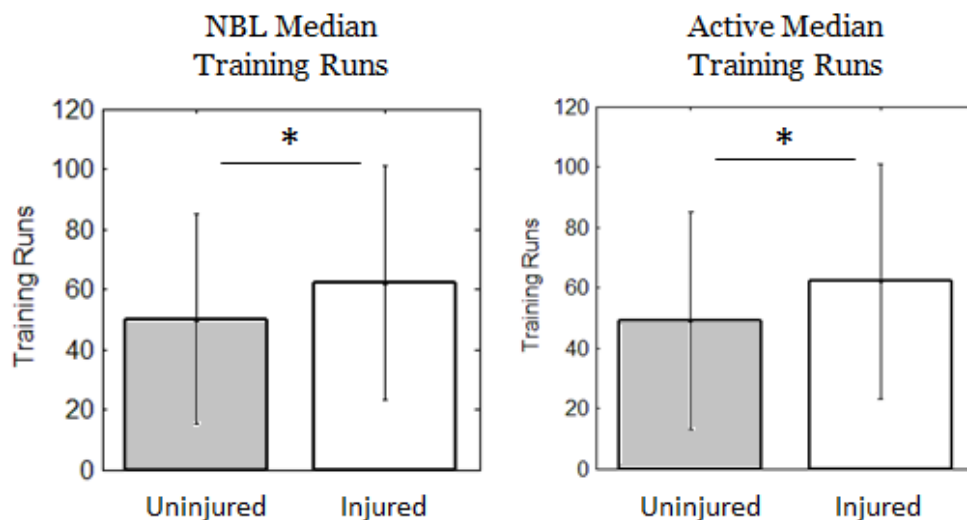


Figure 3.4. Plot of median and median average distance for injured and uninjured subjects. For both groups, the injured subjects performed more training runs than uninjured subjects, with $*p < 0.05$.

subjects ($p = 0.04$), also shown in Figure 3.4. In both groups, injured subjects performed more training runs than uninjured subjects. Therefore, rather than comparing by absolute numbers, HUT sizing information will be scaled by the median of each group.

The total number of runs per subject performed in each HUT size was calculated for both groups. For the NBL subjects, there was no statistical difference between injured and uninjured subjects wearing the medium HUTs ($p = 0.32$) nor when wearing the large HUT ($p = 0.41$) respectively. There was a statistical difference between subjects wearing extra-large HUTs ($p = 0.015$). However, the histogram of subject sizing, shown in Figure 3.5, reveals that for injured subjects in the large HUT, there is a group of subjects 2-3 times the median number of training runs as compared to uninjured subjects. The same pattern may be seen for the medium HUT, but is not as pronounced. This effect is not dominant, however, since the uninjured group has several subjects further on the tail of the distribution. For the extra-large HUT, injured subjects used the HUT for a fraction of their training. There is no statistical difference for the Active subjects in any size (medium $p = 0.89$, large $p = 0.17$, and extra-large $p = 0.20$). No visual substantive difference is seen in the histogram plot for Active subjects.

From the logistic regression, HUT style was found to be a factor related to injury. The effect of both style and size was assessed simultaneously. Each subject was categorized by the size and style combination he or she used most frequently. Table 3.6 shows the percentage of subjects within a category using a particular HUT combination as their most preferred choice. For example, there are 35 injured NBL subjects. Of these, 15 subjects, or 43%, primarily used the medium planar HUT in training.

Injured subjects for both the NBL and Active groups primarily did their training in the planar HUT. Uninjured subjects also had a tendency to train in the planar HUT, but their categorizations are more distributed. These results are unsurprising given the

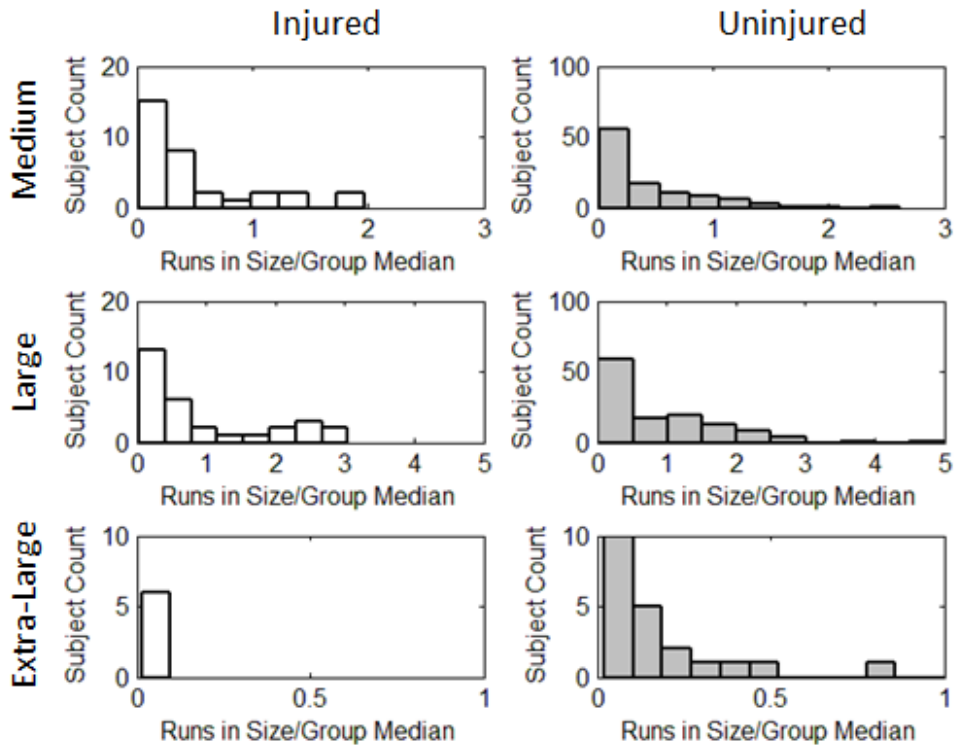


Figure 3.5. Histogram of NBL subjects by injury and their chosen size HUT. *There is no statistical difference for medium and large, but graphically there is a large group of injured subjects performing many times the median number of total runs. There is a statistical difference for extra-large HUTs because nearly none of the injured subjects used this size.*

logistic regression model showing training in the planar HUT leads to a greater propensity for injury.

However, since astronauts iterate on suit fit and may change their sizing over the course of their career, the previous analysis may be oversimplified. Table 3.7 shows the same data when presented in terms of percent total training runs. For example, of the 2,785 total training runs performed by injured NBL subjects, 920 were performed in the planar medium HUT, or 33%. Here, an interesting variation emerges over the patterns noted previously. Although from Table 3.6 43% of subjects preferred the planar medium, and only 8% preferred the pivoted large, when evaluated by total runs, the percentages shift to 33% and 18% respectively. It appears that injured NBL subjects may oscillate between these two sizes. This pattern is also true for active duty subjects. Due to minor differences in the HUT design, astronauts often trade the planar medium and pivoted large, since their fits are similar (as opposed to trading between a planar medium and large). Although this work cannot confirm nor refute the relation between these sizes and injury, it does indicate that further analysis into this area is promising. Additionally, it shows the importance of taking into account each training run as it relates to sizing, since details may be lost if only the most frequent sizing information is considered.

Given this analysis on anthropometry and HUT sizing information, future work should evaluate how bodily geometry compares to the HUT size chosen by an astronaut. As described in Chapter 2, subjects at the extremes of HUT fit, those with too much space

Table 3.6. Comparison of preference of planar and pivoted HUT sizes for both NBL and Active groups. Percentages shown are percentage of subjects with in a group using the size most frequently. Values are consistent among all 4 groups of subjects.

MOST FREQUENTLY USED PER SUBJECT					
NBL Subjects			Active Subjects		
<i>Injured</i>			<i>Injured</i>		
	Planar	Pivoted		Planar	Pivoted
Medium	43%	0%	Medium	29%	0%
Large	49%	8%	Large	48%	20%
X-Large	0%	0%	X-Large	0%	3%
<i>Uninjured</i>			<i>Uninjured</i>		
	Planar	Pivoted		Planar	Pivoted
Medium	27%	8%	Medium	31%	11%
Large	36%	24%	Large	31%	22%
X-Large	0%	5%	X-Large	0%	5%

to articulate the suit properly and those with too little clearance to perform normal scapulothoracic motion, are hypothesized to have a greater propensity for injury. The issue of “too much room” may be reflected in the fact that few of the astronauts chose to work in the extra-large HUT. Alternatively, astronauts at the smaller end of the spectrum must work in the medium size HUTs. Analyzing clearance with 3D models of the body and HUT would allow this theory to be explored. Some astronauts have 3D body scans, but their scanned postures are not similar to those induced by space suited motions. Work at Brown University and the Max Planck Institute may provide a mechanism by which to generate a 3D body representation from the anthropometry presented here, and then morph the model into the desired position. The modeling work uses measurement heuristics for predicting body geometries that are accurate when compared against actual body scans (Guan, A. Weiss et al. 2009) Using this or similar modeling techniques in conjunction with HUT sized models could give the best insight not currently possible into astronaut injury.

3.5. Conclusion

The logistic regression models presented here are able achieve the first specific aim of this work to identify relevant factors that increase propensity for injury. Two groups of subjects were analyzed, those whose reported shoulder incident is specifically attributable to the NBL or working in the suit, and those whose shoulder problems began in active duty, meaning training could have been a related causal factor. For both models, percent of training incidence in the planar HUT, frequency of training, and recovery between training were identified as important metrics. These variables can be monitored and modified operationally to reduce the impacts on the astronaut’s health. Several anthropometric dimensions were also found to have explanatory power for injury. Expanded chest depth was present in both models, while bi-deltoid breadth was relevant for NBL subjects and shoulder circumference was relevant for Active subjects. These dimensions may be targeted as particularly important to accommodate in future

Table 3.7. Comparison of total training incidence in planar and pivoted HUT sizes for both NBL and Active groups. Percentages shown are percentage of total training runs within a group using the size. Injured NBL subjects train more in the planar medium and when uninjured in the pivoted large. For active duty subjects uninjured subjects also train more in the pivoted large. Otherwise values are consistent among all 4 groups of subjects.

TOTAL TRAINING RUNS ACROSS ALL SUBJECTS					
NBL Subjects			Active Subjects		
<i>Injured</i>			<i>Injured</i>		
	Planar	Pivoted		Planar	Pivoted
Medium	33%	3%	Medium	25%	3%
Large	48%	16%	Large	46.0%	24%
X-Large	0%	0%	X-Large	0.5%	1%
<i>Uninjured</i>			<i>Uninjured</i>		
	Planar	Pivoted		Planar	Pivoted
Medium	20%	8%	Medium	23.0%	10%
Large	41%	28%	Large	39%	25%
X-Large	0%	3%	X-Large	0.3%	3%

designs of the HUT or any advanced concept space suit. Finally, for the NBL subjects, previous record of injury was found to be an important factor. Further descriptive analysis implies that analyzing the HUT style and size together may be critical for future detailed studies on fit and accommodation.

These models are not fully descriptive and are likely missing relevant factors. The models ability to separate injured from uninjured subjects is an improvement over the current state, although additional data may improve explanatory power. Regardless, the variables identified here not only allow the identification of between 30-60% of injured subjects correctly, but also provide quantitative confirmation of many of the assertions made previously by flight doctors, trainers, suit designers, and astronauts about relevant factors of injury. Perhaps given individual variability seen in any injury or epidemiological study, there is no factor that might be able to separate out injured from uninjured subjects. Future work includes evaluating more complicated modeling paradigms. Several techniques have already been explored to establish their relative utility. These methods are linear discriminant analysis, partial least squares regression, principal component analysis, decision trees, and random forests.

The first specific aim of this thesis is to analyze data for correlations between anthropometry, space suit components, and shoulder injury. Four hypotheses were proposed to relate injury to 1) body morphologies, 2) space suit HUT components, 3) training variables, and 4) previous injury. Each hypothesis was confirmed, since for both models variables for each of the first three hypotheses were identified and record of previous injury was associated with the NBL model. The major contributions of this work are to:

- 1) Add quantitative statistical analysis to the causal mechanisms of injury found in the literature.
- 2) Provide a framework for identifying relevant predictor variables related to injury given the small number of data points, large number of predictor variables, and the differences in their distributions.
- 3) Identify variables related to injury which can be addressed and resolved through operational changes to training, suit design and accommodation, and identification of higher risk subjects given previous medical history.
- 4) Propose future areas of study for which additional data may continue to be collected and analyzed, such as HUT sizing information as related to clearance anthropometry.

These contributions address the current gap in our understanding of the causal mechanisms of injury. Although HUT style has been reported as a major cause based on anecdotal evidence (Williams and Johnson 2003, Strauss 2004), it has not been until recently that this causal mechanism has been quantitatively evaluated (Scheuring, McCullouch et al. 2012). This research corroborates these findings, but expands upon them to include additional relevant factors not previously explored. It also includes other shoulder incidents, which, although not defined as medical injuries, have had negative impact on crew comfort and health, as well as impacting an astronaut's operational availability. This work also supports the conclusions reached by (Williams and Johnson 2003) regarding the import of the training environment as a contributory factor, but this is the first quantitative assessment of the impacts of training frequency and recovery. Finally, it supports that suit fit is essential to achieve the optimal working environment (Benson and Rajulu 2009, Gast and Moore 2010) and allows future designs to pinpoint the most relevant anthropometric dimensions for suit fit accommodation. This work provides a quantitative analysis through data mining grounded in our historical understanding of the use of the EMU and NBL training environment. The remainder of this thesis allows a look forward into how additional data collection on human-space suit interaction can help prevent the occurrence of future injury and discomfort.

4. WEARABLE PRESSURE SENSING SYSTEM

There is currently no way to quantitatively measure the interaction between a person and the space suit. Joint angle measurements using IMUs inside and outside the space suit provide useful insight into biomechanics, but are nascent work (Di Capua and Akin 2012, Kobrick, C. Carr et al. 2012, Bertrand, Anderson et al. 2014). Currently there is no technological system to measure contact pressure within the suit in the low-pressure range (~0-60 kPa), which are typical of dynamic space suit motions. To address this need, a wearable pressure sensing system was developed to quantify the contact pressure between the person and the space suit during EVA motions. This work focuses on the upper body with two anticipated pressure loading regimes: 1) High-pressure (~>50 kPa) underneath the space suit hard upper torso (HUT) component over the person's shoulder and upper torso, and 2) Low-pressure (~0-60 kPa) under soft goods and bearings covering the arm. A custom sensor suite was developed to quantify astronaut space suit interaction and is specifically tailored to the space suit environment. The design, fabrication, and testing processes used to create the system are described herein. Requirements to ensure the system was properly designed for the space suit environment are presented. A great deal of design and construction iteration on both the sensor itself and the associated hardware (such as wiring, electronics, and power) achieved the current design. Data to evaluate the success or failure in meeting the design requirements are presented. The advantages, limitations, and future work and design concepts for the next generation wearable pressure sensing system for use inside the space suit and extreme environments are discussed.

4.1. System Requirements

Table 4.1 A&B shows the design requirements established for this system and the method by which the requirements were validated. For wearable sensors, the most critical requirements are pressure measurement, range, spatial resolution, response profile, and applicability. Other aspects, such as low power and design simplicity, are

also considered desirable (Tegin and Wikander 2005). The design requirements are divided into two critical aspects of pressure sensing inside the space suit: utility and wearability. Utility refers to the requirements that ensure the sensor system measures pressure as intended by defining the range, accuracy, resolution, and surface area coverage of the sensors. Wearability refers to the system as seen by the user in evaluating its mobility, comfort, and safety. All requirements were developed in reference to the realistic operational environment of the space suit. After an initial evaluation, a discrete sensor architecture was chosen over a sensor mat configuration to allow for movement and greater versatility. Additional advantages to pressure sensing with discrete sensors include simplicity in design architecture and the ability to optimize sensor placement for pressure detection application. Because of these advantages, the requirements were written for a discrete sensor configuration. Appendix C gives justification for each requirement.

This research is directed toward the second specific aim, to quantify and evaluate human-space suit interaction with a pressure sensing tool. Design Requirement 1, “*A pressure sensing tool will achieve both high wearability and high utility in a space suit environment*” is evaluated by using the defined Utility and Wearability requirements.

4.2. Sensor Utility

The following describes the process by which each of the Utility requirements were targeted and evaluated. The major factors considered for ensuring sensor utility were design of the sensor itself, sensor performance when loaded, and system complexity.

4.2.1. Design and Fabrication

Soft hyper-elastic sensors were developed to measure low-pressures applied to the body under the soft goods. The sensors were created in conjunction with researchers at the Wyss Institute for Biologically Inspired Engineering at Harvard (Cambridge, MA). A detailed description of their fabrication may be found in (Park, Chen et al. 2012) but the specific design for the purposes of this project is described herein. The design and fabrication process is highly iterative with the best results achieved using the following method.

The sensors are made in a three step process of casting, bonding, and injection (Park, Chen et al. 2012). Figure 4.1 shows each step in the fabrication process. The sensors are cast from a silicon rubber (EcoFlex0030, Smooth-On, Inc., Easton, PA), making them hyper-elastic and easily conformal to the body. Two plastic molds, shown in Figure 4.2, are 3D printed and the elastomer is poured into the well. One mold is printed with a microfluidic channel positive relief. The molds are placed in a vacuum chamber to remove any gas that may be trapped in the microfluidic channels. The halves are cured at 60 C for 20 minutes, and bonded together. The sensor half without the microfluidic channels will form the base upon which the sensor half with the channel design will be laid. The base is spin-coated with more elastomer and allowed to

Table 4.1A. Detailed Utility design requirements for a pressure sensing capability.
Utility requirements ensure measurements are targeted appropriately for the space suit environment and the system is not overly complex.

Category	Trait	Requirement	Validation
1. Resolution	1.1 Temporal	Response time will be no slower than .25 seconds.	Measure time constant with step function loading profile.
	1.2 Discrimination	Sensors will discriminate pressure changes of at least 1 kPa.	Vary loading profile and compare against output response.
	1.3 Range	Sensors should detect pressures between 5 and 60 kPa	Vary loading profile and compare against output response.
	1.4 Size	Sensors will be no larger than 2x2 cm.	Design to match requirement.
	1.5 Spatial	Sensors should be preferentially placed to cover anticipated “hotspots”. In no case should there be more than a 10cm longitudinal and 6 cm circumferential gap.	Design to match requirement.
2. Accuracy	2.1 Hysteresis	Sensors will not exhibit more than 10% hysteresis over a range of loading profiles.	Vary loading profile and compare against output response.
	2.2 Value	Sensors will not deviate by more than 10% from known pressure.	Vary loading profile and compare against response curve.
	2.3 Drift	Sensors will drift no more than 10% with static loading.	Apply static load and compare against output response.
3. Data Processing	3.1 Real-time	Data output will be displayed within .5 seconds of motion.	Evaluate with load and subsequent data display.
	3.2 Complexity	Data collection software will be able to run on standard laptop computer.	Design to match requirement.
	3.3 Data transfer	Data should be transferred wirelessly or logged from single source.	Design to match requirement.

Table 4.1B. Detailed Wearability design requirements for pressure sensing capability.
Wearability requirements ensure the system is safe and unrestrictive in the space suit environment over a broad range of subjects.

Category	Trait	Requirement	Validation
1. Mobility	1.1 Placement	Sensors and wiring will follow body radii of curvature.	Design to match requirement.
	1.2 Accommodation	Sensors and wiring should accommodate 50% female to 95% male.	Design to match requirement.
	1.3 Integration	Sensors and wiring will be integrated to body garment.	Design to match requirement.
	1.4 Anatomical mapping	Sensor center point will shift no more than 1cm in any direction.	Perform human subject shirt-sleeve range of motion testing.
2. Environment	2.1 Temperature	Sensor readings will change no more than 5% when donned	Perform human subject test.
	2.2 Electrical	Electronics architecture should be robust to mixed gas regimes and pressure.	Space suit design review.
	2.3 Materials	All materials will be safe for human exposure in mixed gas and variable pressure regimes.	Space suit design review.
	2.4 Durability	System performance and components should not break after 50 uses.	Evaluate after each use with visual inspection and data quality.
3. Stand Alone	3.1 Untethered	The pressure sensing system will be self-contained in the garment using onboard data storage and battery power.	Design to match requirement.
	3.2 Power	System will be low power, allowing for at least 3 hours of test time.	Design to match requirement.

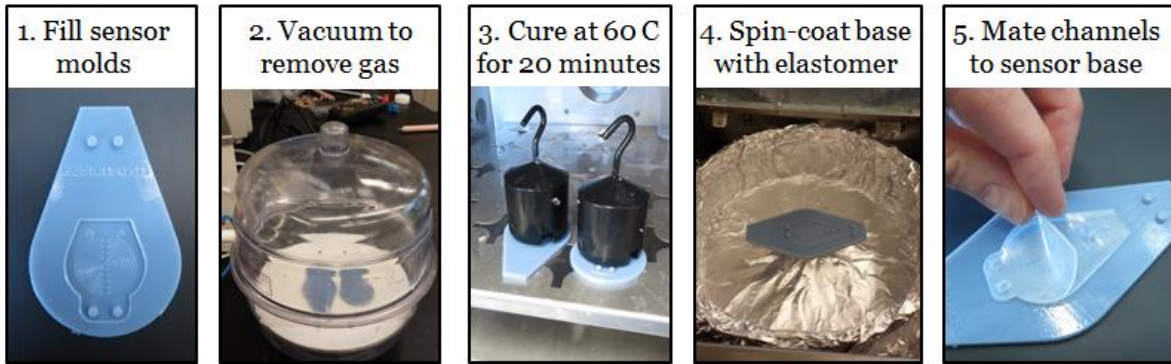


Figure 4.1. Each step in the sensor construction process. First, sensor molds are 3D printed and filled with elastomer. The molds are placed in a vacuum chamber to remove any gas which may be trapped in the microfluidic channels. Next, they are allowed to cure for 20 minutes at 60 C. To mate the sensor halves together, the base without the channel design is spin coated with additional elastomer. The sensor half with the channel design is laid on the base and allowed to cure.

cure for 45 seconds at 60 C to prevent the bonding silicon from wicking into the channels. The second half is laid on top, channel side down, to create the empty sensor. Alignment posts are printed in the mold to ensure proper placement. The sensor is then injected with a highly conductive liquid metal, galinstan (Gallium-Indium Tin eutectic, 14364, Alfa Aesar, Ward Hill, MA). The air inside the empty channel is removed with a syringe and the channel is filled with galinstan using a second syringe. The injection process and a final sensor are shown in Figure 4.3.

Prior to mating the sensors, a flex circuit is sandwiched between the two sensor layers. The flex circuit, shown in Figure 4.4, is a piece of kapton that has been coated with copper, then laser cut and chemically etched with the circuit pattern. Additionally the flex circuit is laser cut with perforations to allow the sensor halves to bond around the flex circuit, increasing durability and preventing the flex circuit from curling up in the construction process, as shown in Figure 4.4 describing the flex circuit performance. Additional flex circuit designs were printed on a slightly stiffer material, to prevent delamination. These designs, however, failed as the sensor bent and flexed with

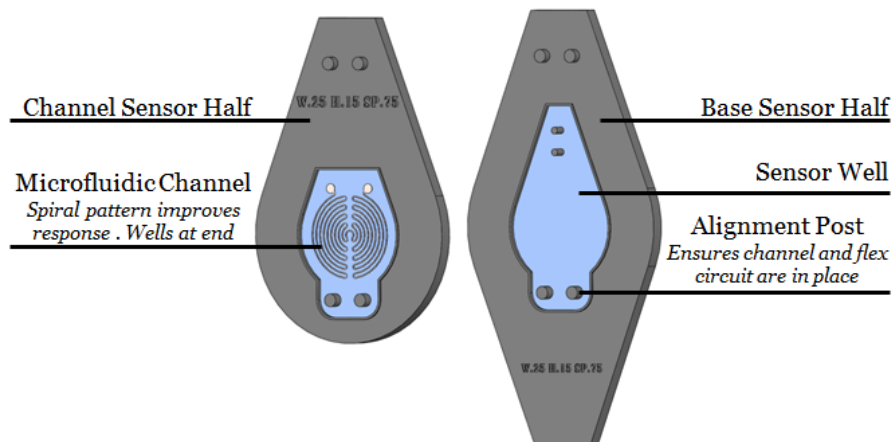


Figure 4.2. Sensor molds components and features. Two sensor halves are 3D printed with a well into which elastomer is poured. The channel half has the positive of the microfluidic channel and sensor wells. The base is printed with alignment posts to ensure proper construction.

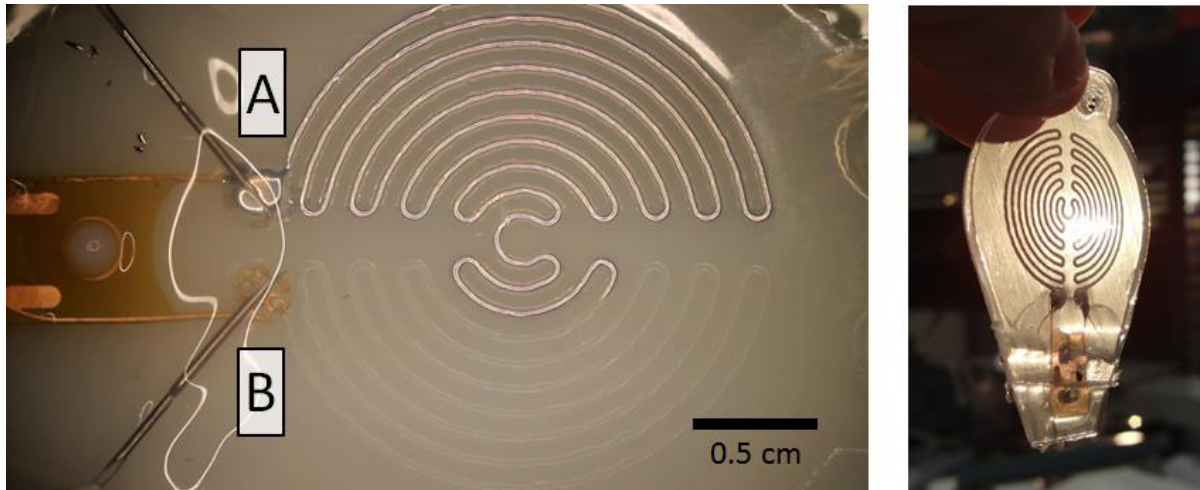


Figure 4.3. Channel filling and completed sensor. Two syringes are used to create a vacuum in the sensor channel from one side B, and to fill it with galinstan, a liquid conductive metal, from the A side. Right, a completed sensor with filled channel and flex circuit.

movement. Additionally, the spacing between the flex circuit pads was increased to prevent sensor failure through the potential leak path between the wells. The flex circuit is also mounted in place using alignment posts. The pads of the flex circuit correspond to wells printed in the microfluidic channel. This completes the connection between the conductive metal and allows wire leads to be soldered onto the sensor at the copper mount.

As normal pressure is applied to the completed sensor, the channel walls deflect. This causes a change in resistance of the galinstan, corresponding to a change in voltage. The response profile is calibrated to correspond to the pressure value. To detect normal pressure and decrease sensitivity to lateral strains, the microfluidic channels is designed as a spiral pattern. Linear patterns are sensitive to detecting strains, in a manner similar to a strain gauge (Park, Majidi et al. 2010) and are therefore avoided for this application. The spiral design adopted for space suit implementation were designed with a 2 cm diameter to satisfy requirement U.1.4 Size. The total sensor diameter is 2.5 cm.

These sensors were designed for the specific application to be used



Figure 4.4. Flex circuit components and improvement features over previous designs. Copper coated kapton is chemically etched (outline in red) to create the circuit pathway from the pad to the mount. Laser cut perforations (outline in blue) allows for better mating between sensor halves and improves durability. Pads were separated to prevent leakage under pressure.

in the space suit. To achieve the range and resolution requirements (requirements U.1.2 Discrimination and U.1.3 Range), an experiment was conducted to optimize channel design to ensure the desired sensitivity. The channel cross section was varied in both width and height, each with the dimensions 150 μm , 250 μm , and 500 μm , creating 9 total sensor channel configurations. These values were chosen based on previous promising sensor designs and the resolution available on the 3D printer. Data from the optimization experiment can be found in Appendix D. It was found that the most sensitive configurations had 150 μm height with 150 μm and 250 μm in width. However, the 150 μm width channel design was abandoned due to the high failure rate during construction caused by elastomer wicking into the channel cross section. Therefore, the final channel design uses 250 μm width by 150 μm height cross section.

4.2.2. Sensor Performance

To characterize the performance of the sensors, they were calibrated to known pressures. The calibration apparatus was purchased commercially from Novel, GmBH (Munich, Germany). It consists of two rigid plates bolted together with an inflatable bladder inside, shown in Figure 4.5. Sensors are placed between the plates under the bladder and air is fed into the system from an air compressor. The bladder's pressure is read from a manometer, while the voltage change of the sensor is recorded. The resolution on the manometer is ± 1 kPa. Sensors were loaded with a constant pressure at 10 kPa increments from 0-60 kPa.

As further discussed in Chapter 6, the sensors and pressure sensing system were used to perform an experiment inside a space suit. The 14 sensors are evaluated here for an assessment of sensor variability and performance. The voltage response of the sensors was fit to an exponential curve corresponding to each pressure increment. The wires and solder connection increase the resistance of the system, altering the voltage output, and therefore affect the calibration curve. The data was zeroed using the initial resistance of the sensor so that a change in sensor output was due to a change in the sensor response



Figure 4.5. Calibration apparatus. Sensors loaded with constant pressure at 10 kPa increments from 0-60 kPa. Pressure measured with manometer with resolution of ± 1 kPa.

with loading, rather than other aspects of the system that could cause artificially high resistance. Figure 4.6 graphically shows the effect of initializing the sensors in this way. The initial resistance was measured for each sensor when possible, and was between 0.9-2.0 Ohms. However, because some sensors failed over the course of human subject testing¹, their initial resistance could not be measured and the average resistance of 1.2 Ohms was used. Five sensors exhibited linear, rather than exponential, responses to increased pressure and were calibrated accordingly. It is not clear why these sensors behaved in this manner, but is likely caused by minute variations in construction such as deformation of the channel walls (Park, Majidi et al. 2010) or delamination of the sensor halves near the sensor wells increasing the size of the reservoir.

Calibration fit varied by sensor. Figure 4.7 shows both the best and worst fit calibration curves with a 95% confidence interval on the fit coefficients up to 75 kPa for both exponential and linear fits. Appendix E shows the remaining calibration curve fits. For both the exponential and linear curve fits, the more sensitive sensors correspond to higher output response. Less sensitive sensors had poorer curve fit since as their profile is extrapolated to larger pressures and the uncertainty increases. All sensors were able to detect pressures within the targeted range of 5-60 kPa, validating the requirement U.1.3 Range was met.

The discrimination, or resolution of pressure/bit output, of each sensor was evaluated to assess requirement U.1.2 Discrimination to achieve 1 kPa. For linear sensors, the resolution is the slope of the calibration curve. Table 4.2 shows the slope coefficient for each linear sensor, all of which satisfy requirement U.1.2 Discrimination over the entire pressure range. For exponentially fit curves, the discrimination, D , is not constant but governed by the equation:

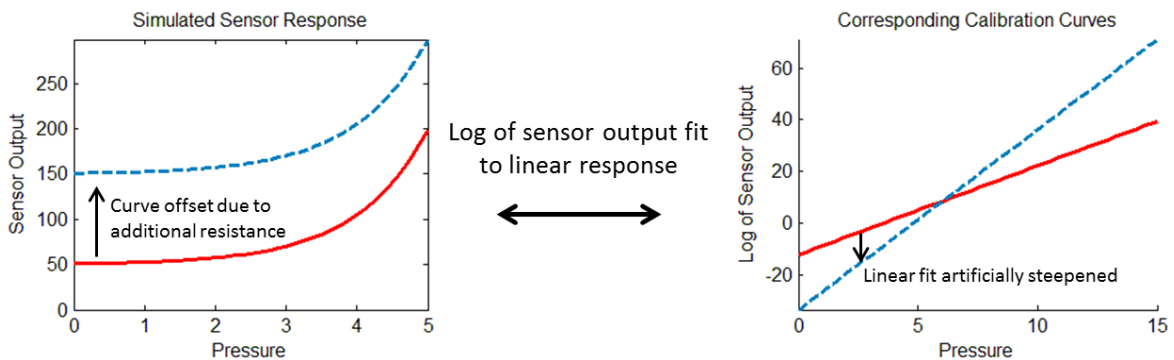


Figure 4.6. Simulated calibration data. The sensor response is exponential to increasing pressure. However, adding resistance to the system with wires and circuit connections increases resistance. This steepens the calibration curve artificially. For this reason, the offset was removed prior to calculating the calibration linear fit.

¹ The experimental protocol was approved by MIT's institutional review board, the approval for which can be found in Appendix J

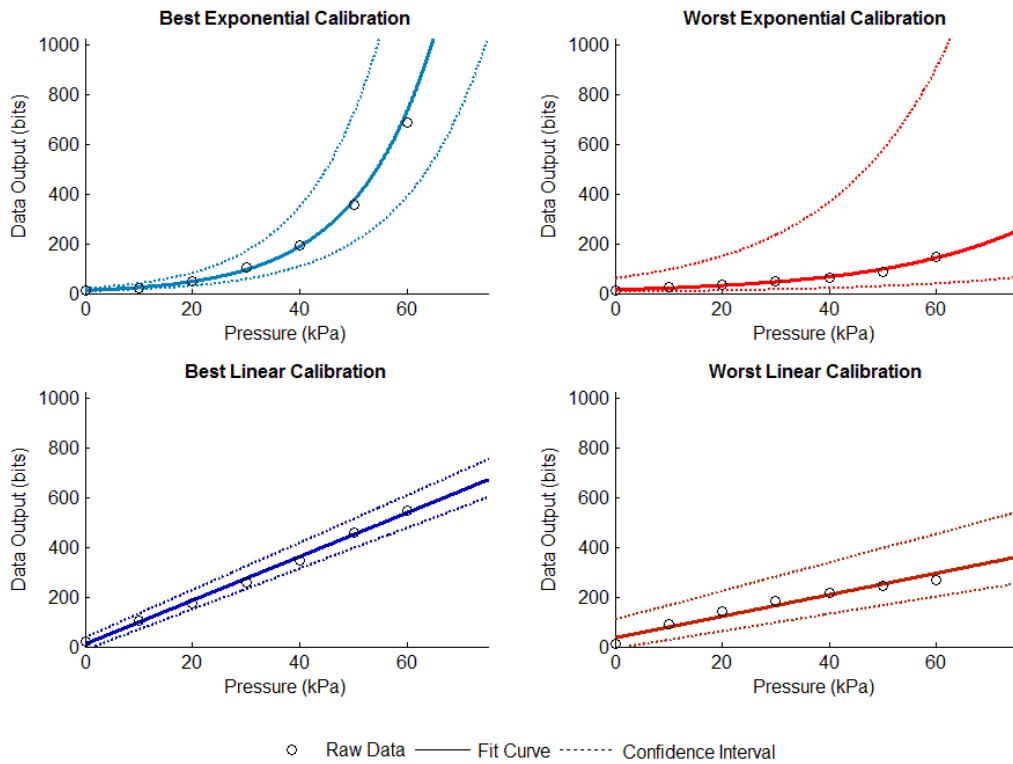


Figure 4.7. Variation on curve fit. The first row shows examples of the best and worst calibration data for the exponentially fit date. The second row shows examples of the best and worst calibration data for linearly fit data. In both types of curve fits, the poorest curve fits are those with less sensitivity, corresponding to a smaller output within the pressure range. As a result, the uncertainty increases with system output.

$$D = \alpha \ln \left(\frac{x+1}{x} \right) \quad (4.1)$$

where α is the coefficient fit to the exponential function and x is the bit output response of the sensor. Derivation of Equation 4.1 is given in Appendix F. Table 4.2 shows the data resolution for each sensor at the high and low end of targeted pressure regime, 5kPa and 60 kPa. Most sensors do not achieve 1 kPa discrimination at 5 kPa of pressure, whereas all sensors have better than 1 kPa discrimination at 60 kPa. Equation 4.1 was rearranged to solve for the pressure at which the discrimination D is 1 kPa. This equation is also derived in Appendix F. This is shown in Table 4.2. This varies for each sensor since it is a function of the calibration curve coefficients. However, because all sensors achieved 1 kPa discrimination, requirement U.1.2 Discrimination is marginally achieved for the system. It is desirable for the sensor to achieve 1 kPa of discrimination throughout the entire pressure sensing regime, which would come with greater sensitivity and uniform sensor construction.

The variability associated with the calibration fit is also associated with an inherent limitation to using hyper-elastic sensors. Although ideal in their sensitivity, ability to morph shape, and conformance to the person's body without artificial measurements, the polymers from which they are made do not behave uniformly with time under

Table 4.2. Discrimination of sensors (marginally satisfying requirement U.1.2 Discrimination) A) The sensors with a linear response achieved the desired resolution over the entire pressure range. B) The exponentially fit sensors did not achieve 1 kPa resolution at the lower end of the sensing region, but all achieved the desired resolution at the higher end of pressure sensing at 60 kPa. C) To determine the cross-over pressure at which the targeted discrimination was achieved, Equation 4.1 was rearranged and the pressures are shown. The values vary based on curve fit coefficients.

Linear Sensors		Exponential Sensors			Pressure for $D = 1\text{ kPa}$	
Sensor	Discrimination	Sensor	D at 5 kPa	D at 60 kPa	Sensor	Pressure
1	0.66 kPa	1	1.8	0.27	1	23 kPa
2	0.23 kPa	2	3.3	0.97	2	60 kPa
3	0.10 kPa	3	2.5	0.5	3	37 kPa
4	0.11 kPa	4	1.4	0.19	4	15 kPa
5	0.47 kPa	5	2.8	0.7	5	47 kPa
		6	0.79	0.02	6	2 kPa
		7	1.2	0.06	7	9 kPa
		8	3.2	0.57	8	43 kPa

pressure. For a constant load, the sensors exhibit a creep over time as the elastic polymers slowly stretch to alleviate internal loading. This is exhibited by the hysteresis seen when the sensors are loaded and then subsequently unloaded, as shown in Figure 4.8. The sensor was transitioned in 10 kPa increments up to 60 kPa and back down to 0 kPa. At each pressure level, the sensor was allowed to equalize for approximately 10 seconds before being slowly brought up to the next increment. The table with Figure 4.8 shows for each level of pressure the bit output read from the sensor and subsequently the change in total pressure read. A clear hysteresis effect can be seen between loading and offloading. Although there is hysteresis in any system where energy is dissipated, the effect is worsened as the energy is allowed to dissipate more freely through the stretching of the polymer chains. In all loading conditions, the loss from hysteresis is greater than 10%, therefore the requirement U.2.1 Hysteresis was not satisfied.

The sensor's creep can be seen by loading the sensors to a known compression. A materials testing machine (5544A, Instron Corporation, Norwood, MA) was used to measure vertical compression distance, resulting load, and corresponding voltage

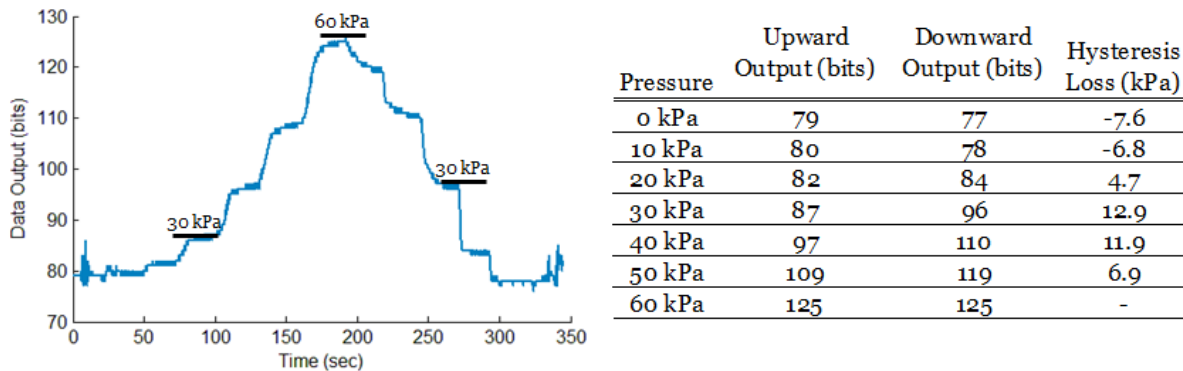


Figure 4.8. Hysteresis effect of loading and unloading (requirement U.2.1 Hysteresis not satisfied). Pressure was applied and released at 10kPa increments to the sensor, up to 60 kPa. The sensor output varied at each pressure level, adding to the ambiguity associated with sensor

output from the sensor. This test setup is shown in Figure 4.9. The upper compression plate was moved in the vertical direction a set distance. The sensor was loaded for 60 seconds before being offloaded for another 60 seconds. The loading profile was repeated four times. The load cell measured force in Newtons, which was converted to pressure by dividing by the loading area, shown on the left vertical axis in red of Figure 4.9. The corresponding output voltage is shown plotted against the right vertical axis in blue. Although the vertical distance of the plate did not change, the pressure on the sensor did, a measure of the creep associated with the sensor's elastomer. The sensor is expanding to alleviate the internal tension, and therefore reducing the load read from the force transducer on the materials testing machine. Similarly, the voltage slowly increases over time. As the sensor expands, the microfluidic channels also expand, increasing resistance and increasing the output voltage. Although in a real world scenario, the load would remain constant (i.e., a weight placed on the sensor would not gain or lose mass), the creep and voltage response is still seen.

Figure 4.10 shows the response when the test set up is modified to apply a constant force (rather than constant compression) and the associated artificial change in pressure. Note that the load in Newtons and pressure as measured by the sensor in kPa are not plotted on the same axis. The sensor was loaded with a constant 6 N for 60 seconds, corresponding to 30 kPa. Over the course of this 60 second period, the sensor drifted by 11%. Although this meets requirement U.2.3 Drift, the effects of drift (and hysteresis) are magnified with increasing pressure. Therefore, this requirement is marginally met, satisfying the condition near the low-end of the pressure region but not at higher pressures.

Due to confounding effects of creep, the time response of the sensors was evaluated when transitioning from loaded to unloaded. The time constant τ was calculated both

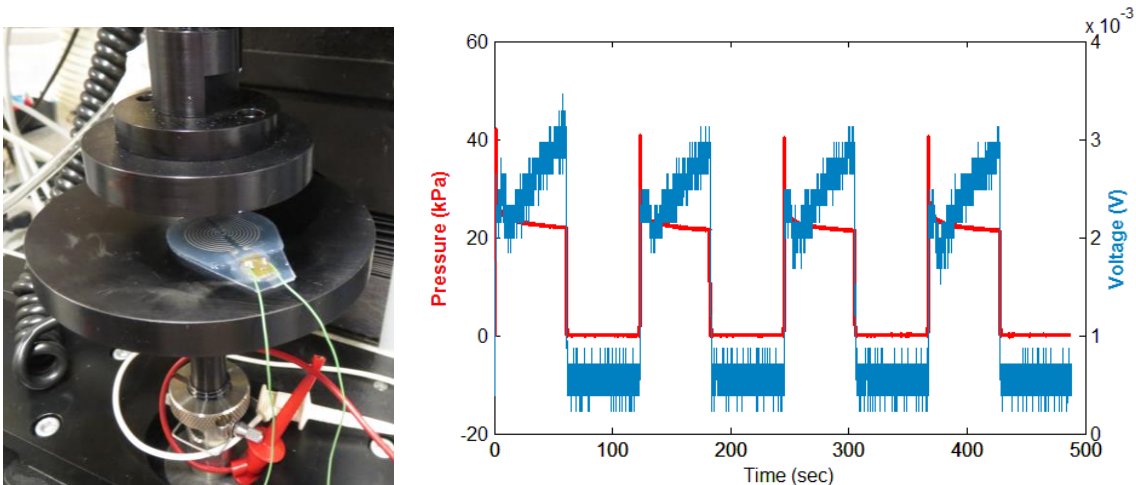


Figure 4.9, Sensor creep demonstrated. *The sensor was tested using the set up shown in Figure A. The top plate was moved to a vertical offset to compress the sensor. The pressure on the sensor and corresponding voltage is shown in Figure B. The pressure is relieved over time due to sensor creep. As a result, the voltage, and therefore pressure, is artificially increased.*

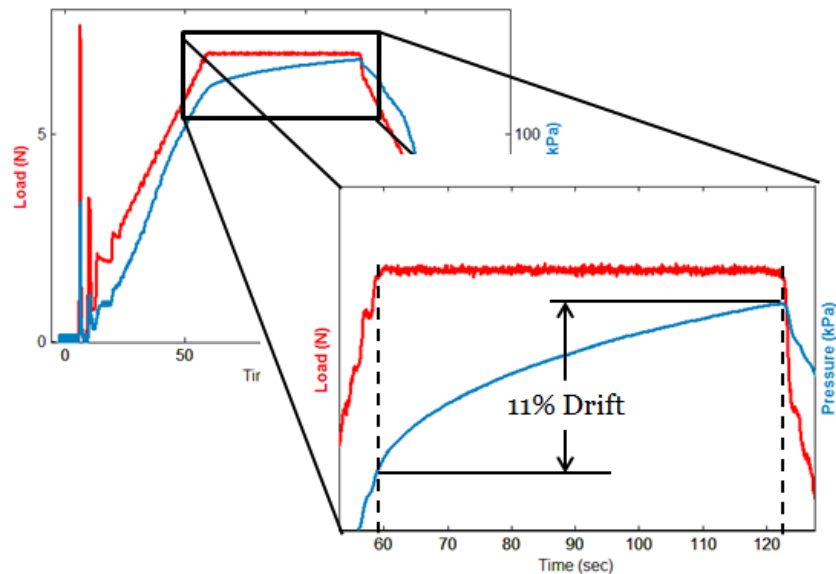


Figure 4.10. Drift associated with a constant load (satisfies requirement U.2.3 Drift). A constant load was applied to the sensor for 60 seconds. At the load pressure of 30 kPa an 11% drift was measured. However, response is dependent on load pressure and increases as pressure for the pressure and the voltage response. The pressure on the sensor after 60 seconds of loading was 22 kPa, or one third of the desired pressure range. When unloaded, the measured pressure time constant was $\tau_p = 0.08$ seconds, indicating a near step function in offloading. The voltage response measured during offloading had a time constant $\tau_v = 0.1$ seconds. This satisfies requirement U.1.1 Time, where the targeted response time was 0.25 seconds.

Although the effects of creep cause erroneous results when loaded statically, this sensor suite was designed for dynamic movement to test the interaction between the person and the space suit during EVA movement. Therefore, their response when loaded dynamically is evaluated to assess requirement U.2.2 Value. The sensors were tested using the Instron test configuration described previously. A constant load rate was used to apply a pressure to the sensor area up to 30 kPa. Figure 4.11 shows the pressure applied to the sensor and the resulting pressure measured by the sensor system. There are several important points to note about this response. The first is that the output from the sensor is very repeatable. The response consistently follows the applied pressure on the loading portion of the profile. The second point to note is that the effects of hysteresis can be seen even in dynamic conditions, but to a much smaller degree. The greatest deviation from the actual pressure occurs during offloading. One limitation to the loading profile was due to the response of the machine's internal feedback loop to maintain a constant load rate. This caused large pressure spikes at the transition from unloaded to loaded, and again to a lesser extent at the turn-around transition at 30 kPa. Very rapid fluctuations in pressure produced a muted response from the sensor, again due to the nature of the elastomer.

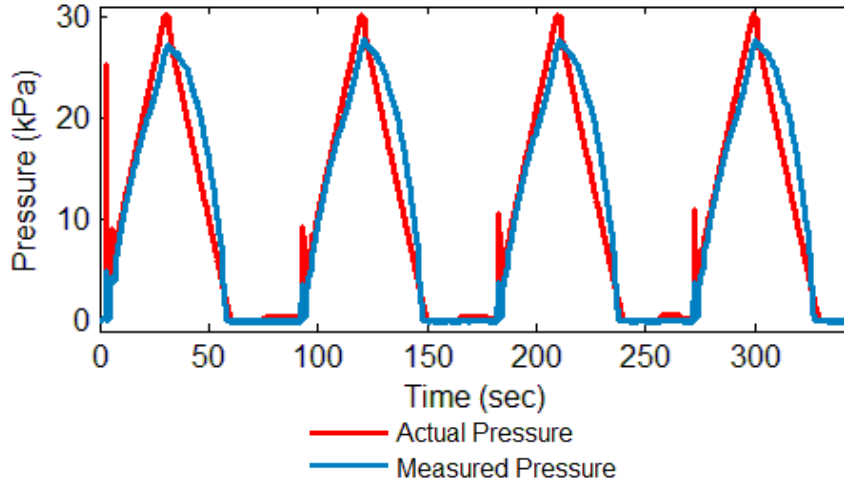


Figure 4.11. Dynamic response of the sensor to known loading. *The system was designed for dynamic movement. When measured at loading speed corresponding to human movement, the sensors track the known pressure profile to a root mean square error of 3 kPa.*

The sensor's accuracy was measured by the root mean square error (RMSE) of the deviation between the actual and measured pressures. The data shown in Figure 4.11 was loaded and unloaded over the course of 30 seconds with RMSE = 2.97 kPa. The load time to produce the dynamic motion was doubled to 60 seconds and halved to 15 seconds in order to evaluate the sensor's response over a broader range of dynamic conditions. The RMSE was 3.76 kPa for 60 second loading step, and the effects of hysteresis are more pronounced. However, it is unlikely a subject would perform a motion that required them to move for 60 seconds. The RMSE was 3.04 kPa for a 15 second loading step. This is much closer to the duration of normal movement. Both the 30 second and 15 second loading condition produced RMSE deviation from a known loading profile of about 3 kPa. The peak loading condition is 30 kPa. The RMSE is a measure of deviation over the entire profile, rather than a constant error. It will be compared to the maximum pressure to assess requirement U.2.2 Accuracy, where the RMSE is approximately 10% of the maximum load. Therefore, the Utility requirement U.2.2 Value was satisfied under dynamic conditions for which the sensory system was designed.

4.2.3. Remaining Utility Requirements

The electronics hardware is described in greater detail in section 4.3.3, but is mentioned here for the discussion of the third group of Utility Requirements, Data Processing. A single Arduino Micro microprocessor (Arduino, Turin, Italy) is used to control and log the output from each sensor, satisfying requirement U.3.3 Data Transfer. The data can also be collected and visualized in real-time in a tethered configuration. A Matlab (Natick, MA) interface allows data collection in real-time and can be run from both standard Macintosh and PC computers, satisfying both requirements U.3.1 Real-Time and U.3.2 Complexity.

The assessment of requirement U.1.5 Spatial is presented in section 4.3.1 where sensor placement is discussed.

4.3. Sensor System Wearability

The following is a review of the design process undertaken to satisfy the mobility requirements for the entire sensor system. The major factors in meeting these objectives are human accommodation, wiring design, and creating an untethered stand-alone, wearable system.

The pressure sensing system has three major components, shown in Figure 4.13: 1) the Base layer, 2) the “Polipo” or octopus in Italian, and 3) the Cover shirt. Each of these components was constructed in conjunction with colleagues at Dainese, SpE (Molvena, Italy). The base layer is a conformal elastic garment worn by the subject. The Polipo is the system of 12 sensors developed for low-pressure sensing under the soft goods in the space suit environment. The sensors are detachable from the base layer, allowing an independent pressure sensing system. The base layer also has a pocket interface over the shoulder to house the high-pressure sensor mat. Finally, the cover shirt slides easily over the sensors to prevent the wires from catching and ensure proper sensor placement. The design and implementation of each component is described in the following sections. All materials and manufacturers used in the construction of the system are found in Appendix G.

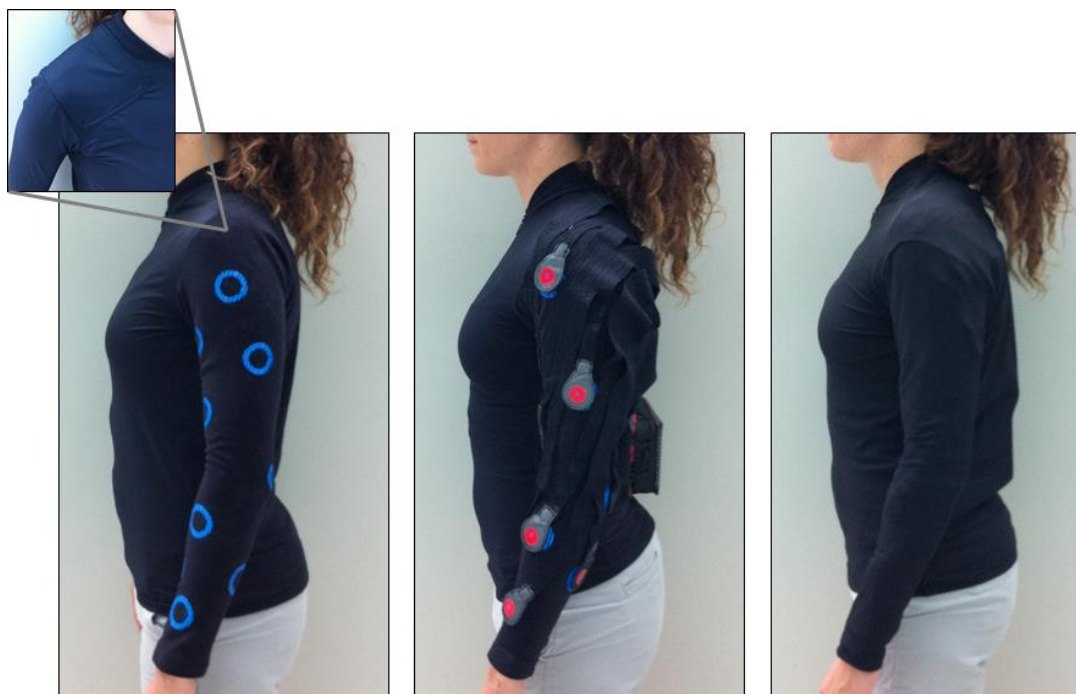


Figure 4.12. Components of the pressure sensing system. A) The base layer garment with sensor target spots. The opposite shoulder has a pocket built to house a high-pressure sensor mat. B) The Polipo sensor system attached to the base layer, C) The cover shirt over the Polipo sensor system to prevent catching of the wires or movement of the sensors.

4.3.1. Human Accommodation

The U.S. astronaut corps is restricted anthropometrically to the population 5th percentile female as the lower bound and 95th percentile male as the upper bound. Although flight hardware must be designed to accommodate the entire astronaut population (NASA 2011), this criteria was prohibitively restrictive for this research project. As noted in Design requirement W.1.2 Accommodation, the objective of this system was to accommodate a 50th percentile female to a 95th percentile male. The U.S. Army Anthropometric Survey (ANSUR (Gordon 1988)) database was used to evaluate how the wire lengths should be properly sized. Several upper body dimensions were collected at the 50th percentile female and 95th percentile levels for each measurement, shown in Table 4.3. The dimensions used were the acromium-radiale length, shoulder-elbow length, the difference between elbow-fingertip length and wrist-fingertip length, and finally, the wrist-wall length. The percent increase in length between male and female data points was calculated to be 19% for each dimension. This increase in length was taken as the minimum elasticity or accommodation length needed for the wiring.

Next, approximate sensor placement was determined. The functional upper limit to the number of sensors possible was 12 sensors based on the electronics architecture (described in the following section). Discussions with subject matter experts identified the anticipated “hot spots” astronauts were likely to encounter while working in the space suit. This determined the initial placement of the first eight sensors on the inner wrist, back of the elbow, front of the elbow near the crease (one above and one below), the triceps muscle near the armpit, outside of the biceps muscle near the upper arm bearing of the space suit, and on the top of the shoulder. The remaining four sensors were placed to achieve uniform spatial distribution over the rest of the arm to meet requirement U.1.5 Spatial. A schematic of the designed sensor location is seen in Figure 4.13, as well as a brief summary of the entire construction process.

4.3.2. Wiring mobility

Wiring and data transfer can often be the limiting factor in wearable electronic systems. Therefore many concept prototypes were constructed and iterated upon to achieve the optimal solution for this system. The final design solution is presented herein.

Table 4.3. ANSUR database body dimensions for 50th percentile female and 95th percentile male. *Body dimensions were used to determine the percent change in length required for the wiring to accommodate the target population.*

Dimension	50% Female (cm)	95% Male (cm)	Change in Length
Acromium-Radiale	300	370	19%
Shoulder-Elbow	335	399	19%
Elbow-Wrist	274	327	19%
Wrist-Wall	619	738	19%

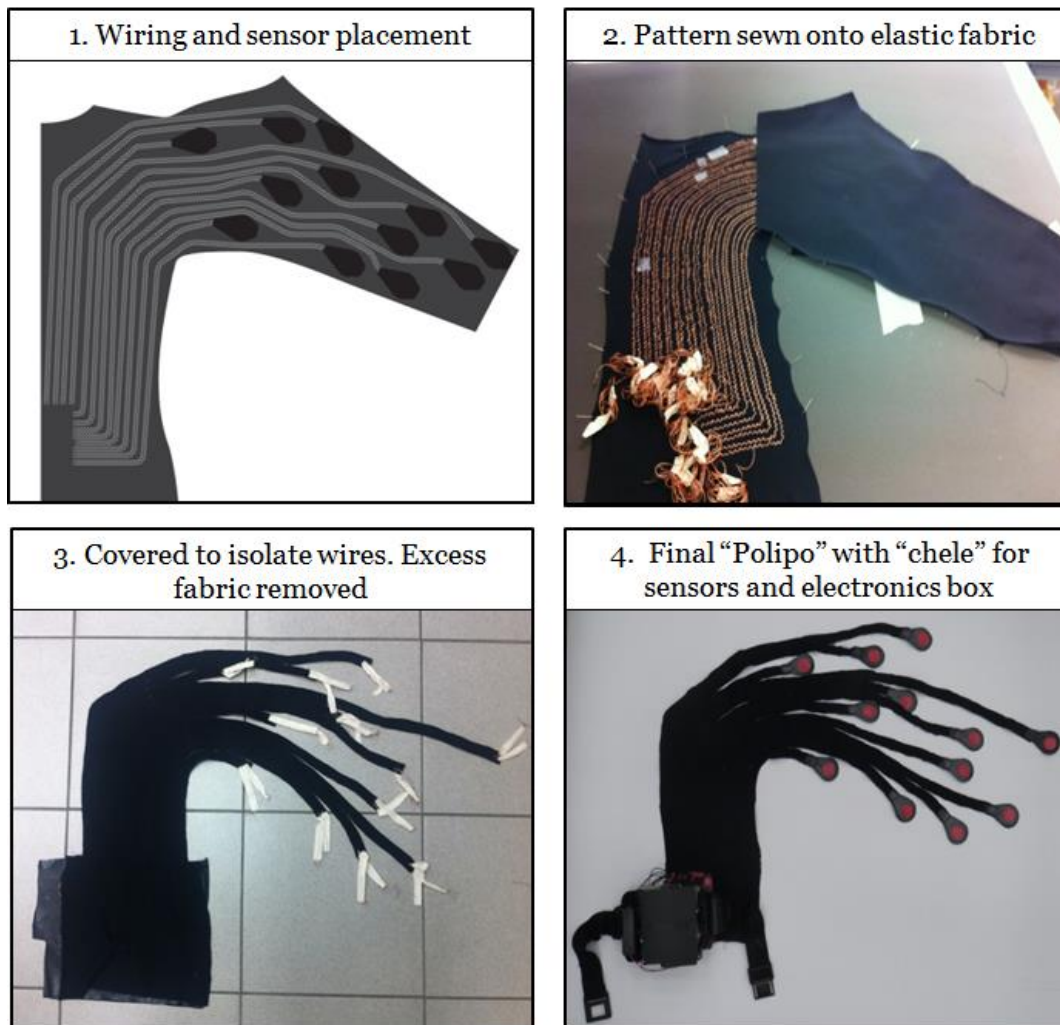


Figure 4.13. Wiring design and construction of the Polipo. 1) Initial design of the sensor placement and wiring. 2) Wires were sewn in zig-zag pattern onto an elastic fabric backed by a water soluble stiffener. The wiring was then covered in a glue-backed elastic fabric and heat pressed to isolate them and prevent a short circuit. 3) Excess fabric is removed and relief slits are cut to allow for greater mobility. 4) The “chele” to house the sensors are numbered and added. Electrical connections are fed from each sensor into the electronics box to complete the design.

One of the greatest challenges to designing the Polipo was developing a system of wiring that could accommodate the population and range of motion requirements. Selecting the correct wiring scheme was a trade-off between mobility (i.e., flexibility), resistance (i.e., wire diameter), and durability (i.e., material properties). Many wires and conductive threads were evaluated, and the final solution implements seven strands of copper wrapped polyester (Tecnospir, 24066 Pedrengo, Italy). The copper gives the wire a low resistance of 0.6 ohms/meter, while the polyester core allows it to be very durable and flexible. The wire’s primary limitations, being inelastic and not electrically isolated with a protective coating, were resolved in the fabrication technique of the Polipo.

The wire was sewn in a zig-zag pattern on an elastic material called *Carrezza* to achieve elasticity. A special sewing machine was used to create the design since the diameter of the wire would not allow it to be stitched in a normal machine. Additionally, the *Carezza* was so soft and pliable it could not maintain its shape during sewing. A water soluble backing was used over the *Carezza* to provide stiffness, and later dissolved away. The two wires of the circuit were sewn next to each other, each with a 0.5 cm zig-zag and 0.2 cm spacing, giving a total 1.5cm width for each sensor. To isolate the wires, an additional layer of elastic fabric with a glue backing called *Tess 0917 Charmeus + Web 35* was heat pressed to the top. This prevents short circuits and allows each sensor's wires to be cut away from the others, increasing mobility and allowing for easy sensor placement. Excess fabric was removed and strain relief slits were cut, giving the Polipo near shirt-sleeve mobility.

Wiring constructed using this method had a measured strain of 20%. This met the previously calculated desirable strain of 19% for population accommodation. However, the wires would also need to accommodate movement of the wearer. Three subjects within the target population were measured in a resting posture, arm fully abducted, and arm fully extended in front of the body to determine the additional change in length needed to accommodate full range of motion. Subjects needed between 10-15% additional wire lengths to accommodate movement. This was added to the wiring design to satisfy requirement W.1.2 Accommodation.

The wire patterning was based on sensor placement and body joint axes of rotation. Placing the wiring along the neutral axis is desirable because it minimizes the stretch required to accommodate movement (i.e., along the side of the arm rather than around the back of the elbow). As previously described, the approximate sensor locations had been determined. Because each set of wires required 1.5 cm width path along the arm, the wire's paths were mapped out virtually prior to construction and printed using a pattern plotter to guide fabrication. In this way, wiring pathways were directed along the neutral axis of the arm where possible, with the remaining wires running along the arm between sensors. This satisfies requirement W.1.1 Placement.

To house the sensors themselves, a “chele”, or claw in Italian, was attached at the base of the wires for sensor attachment. The final chele design is seen in Figure 4.14. Initial prototypes revealed it was important to have access to the sensors should they need to be



Figure 4.14. Components of the Chele. A) Open view of the chele with bare wires B) Sensors are soldered into place and wires are fixed and isolated, C) Final configuration with sensor integrated.

replaced, repaired, or the design improved. Additionally, because the sensors are hyper-elastic, there may be an ambiguity between strain forces and normal pressures on the sensor, leading to erroneous voltage readings. Any strain seen in the fabric upon which the sensor is mounted must not be transferred to the sensor itself. Finally, the sensor's housing must not reduce sensitivity, since the primary function of the sensors is for low-end pressure detection.

The designed chele solution is a sensor bed made from inelastic fabric called *Textile 3 Storm 3 Layers* that is able to be opened. The sensor rests in the chele, but it not directly attached to it. This allows the sensor to be removed and does not allow any strain to be transferred to the sensor. The chele closes with a thin layer of Velcro® laser cut to match the shape of the housing and sewn around the perimeter so as not to interfere with the sensor itself. At the base, near the insertion points for the wire, the two wires are isolated with 1.2mm shrink tubing and permanently fixed into position with hot glue. As the wires stretch with movement, the ends of the wires are fixed into place, preventing the wiring from tearing away from the flex circuit. The sensors are then soldered into place. The top side of the chele has a number heat pressed onto it, corresponding to the sensor number.

Finally, the Polipo is integrated to the base layer using small strips of Velcro® sewn to the back side of the system, satisfying requirement W.1.3 Integration. A list of all materials used in the Polipo, their manufacturers, and their primary characteristics can be found in Appendix G.

Although a great deal of effort was put into selecting and designing the best wiring system, ultimately it remained the greatest limitation in evaluating requirement W.2.4 Durability. The wires were covered with a glue-backed fabric to isolate each one. However, over time as the system flexes, stretches, and folds, the fabric can become delaminated over the wiring. With each movement, friction on the wire's surface can degrade the copper strands. This effect can be seen in Figure 4.15. Although low in resistance, copper does not perform well under repeated stress. The failure rate of the wiring varied, but as each strand within the wire broke, the overall resistance of the wires increased. Additionally, broken strands came in and out of contact with one another as the subject moved, causing the data to jump between high and low voltage values, making it unusable. This is discussed in greater detail in Chapter 5 in reference to the human subject experiment. Requirement W.2.4

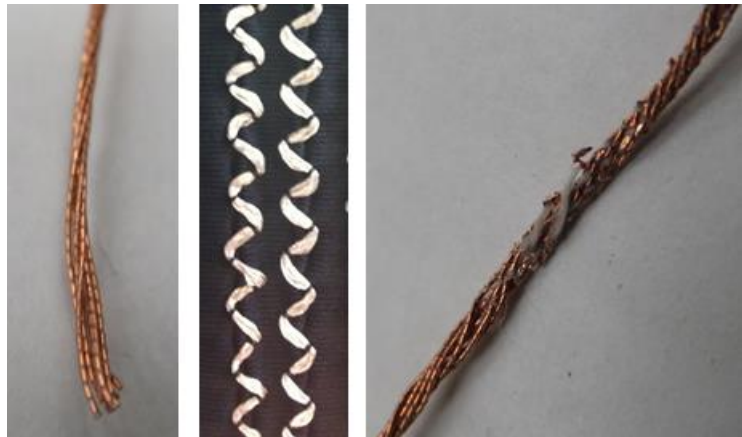


Figure 4.15. Wiring, implementation, and wear. A) Wires are combination of 7 strands of copper wrapped polyester. B) Flexible wires sewn in pairs in a zig-zag pattern to allow additional stretch. C) Over time, friction causes the strands to break, causing slow, steady deterioration.

Durability states the system should function for 50 uses. The system was used outside the space suit in fit trials, sensor testing, and data demonstrations. The system was used inside a space suit for data collection trials in the laboratory vacuum chamber with a space suit arm, experimental design evaluation on the same vacuum chamber, and in 4 long duration (more than 2 hours each) full space suit experiments. This amounts to approximately 40-50 uses. Currently, 10 of the 12 circuits are now unusable due to wiring failure. One set of wires became inoperable in as few as an estimated 30 uses. There was a marked increase in wire deterioration after the space suit experiments due to the length of the tests and large number of movements performed by the subjects. Therefore, Requirement W.2.3 was marginally met since the upper limit on durability has not been reached for some sensors.

4.3.3. Electronics and Data Transfer

To satisfy requirements W.3.1 Untethered and W.3.2 Power, the electronics architecture was created to ensure the system would be low power and would log data onboard. A custom circuit board was printed in collaboration with researchers at the Wyss Institute for Biologically Inspired Engineering at Harvard (Boston, MA). The board, electronics housing, and wiring input into the electronics are shown in Figure 4.16. The system uses a constant current configuration. Changes in resistance of the sensor are measured as changes relative to the reference voltage. The signal is magnified, allowing even finer pressure detection than was previously possible. The microprocessor used to control the



Figure 4.16. Electronics housing and configuration. A) The deformable electronics box with sensor wiring, B) The transition from the elastic wires to the input into the electronics boxes are labeled by sensor. C) The electronics board was custom designed with 12 sensor inputs collected with an Arduino Micro and stored on a micro SD card. D) The smaller profile electronics box and battery mount. This is the configuration used for human-space suit testing.

system and log the data is mounted onto the board. The analog voltage is read by an Arduino Mirco microprocessor (Turin, Italy), which collects up to 12 analog signals at once. The system can be operated in two modes: tethered and data logging. In tethered mode, the system is powered and data is transferred over USB directly to computer. The data is collected and visualized in real-time with Matlab (Natick, MA). In the data logging configuration, data is stored onto an SD card, up to 2GB. The SD card interface is built into the custom electronics board. The schematic of the custom circuit board is found in Appendix K.

Each sensor is run in at 0.5 mA, and with the microprocessor and data logging, the entire system runs at 100mA. To satisfy the power requirement W.3.2 Power, an alkaline 9 Volt battery was chosen. The Arduino Micro requires a minimum input of 5V. The excess voltage is down regulated, making the 9V battery a potentially inefficient choice. However, its small profile, ease of availability, and high safety made it an appealing choice. An experiment was run to determine the upper limit of available testing time. All sensors were logging data onboard the SD card. Data began dropping after 4 hours and 30 minutes. Therefore this electronics configuration satisfied the requirement W.3.2 Power.

All of the electronics for the Polipo are housed in an electronics box located at the base of the back. At the point where the wiring enters the box, the sensors are numbered for troubleshooting. Two boxes to house the electronics are used, both shown in Figure 4.16. The first is a modified case used at Dainese for their D-Air project. This box is made of thermoformed plastic made by injection molding. The box is designed for the curvature of the lower back and is 12x10x4 cm in each length, width, and height respectively. It has an elastic belt which clips in the front of the subject's waist to hold it securely in place. The second box design is multi-layered foam to ensure comfort against the user's body and prevent hard contact points. It uses four layers of foam with different thicknesses and densities, sandwiched between three layers of plexiglass to provide structural support. The box gives with loading, without allowing the hardware to be compressed. The electronics hardware is mounted on a removable plexiglass base. The first electronics box configuration was used for human subject testing. Future iterations of each box type may decrease the overall size of associated hardware.

4.3.4. *Garment Design*

The base layer shirt was also designed specifically for our space suit pressure sensor system. It comes in two sizes based on standard patterns used at Dainese (male small (to accommodate male and female subjects) and male large). The garment, seen in Figure 4.17, is sewn from a bi-directional elastic fabric called *Velentino Bi-elastico* that is highly sensitive to the link side of Velcro®. This material allows for secure and easy integration of the Polipo. The left sleeve and back panel of the shirt are cut from one unique piece of fabric creating a seamless garment. On the sleeve, sensor placement is directed with a numbered "target" to ensure proper sensor placement. The targets were heat pressed onto the elastic fabric and are segmented vertically to allow for elastic strain relief as subjects move. To prevent the sensors from shifting over the body with movement, silicone backing is placed on the skin-side of the target. The material around the sensors stretches to accommodate movement, while the sensors themselves do not

shift. Additionally, a silicon strip is placed at the wrist to prevent the sleeve from shrinking longitudinally up the arm. Mobility tests on nine subjects within the target population validated that requirement W.1.4 Anatomical mapping was achieved after adjusting sensor placement. Subjects were asked to move through their full range of motion and compare mobility to their opposite arm, achieving full range of motion.

Additional features of the base layer include front zip entry, high collar for easy integration of future injury padding systems, a soft second fabric called *Carezza* making up the rest of the garment to allow for greater breathability.

The final Polipo system worn on the body is shown in Figure 4.18. The last piece of the system is a cover layer worn to hold the wires close to the body to prevent the wires or hardware from catching and prevent shifting of the sensors.

4.3.5. Novel™ Sensor Integration

The Polipo sensor system is used to measure low-pressures against the body. To measure high-pressures against the body a commercially available pressure sensor from Novel, GmbH (Munich, Germany), was selected. The advantage to purchasing a sensor system is that it is well characterized and reduces developmental time. However, the sensors are prohibitively expensive and are not ideal for high mobility applications. The Pliance S2073 sensor mat was modified to have 8x16 sensors. The Pliance sensors are a segmented grid of sensors that changes capacitance with normal pressure. The S2073 has a pressure range of 20-600kPa. Each of the 128 sensors is 1.4cm, and the sensor pad covers the clavicle, shoulder, and acromion. The sensor is set up in the I-Configuration, meaning the tail of the electronics travels down the subject's back, where it connects to the electronics specific to the Novel system.

A modified pocket was constructed to house the Novel sensor. The pocket has a one-way insertion flap that allows the sensor to easily slip inside, but not to then slide out again. Near the neck, an additional neoprene comfort strip has been added. The sensor is able to bend well in one dimension, but not bi-directionally. As a subject performs a shoulder abduction, the sensor has difficulty flexing with the additional dimension of curvature. This causes the sensor to shift up on the person's body and slip uncomfortably into the neck. The neoprene and placement against the body with the base layer prevents the sensor from shifting and ensures subject comfort.

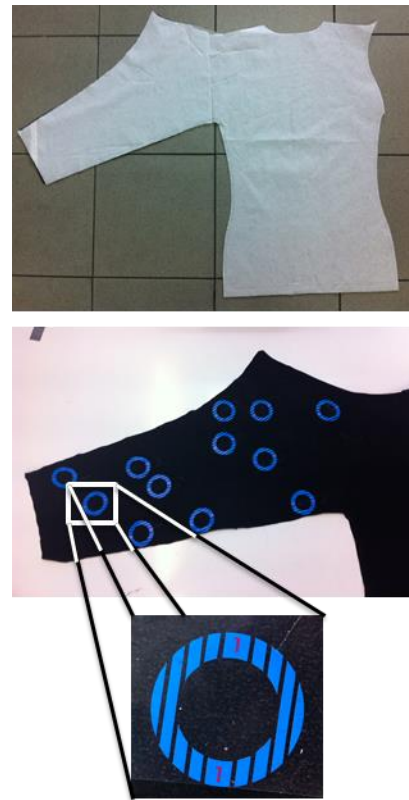


Figure 4.17. Design and fabrication of the base layer garment. A) A seamless pattern design allows full movement. B) Sensor “targets” were heat pressed to the base layer to ensure proper sensor placement. The targets are numbered and segmented for strain relief.

4.3.6. Environment

Subject safety is the most important requirement for wearable electronics. The harsh nature of the testing environment inside the space suit posed additional concerns. The space suit is a pressurized, confined environment, potentially using a mixed gas atmosphere. This poses problems for materials off-gassing and flammability. Also, the subject is confined to the space suit and cannot be removed easily in an emergency situation. The cooling system of the liquid cooling garment uses water to maintain body temperature. Potential leaks, along with additional moisture accumulation through sweat and respiration increase concern for electrical shock and battery hazards.



Figure 4.18. Final design of the Polipo pressure sensing system worn on the body. *An additional layer (not shown) is worn over the system to prevent the wires from catching or sensors moving.*

Before the human subject experiment, a full review was conducted in conjunction with engineers and managers at NASA Johnson Space Center. A full hazard analysis and list of materials used in the sensor system was compiled. The details of each potential hazard that was analyzed can be found in Appendix H. The hazards analyzed were 1. Subject overheating, 2. General personnel injury, 3. Electrical shock, 4. Battery failure, 5. Subject-borne bulk, 6. Hammering, and 7. Loss of habitable environment. All potential hazards were mitigated to a NASA defined risk assessment code of 4 or higher, where each risk is considered “Acceptable with controls”, satisfying requirements W.2.2 Electrical and W.2.3 Materials.

Finally, a test was performed to satisfy requirement W.2.1 Temperature. A subject wore the system while performing practice EVA motions inside a space suit arm pressurized using a vacuum chamber. No deviations in baseline readings beyond normal fluctuation were measured, indicating body temperatures did not affect readings.

4.4. Discussion

The wearable Polipo pressure sensing system was designed for the environment of the space suit, which imposes extreme conditions for implementing wearable electronics. The sensor system measures the pressure between a person’s body and the space suit, for the first time, and was evaluated against requirements, establishing its utility in sensing resolution, accuracy, and with minimal system complexity. It was also designed to be worn for multiple subjects requiring high mobility, safety in the environment in which it’s used, and to be a stand-alone system.

The requirements and the Polipo's success/failure at meeting the requirements is reviewed in Table 4.4 A&B. The Polipo system meets nearly all of the Utility design requirements. Its resolution allows for pressure detection in the anticipated range over the desired area of the body. It responds temporally in near real-time with movement. Sensor discrimination varies by sensor based on its sensitivity measured in calibration. All sensors achieved pressure resolution of 1 kPa within, but not throughout, the targeted pressure sensing range.

The sensors are accurate when used under intended dynamic conditions, but are limited in their utility under static loading. As shown, this is due to creep as energy dissipates. As a result, the sensors exhibit hysteresis as well as drift at higher pressures. This effect is not as pronounced at lower pressures. However, when the sensors are loaded dynamically, their response is greatly improved. The range under which the sensor response is accurate corresponds to the duration of normal movement. The effect of the elastomer can be thought of as a dashpot in a mechanical system model. With rapid fluctuation the response is dampened by the elastomer. However, with constant load, the elastomer will slowly reach a steady state response of minimum energy. Within the velocities of normal human movement, the response can be calibrated to correspond to the actual load. Future work includes modeling the sensor's response to pressure to improve channel designs and accommodate a broader range of responses. Initial work in collaboration with researchers at the Wyss Institute has evaluated the deformation under load using finite element analysis. The Polipo also satisfied each wearability requirement. The system accommodates a broad range of people with shirt-sleeve motion. It is conformal on the body and can be transferred to different subjects easily as a stand-alone system. All components were evaluated for the safety of the user in the space suit environment and all electrical, material, and battery hazards were minimized. The primary wearability limitation is the durability of the system. With the wires and materials available, the wiring chosen was the best achievable design. Over time, however, the integrity of the wires deteriorates. Durability would have likely improved if the wires had been re-heat pressed after each use. In future versions, the wires could be implemented in a different manner by using another material with less friction to isolate the wires, such as an elastomer, to increase durability. A better wiring solution with the same flexibility and low resistance but without the fracture characteristics of copper may be sought. To the author's knowledge, however, this wire still offers the best solution for this sensor system and the most promising future iteration would be to improve implementation, rather than changing the wire itself. The current system's durability is acceptable for a baseline from which to iterate on design and, therefore, it is desirable to improve the system performance on this metric.

Finally, the Polipo achieved all requirements for data processing, power, and electronics architecture. The system was very versatile in that it could be worn in a tethered configuration for visualizing data in real-time, or in a stand-alone configuration using onboard power and data storage. The electronics board has the capacity to transmit data over Bluetooth, but this feature has not been evaluated. For space suit testing, transmitting data wirelessly could interfere with communication systems. Additionally, if used in the neutral buoyancy lab, data transmission in this way is impossible.

Table 4.4A. Detailed Utility design requirements for a pressure sensing capability. *Utility requirements ensure measurements are targeted appropriately for the space suit environment and the system is not overly complex.*

Category	Trait	Requirement	Validation
1. Resolution	1.1 Temporal	Response time will be no slower than .25 seconds.	Measure time constant with step function loading profile.
	1.2 Discrimination	Sensors will discriminate pressure changes of at least 1 kPa.	Vary loading profile and compare against output response.
	1.3 Range	Sensors should detect pressures between 5 and 60 kPa	Vary loading profile and compare against output response.
	1.4 Size	Sensors will be no larger than 2x2 cm.	Design to match requirement.
	1.5 Spatial	Sensors should be preferentially placed to cover anticipated "hot spots". In no case should there be more than a 10cm longitudinal and 6 cm circumferential gap.	Design to match requirement.
2. Accuracy	2.1 Hysteresis	Sensors will not exhibit more than 10% hysteresis over a range of loading profiles.	Vary loading profile and compare against output response.
	2.2 Value	Sensors will not deviate by more than 10% from known pressure.	Vary loading profile and compare against response curve.
	2.3 Drift	Sensors will drift no more than 10% with static loading.	Apply static load and compare against output response.
3. Data Processing	3.1 Real-time	Data output will be displayed within .5 seconds of motion.	Evaluate with load and subsequent data display.
	3.2 Complexity	Data collection software will be able to run on standard laptop computer.	Design to match requirement.
	3.3 Data transfer	Data should be transferred wirelessly or logged from single source.	Design to match requirement.

Table 4.4B. Detailed Wearability design requirements for pressure sensing capability. *Wearability requirements ensure the system is safe and unrestrictive in the space suit environment.*

Category	Trait	Requirement	Validation
1. Mobility	1.1 Placement	Sensors and wiring will follow body radii of curvature.	Design to match requirement.
	1.2 Accommodation	Sensors and wiring should accommodate 50% female to 95% male.	Design to match requirement.
	1.3 Integration	Sensors and wiring will be integrated to body garment.	Design to match requirement.
	1.4 Anatomical mapping	Sensor center point will shift no more than 1cm in any direction.	Perform human subject shirt-sleeve range of motion testing.
2. Environment	2.1 Temperature	Sensor readings will change no more than 5% when donned	Perform human subject test.
	2.2 Electrical	Electronics architecture should be robust to mixed gas regimes and pressure.	Space suit design review.
	2.3 Materials	All materials will be safe for human exposure in mixed gas and variable pressure regimes.	Space suit design review.
	2.4 Durability	System performance and components should not break after 50 uses.	Evaluate after each use with visual inspection and data quality.
3. Stand Alone	3.1 Untethered	The pressure sensing system will be self-contained in the garment using onboard data storage and battery power.	Design to match requirement.
	3.2 Power	System will be low power, allowing for at least 3 hours of test time.	Design to match requirement.

Therefore, onboard data logging was the most appealing option to develop, and was achieved.

Additional design factors beyond the requirements should also be considered. The solder joint or connection between the sensor and wiring should be improved. The flex circuit is a great solution since it can be built directly into the sensor. However, the solder joint became a weak point and broke frequently under use. In these instances, the sensor had to either be replaced or reconnected and the data was lost for the duration of the experiment. Potential solutions include embedding wires into sensor channels. Initial iterations of these concepts had mixed results, but is a promising area of development. One of the most important improvements to sensor design is to improve consistency in manufacturing. Building each sensor is a highly skilled time intensive process. Currently, the sensors can only be constructed two at a time, with each sensor taking approximately an hour and a half. Even at this rate, approximately 50% of sensors fail in the construction process, whether that be from the channel walls closing off, poor mating of the sensor halves, misalignment, or flex circuit delamination. Finally, increasing the initial resistance of the sensor would improve the resolution of data the sensor is able to collect.

After using the sensors for a human subject experiment, it became clear that multiple versions of the Polipo would be useful to characterize pressures over different areas of the body or to increase sensor density over a particularly targeted area. To that effect, sensor size could be changed to cover larger or smaller areas. The electronics architecture was sufficient for the purpose of this work, however if future iterations use more than 12 sensors, additional microprocessors must be added to consolidate and store the data from multiple sources. As with this version, future development should be mindful of the operational environment and remain a standalone system with limited electrical, material, and battery hazards.

4.5. Conclusions

The novel Polipo low-pressure sensing system for extreme environments achieved here has many advantages. With the Polipo human-suit interaction can be measured for the first time through dynamic movement. It can accurately measure low-pressures against the body over underneath the soft-goods. The system of 12 sensors is transferrable between many different people, creating an independent stand-alone pressure-sensing system. Sensors can easily be changed to allow for improved designs or to accommodate different target pressures. The wiring was intentionally designed to achieve the best trade-off between flexibility, resistance, and stretch ability. The system achieves near shirt-sleeve mobility as sensors are moved to accommodate users. It can also be used in conjunction with a high-pressure sensing mat placed over the shoulder to measure loading between the person and HUT. The electronics architecture allows for low power onboard or real-time data collection. The entire system has been designed with extreme environments in mind, where considerations of shock, battery hazards, and material properties in mixed gas environments were minimized to ensure user safety. Finally, it has a cover shirt to slide easily over the system and prevent catching and ensure proper placement. Nearly all requirements were met and those which were not were evaluated

for extent of their impact on the system performance. Therefore, this work confirms Design Requirement 1 “*A pressure sensing tool will achieve both high wearability and high utility in a space suit environment*”. This system could easily be extrapolated to other environments where biomechanics and comfort under load needs to be evaluated, for example soldier pack accommodation or wearable protective devices for the elderly where discomfort substantially decreases compliance.

The Polipo system in its described configuration was used in a human subject experiment inside the space suit, as will be described in Chapter 5. These experiments validated the system’s performance in the space suit environment and confirmed the conclusions reached after the assessment of the requirements presented here.

The primary contributions of this work are to:

- 1) Establish baseline requirements for in-suit sensing and wearable electronics.
- 2) Develop pressure sensors and evaluate their performance for human movement applications.
- 3) Develop a wearable, stand-alone pressure-sensing system to be used for a large group of subjects in harsh working environments.
- 4) Create a system that is specifically targeted to provide quantitative information about human-space suit interaction not previously possible.

The Polipo system as designed overcomes the issues associated with wearable electronics in that it allows for high mobility at low-pressure with less encumbrance from hardware and wired data transfer (Cork 2007, Witt and Jones 2007, Brimacombe, D. Wilson et al. 2009). It builds upon previous sensor designs (Park, Majidi et al. 2010, Park, Chen et al. 2012) to measure normal pressures targeted to the 5-60 kPa range through dynamic motion. In-suit sensing concepts have focused on traditional physiologic measures (Carr 2000, Dismukes 2002, Dismukes 2002, Catrysse 2004, Tang 2007) or display and control information (Rochlis 2000, Graziosi 2005, van Erp 2005, Graziosi 2006). The Polipo builds from previous in-suit wearable electronics, but expands upon it to establish design requirements and a precedent for implementation. Future iterations of the pressure sensing system could utilize work done on distributed computing and data collection in a space suit environment to allow for sensor coverage over the entire body (Carr 2002, Simon 2013, Taj-Eldin 2013). The results presented in this chapter demonstrates the Polipo’s success in meeting its targeted design. The following chapter demonstrates its performance in the pressurized suit environment and its utility to elucidate human-space suit interaction.

5. PRESSURE INTERFACE EXPERIMENT

The second specific aim of this work is to quantify and evaluate human-space suit interaction to develop an understanding of how the person moves with the space suit during normal EVA motions. Results may be used to assess and mitigate injury as well as the biomechanics of suited movement and space suit performance. Two pressure sensing tools, focusing on arm and shoulders motions under different loading regimes, were used to quantify and evaluate human-space suit interaction. Additionally, inertial measurement units (IMUs) were placed internal and external to the space suit arm to assess the biomechanics of movement. The custom and commercially produced sensors were incorporated into a modified athletic garment described in Chapter 4. The sensor suite experiment establishes a precedent and proof of concept for this methodology and opens the doorway for future technology development.

The Polipo sensor system was described in detail in Chapter 4. The two remaining sensor systems are reviewed below. Data analysis and lessons learned from the experiment focus on the low-pressure sensing Polipo system, with general recommendations for experimental design and integration with the other sensor systems discussed. The experiment was designed to evaluate Design Requirement 2, *“Human and space suit interaction characterized by interface pressures will show trends consistent with expected loading regimes.”* Requirement 2 assesses the Polipo pressure sensing tool in the environment for which it was designed. Additionally, Hypothesis 5 is tested, *“Subjects with experience working in the space suit will perform motion tasks with consistent movement strategies.”* This research question evaluated changes in pressure that may be due to alterations in biomechanical strategies or fatigue, both of which could be precursors for injury and discomfort.

5.1. Experimental Methods

5.1.1. Sensor Systems

How a human moves in a suit and how suit rigidity constrains movement is essentially unknown. Pressure and joint angle measurements would allow greater insight into how

these interactions occur and help characterize suit performance. The two pressure sensing systems and inertial measurement units (IMUs) used to measure kinematics are seen in Figure 5.1. A schematic of all sensors integrated into a wearable garment are shown in Figure 5.2.

The Polipo, described in Chapter 4, is a system of 12 sensors developed for low-pressure sensing under suit soft goods. The sensors are molded using a hyper-elastic polymer that is cured to have a microfluidic channel into which liquid conductive metal is deposited. The sensors measure normal pressure by a change in resistance of the conductive metal when the channel is deformed. These sensors are placed over the arm in a way that targets anticipated hot spots and for uniform coverage. The Polipo is integrated into a conformal athletic garment with areas onto which the sensors are attached with Velcro. The system is detachable from the garment which allows the pressure sensing system to be used on differently sized people. It also allows the experimenter to move the sensors to concentrate them over a certain region of the body. The Polipo is run on battery with on-board data collection and electronics are attached at the base of the back. An Arduino Microprocessor is used for data collection. Each sensor is powered with constant current of 0.5mA. The entire board in nominal operation with 12 sensors runs around 100mA, giving a test upper limit of four hours.

The garment used to attach the Polipo also has a pocket interface over the right shoulder to house the Novel pressure-sensing mat, which is used for high-pressure sensing. The mat is located at the interface between the person's body and the HUT. A Novel pressure sensing mat was used previously in a study by the Anthropometry and Biomechanics Facility (ABF) on an Extravehicular Mobility Unit hard upper torso. However the results are unpublished, so comparisons are left for future work. For the current experiment a modified S2073 sensor mat with 128 sensor points is used. Each sensor is 1.4cm in each dimension and has a pressure range between 20-600kPa. The Novel system uses ten 1.2V nickel metal hydride batteries with 2000 mAh. The sensor is run at 330mA. Like the Polipo, data collection hardware is mounted at the base of the back and data is stored onboard. Finally, a cover shirt slides easily over the hardware to prevent catching

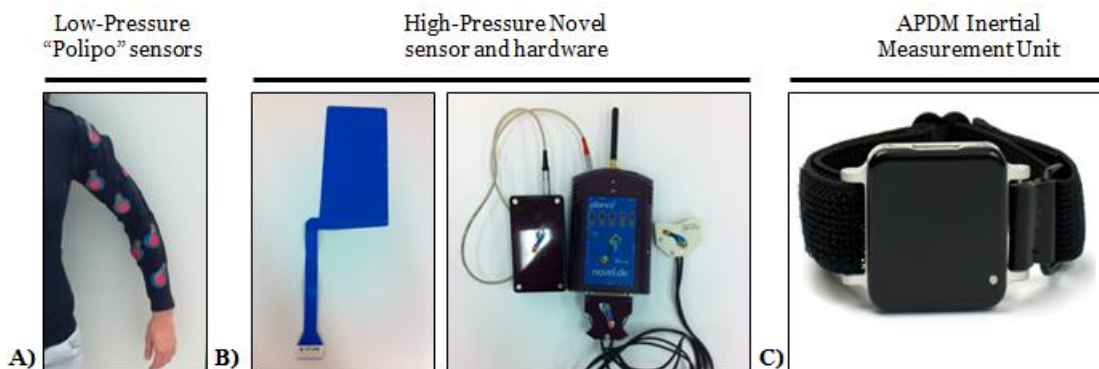


Figure 5.1. In-suit sensor systems. A) Polipo low-pressure sensors to measure the pressure between the arm and soft goods. B) Novel high-pressure sensor and associated hardware to measure pressure on shoulder under the HUT. C) APDM Opal inertial measurement unit with three place internally and three placed externally to the suit to measure joint angle differences.

and ensure proper sensor placement.

The inertial measurement units (IMUs) chosen for this experiment are the APDM Opal IMU Sensing System (Portland, OR), which are commercially available and are the highest quality sensor system offered by APDM. The IMUs are shown in Figure 5.1. Each IMU consists of three accelerometers, three gyroscopes and three magnetometers. The integration of these signals by a Kalman filter developed by APDM gives the orientation quaternion of each IMU. Three sensors were mounted internally on the upper arm, lower arm, and chest. The IMUs were placed in-plane with one another to optimize the output for isolated joint movements, but their relative orientations allow the detection of off-axis rotations. Three externally mounted sensors on the upper and lower spacesuit arm and suit torso were attached to the suit such that they corresponded to the internal sensors. The internal sensors were attached to the body with a harness or straps and were secured with athletic tape to prevent them from moving during the experiment. The external IMUs were fixed by elastic straps and athletic tape, or Velcro®. Each sensor is 4.8x3.6x1.3 cm and weighs less than 22g. The gyroscopes and magnetometers were recalibrated before placed on each subject to take into account the magnetic environment and minimize the gyroscope drift over time. They are powered by a lithium ion battery at 3.7V nominal. The maximum current through the sensor is approximately 56 mA. IMU sensor data was collected wirelessly and continuously synchronized in real time. In addition, the unsynchronized data was saved on board the sensor in the event of a wireless signal failure.

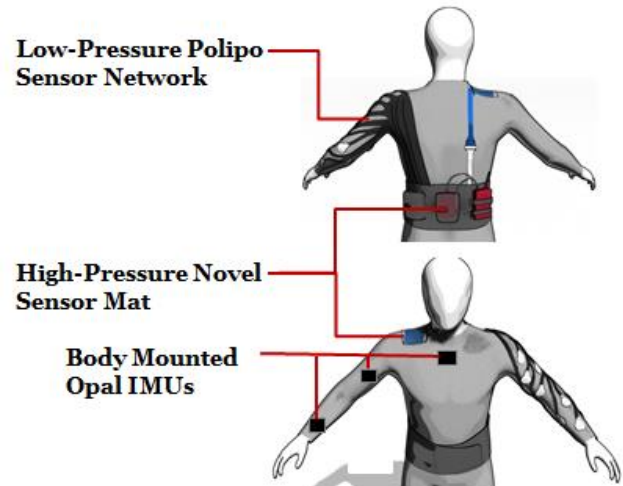


Figure 5.2. In-suit sensor systems. Each of the three sensor systems are attached to the person's body before donning the space suit. The two pressure sensing systems, the Polipo and Novel, are integrated to a conformal garment, while the IMUs are placed directly on the subject's body.

Three externally mounted sensors on the upper and lower spacesuit arm and suit torso were attached to the suit such that they corresponded to the internal sensors. The internal sensors were attached to the body with a harness or straps and were secured with athletic tape to prevent them from moving during the experiment. The external IMUs were fixed by elastic straps and athletic tape, or Velcro®. Each sensor is 4.8x3.6x1.3 cm and weighs less than 22g. The gyroscopes and magnetometers were recalibrated before placed on each subject to take into account the magnetic environment and minimize the gyroscope drift over time. They are powered by a lithium ion battery at 3.7V nominal. The maximum current through the sensor is approximately 56 mA. IMU sensor data was collected wirelessly and continuously synchronized in real time. In addition, the unsynchronized data was saved on board the sensor in the event of a wireless signal failure.

Three high-resolution cameras were used to record the motions of the subjects from both head on and profile views during the experiment. Video was helpful to review the details of the experiment and to track the kinematics to compare to IMU results. The results of the IMU and Novel pressure sensor data are reported elsewhere (Anderson 2014, Bertrand, Anderson et al. 2014)

5.1.2. Experimental Design

Subjects were asked to perform a series of upper body motions while wearing the space suit. The pressure profiles and joint angle histories were recorded for each subject. The test protocol consisted of 12 repetitions of five motions inside the space suit. A representative schematic of the test protocol is shown in Figure 5.3. The selected movements engage the upper body, particularly where the sensors are placed. The five motions are three isolated joint movements (Elbow flexion/extension, Shoulder flexion/extension, and Shoulder abduction/adduction) and two functional tasks

(Overhead hammering, Cross body reach). These tasks are described in detail in Figure 5.4. Prior to the test, subjects were trained on each movement and allowed to repeat it as many times as they desired until they felt proficient. For each movement, the 12 repetitions were further subdivided into three groups of four repetitions. This was done to evaluate changes in pressure response over time, either an indicator of subject fatigue or potential change of biomechanical strategies. After each group of movements, the subject rested for a minimum of five minutes and qualitative information was gathered on subject comfort, fatigue, perceived contact with the suit, and perceived consistency of movement. Appendix N gives the subjective feedback form. Each test condition was counterbalanced and randomized for each subject, performed in the order given in Appendix O. Unsuiting data were collected after the suited test to form the baseline pressure profile used to mitigate the effects of erroneous readings caused by movement without contact with the suit. For the unsuited runs, subjects were asked to perform the task matching the pace and range of motion while suited. There was no practical method, however, to ensure the subject performed the same motion as the suited case.

Outside of the experimental protocol, additional data were taken in static positions and through additional dynamic motions for the purpose of calibrating the IMUs and determining baseline loading from the suit. This was done before the subject donned the suit, while pressurized inside the suit, and after the experiment to determine changes from the pre-experiment data.

A full list of the procedures can be found in Appendix I.

5.1.3. Subject Selection

This experiment was performed on a total of four subjects. The first experiment was performed as a pilot study in conjunction with the David Clark Company, Incorporated (DCCI) where one subject was tested in their Mobility Mock-Up, which is an internal

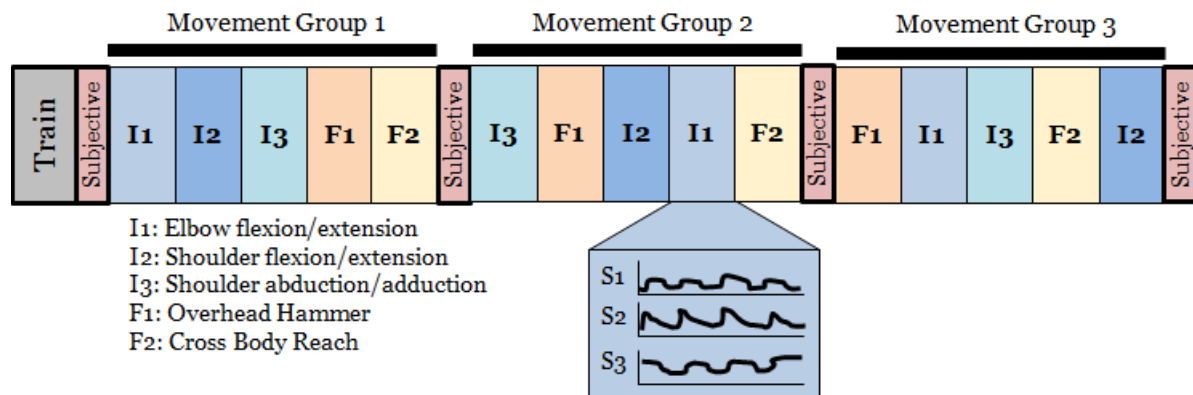


Figure 5.3. Experimental test protocol for a single subject. Subjects are given time to train each of the five movements in the suit. Subjective information is taken on comfort and pressure hot spots. The movements are performed in three groups with subjective information taken after each group. The order is counterbalanced within the group and randomized between subjects and space suits. Each of the movements is repeated four times each. Sensor pressure profiles over time are recorded for analysis.

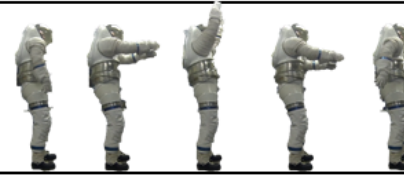
Elbow Flexion/Extension

The subject stands away from the donning stand supported by their own effort. Beginning with both arms relaxed at their side, palms facing anterior, the subject bends the arms at the elbow through their maximum range of motion. The subject then releases to the relaxed position.



Shoulder Flexion/Extension

The subject stands away from the donning stand supported by their own effort. Beginning with both arms relaxed at their side, the subject bends the arms at the shoulder through the sagittal plane. The subjects move through their maximum range of motion. The subject then releases to the relaxed position.



Shoulder Abduction/Adduction

The subject stands away from the donning stand supported by their own effort. Beginning with both arms relaxed at their side, the subject bends the arms at the shoulder through the coronal plane. The subject moves through his or her maximum range of motion. The subject then releases to the relaxed position.



Cross Body Reach

The subject begins in a relaxed position and reaches across their body to touch their hip on the opposite side. The subject moves their arm up to chest level and sweeps in front of their body. When the arm is extended in front of the shoulder, the subject touches the helmet on the same side. The movement is then repeated with the opposite arm.



Overhead Hammering

Subjects are given a rubber mallet to be grasped with both hands. The subject aims for a flat 7" rubberized square pad. The subject will hammer with both hands beginning the movement overhead and ending at approximately waist level at the height of the stand to which the rubber pad is attached.



Figure 5.4. Movement tasks performed by each subject. *Three isolated joint tasks are performed: Elbow Flexion/Extension, Shoulder Flexion/Extension, and Shoulder Abduction/Adduction. Two functional tasks were performed: Cross Body Reach and Overhead Hammering. Subjects were given very specific instructions on how to perform the isolated joint tasks, while subjects were given way-point markers to meet and allowed to develop their own biomechanical strategies for the functional tasks. Subject suited in Mark III suit is shown.*

test article that was used in the development of the “Demonstrator Suit”(Jacobs 2011). The same experimental protocol was performed at NASA’s Johnson Space Center (JSC) in the Advanced Space Suit Lab. The test was performed in the Mark III space suit. Both suits are shown in Figure 5.5. For all tests, the criteria for participation were: 1. Current fit-check in relevant suit, 2. Current test subject medical approval, 3. Extensive experience working in the pressurized suit to aid in comfort and stability while performing identified functional tasks and to ensure the subject would not develop new, potentially confounding movement strategies. Subjects were employees of the Advanced Suit Lab who have participated in many experimental evaluations of the Mark III.

Each subject was briefed on the experiment and potential hazards associated with participating prior to signing an informed consent. This protocol was reviewed and approved by both the MIT Committee on the use of Humans as Experimental Subjects and NASA Johnson Space Center’s Institutional Review Board. Experimental forms can be found in Appendix J. Additionally, each sensor system was reviewed for electrical,

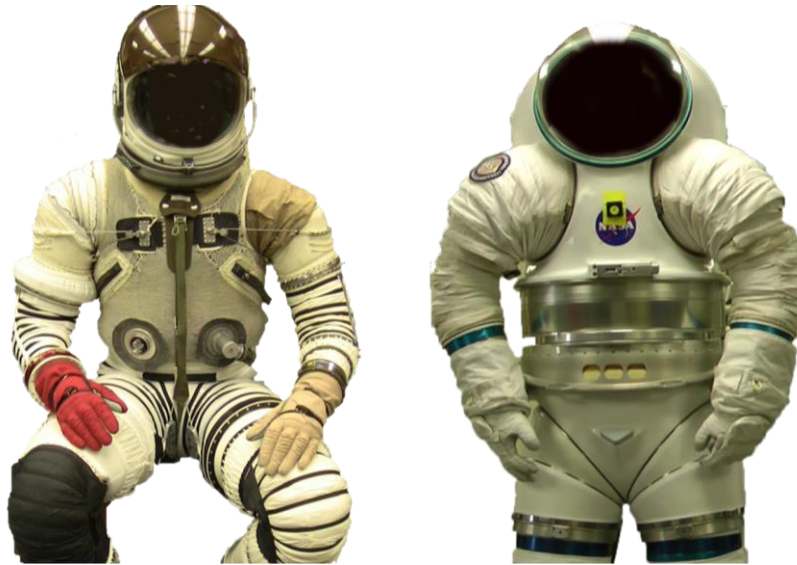


Figure 5.5. Advanced concept space suits for technology demonstration used in this experiment. A) *The David Clark Mobility Mock-Up suit. The Mobility Mock-up is used to quickly implement technology for the Demonstrator suit.* B) *The Mark III worn during the experiment presented here in.*

encumbrance, and material hazards. All materials associated with the hazards review are found in Appendix H. The experiment could be terminated by the subject at any time for any reason, or by the test conductor, suit technicians or suit engineer due to any safety or hardware concerns or concern for the suited subject.

For the experiment performed at JSC, Subject 1 was left handed, while Subjects 2 and 3 were right handed. This did not have an effect in the way subjects performed the experiment. It is not possible to determine if this affected the pressure responses since so many other variables may contribute to differences across subjects.

5.1.4. Polipo Sensor Calibration

Sensors were calibrated at MIT prior to experiment in the manner described in Section 4.2.2. Over the course of the experiment, several sensors broke and were replaced. Sensors 2, 5, and 9, were calibrated upon returning to MIT after the experiment had concluded. Sensor 10 was replaced between subjects, but broke before it could be calibrated. For this sensor, the original sensor was used for analysis, but the data will be evaluated qualitatively rather than by the values of the response.

The calibration curves used for each sensor and for each subject can be found in Appendix E.

5.1.5. Data Processing

The data were divided by each of the five tasks for each movement group. Data two seconds prior to and after the recorded time of movement was included in the profile to ensure each of the four repetitions was included. All code used to process the data can be found in Appendix L. Static data taken prior to donning the suit was used to establish the zero-pressure value while on the subject's body. Once the suit was donned and

pressurized, static data collected during IMU calibration was used to determine the suit loading on the person's body. After the pressurized portion of the experiment, static data collected during unsuited IMU calibration was used to determine any shifts from the baseline readings and to determine sensors that broke over the course of the experiment. Additionally, sensors were identified as broken when they began displaying erratic behavior. This is discussed in further detail for each subject. Sensor 8 is excluded from the experiment because it had a wire break inside the Polipo cover. Sensors 7 and 12 were known to give erratic responses prior to the beginning of the experiment due to internal fraying of the copper wiring inside the Polipo's fabric cover. With movement, however, these sensors gave some useful responses, but their recorded profiles were treated with particular caution.

The three subjects performed five movement tasks spread over three movement groups. Data were collected by 11 sensors, for a total of 495 response profiles to evaluate. Each profile was examined to determine if the output was usable by looking for a consistent peak response and the absence of erratic sensor readings which would indicate wiring issues. When the sensor response was useful, the peak pressure for the four repetitions within the response was recorded. When the peak pressure was collected for all 12 repetitions, a Kruskal-Wallis H-Test was performed to evaluate the subject's consistency between movement groups². When this test is significant, the peak pressures within at least one movement group is significantly different than the others. It cannot give insight as to which movement group(s) was different nor the magnitude of difference, although this may be inferred by looking at the data. Note that when data are highly variable within the movement group itself, the H-test would not yield a significant result. Therefore, it is not a measure of consistency, but rather inconsistency.

5.1.6. Pilot Study

A pilot study experiment was performed on one subject at the DCCI inside their Mobility Mockup space suit. The suit was pressurized to 3.5 psi and used an air cooling system. The subject wore comfort garments and padding as desired. DCCI uses this suit to evaluate new suit concepts, and therefore the upper body configuration was different for each arm/shoulder. In addition to the test protocol outlined previously, the subject also performed the experiment suited while un-pressurized.

The testing at DCCI proved extremely useful for final adjustments to the experimental protocol. To gain clearly defined data, the subject was given very specific instructions as to arm orientation during the motion and when to focus on a particular isolated joint movement. This evolved over the course of the experiment based on the subject's feedback and observation. For example, the protocol was modified to ensure the subject returned to a neutral position before beginning the next repetition. The order of tasks, such as changing cross body reach to four repetitions with the right arm followed by four with the left, was also modified during the pilot study. It became clear that taking subjective feedback after each motion, rather than after each movement group,

² This test is the nonparametric equivalent of a single factor ANOVA and is based on ranks of data. Reference can be found in Kutner, M., C. Nachtsheim, J. Neter, W. Li (2005). Applied Linear Statistical Models. Boston, MA, McGraw-Hill Irwin.

improved results since the movement was fresh in the subject's memory. Finally, the pilot study improved the data collection timing-tool to improve synchronization from the three sensor systems after the experiment.

The experiment was also important to the implementation of the Polipo system. Due to technical issues, the data logged once every seven seconds, rather than the intended 0.3 seconds. This made interpreting any results from the data very challenging, as it is not clear from which portion of the movement the pressure was read. The technical issues were resolved before performing any additional experiments. The subject was asked to evaluate the pressure sensing garment fit and evaluate the degree to which the system inhibited motion. Adjustments were made in real time, a practice that was used in subsequent experiments. Initializing the Polipo prior to initializing the Novel system was necessary since the Novel hardware covers that of the Polipo.

5.2. Results

The experiment was performed with three subjects at NASA Johnson Space Center inside the MK III space suit. Suit pressure was maintained at 4.3 psi for this test. As per normal operation, the subjects also wore a liquid cooling garment, thermal comfort undergarment, wristlets, comfort gloves, and socks to aid in comfort and thermal control. Padding was used based on the subject's normal suit requirements; however any shoulder padding was removed to prevent interference with the Novel system located over the shoulder.

5.2.1. Data Integrity

Figure 5.6 reviews the sensor placement on the subject's arm. Table 5.1 summarizes the useful pressure profiles of the Polipo sensors inside the space suit environment for all subjects across all movement tasks. These sensors gave useful results when the sensor was intact and loaded within the movement group. Profiles are divided by subject and movement task for each sensor. The table indicates under which movement group the sensor was loaded and the profile was readable. Sensors which also gave a reading during the unsuited movement are designated with a "U". Of the 165 possible sensor loading regimes (3 subjects, 5 motions, 11 sensors), 43% of the profiles were useful. The integrity of the data deteriorated as the experiment progressed. Subject 1 registered a sensor response for 60% of his loading scenarios, while Subjects 2 and 3 had 45% and 24% respectively.

Table 5.1 shows all useful profiles, but not all missing data was due to the absence of load on the sensor. Some sensors broke over the course of the experiment for two primary reasons. The first is due to losing the connection at the solder joint between the wiring and the sensor itself. This typically resulted in a total loss of signal. However, for some sensors, the movement itself would reestablish the circuit's connection, allowing some intermittent data to be used. The continual decrease in data integrity reflects deterioration of the sensor system with use. The most common form of failure was in the slow deterioration of the wiring. Internal breakage of the copper strands in the wires, described in detail in section 4.3.2, caused the data to be erratic, either increasing or decreasing the resistance as the subject moved and copper strands came in and out of

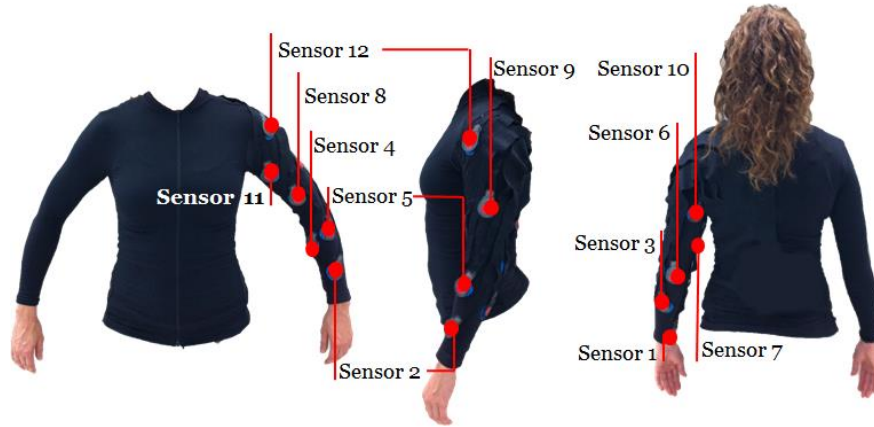


Figure 5.6: Polipo sensor locations. The Polipo low-pressure sensing system is placed on the subject’s left arm and is designed for anticipated pressure hot spots and for even distribution over the sleeve. Sensors 1 and 2 are located on the wrist; Sensors 3 and 4 on the forearm; Sensors 5 and 6 on the elbow; Sensors 7-9 on the upper arm; and Sensors 10-12 near the shoulder.

contact with one another. This progressively became more problematic with each subject as wear on the system increased.

5.2.2. Neutral Posture Pressure Loads

In the static relaxed posture, all subjects applied a constant load to Sensor 10, which is on the back side of the upper arm. All measurable profiles, examples of which are shown in Figure 5.7, are indicative of an “offloading” scenario, where the pressure is initially high, but drops with movement as the subject lifts his arm off the suit components. During subjective feedback, Subject 2 noted constant contact at the tricep where Sensor 10 is located. For Subject 1, the static pressure was 53.1 kPa. For Subjects 2 and 3 the curve is representative since the sensor broke before calibration was possible. The shape of the curve, however, is accurate. Additionally, Subject 1 experienced a nominal static load of 14.5 kPa on Sensor 6 on the back of the elbow. Subject 2 saw 19.2 kPa of loading

Table 5.1: Useful movement profiles. Summary of sensors detecting pressure over each subject, movement task, and movement group. Movement tasks are E – Elbow flexion/extension, S – Shoulder flexion/extension, A – Shoulder abduction/adduction, C – Cross body reach, and O – Overhead hammering. The movement groups are numbered 1, 2, and 3, while an unsuited profile is listed as “U”.

	Subject 1					Subject 2					Subject 3				
	E	S	A	C	O	E	S	A	C	O	E	S	A	C	O
Sensor 1				1 2 3							1 2 3 U				
Sensor 2	1 2 3	1 2 3	1 2 3	1 2 3	1 2 3	1	1	1	1	1	1 2 3			1 2 3	
Sensor 3	1 2 3														
Sensor 4	1 2	1	1	2		1 2 3 U	1 2	1 2 3		1 2 3					
Sensor 5	1 2	1 2 3	1 2	1 2 3		1			1 2		1 2 3	1 2 3 U	1 2 3 U	1 2 3	1 2 3 U
Sensor 6	1 2 3 U	1	1 2 3	1 2 3 U		1 2 3 U	1 2 3	1 2 3	1 2 3 U	1 2 3 U	1 2	1 2		1	1 2
Sensor 7		3													
Sensor 8															
Sensor 9		3	1 2 3						1				1 2 3		
Sensor 10	2	1		1	1 2	1 2	1	1 2	1 2	1 2		1			
Sensor 11	1 2 3	1 2 3 U	1 2 3 U	1 2 3 U	1 2 3										
Sensor 12	1 2 3				1 2		1								

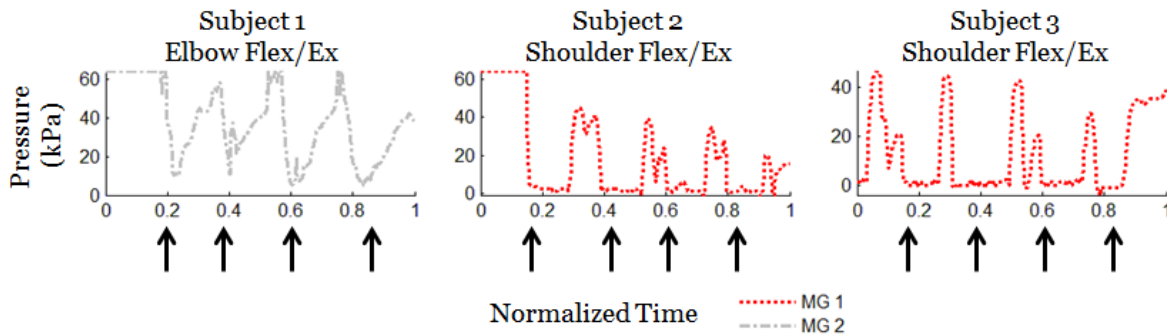


Figure 5.7. Offloading pressure response profiles from Sensor 10. Offloading profiles for each subject shown. One movement group (MG) plotted for each subject. Arrows indicate the period at which other sensors reached their peak loading, corresponding to Sensor 10 offloading. Response values are representative for Subjects 2 and 3.

over Sensor 9 during the static posture, which is consistent with the sensor loading and lead ultimately to its rupture after several movement tasks. The rupture is linked to impact against the upper arm bearing, and was not seen for the other two subjects indicating a difference in suit fit. Subject 3 did not have any other sensors loaded in the static configuration.

5.2.3. Maximum Pressure Profiles

To evaluate how pressure responses change over each movement group, four subsets of data are shown. Sensor 2 for Subject 1, located at the wrist, Sensor 11 for Subject 1 located on the upper arm, Sensor 6 for Subject 2 located at the back of the elbow, and Sensor 5 for Subject 3 located on the upper arm near the bend of the elbow. A schematic of where sensors are located on the arm is seen in Figure 5.8. Note that these results are presented because they are nearly complete data sets. The results are expected to change for each subject and for each sensor. The purpose of the comparison is to show the utility of the pressure sensors in evaluating human-space suit interaction, not to provide generalizations for all instances. All profiles and peak pressures can be found in Appendix M.

Profiles are plotted by movement group and are normalized by time of the movement. The peak pressure at each of the 12 repetition is given in the corresponding table, as is the mean (μ) and standard deviation (σ) of the peaks. Mean responses found to be inconsistent with the H-Test at the $p = 0.05$ level are indicated with an asterisk.

Table 5.2 shows the movement profiles for Subject 1 as measured by Sensor 2. For Subject 1, pressures at Sensor 2 generally remained within

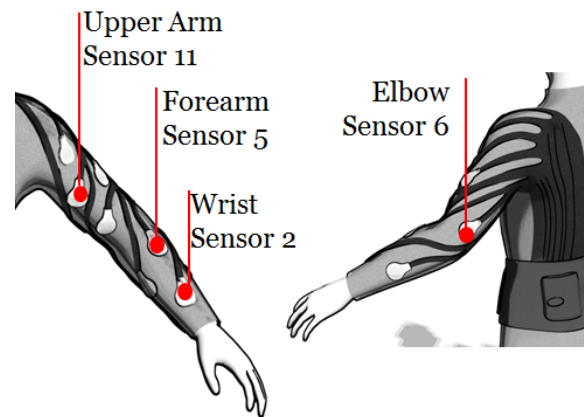


Figure 5.8. Sensor placement over the arm. Sensor 2 is placed near the wrist while sensor 11 is on the upper bicep. These sensors are analyzed for Subject 1. Sensor 5 is located near the elbow on the forearm and is analyzed for Subject 3. Sensor 6 is located on the back of the elbow and is analyzed for subject 2.

Table 5.2
Subject 1, Sensor 2 maximum pressure
(kPa)

Task		R 1	R 2	R 3	R 4	μ (σ)	- - - MG 1 - - - MG 3 - - - MG 2 — Unsuited
Elbow Flex/Ex	MG 1	49.4	29.1	20.5	17.3	28.2 (14.5)	
	MG 2	54.1	23.6	26.4	13.8		
	MG 3	49.4	20.5	20.5	13.8		
Shoulder Flex/Ex	MG 1	25.4	37.4	37.4	45.1	23.3* (13.4)	
	MG 2	36.1	27.7	17.3	17.3		
	MG 3	8.9	8.9	8.9	8.9		
Shoulder Ad/Ab	MG 1	55.9	30.6	33.0	30.6	28.3* (11.5)	
	MG 2	39.4	28.1	30.6	19.5		
	MG 3	16.3	16.3	16.3	22.6		
Cross Body Reach	MG 1	6.2	6.2	6.2	8.2	7.5 (2.3)	
	MG 2	4.2	6.2	8.2	12.0		
	MG 3	10.1	6.2	6.2	10.1		
Overhead Hammer	MG 1	16.3	4.8	4.8	4.8	13.9* (10.4)	
	MG 2	39.4	22.6	12.8	22.6		
	MG 3	16.3	8.9	8.9	4.8		

a consistent regime of 0-50 kPa. However, the pressure fluctuated within the movement group with each repetition. This is particularly evident in elbow flexion/extension where for all three movement groups Subject 1 had a strong initial peak between 49-55 kPa, with remaining peaks closer to 14-30kPa. The pressure decrease may reflect the initial torque needed to “break” the soft goods of the elbow during articulation with the wrist. After the initial movement, the fabric has a tendency to crease where it folded initially and requires less torque thereafter. An alternative reason would be if Subject 1 put forth more effort with the initial movement, then altered strategy either from fatigue or

motivation. However, the consistent pattern and subjective feedback that elbow flexion/extension was one of the least fatiguing movements making this unlikely.

Significant fluctuation between movement groups can be seen for shoulder flexion/extension ($p = 0.012$). During the first movement group, Subject 1's pressure response builds over time up to 45 kPa. During the second movement group, however, he begins with an initial peak pressure of 36 kPa and declines over time. It is not clear why the change occurred. The pressure response remains constant in the third movement group with peaks at 50% smaller than the lowest values in movement groups 1 and 2. It is likely that Subject 1 made a small internal shift in the way the suit was articulated, making the sensor less loaded in the third movement group compared to the previous two movement groups. He indicated he was "Very Consistent" for every movement group in this movement task. He did not indicate in the subjective feedback that this task was particularly difficult, making fatigue unlikely.

During shoulder abduction/adduction Subject 1 showed a significant decrease in peak pressure ($p = 0.026$). According to subjective feedback, shoulder abduction/ adduction was the most fatiguing task, and the decrease in pressure over time may reflect this. Additionally, he indicated he was initially inconsistent with his movement, but by the end of the experiment felt he was "Very Consistent". Within the movement group, there was no clear pattern of fluctuation.

Subject 1 did not appear to load Sensor 2 heavily during cross body reach. Expected loads, for example during elbow flexion to reach the helmet, were not discernible. The peak pressures seen are similar to the smallest peaks during the isolated joint movement. A general pressure response for the task is discernible. He rated his movement as less consistent for the cross body reach compared to other tasks. Also of note, Sensor 1, located on the inside of the wrist, was loaded very strongly in this movement. He was allowed to perform this task "naturally", and may have rotated the wrist bringing Sensor 1 into contact and Sensor 2 out of contact with the suit accordingly.

For all subjects, the overhead hammering task produced some of the lowest pressure responses. Expected pressure responses would be consistent with the shoulder flexion/extension isolated joint movement. In the second movement profile sharp peaks were seen and the Subject 1's motion was inconsistent ($p = 0.05$). Perhaps because grasping the hammer also requires a pronation at the wrists the sensor is less loaded under this regime. The muted pressures seen for this movement across all sensors may be caused by a delayed time response since overhead hammering was the quickest movement. Sensor response delay when pulsed too quickly was discussed in Chapter 4. To contrast the loading on wrist Sensor 2, the upper arm Sensor 11 is also shown for Subject 1. The peak pressure profiles are shown in Table 3.3. In elbow flexion/extension, the sensor is loaded consistently over all movement groups, 24 kPa on average. Although he was not producing a movement at the shoulder joint, achieving full range of motion brought his upper arm into contact with the suit.

During shoulder flexion/extension the pressure profile is also very clear. Subject 1 has a double peak response with the first peak being sharp and for a short period of time, while the second peak is to approximately half the level of pressure and over a longer duration. The second pressure response, however, is significantly inconsistent in the peak pressure attained ($p = 0.015$). The first peak corresponds to forward arm flexion, while the second peak corresponds to loading as the arm is lowered and moved into extension. This represents a constant load on the sensor. Due to placement, this type of

Table 5.3
Subject 1, Sensor 11 maximum pressure
(kPa)

Task	R 1	R 2	R 3	R 4	μ (σ) MG 1 - - - MG 3 - - - MG 2 — Unsuitd	
Elbow Flex/Ex	MG 1	24.4	23.4	30.1	23.7	24 (2.4)	
	MG 2	24.4	21.9	24.1	22.6		
	MG 3	21.1	22.6	23.4	26.6		
Shoulder Flex/Ex, Peak 1 and Peak 2	MG 1	5.3	17.8	19.3	27.8	24.2 (8.2)	
	MG 2	34.8	25.0	27.9	33.8		
	MG 3	18.8	23.6	31.6	25.3		
	MG 1	10.4	10.4	12.6	14.0	14.9^* (3.8)	
	MG 2	19.3	20.1	18.1	20.8		
	MG 3	14.1	13.7	10.7	14.1		
	Unsuit	6.2	5.8	2.2	6.2	5.1 (1.9)	
Shoulder Ad/Ab	MG1	9.6	8.1	8.1	8.1	12.6^* (10.3)	
	MG 2	6.3	6.3	6.3	6.3		
	MG 3	6.3	22.3	37.9	25.1		
	Unsuit	17.0	19.0	17.0	14.3	16.8 (1.9)	

Table 5.3, contd.
Subject 1, Sensor 11 maximum pressure
(kPa)

Task		R 1	R 2	R 3	R 4	μ (σ)	
Cross Body Reach	MG 1	4.4	12.5	22.6	8.1	14.9 (11.3)	
	MG 2	12.5	18.0	8.9	6.3		
	MG 3	8.1	46.7	16.5	14.3		
	Unsuit	8.9	10.1	14.4	11.5	9.0 (1.0)	
Overhead Hammering	MG 1	28.7	27.2	18.0	14.0	29.8* (5.3)	
	MG 2	49.0	47.4	37.1	47.9		
	MG 3	35.4	37.8	6.9	7.8		

loading corresponds either to a shoulder rotation bringing the front of the bicep in contact with the suit to push the arm behind or from the suit resting on the arm.

For both shoulder abduction/adduction and cross body reach, the sensor is loaded intermittently with random spikes occurring as the sensor impacts the suit. This is particularly surprising for cross body reach since the sensor showed a clear and consistent response for elbow flexion/extension, a component of the cross body reach. The elbow flexion/extension is done in a different orientation beginning the arm extended, so it is feasible that the sensor is not loaded in the newer condition. Shoulder abduction/adduction is also a component of cross body reach, and may be linked to the sharp increases in pressure seen. This movement was inconsistent with $p = 0.05$.

Finally, during overhead hammering, we see a large initial response for all repetitions in each of the three movement groups. Subject 1, however, is inconsistent across the movement groups ($p = 0.04$). The first movement group also exhibited a second peak response. It appears he may change his movement strategy in the second and third movement groups, preventing the sensor from being loaded in the upward swing as well as the downward swing. The response is greatest for the second movement group.

Also note the sensor shows an unsuited response for several movements. The unsuited response is evidence of wiring deterioration over the course of this experiment. For abduction/adduction and flexion/extension, it occurs later in the movement, during the adduction and extension phases. Additionally, adduction is part of the cross body reach where a similar unsuited response was seen. The wires are stretched as the garment is

stretched over the front of the bicep at the extreme range of motion. The broken wires produced the artificial reading, and Sensor 11 became unusable for the subsequent subjects.

Looking next at Subject 2, Sensor 6 is evaluated. This sensor is located over the back of the elbow. This sensor is prominently loaded in elbow flexion/extension for all subjects. However, it can be seen from the graph in Table 5.4 that there is a motion artifact associated with this movement detected in the unsuited case. This is due to the stretching of the material and bending of the sensor around the elbow with flexion which applies a normal pressure on the sensor, creating an artificial reading. Note that for Subject 2 the unsuited loading profile was higher than for the suited profile. This is one of the limitations to analyzing unsuited data, where the subject may produce a greater range of motion than while suited. Therefore, the effect cannot be directly subtracted out but should be matched by joint angle. Subject 2 noted contact at the back of the elbow with maximum flexion. The movements were also found to be inconsistent across the movement groups ($p = 0.007$), despite rating his movement as “Extremely Consistent”.

During shoulder flexion/extension, Sensor 6 is only loaded for the end of movement group 2 and for movement group 3. The profiles are initially broad and flat, finally shifting to a spike response. This indicates that Subject 1 shifted his arm inside the suit somewhere in the second movement group and continued to move with that strategy for the remainder of the experiment ($p = 0.018$). This is corroborated with changes in the subjective feedback where initially he reported contact was only felt along the arm at the extremes of the range of motion, but toward the end of the experiment on the torso against the HUT.

For shoulder abduction/adduction, the response is a transient spike for certain repetitions, but for each movement group the second repetition is loaded. It is unclear if this is due to random variation or if after the initial repetition there is a consistent shift in the suit's orientation. Subjects were asked to perform this task with palms facing inward and without bending elbows. Presumably, any response from Sensor 6 would be due to shifting inside the pressurized suit arm. On several occasions, however, Subject 2 noted the ease with which the elbow bent as compared to the other joints. He stated he used elbow flexion to improve range of motions in the other tasks, particularly in shoulder abduction/adduction. This may be the source of the readings for this movement task.

During cross body reach, a loading response can be seen, although the maximum pressure fluctuates between movement groups ($p = 0.037$). Again, an unpressurized response can be seen, likely due to the elbow flexion/extension component of the task. Subject 2 also noted that this movement was particularly difficult on the left side of the body, where the Polipo was located, because he felt he was fighting against the suit programming more so than the right side.

Finally for overhead hammering, the peak response is small and the values decrease over the course of the experiment. Subject 2 was inconsistent with his

Table 5.4
Subject 2, Sensor 6 maximum pressure
(kPa)

Task	R1	R2	R3	R4	μ (σ)		
Elbow Flex/Ex	MG 1	2.0	3.1	4.1	2.7	5.3* (2.5)	
	MG 2	4.8	4.5	5.7	4.3		
	MG 3	7.1	6.6	6.6	11.5		
	Unsuit	18.2	8.7	10.8	9.4	11.8 (4.4)	
Shoulder Flex/Ex	MG 1	1.5	2.0	1.1	5.7	24.5* (27.3)	
	MG 2	0.4	5.9	13.1	29.0		
	MG 3	61.4	65.5	41.5	67.4		
Shoulder Ad/Ab	MG 1	2.4	8.2	1.3	1.1	14.9 (14.7)	
	MG 2	9.1	39.0	31.6	0		
	MG 3	0	26.7	2.9	0		
Cross Body Reach	MG 1	8.0	1.5	2.2	2.0	20.5* (20.3)	
	MG 2	56.1	10.8	11.5	36.4		
	MG 3	3.6	54.2	35.0	24.9		
	Unsuit	8.0	6.4	7.3	2.0	5.9 (2.7)	
Overhead Hammering	MG 1	5.9	4.3	2.9	4.1	2.3* (1.9)	
	MG 2	0.4	0.6	1.7	0.4		
	MG 3	0.6	2.0	0.4	0.8		
	Unsuit	3.1	2.9	4.7	2.2	3.2 (1.0)	

movement ($p = 0.022$). To grasp the hammer, subjects must produce a slight elbow bend. This is seen both in the suited and unsuited conditions. As the subject swings the hammer down, there may be additional loading due to impact with the suit.

For Subject 3, the movement pattern measured by Sensor 5 was clearly defined for each movement. This is consistent with subjective feedback where for every task he indicated they felt contact broadly over the upper forearm. Pressures remained within 0-80 kPa. During elbow flexion/extension Subject 3 experienced a mean and standard deviation pressure of 55.8 (3.0) kPa. His movement was consistent across all movement groups and each repetition. In the third movement group, his response profile began at a non-zero offset, which is likely due to positioning his arms prior to beginning the test. There is a small dip in the third movement group, likely corresponding to complete offloading of the sensor as he attempted to fully extend his elbow.

For shoulder flexion/extension, Subject 3 exhibited a pattern of steady increase in pressure for each movement group. For each profile, the first peak produced was the smallest by about 20 kPa. Additionally, the 4th repetition in the 1st movement group is undetectable. It is unclear why the sensor was unloaded in this scenario because he completed four repetitions and pressure response is seen from other sensors. Subject 3 did not indicate any change of motion in subjective feedback. Therefore this represents a substantial change in the way the subject interacted with the suit over his forearm.

Shoulder abduction/adduction shows a clear change in response profiles between movement groups. In the first two repetitions, Subject 3 exhibited a double peak response. This indicates he loaded the sensor in both abduction and adduction. However, this pattern is not seen again for subsequent repetitions. After the first movement group he rated shoulder abduction/adduction the least consistent of the movement tasks. He did not, however, explicitly change movement strategies. Subject 3 showed a consistent response during the 2nd movement group, but a decreasing pressure peaks during the 3rd movement group. He reported shoulder abduction/adduction was the most fatiguing, so this may be evidence of the slow build-up of fatigue. However, he rated his movements as ‘Very Consistent’ for the second and third movement groups.

For cross body reach, Subject 3 exhibited a movement profile which is a combination of the isolated joint responses, as expected. The initial peaks are associated with shoulder adduction and flexion. Note that these values are smaller in magnitude than the isolated joint movements, potentially due to the added mobility achieved through rotation of the hip bearing. Hip rotation allows the subject to achieve the position without forcing them to be at the extreme of his range of motion where maximum pressures are seen. The largest peak is associated with elbow flexion/extension and is higher in magnitude than the isolated joint movement. This is potentially due to performing this motion with an elevated arm, shifting the arm’s position in the suit. Subject 3 noted a sharp increase in pressure with the elbow bend described at the location of Sensor 5.

Table 5.5
Subject 3, Sensor 5 maximum pressure
(kPa)

Task	R1	R2	R3	R4	μ (σ)		
Elbow Flex/Ex	MG 1	53.6	54.4	58.4	53.8	55.8 (3.0)	
	MG 2	60.1	55.3	58.1	60.6		
	MG 3	52.1	52.0	54.0	57.7		
Shoulder Flex/Ex	MG 1	58.9	77.6	80.9	0.0	68.3 (23.5)	
	MG 2	54.4	76.1	76.5	80.8		
	MG 3	70.0	87.4	81.4	75.4		
	Unsuit	20.4	20.4	20.4	18.7	20 (0.9)	
Shoulder Ad/Ab	MG 1	66.1	73.9	75.1	75.6	72.1 (7.2)	
	MG 2	66.4	70.8	75.6	59.8		
	MG 3	86.0	80.8	67.3	67.5		
	Unsuit	18.8	18.8	18.8	17	18.4 (0.9)	
Cross Body Reach	MG 1	80.2	71.5	71.4	70.0	69.7* (5.5)	
	MG 2	63.3	59.9	66.3	73.3		
	MG 3	64.9	70.1	70.9	75.2		
Overhead Hammering	MG 1	52.5	49.6	39.7	31.5	52.5* (11.2)	
	MG 2	62.5	55.7	64.6	72.7		
	MG 3	58.0	49.4	47.4	46.6		
	Unsuit	7.3	9.5	2.1	8.4	6.8 (3.3)	

Finally, for overhead hammering, Subject 3 exhibited a large steady peak in pressure followed by a short spike in pressure for each repetition. The magnitude of these peaks, however, changes over the movement groups ($p = 0.04$), with the largest values in the second movement group and the smallest in the first movement group. The first peak is likely due to the shoulder flexion and elbow flexion in order to hold the hammer, while the small peak may be caused by the forceful impact when the hammer reaches its target. The second peak is less discernible during the first movement group.

5.2.4. Temporal Analysis

In addition to analyzing peak pressures, one of the primary benefits to using pressure sensing to detect human-suit interaction is in assessing the nature of more complicated movements temporally. Figure 5.9 shows the activation of sensors for Subject 1 during the cross body reach task. The data presented is the mean and standard deviation of all repetitions within the first movement group. The data are normalized by time and aggregated to show the relative activation of the sensors over time. Standard deviations show that the variability is higher for loading certain sensors than others. Subject 1 initially begins in a resting posture. In this posture only Sensor 10 is loaded. The first 10-30% of the movement is associated with moving the arm from the neutral position across the body to the opposite hip. Sensor 1 is strongly loaded during the portion of the movement since it is on the inside of the wrist and the subject is moving his arm across the body. Next he raises his arm to chest level on the opposite side. Sensor 11, located on the upper bicep, is the only sensor activated during this period due to the weight of the suit resting on his arm. Between 40-60% of the movement the subject sweeps his arm in front of his body at chest level in front of his shoulder. Sensor 2 is slightly loaded over this period, while Sensor 5 becomes loaded half way through this section. As Subject 1 crossed the body, he also performed a shoulder rotation to prepare for the next phase of movement, the elbow bend. This rotation is likely what caused Sensor 5 to be loaded on the inside of the forearm near the elbow. Between 60-80% of the movement an elbow flexion/extension is done to touch the helmet near his ear. As expected, this loads Sensors 1, 2, 5, and 6, all the lower arm and elbow sensors. Although the loading profiles are seen with the pure isolated joint movement, the magnitude of loading is slightly different, as was noted previously. Finally, he extends his elbow and lowers his arm to neutral position in the last 90-100% of the movement. This re-loads Sensor 10, as discussed previously since it is loaded in the neutral posture as the arm rests on the suit. Sensor 11 is also slightly loaded as the subject brings his arm down causing contact with the bicep due to the weight of the suit arm.

This sequence of loading is consistent for Subject 1 over all three movement groups. Due to sensor failures, it is not possible to analyze the functional tasks with temporal activation patterns for the remaining subjects. However, the capability to discern movement patterns as a subject performs a task shows in great detail how the person's body shifts within the suit as he or she attempts to complete a movement.

5.3. Discussion

The second specific aim of this work is to quantify and evaluate human-space suit interaction with a pressure sensing tool. The pressure sensing system was developed

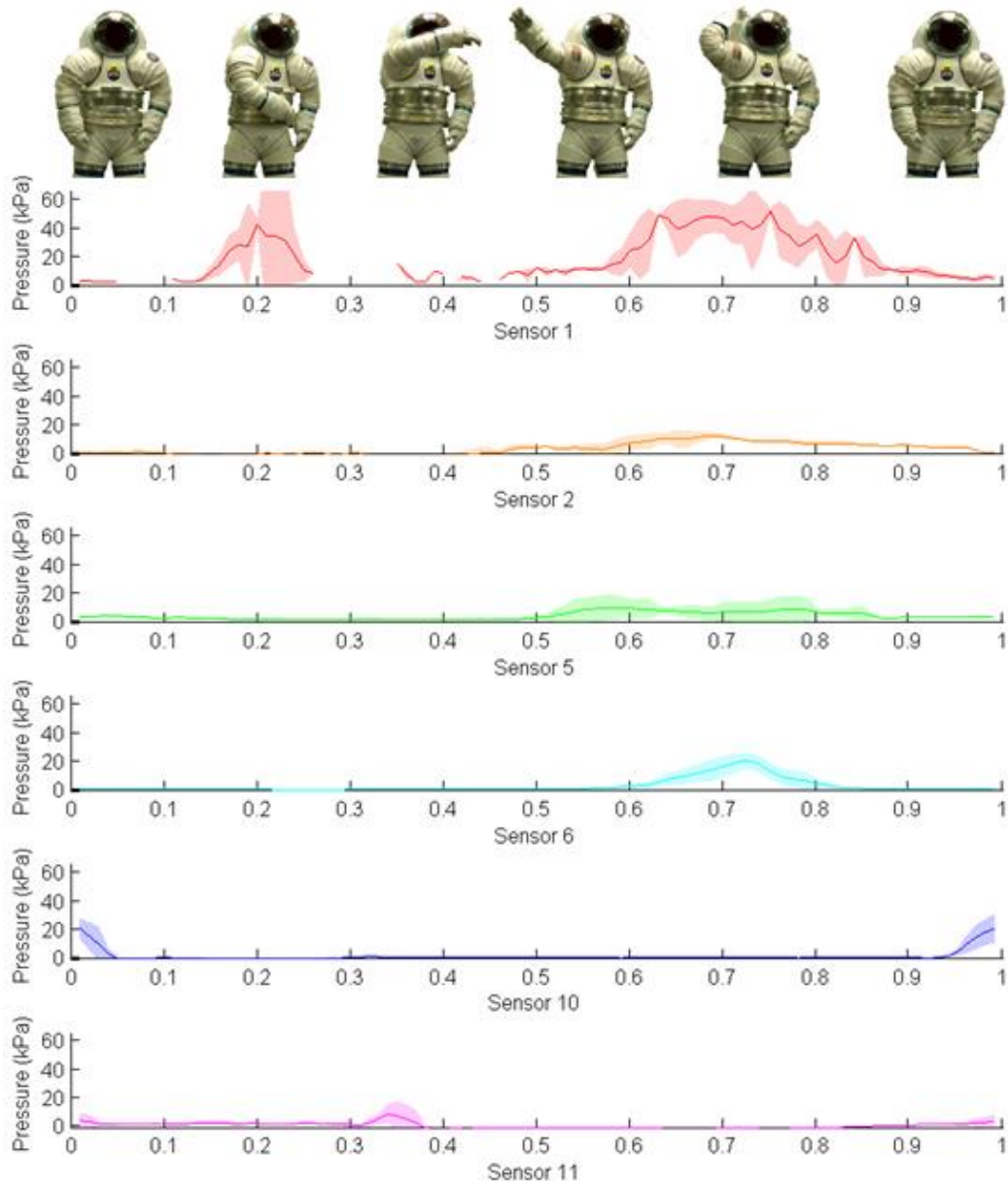


Figure 5.9. Temporal activation of sensors for Cross Body Reach. Results are for Subject 1, movement group 1. Response is averaged over each repetition and normalized by time. Sensors are shown with most distal on top of figure and proximal at the bottom. The Y axis is consistent for all sensors to compare relative pressure magnitudes.

and tested as described in Chapter 4, but had never been used in a full-body pressurized space suit for a human subject test to validate its capabilities. The Polipo pressure sensing system provided much greater insight into human movement inside the space suit than has previously been possible. It was well targeted in its design, but further improvement is desired, as noted in Chapter 4.

In general, Sensor 1 did not provide useful information due to broken wires. The response profiles were erratic, although occasionally a consistent response could be

detected through the noise. Sensor 2 was extremely useful for Subject 1, but broke early during the experiment for Subject 2. The solder connection was repaired and performed well for Subject 3, although it was only loaded during elbow flexion/extension (and therefore also cross body reach). Sensor 3 survived the entire experiment for all three subjects, but it was nearly never loaded. Sensor 3 was located on the back side of the forearm, and seemingly rarely made contact with the suit nor was stressed during unsuited movement. Sensor 4 broke early in the experiment for Subject 1 at the solder joint. It was repaired and provided useful data for Subject 2. However, over the course of the experiment the wires began to break internally, making it unusable for Subject 3. Sensor 5 was very useful for Subject 1, but broke at the solder joint late in the experiment. It broke again at the solder joint early in the experiment for Subject 2, but was repaired for Subject 3 and remained intact, providing useful profiles for the duration of the experiment. Sensor 6 remained intact for all subjects, but broke midway through the experiment for Subject 3. It provided some of the clearest profiles, but also exhibited an unsuited response due to its placement on the elbow. This artifact could be removed from the data before considering pressure magnitudes. Sensor 7 was known prior to the experiment to give erratic responses due to wire breakage, and almost no usable profiles were detected. Sensor 8 was not included in the experiment because its wires had broken prior to the experiment. Sensor 9 remained intact for Subject 1, however was rarely loaded against the suit. Short spikes in pressure were detected on occasion, likely due to intermittent impact with the upper arm bearing. This was confirmed with Subject 2, whose impact with the bearing caused the sensor to rupture. The sensor was replaced and Subject 3 showed similar response profiles to Subject 1. Sensor 10 was constantly loaded for all subjects in the neutral posture, due to its placement on the back of the upper arm. Therefore, the response profiles detected by this sensor are in offloading, rather than in loading. For all subjects, the sensor broke during the course of the experiment. Sensor 11 produced very useful results for Subject 1, but over the course of the experiment its responses deteriorated due to internal breakage of the wires. Finally, Sensor 12 was nearly unusable due to internal breakage, however occasionally response profiles were able to be detected through the noise.

Due to the distributed nature of the system, each sensor's story provides different information about human movement while suited. It may be desirable for future studies to concentrate sensors to a smaller area to provide a pressure map with higher fidelity than would be possible with the system in its current configuration. Additionally, improving sensor integrity will be critical before a programmatic series of tests could be performed. The objective is to use pressure sensing in a variety of conditions to understand the differences between human and suit performance, potentially providing insight into the causal mechanisms of injury. If the system's data are to be extrapolated to this extent, higher confidence in the sensor output must be achieved.

Design Requirement 2, "*Human and space suit interaction characterized by interface pressures will show trends consistent with expected loading regimes*" is achieved by the results from this study. Of the usable profiles, 80% measured average pressures within the anticipated loading regime of 5-60 kPa. For isolated joint movements, sensors are activated as expected based on anatomical locations and subjective feedback. The results when analyzed across movements show activation patterns consistent between isolated

joint movements the functional tasks, although pressure magnitudes differ. These trends are true for all subjects. The temporal activation of pressure profiles shows patterns for complicated dynamic movements in a sequence consistent with sensor placement on the body. Analyzing sequential activation patterns shows how the person shifts inside the suit, a capability not previously possible.

The results from Chapter 4 and the evaluation of Design Requirement 2 give confidence in the Polipo's ability to evaluate Hypothesis 5, "*Subjects with experience working in the space suit will perform motion tasks with consistent movement strategies.*" Each of the subjects tested were experienced working in the Mark III and had performed several experiments inside the suit. From subjective feedback, in general all subjects felt they were consistent in their movements. The tasks which subjects rated as least consistent were shoulder abduction/adduction and cross body reach. The reasons given were the programming of the suit and working against the rotation of the bearings to keep the movements isolated to a single joint. These were also the tasks subjects rated as requiring the greatest level of effort (However overall they felt the tasks required a "Reasonable Effort" or less). Comparing subjective feedback to quantitative pressure profiles, however, gives a much greater sense of the variability of movement and minor changes in loading on the body. There were 34 complete movement profiles with 12 repetitions for which the H-test was calculated. Of these, 18 tests were found to be inconsistent ($p < 0.05$), with 65% of tests with $p < 0.1$. The magnitude of the differences in peak pressures is not taken into account with the H-test, nor is variability within a single movement group. Therefore, when comparing the peak pressures qualitatively, an even greater degree of variability is apparent. It cannot be extrapolated from these results how these changes would affect a subject's propensity for injury. However, it is clear that inconsistencies in movement are present in many motions both within movement groups and across movement groups. With the results from this work it cannot be assessed to what extent changes in pressure are due to alterations in biomechanical strategies, fatigue, or normal fluctuation during movement. However, changes in movement strategy or fatigue could be early indicators for injury and discomfort. Based on the data presented herein, Hypothesis 5 is rejected, experienced subjects were not found to be consistent in movement.

Comparing subjective feedback to quantitative data, subjects did not always note contact where the pressure sensors indicated contact was being felt. Despite being given a body graphic aid to assist in describing contact locations, found in Appendix N, some subjects felt it was difficult to describe the location and nature of the contact since they were, "Feeling contact all over." However, some sensors, such as Sensor 3, never registered a contact response, despite being functional for the duration of the experiment. Adding quantitative information to subjective feedback gives more precision to space suit assessment. Despite the subject's best efforts, it is not possible to be aware of every detail of a movement. Using pressure sensing to get a clearer understanding of human-suit interaction will be particularly important as EVA objectives move toward planetary exploration, where subjects will not be under ideal conditions performing isolated joint movements. Rather, the nature of space suit testing will be focused on comfort, fit, and performance for complicated EVA tasks.

The process of acquiring approval for this experiment identified additional lessons learned from this study regarding evaluating potential hazards to the test subjects. Each sensor system was designed/selected to be stand-alone and wearable in the suit environment. As a result, this work was able to move beyond traditional barriers of creating a suit pass-through or potential movement inhibition due to tethered data collection systems. Demonstrating a safe, well executed experiment will allow future iterations of this work to be completed more rapidly and with a track record for implementation, reducing uncertainty.

These experiments also evaluated the sensor systems in the suit environment. In addition to the improvements to the Polipo previously noted, improvements should also be made to the Novel sensor. The sensor was bent and the cover began peeling near the edges with use. Although this did not negatively impact the results, future tests should not be performed until the sensor can be reconditioned. The sensor could be housed differently to prevent the cover peel, but the bending cannot be fixed given the sensor's size. Potentially in the future a smaller sensor mat or newly developed stretchable sensors may be better suited for these tests. To improve the IMU results, further study could be performed to quantify the magnetometer perturbations and its effects on the estimation of the orientation of the IMUs. A 3D visualization tool of suit joint angles is being developed to better understand the multi-axis rotation of joints through the bearings, and will aid in comparing the human and space suit motions.

Coupling the data from the kinematics sensors with the pressure sensors is ideal to determine the contact between the human and the suit. Future iterations of this experiment should improve the integration of the three data collection systems. Due to potential concerns of interference with the communications system, not all the data were collected wirelessly. Currently, this problem is resolved by keeping individual timelines for each system, and the data are synced post-test, increasing the potential for error. Either a new data initialization process should be developed, or the data should be collected by one central processor.

5.4. Conclusions

This research is, to our knowledge, the first experiment to characterize human-space suit interaction with pressure sensors placed inside the pressurized suit environment. Unpublished work from the NASA Anthropometry and Biomechanics Facility performed a similar study and future work includes comparing results and procedures. This research builds from previous work on measuring joint angles both internal and external to the suit and is our first glimpse “inside the space suit” and will be the baseline for future studies.

There were many successes in implementing this experiment that should be carried further into future experiments. The Polipo sensor system was built from scratch for this application. It was designed to be wearable through the full range of motion, stand alone for power and data collection, be transferrable between subjects, and was targeted at detecting pressure at the low-pressure range and resolution expected under the soft goods. Each of these design objectives was achieved. As a result, its applicability to the

space suit environment was validated with this experiment. The Novel pressure sensing system also proved to be extremely useful even in the loading regime that was less than it was originally designed for. The experiment also proved that kinematics could be efficiently tracked inside the suit, wirelessly, and compared to the suit motions, with the use of inertial measurement units.

These experiments were successful in opening the door for this type of space suit testing. The data provide valuable insight into how motions occur, how consistent subjects are, and how discomfort and fatigue may build up over time while working in the suit. It demonstrates the value in using pressure sensing to characterize human-suit interaction in a way not previously possible. The implications of the test are valuable in finding an initial baseline of human-suit interaction and will guide future tests to optimize sensor design, influence space suit design, and ultimately prevent injuries that occur inside the space suit.

The primary contributions of this work are to:

- 1) Establish a precedent for pressurized human subject testing in the space suit and a baseline for pressure interface interaction.
- 2) Validate the use of the Polipo in the space suit environment and suggest future pressurized suit testing work.
- 3) Add quantitative information to subjective feedback on human suit interaction.
- 4) Assess human movement inside the suit through the temporal activation of sensor located over the arm.
- 5) Use peak pressures to assess the consistency of subjects' movement as a means to evaluate discomfort, fatigue or change in movement with an eye toward injury prevention.

This thesis is the first published work to use untethered pressure sensing systems to measure the contact interface between the person and space suit. Space suit evaluation is traditionally measured treating the human and space suit as a system, evaluating gross metrics of performance (Morgan, Wilmington et al. 1996, Jaramillo, Angermiller et al. 2008, Matty and Aitchison 2009, Norcross, Lee et al. 2009, Norcross 2010, Aitchison 2012, Valish and Eversley 2012). Previously, no technology has allowed their separation. This system is the first to specifically target the interface between the person and space suit at the body's surface to overcome this limitation, allowing us to move beyond external visual measures, such as motion capture and photogrammetry. Recent work on joint angle kinematics of the person and space suit as measured independently have allowed us to look at these differences (Di Capua and Akin 2012, Kobrick, C. Carr et al. 2012, Bertrand, Anderson et al. 2014), but they provide limited information regarding the injury mechanisms of space suited motion. This new capability allows us to index a person inside the suit and quantify contact pressures to assess propensity for injury and discomfort.

6. CONCLUSION

Astronaut injury resulting from tasks performed in the space suit, during training and operational missions, is one of the most important issues to be resolved with the current space suit design (Longnecker 2004, Strauss 2004, Jones, Hoffman et al. 2008, Scheuring, Jones et al. 2008, Gernhardt, Jones et al. 2009, Scheuring, Mathers et al. 2009). The space suit is gas-pressurized, giving it inherent stiffness as the astronaut moves to perform his or her tasks (Parry, L. Curry et al. 1966, Schmidt 2001, Holschuh, Waldie et al. 2009). Additional programming due to rotational bearings in the suit causes the astronaut to move differently, in biomechanical terms, than when unsuited and performing natural motions. The challenges of working in a gas-pressurized space suit lead to fatigue, wasted energy, discomfort, and a variety of injuries such as abrasions, contusions, or more serious injuries such as rotator cuff injuries to the shoulder (Morgan, Wilmington et al. 1996, Williams and Johnson 2003, Longnecker 2004, Strauss 2004, Viegas, Jones et al. 2004, Carr 2005, Hochstein 2008, Jones, Hoffman et al. 2008, Scheuring, Mathers et al. 2009, Opperman 2010, Scheuring, McCullouch et al. 2012). As we move to suit designs for planetary exploration missions, it will be critical to resolve these issues for the successful implementation of habitat construction and exploration (Parry, L. Curry et al. 1966, Gernhardt, Jones et al. 2009, Norcross 2010).

Prior to this research effort, there was no established method to assess how the person interacts with the space suit, and wearable technology had not been implemented to quantify human–space suit interactions. Current performance evaluation metrics like joint torque, suited strength, range of motion, and work envelope are measured externally, rather than looking at the differences between the suit and human inside (Morgan, Wilmington et al. 1996, Jaramillo, Angermiller et al. 2008, Matty and Aitchison 2009, Norcross, Lee et al. 2009, Norcross 2010, Aitchison 2012, Valish and Eversley 2012). Additionally, most studies have not focused on injury prevention. Generally, the EVA literature addressing injury has been performed through

retrospective studies and evaluating the reporting of injury incidence (Williams and Johnson 2003, Longnecker 2004, Strauss 2004, Viegas, Jones et al. 2004, Scheuring, Jones et al. 2008, Scheuring, Mathers et al. 2009, Scheuring, McCullouch et al. 2012). Many of the proposed mechanisms of injury had never been quantitatively evaluated in combination to determine the relative contribution.

This work addresses astronaut injury inside the space suit through two specific aims:

- 1) To analyze data for correlations between anthropometry, space suit components, and shoulder injury.
- 2) To quantify and evaluate human–space suit interaction with a pressure sensing tool.

A logistic regression was performed on the largest NASA database to date to identify relevant variables associated with shoulder injury. Two models were developed, the relevant variables and fit coefficients shown in Tables 6.1 and 6.2 for the NBL and Active duty groups of subjects respectively. The most important predictor of injury was percent of total training runs the astronaut trained in the planar HUT as opposed to the pivoted HUT, supporting the claim found in the literature that the planar HUT is the primary cause of shoulder injury (Williams and Johnson 2003, Scheuring, McCullouch et al. 2012). However, there are several additional factors contributing to injury identified in this research effort. Training frequency and recovery time between runs were also important predictors for injuries. These two variables can be altered operationally to improve crew health and safety. Previous work has suggested changing orientation during training and providing additional assistance to astronauts would reduce injury (Williams and Johnson 2003), but since injuries have persisted, this research suggests additional alterations to training to reduce frequency and increase recovery should be implemented. Bi-deltoid breadth, expanded chest depth, and shoulder circumference were found to be the anthropometric dimensions most strongly related to injury. These dimensions affect how the person fits inside the HUT and therefore how their motions are achieved. These particular body dimensions should be the focus for future space suit design studies, and to ensure astronauts are working in the HUT that fits them best

Table 6.1. Model fit to subjects whose incident was reported as a result of working in the NBL. Six predictor variables were found to be important for identifying injury: three related to training, two anthropometric dimensions, and record of previous injury.

	Coef.	Variable	Wald	p-value
β_0	-1.79	Constant	-6.59	-
β_1	1.06	Percent in planar HUT	3.44	.0006*
β_2	0.073	Training frequency	0.47	0.64
β_3	0.42	Recovery metric	2.09	.037*
β_4	-0.33	Expanded chest depth	-1.15	0.25
β_5	0.19	Bi-beltoid breadth	0.7	0.48
β_6	0.98	Previous injury	1.66	0.1

Table 6.2. Model fit to subjects whose incident was reported during active duty and while working in the NBL. Five predictor variables were found to be important for identifying injury: three related to training and two anthropometric dimensions.

	Coef.	Variable	Wald	p-value
β_0	-0.37	Constant	-2.2	-
β_1	0.55	Percent in planar HUT	3	.003*
β_2	0.23	Training frequency	1.89	0.06
β_3	0.37	Recovery metric	2.36	.02*
β_4	-0.31	Expanded chest depth	-1.36	0.17
β_5	0.5	Shoulder circumference	2.34	.02*

(Benson and Rajulu 2009, Gast and Moore 2010). Finally, a record of previous injury was shown to be a significant predictor of subsequent injury. This allows flight surgeons and astronaut strength and conditioning personnel to identify higher risk astronauts to ensure they are properly trained and healthy before entering the NBL training environment. The statistical models, however, cannot identify all astronauts that may be injured as a result of working inside the space suit. Due to individual variability and the data available, this model represents an improvement over the current understanding. This research also shows how HUT size in conjunction with HUT style may be used in future work to identify the clearance between an astronaut and the space suit as measured through matching 3D models (Guan, A. Weiss et al. 2009), one of the interaction effects not currently evaluated.

To improve the statistical analysis, additional information is desirable. Injuries are not reported in a uniform manner. Additional detail would improve the categorization of injured and uninjured subjects, or even allow detailed analysis to be performed on specific injuries. NASA’s current efforts to centralize injury reporting may address this issue in the future. Higher fidelity human body models using body scans would allow clearance analysis to be performed. However, to achieve this, high fidelity models of the HUT designs are required. There are currently no 3D models of the inside contour lines of the HUT and no engineering drawings were released to further our research investigation. Improved results can only come when there is more precise understanding of how the astronaut fits inside the space suit, and the most promising way to do this is through 3D biomechanical modeling. These contributions address the current gap in our understanding of the causal mechanisms of injury.

This research effort also contributes a wearable pressure sensing system, which directly quantifies interaction between the person and the space suit, revealing interface pressures underneath the soft goods for the first time. Prior to this work, no sensor system was viable for this application (Cork 2007, Judnick 2007, Witt and Jones 2007, Brimacombe, D. Wilson et al. 2009, Anderson 2011). This is particularly true when considering the harsh environmental requirements of working inside the suit (Carr 2000, Carr 2001, Canina 2006, NASA 2011). This system was specifically designed for the space suit environment to be used for dynamic upper-body motions. The sensors

build upon previous research (Park, Majidi et al. 2010, Park, Chen et al. 2012) to measure normal pressures targeted to the 5-60 kPa range. Sensor dynamic performance can be seen in Figure 6.1 where the root mean square error from the known loading pressure is 3 kPa. This data also shows that the sensor system is highly repeatable. It has a measured time constant of 0.1 seconds allowing for near real time pressure sensing. It addresses each of the primary issues associated with wearable electronics such as power, data storage, wiring, and signal detection, with additional constraints placed on the system due to the unique environment for which it was developed, such as materials, electrical, and confinement hazards. The Polipo implements wearable electronics inside the suit beyond traditional physiologic measures (Carr 2000, Dismukes 2002, Dismukes 2002, Catrysse 2004, Tang 2007) or display and control information (Rochlis 2000, Graziosi 2005, van Erp 2005, Graziosi 2006). The final iteration of the entire Polipo sensors and system is shown in Figure 6.2.

The pressure-sensing system achieved both high wearability and utility. The primary design concern for future iteration is improving individual sensor wiring durability, shown to be a limitation after several hours of wear inside the space suit performing EVA motions. Future versions could improve durability by changing the material used to cover the wires, such as using a polymer or another fabric that more securely adheres to the base fabric. Alternatively, other wiring solutions that give the same flexibility, resistance, and elasticity may be envisioned. Another major design concern is the connection between the wires and the sensors. Better solutions, such as imbedding the wires in the sensors or creating a circuit connector that can be detached may prevent sensor failure with movement. Current attempts at these solutions have torn the elastomer causing sensor failure, but are still a promising area for design iteration. Additionally, the sensors perform best under dynamic loading conditions rather than static loading. Ideally the sensors would be calibrated dynamically, ensuring the effects of creep do not produce erroneous results in sensor readings. Another important area of

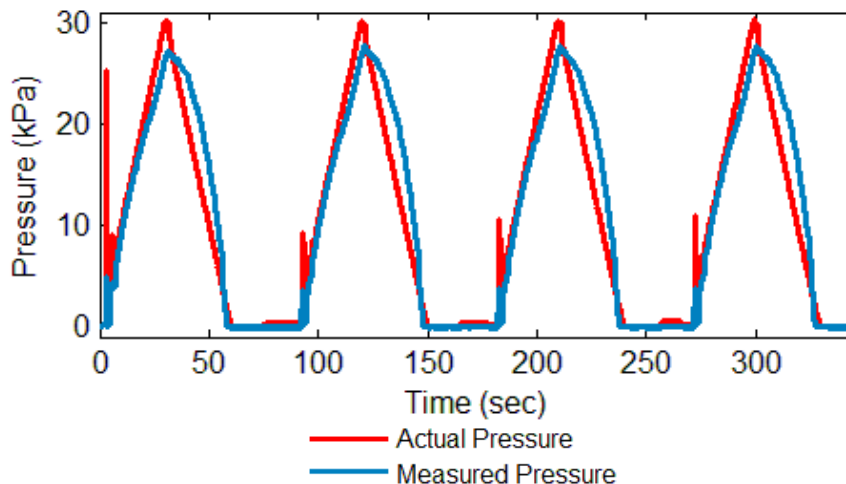


Figure 6.1 Dynamic response of the sensor to known loading. *The system was designed for dynamic movement. When measured at loading speed corresponding to human movement, the sensors track the known pressure profile to a root mean square error of 3 kPa.*



Figure 6.2. Each component of the Polipo pressure sensing system. *The pressure sensors are molded with a silicon elastomer filled with an electrically conductive liquid metal, gallinstan. The sensors are integrated to a wearable electronics system designed for the 50th percentile female to the 95th percentile male in upper body dimensions. The system takes into account the unique environmental of the space suit allowing for over 4 hours of continuous pressure measurement between the space suit and person’s arm during dynamic movement.*

future work is to improve manufacturability such that the process is less highly-skilled, takes less time, and fewer sensors fail during the construction process.

Human-Suit interaction was then characterized for three subjects performing a series of upper body EVA movements while suited in NASA’s Mark III space suit. For the first time, this capability allows researchers a “window inside the suit” to index a subject through complex motion tasks. Figure 6.3 shows the temporal activation of sensors through the cross body reach motion, placing the subject inside the suit in a way internally measured joint angles cannot (Di Capua and Akin 2012, Kobrick, C. Carr et al. 2012, Bertrand, Anderson et al. 2014). This allows us to move beyond external visual measures, such as motion capture and photogrammetry. Additional results of this experiment show that subjects, although well experienced working in the suit, do not perform suited motions consistently. Inconsistency of movement may be due to fatigue or change in biomechanical strategy. In either case, the changes may be early indicators of astronaut discomfort or potentially injury over many additional repetitions. The pressure data may be used to pinpoint more precisely where contact and human–suit interaction occurs. Despite detailed subjective feedback, subjects were unable to identify many points of contact between their bodies and the space suit, as shown by pressure profiles where the subject had not noted interaction.

Future work remains to compare joint angles measured by internal and external IMUs to the pressure measurements to determine if variability is due to range of motion or internal shifting of the arm. These quantitative kinematic and pressure-sensing capabilities will be an important supplement for future EVA performance studies. The novel pressuring sensing system develop in this research effort will allow higher fidelity

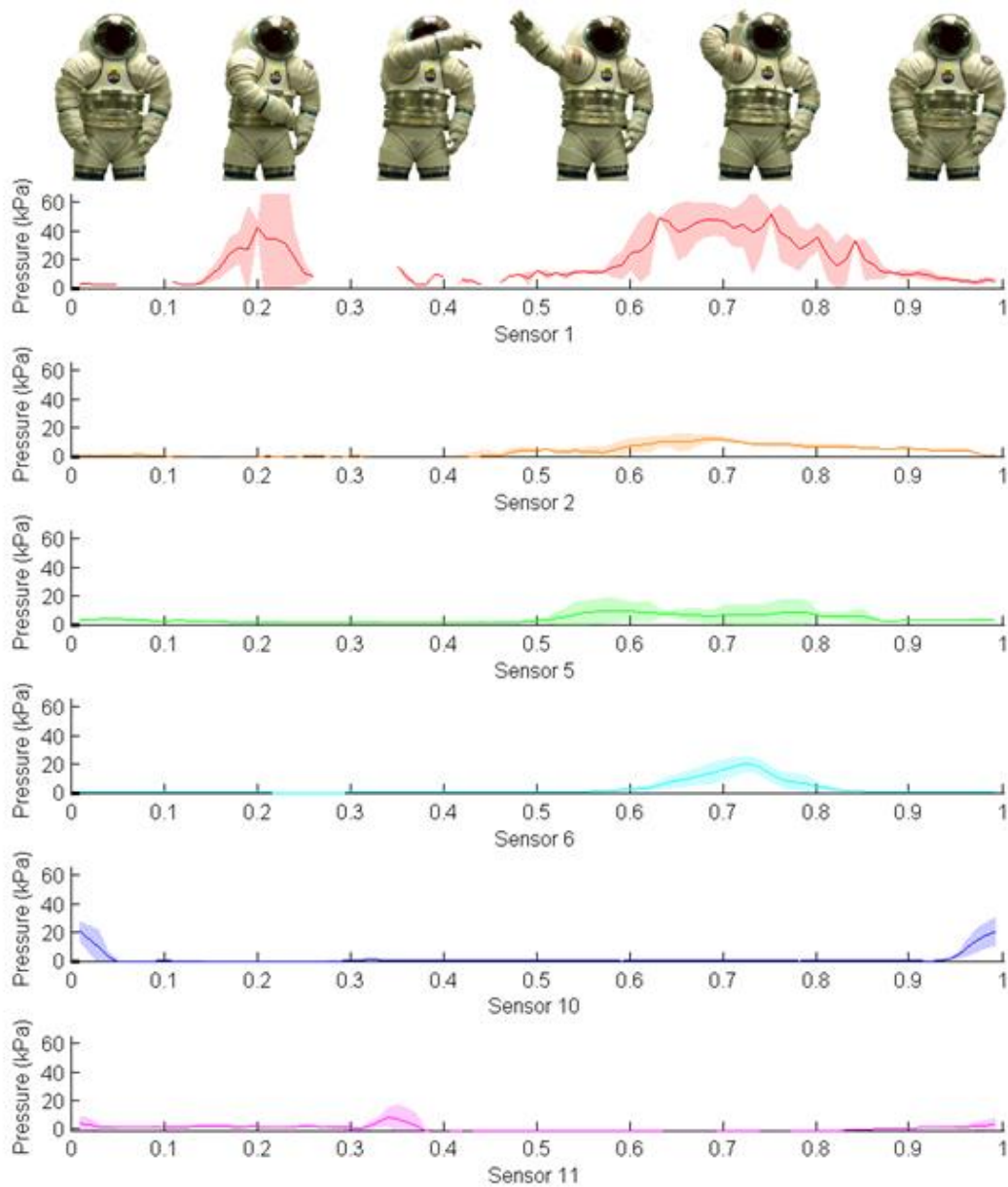


Figure 6.3. Temporal activation of sensors for Cross Body Reach. Results are for Subject 1, movement group 1. Response is averaged over each repetition and normalized by time. Sensors are shown with most distal on top of figure and proximal at the bottom. The Y axis is consistent for all sensors to compare relative pressure magnitudes.

assessment of space suit performance, such as an analog mobility study for future planetary exploration. Adding more sensors will increase the complexity of the electronics architecture, but the increased quality of the data overshadows this issue. It could even be used in collaboration with other researchers for distributed computing and data collection in a space suit environment to allow for sensor coverage over the entire body (Carr 2002, Simon 2013, Taj-Eldin 2013). This would allow pressure detection to be extrapolated to a pressure map over the body, useful for biomechanical modeling and injury, comfort, and injury evaluation.

The primary contributions of this work are to:

- 1) Add quantitative statistical analysis to the causal mechanisms of injury found in the literature.
- 2) Provide a framework for identifying relevant predictor variables related to injury given the small number of data points, large number of predictor variables, and the variability in their distributions.
- 3) Identify variables related to injury which can be addressed and resolved through operational changes to training, suit design and accommodation, and identification of higher risk subjects given previous medical history.
- 4) Propose future areas of study for which additional data may continue to be collected and analyzed, such as HUT sizing information as related to clearance anthropometry.
- 5) Establish baseline requirements for in-suit sensing and wearable electronics.
- 6) Develop pressure sensors and evaluate their performance for human movement applications.
- 7) Develop a wearable, stand-alone pressure-sensing system to be used for a large group of subjects in harsh working environments.
- 8) Create a system that is specifically targeted to provide quantitative information about human-space suit interaction not previously possible
- 9) Establish a precedent for pressurized human subject testing in the space suit and a baseline for pressure interface interaction.
- 10) Validate the use of the Polipo in the space suit environment and suggest future pressurized suit testing work.
- 11) Add quantitative information to subjective feedback on human suit interaction.
- 12) Assess human movement inside the suit through the temporal activation of sensor located over the arm.
- 13) Use peak pressures to assess the consistency of subjects' movement as a means to evaluate discomfort, fatigue or change in movement with an eye toward injury prevention.

This research addresses risks found under the Human Health Countermeasures element in the Human Research Program (HRP) Bioastronautics Critical Path Roadmap. Specifically, it addresses “Risk of Compromised EVA Performance and Crew Health Due to Inadequate EVA System”. It primarily contributes to reducing risk in gap EVA 11: How do suit fit and suit-human biomechanical interactions affect the likelihood of crew injury?, focusing on how suit fit and suit-human biomechanical interaction affects the likelihood of crew injury. However, it also contributes to EVA 6: What physiological & performance capabilities are required for suited operations? through the statistical analysis “... to understand possible correlations of subject characteristics with successful and efficient performance of EVA tasks”. Finally, it contributes to EVA10: How can biosensors be integrated with advanced tools, biofeedback & information systems to improve EVA crew performance and autonomy? The Polipo is the first iteration of a tool that will help astronauts improve EVA space suit sizing and assess comfort prior to a sortie.

Although this research is focused on ground-based operations, future versions may be used on orbit. This would improve autonomy and efficient resizing of suits without access to trained suit technicians. Additionally, the precedent and design requirements established by the Polipo aid in other wearable sensing technologies for space suited applications. Its use could be further extended to any field where humans wear protective hardware, such as evaluating the design of hip protectors for the elderly or personal protection for soldiers. This thesis addresses our gaps in understanding human-space suit interaction both through statistical analysis to evaluate the underlying mechanisms of injury, and through experimental evaluation of human-suit interaction using a pressure-sensing system specifically designed for dynamic movement inside the environment of the space suit.

REFERENCES

1. (2012). "Shoulder and Elbow Anatomy." Retrieved October 31, 2012, from <http://outpatient.stanfordhospital.org/clinics/orthopaedics/sportsmedicine/procedures/shoulder/anatomy.html>.
2. Abramov, I., et al. (1994). Essential Aspects of Space Suit Operating Pressure Trade-Off. International Conference on Environmental Systems. Friedrichshafen, Germany, Society of Automotive Engineers.
3. Aitchison, L. (2012). A Comparison of Methods for Assessing Space Suit Joint Ranges of Motion. International Conference on Environmental Systems. San Diego, CA, American Institute of Aeronautics and Astronautics: 12.
4. Alirezai, H., et al. (2007). A Highly Stretchable Tactile Distribution Sensor for Smooth Surfaced Humanoids. IEEE-RAS International Conference on Humanoid Robots, IEEE: 167-173.
5. Anderson, A. (2011). Addressing Design Challenges in Mechanical Counterpressure Spacesuit Design and Space-Inspired Informal Education Policy. Aeronautics and Astronautics. Cambridge, MA, Massachusetts Institute of Technology. **M.S.:** 161.
6. Anderson, A., A. Hilbert, P. Bertrand, S. McFarland, D. Newman (2014). In-Suit Sensor Systems for Characterizing Human-Space Suit Interaction International Conference on Environmental Systems. Tuscon, AZ, Texas Tech University.
7. Anderson, D. (1999). "EVA Worksite Analysis - Use of Computer Analysis for EVA Operations Development and Execution." Acta Astronautica **44**(7-12): 593-606.
8. Ansari, R. R., et al. (2009). "A Non-Invasive Miniaturized-Wireless Laser-Doppler Fiber-Optic Sensor for Understanding Distal Fingertip Injuries in Astronauts." Optical Diagnostics and Sensing IX **7186**.
9. Beccai, L., et al. (2005). "Design and Fabrication of a Hybrid Silicon Three-Axial Force Sensor for Biomechanical Applications." Sensors and Actuators A(120): 13.
10. Benson, E. and S. Rajulu (2009). Complexity of Sizing for Space Suit Applications. Digital Human Modeling. V. G. Duffy, Springer-Verlag: 599-607.
11. Bertrand, P., et al. (2014). Characterization of Spacesuit Kinematics and Human-Suit Interactions. International Conference on Environmental Systems. Tuscon, AZ, Texas Tech University.
12. Braden, J. R. and D. L. Akin (2002). Development and Testing of a Space Suit Analogue for Neutral Buoyancy EVA Research. International Conference on Environmental Systems. San Diego, CA, Society of Automotive Engineers.
13. Brady, S., et al. (2005). "Inherently Conducting Polymer Modified Polyurethane Smart Foam for Pressure Sensing." Sensors and Actuators A(119): 7.
14. Brimacombe, J., et al. (2009). "Effect of Calibration Method on Tekscan Sensor Accuracy." Journal of Biomechanical Engineering **131**(3): 4.
15. Canina, M., D. Newman, G. Trotti (2006). Preliminary Considerations for Wearable Sensors For Astronauts in Exploration Scenarios. IEEE International Summer School Symposium on Medical Devices and Biosensors. Boston, MA, IEEE: 4.

16. Carlson, J. (2006). "Functional Limitations: From Pain Caused by Repetitive Loading on the Skin: A Review and Discussion for Practitioners, With New Data for Limiting Friction Loads." American Academy of Orthotists and Prosthetists **18**(4): 93-103.
17. Carr, C. (2005). Bioenergetics of Walking and Running in Space Suits. Aerospace and Astronautics. Cambridge, Massachusetts Institute of Technology. **Ph.D.**
18. Carr, C., D. Newman (2000). Applications of Wearable Computing To Exploration in Extreme Environments. Third International Mars Society Convention: To-Mars 2000. Toronto, Canada, Mars Society: 7.
19. Carr, C., S. Schwartz, D. Newman (2001). Preliminary Considerations for Wearable Computing in Support of Astronaut Extravehicular Activity. Cambridge, MA, MIT Human Dynamics Laboratory: 7.
20. Carr, C., S. Schwartz, I. Rosenberg (2002). A Wearable Computer for Support of Astronaut Extravehicular Activity. 6th International Symposium on Wearable Computers. Seattle, WA, IEEE: 8.
21. Carson, M., et al. (1975). Extravehicular Mobility Unit. Biomedical Results of Apollo. J. J. Parker. Houston, TX, Johnson Space Center.
22. Catrysse, M., R. Puers, C. Hertleer, L. Van Langenhove, H. van Egmond, D. Mattys (2004). "Towards the Integration of Textile Sensors in a Wireless Monitoring Suit." Sensors and Actuators A: Physical **114**(2-3): 302-311.
23. Chigusa, H., et al. (2007). Large Area Sensor Skin Based on Two-Dimensional Signal Transmission Technology. EuroHaptics Conference, IEEE: 151-156.
24. Cork, R. (2007). "XSensor Technology: A Pressure Imaging Overview." Sensor Review **27**(1): 5.
25. Cotton, D., et al. (2009). "A Multifunctional Capacitive Sensor for Stretchable Electronic Skins." IEEE Sensors Journal **9**(12): 2008-2009.
26. Cowley, M., et al. (2012). Model for Predicting the Performance of Planetary Suit Hip Bearing Designs. Advances in Human Factors and Ergonomics. V. G. Duffy, CRC Press.
27. de Leon, P. and G. L. Harris (2011). NDX-2: Development of an Advanced Planetary Space Suit Demonstrator System for the Lunar Environment. International Conference on Environmental Systems. Portland, OR, AIAA.
28. Desmoulin, G. and G. Anderson (2011). "Method to Investigate Contusion Mechanisms in Living Humans." Journal of Forensic Biomechanics **2**: 10.
29. Di Capua, M. and D. Akin (2012). Body Pose Measurement System (BPMS): An Inertial Motion Capture System for Biomechanics Analysis and Robot Control from Within a Pressure Suit. International Conference on Environmental Systems. San Diego, American Institute of Aeronautics and Astronautics.
30. Dismukes, K. (2002, April 7, 2002). "Extravehicular Activity Mobility Units." Human Space Flight. Retrieved March 31, 2014, from <http://spaceflight.nasa.gov/shuttle/reference/shutref/orbiter/eclss/emu.html>.
31. Dismukes, K. (2002, April 7, 2002). "Operational Bioinstrumentation System." Human Space Flight. Retrieved March 31, 2014, from <http://spaceflight.nasa.gov/shuttle/reference/shutref/crew/obs.html>.

32. Duchaine, V., et al. (2009). A Flexible Robot Skin for Safe Physical Human Robot Interaction. IEEE International Conference on Robotics and Automation. Kobe, Japan, IEEE: 3676-3681.
33. Dunne, L., et al. (2005). "Initial Development and Testing of a Novel Foam-Based Pressure Sensor for Wearable Sensing." Journal of NeuroEngineering and Rehabilitation **2**(4): 7.
34. England, S. A., et al. (2010). Functional Mobility Testing: Quantification of Functionally Utilized Mobility Among Suited and Unsuited Subjects. A. B. Facility. Houston, TX, Johnson Space Center.
35. Gast, M. and S. Moore (2010). "A Glimpse from the Inside of a Space Suit: Whats it Really Like to Train for an EVA?" Acta Astronautica **2011**(68): 9.
36. Gernhardt, M. EVA Physiology, Systems & Performance (EPSP) Project. Biomedical & Technological Challenges of EVA, NASA.
37. Gernhardt, M., et al. (2009). Risk of Compromised EVA Performance and Crew Health Due to Inadequate EVA Suit Systems. Houston, TX, Human Research Program.
38. Gilkey, A. (2012). Space Suit Simulator for Partial Gravity Extravehicular Activity Experimentation and Training. Department of Aeronautics and Astronautics. Cambridge, MA, Massachusetts Institute of Technology. **M.S.**
39. Gordon, C., T. Churchill, C. Clauser, B. Bradtmiller, J. McConville, I. Tebbetts, R. Walker (1988). 1988 Anthropometric Survey of U.S. Army Personnel: Methods and Summary Statistics. D. a. E. C. United States Army Natick Research. Technical Report.
40. Graziosi, D., J. Ferl, K. Splawn, D. Akin, E. Tie, J. Kosmo, A. Ross (2005). Human and Robotic Enabling Performance System Development and Testing. International Conference on Environmental Systems. Rome, Italy, Society for Automotive Engineering: 11.
41. Graziosi, D., W. Splawn, J. Ferl, A. Ross (2006). Evaluation of the Rear Entry I-Suit During Desert RATS Testing. International Conference on Environmental Systems. Norfolk, VA, Society of Automotive Engineers: 7.
42. Greenisen, M. (1986). Effect of STS Space Suit on Astronaut Dominant Upper Limb EVA Work Performance, University of Houston: 8.
43. Griffin, B., et al. (2009). Creating a Lunar EVA Work Envelope. International Conference on Environmental Systems. Savannah, GA, Society of Automotive Engineers.
44. Guan, P., et al. (2009). Estimating Human Shape and Pose from a Single Image. International Conference on Computer Vision. Kyoto, Japan: 8.
45. Harris, G. L., Ed. (2001). Origins and Technology of the Advanced Extravehicular Space Suit. AAS History Series. San Diego, CA, American Astronautical Society.
46. Hayes, W., et al. (1996). "Etiology and Prevention of Age-Related Hip Fractures." Bone **18**(1).
47. Hochstein, J. (2008). Astronaut Total Injury Database and Finger/Hand Injuries During EVA Training and Tasks. Strausborg, FR, International Space University. **M.S.**
48. Holschuh, B., et al. (2009). Characterization of Structural, Volume, and Pressure Components to Space Suit Joint Rigidity. International Conference on Environmental Systems. Savannah, GA, Society of Automotive Engineers.
49. Hoshi, T. and H. Shinoda (2006). Robot Skin Based on Tough-Area-Sensitive Tactile Element. IEEE International Conference on Robotics and Automation, Orlando, FL, IEEE.

50. Inaba, M., et al. (1996). A Full-Body Tactile Sensor Suit Using Electrically Conductive Fabric and Strings. IEEE-RAS International Conference on Intelligent Robots and Systems, IEEE: 450-457.
51. Interlink FSR: Force Sensing Resistor Integration Guide and Evaluation Parts Catalog. I. Electronics. Camarillo, CA, Interlink Electronics. **Version 1, Rev. D.**
52. Jacobs, S., D. Tufts (2011). Follow-On Development of the Demonstrator Suit for Post-Shuttle Operations. International Conference on Environmental Systems. Portland, OR, American Institute of Aeronautics and Astronautics: 19.
53. Jaramillo, M. A., et al. (2008). Refinement of Optimal Work Envelope for Extravehicular Activity Suit Operations. A. a. B. Facility. Houston, TX, Johnson Space Center.
54. Jones, J. A., et al. (2008). "The use of an extended ventilation tube as a countermeasure for EVA-associated upper extremity medical issues." Acta Astronautica **63**: 763-768.
55. Jones, R., et al. (2007). Development of a Space Suit Soft Upper Torso Mobility/Sizing Actuation System with Focus on Prototype Development and Manned Testing. International Conference on Environmental Systems. Chicago, IL, SAE International.
56. Judnick, D. (2007). Modeling and Testing of a Mechanical Counterpressure BioSuit System. Aeronautics and Astronautics. Cambridge, MA, Massachusetts Institute of Technology. **M.S.**
57. Kannus, P., et al. (2000). "Prevention of Hip Fracture in Elderly People with Use of a Hip Protector." New England Journal of Medicine **343**(21): 8.
58. Kawchuk, G. and P. Elliott (1998). "Validation of Displacement Measurements Obtained from Ultrasonic Images During Indentation Testing." Ultrasound in Medicine and Biology **24**(1): 105-111.
59. Knapik, J., et al. (1990). Relationship of Soldier Load Carriage to Physiological Factors, Military Experience, and Moot States, U.S. Army Research Institute of Environmental Medicine: 39.
60. Kobrick, R., et al. (2012). Using Inertial Measurement Units for Measuring Spacesuit Mobility and Work Envelope Capability for Intravehicular and Extravehicular Activities. International Astronautical Congress. Naples, Italy, International Astronautical Federation: 9.
61. Kolesar, E. and C. Dyson (1995). "Object Imaging with Piezoelectric Robotic Tactile Sensor." Journal of Microelectromechanical Systems **4**(2).
62. Kozloski, L. D. (1994). U.S. Space Gear. Washington D.C., Smithsonian Institute Press.
63. Kutner, M., C. Nachtsheim, J. Neter, W. Li (2005). Applied Linear Statistical Models. Boston, MA, McGraw-Hill Irwin.
64. Kuznetz, L. (1969). Real Time Determination of Metabolic Rate and Life Support Consumables During EVA. Houston, TX, Crew Systems Division: 63.
65. Lacasse, M.-A., et al. (2010). Characterization of the Electrical Resistance of Carbon-Black-Filled Silicone: Application to a Flexible and Stretchable Robot Skin. IEEE International Conference on Robotics and Automation. Anchorage, AK, IEEE.
66. Lee, M. and H. Nicholls (1999). "Tactile Sensing for Mechatronics - A State of the Art Survey." Mechatronics **9**: 31.

67. Lee, N., et al. (2001). "A Flexible Encapsulated MEMS Pressure Sensor System for Biomechanical Applications." Microsystem Technologies 7: 13.
68. Longnecker, D., et al. (2004). Review of NASA's Longitudinal Study of Astronaut Health. I. o. Medicine. Washington, D.C., National Academies Press.
69. Mailler, E. and B. Adams (2004). "The Wear and Tear of 26.2: Dermatological Injuries Reported on Marathon Day." Biomedical Journal of Sports Medicine 38: 498-501.
70. Martin, J. and R. Hooper (2001). Military Load Carriage: A Novel Method of Interface Pressure Analysis. RTO HFM Specialists' Meeting. Kingston, Canada, RTO. **MP-056**.
71. Matty, J. and L. Aitchison (2009). A Method for and Issues Associated with the Determination of Space Suit Joint Requirements. International Conference on Environmental Systems. Berlin, Germany, SAE International
72. Metzger, C., et al. (2008). "Flexible-foam-based Capacitive Sensor Arrays for Object Detection at Low Cost." Applied Physics Letters 92(013506): 3.
73. Meyen, F., et al. (2011). Robotic Joint Torque Testing: A Critical Tool in the Development of Pressure Suit Mobility Elements. International Conference on Environmental Systems. Portland, OR, AIAA.
74. Meyer, J. (2008). Textile Pressure Sensor: Design, Error Modeling, and Evaluation. Zurich, SW, ETH Zurich. **PhD**: 133.
75. Meyer, J., et al. (2006). "Textile Pressure Sensor for Muscle Activity and Motion Detection." IEEE Xplore.
76. Morgan, D. A., et al. (1996). Comparison of Extravehicular Mobility Unit (EMU) Suited and Unsited Isolated Joint Strength Measurements. Houston, TX, Johnson Space Center.
77. NASA (2002). NASA Extravehicular Mobility Unit (EMU) LSS/SSA Data Book, Hamilton Sunstrand. **Rev H**.
78. NASA (2011). NASA Space Flight Human System Standard Volume 2: Human Factors, Habitability, and Environmental Health. NASA-STD-3001 VOL II.
79. Newman, D. (1992). Human Locomotion and Energetics in Simulated Partial Gravity. Aeronautics and Astronautics. Cambridge, MA, Massachusetts Institute of Technology. **PhD**: 219.
80. Newman, D. and H. Alexander (1993). "Human Locomotion and Workload for Simulated Lunar and Martian Environments." Acta Astronautica 29(8): 613-620.
81. Newman, D., et al. (2000). Modeling the Extravehicular Mobility Unit (EMU) Space Suit: Physiology Implications for Extravehicular Activity (EVA). International Conference on Environmental Systems. Toulouse, FR, SAE International.
82. Newman, D. J., J. Hoffman, K. Bethke, C. Carr, N. Jordan, L. Sim, N. Campos, C. Conlee, B. Smith, J. Wilcox, G. Trotti (2005). Astronaut BioSuit System for Exploration Class Missions: NIAC Phase II Final Report. Cambridge, MA, Massachusetts Institute of Technology: 34.
83. Newman, D. J. and G. Schaffner (1998). "Computational Dynamic Analysis of Extravehicular Activity: Large Mass Handling." AIAA Journal of Spacecraft and Rockets 35(2): 225-227.
84. Noda, K., et al. (2010). Stretchable Liquid Tactile Sensor for Robotic-Joints. IEEE International Conference on Robotics and Automation. Anchorage, AK, IEEE: 4212-4217.

85. Norcross, J., K. Clowers, T. Clark, L. Harvill, R. Morency, L. Stroud, L. Desantis, J. Vos, M. Gernhardt (2010). Metabolic Costs and Biomechanics of Level Ambulation in a Planetary Suit. Houston, TX, Johnson Space Center: 74.
86. Norcross, J., et al. (2009). Feasibility of Performing a Suited 10-km Ambulation on the Moon - Final Report of the EVA Walkback Test (EWT). Houston, TX, Johnson Space Center: 48.
87. Opperman, R. (2010). Astronaut Extravehicular Activity - Safety, Injury, and Countermeasures & Orbital Collisions & Space Debris - Incidence, Impact, and International Policy. Aeronautics and Astronautics, Technology Policy Program. Cambridge, MA, Massachusetts Institute of Technology. **M.S.:** 183.
88. Opperman, R., et al. (2009). EVA Injury, Comfort, and Protection: Improving the Plight of the Hand and Shoulder for the Constellation Program. International Conference on Environmental Systems. San Francisco, CA, AIAA.
89. Opperman, R. A., et al. (2010). "Probability of spacesuit-induced fingernail trauma is associated with hand circumference." Aviat Space Environ Med **81**(10): 907-913.
90. Park, Y.-L., et al. (2012). "Design and Fabrication of Soft Artificial Skin Using Embedded Microchannels and Liquid Conductors." IEEE Sensors Journal **12**(8).
91. Park, Y.-L., et al. (2010). "Hyperelastic Pressure Sensing with a Liquid-Embedded Elastomer." Journal of Micromechanics and Microengineering **20**.
92. Parry, D., et al. (1966). A Study of Techniques and Equipment for the Evaluation of Extravehicular Protective Garments. Dayton, OH, Hamilton Standard: 427.
93. Proctor, R., T. Van Zandt (2008). Anthropometrics and Workspace Design. Human Factors in Simple and Complex Systems. Boca Raton, FL, CRC Press.
94. Reinhardt, A. and J. Magstad (1990). AX-5 Space Suit Reliability Model. International Conference on Environmental Systems. Williamsburg, VA, SAE. **99:** 1057-1065.
95. Rice, J. (2007). Mathematical Statistics and Data Analysis. Belmont, CA, Brooks/Cole.
96. Ripps, T., et al. (2011). The Demonstrator Suit: Evaluating a Full Pressure Suit Through Manned and Unmanned Testing. International Conference on Environmental Systems. Portland, OR, American Institute of Aeronautics and Astronautics.
97. Rochlis, J., D. Newman (2000). "A Tactile Display for International Space Station (ISS) Extravehicular Activity (EVA)." Aviation, Space, and Environmental Medicine **71**(6): 571-578.
98. Roh, J.-S., et al. (2011). Robust and Reliable Fabric, Piezoresistive Multitouch Sensing Surface for Musical Controllers. NIME. Oslo, Norway.
99. Rubins, K. (2014). Science in Extreme Environments: Building Extraterrestrial and Earth-Based Capacities. M. S. G. Consortium.
100. Scheuring, R., et al. (2008). "The Apollo Medical Operations Project: Recommendations to Improve Crew Health and Performance for Future Exploration Missions and Lunar Surface Operations." Acta Astronautica **2008**(63): 8.
101. Scheuring, R., et al. (2012). Shoulder Injuries in US Astronauts Related to EVA Suit Design. Aerospace Medical Association. Atlanta, GA.

102. Scheuring, R. A., et al. (2009). "Musculoskeletal injuries and minor trauma in space: incidence and injury mechanisms in U.S. astronauts." Aviat Space Environ Med **80**(2): 117-124.
103. Schmidt, P. (2001). An Investigation of Space Suit Mobility with Applications to EVA Operations. Aeronautics and Astronautics. Cambridge, MA, Massachusetts Institute of Technology. **PhD**: 254.
104. Sergio, M., et al. (2002). "A Textile Based Capacitive Pressure Sensor." IEEE: 1625-1630.
105. Simon, C. (2013, 2013). "Wearable Technology " Virtual Science Symposium. 2014, from <http://www.ustream.tv/recorded/34919643>.
106. Strauss, S. (2004). Extravehicular Mobility Unit Training Suit Symptom Study Report. Houston, TX, Johnson Space Center.
107. Strauss, S., et al. (2005). "Extravehicular mobility unit training and astronaut injuries." Aviat Space Environ Med **76**(5): 469-474.
108. Taj-Eldin, M., B. Kuhn, A. Hodges, B. Natarjan, G. Peterson, M. Alshetaiwi, S. Ouyang, G. Sanchez, E. Montfort-Nelson (2013). Wireless Propagation Measurements for Astronaut Body Area Network. International Conference on Wireless for Space and Extreme Environments. Baltimore, MD, IEEE: 7.
109. Takei, K., et al. (2010). "Nanowire Active-Matrix Circuitry for Low-Voltage Macroscale Artificial Skin." Nature Materials **9**: 6.
110. Tang, S. (2007). "Recent Developments in Flexible Wearable Electronics for Monitoring Applications." Transactions for the Institute of Measurement and Control **29**(3/4): pp. 283-300.
111. Tegin, J. and J. Wikander (2005). "Tactile Sensing in Intelligent Robotic Manipulation - A Review." The Industrial Robot **35**(1): 64-70.
112. Thomas, K. and H. McMann (2006). US Spacesuits. Chickester, UK, Springer-Praxis Publishing Ltd.
113. Tseng, W.-Y., et al. (2009). "A Slow-Adapting Microfluidic-Based Tactile Sensor." Journal of Micromechanics and Microengineering **19**.
114. Valdastrì, P., et al. (2005). "Characterization of a Novel Hybrid Silicon Three-Axial Force Sensor." Sensors and Actuators A(123): 8.
115. Valish, D. and K. Eversley (2012). Space Suit Joint Torque Measurement Method Validation. International Conference on Environmental Systems. San Diego, CA, American Institute of Aeronautics and Astronautics: 14.
116. van Erp, J., M. Ruijsendaal, H. van Veen (2005). A Tactile Torso Display Improves Orientation Awareness in Microgravity: A Case Study in the ISS. Soesterberg, Netherlands Organization for Applied Scientific Research: 35.
117. Ventrelli, L., et al. (2009). Development of a Stretchable Skin-Like Tactile Sensor Based on Polymeric Composites. International Conference on Robotics and Biomimetics. Guilin, China, IEEE: 6.
118. Viegas, S., et al. (2004). "Physical Demands and Injuries to the Upper Extremity Associated with the Space Program." Journal of Hand and Surgery **29**(3): 7.

119. Villar, T., et al. (1998). "Will Elderly Rest Home Residents Wear Hip Protectors?" Age and Ageing **27**: 4.
120. Waligora, J. and D. Horrigan (1975). Metabolism and Heat Dissipation During Apollo EVA Periods. Biomedical Results of Apollo. J. J. Parker. Houston, TX, Johnson Space Center.
121. Wang, Y., et al. (2011). "Novel Fabric Pressure Sensors: Design, Fabrication, and Characterization." Smart Materials and Structures **20**: 7.
122. Wettels, N., et al. (2008). "Biomimetic Tactile Sensor Array." Advanced Robotics **22**: 829-849.
123. Williams, D. R. and B. J. Johnson (2003). EMU Shoulder Injury Tiger Team Report. Houston, TX: 104.
124. Witt, J. and J. Jones (2007). Evaluation of the Hard Upper Torso Shoulder Harness. Houston, TX, NASA.
125. Xing, M., et al. (2007). "Skin Friction Blistering: Computer Model." Skin Research and Technology **13**: 310-316.
126. Yoshikai, T., et al. (2009). Development of Soft Stretchable Knit Sensor for Humanoids' Whole-body Tactile Sensibility. IEEE-RAS International Conference on Humanoid Robots. Paris, France, IEEE: 624-631.

APPENDICES

APPENDIX A: ASTRONAUT INJURY CATEGORIZATION

The following is the division of subjects used for grouping injures in statistical analysis. The subject numbers have been de-identified but are provided here for those with access to the injury database for comparison.

Injuries known not to be attributable to working in the NBL:

- Pre-existing injury only: 245, 279, 312, 397, 462, 498, 542, 609, 645, 664, 730, 737, 738, 771, 793
- Launch and Entry Suit is only injury: 116, 506, 507, 708, 719
- Active injury attributable to traumatic event: 148, 194, 169, 206, 221, 233, 284, 300, 451, 537, 616, 648, 683, 702, 705, 756 (precursor, also attributable), 784, 787
- Not shoulder related: 623 (decompression sickness), 655
- Active prior to EMU: 175, 239, 254, 327, 374, 671
- Retirement injury attributable to traumatic event: 113, 259, 307, 335, 440, 479, 505, 519, 535, 539, 604, 698

NBL Attributable:

- Pre-existing injury with Suit or NBL identified as active injury: 158, 212, 215, 218, 474, 527
- Active only, NBL: 146, 152, 258, 291, 294, 308, 356, 413, 430, 458, 472, 513, 543, 556, 564, 580, 610, 636, 720, 739
- Active only, Suit: 196, 262, 405, 544, 638, 733, 769
- Active NBL then related retirement: 798

Active Subjects:

- Active duty only: 110, 134, 139, 179, 189, 157, 260, 271, 277, 283, 304, 315, 322, 330, 336, 347, 350, 362, 365, 372, 376, 377 (Old shoulder injury cited, but not in report so not clear if pre-selection or active), 388, 406, 452, 459, 491, 495, 511, 522, 541, 550, 552, 561, 563, 593, 633, 640, 658, 670, 674, 678, 681, 704, 707, 725, 729, 735, 744, 761, 765, 781, 794, 795, 797
- Active and Retirement: 228, 265, 285, 432, 764

Injury potentially from shoulder degeneration:

- Pre-selection event and retirement: 149, 161, 314, 494
- Pre-selection and active: 150, 200, 329, 410, 469, 534, 591, 635, 746, 790
- All 3 Active Attributable: 427
- All 3 active unspecified: 112, 117, 253, 448, 774
- Retirement only: 100, 128, 132, 133, 143, 173, 243, 251, 321, 408, 423, 547, 553, 569, 570, 595, 597, 599, 608, 631

APPENDIX B: MATLAB CODE FOR STATISTICAL SHOULDER INJURY ANALYSIS

B.1 Logistic Regression

```
clear all
close all
clc

filename = 'LSAH Shoulder Injury Data 1.2.2014.xlsx';

% Anthropometry
anthro = xlsread(filename, 3);
[g,h] = size(anthro);
outliers = [682, 3; 350, 10; 661, 12; 448, 12; 655, 17; 709, 16; 271, 8];
for ll = 1:length(outliers)
    xx = find(anthro(:,1) == outliers(ll,1));
    anthro(xx,outliers(ll,2)) = NaN;
end

[g,h] = size(anthro);
manth = nanmean(anthro);
stdanth = nanstd(anthro);
for mm = 1:g
    for pp = 2:h
        if isnan(anthro(mm,pp))
            nanthro(mm,pp) = NaN;
        else
            nanthro(mm,pp) = (anthro(mm,pp) - manth(1,pp))./stdanth(1,pp);
        end
    end
end
nanthro(:,1) = anthro(:,1);

% Select the anthro columns that make sense
inanth = [1 2 3 4 5 6 7 8 9 10 11 12 13 14 15 16 17]; % excluded arm reach (7,8) and lower arm
lengths (15,16)
anthkeep = nanthro(:,inanth);

% [cor, corp] = corrcoef(anthkeep(:,8:11), 'rows', 'complete')
% corrplot(anthkeep(:,8:11), 'rows', 'complete') % Example colinearity plots

% Training
[nothing1, nothing2, train] = xlsread(filename, 5);
m = length(train);
for i = 2:m-1
    emins(i-1,1) = str2double(train(i,4));
end
x = 'Pivoted';
y = 'Planar';
piv = strcmp(x,train(2:m-1,5));
plan = strcmp(y, train(2:m-1,5));
piv = zeros(m-2,1);
hut_style = piv+plan;
t = 'Medium';
u = 'Large';
v = 'X-Large';
w = 'Not Recorded';
med = strcmp(t,train(2:m-1,6));
lg = strcmp(u, train(2:m-1,6));
lg = lg*2;
xl = strcmp(v,train(2:m-1,6));
xl = xl*3;
hut_size = med+lg+xl;
for bb = 1:length(hut_size)
```

```

    if hut_size(bb,1) == 0
        hut_size(bb,1) = NaN;
    end
end

train2 = [nothing1(:,1:3), emins, hut_style, hut_size];
missingsize = 0;
fill = 100;
count = 1;
for j = 1:m-2
    % find the next subject number
    if train2(j,1) > fill
        fill = train2(j,1);
        % Subject number
        tvar(count,1) = fill;
        x1 = find(train2(:,1) == fill, 1, 'first');
        x2 = find(train2(:,1) == fill, 1, 'last');
        % Incidence rate
        tvar(count,2) = x2-x1 + 1;
        % Subset of data
        sub = train2(x1:x2, :);
        % Incidence in planar
        tvar(count,3) = sum(sub(:,5));
        % Percent in planar
        tvar(count,4) = tvar(count,3)/tvar(count,2);
        % Training longevity
        [n,p] = size(sub);
        tvar(count,5) = sub(n,2) - sub(1,2) + 1;
        % Frequency
        tvar(count,6) = tvar(count,5)./tvar(count,2);
        % Recovery, for each group of training sessions by 1/days between
        % sessions
        rec = 0;
        for k = 1:n-1
            q = sub(k+1, 2) - sub(k,2);
            if q > 0
                rec = rec + 1/q;
            else
                continue
            end
        end
        if rec == 0
            rec = NaN;
        end
        tvar(count, 7) = rec;
    %
    count = count+1;
    else
        continue
    end
end
tvar(:, [2,6,7]) = log(tvar(:, [2,6,7]));
% tvar(:,4:5) = sqrt(tvar(:,4:5));
[e,f] = size(tvar);
mtvar = nanmedian(tvar);
tvar_mad = mad(tvar, 1);
for qq = 2:f
    tvar(:,qq) = (tvar(:,qq) - mtvar(1,qq))/tvar_mad(1,qq);
end

include = [2,4:7];
% [cor, corp] = corrcoef(tvar(:,include), 'rows', 'complete')
% corrplot(tvar(:,include), 'rows', 'complete') % Example colinearity plots

% Injury
in_nbl = [158, 212, 215, 218, 474, 527, 146, 152, 258, 291, 294, 308,...
    356, 413, 430, 458, 472, 513, 543, 556, 564, 580, 610, 636, 720, 739,...
    196, 262, 405, 544, 638, 733, 769, 798, 668];
in_nbl = sort(in_nbl', 1, 'ascend');
in_active = [110, 134, 139, 179, 189, 157, 260, 271, 277, 283, 304, 315,...
    322, 330, 336, 347, 350, 362, 365, 372, 376, 377, 388, 406, 452, 459, ...

```

```

    491, 495, 511, 522, 541, 550, 552, 561, 563, 593, 633, 640, 658, 670, ...
    674, 678, 681, 704, 707, 725, 729, 735, 744, 761, 765, 781, 794, 795, ...
    797, 228, 265, 285, 432, 764, 481, 666];
in_active = sort(in_active', 1, 'ascend');
in_degen = [149, 161, 314, 494, 150, 200, 329, 410, 469, 534, 591, 635,...
    746, 790, 427, 112, 117, 253, 448, 774, 100, 128, 132, 133, 143, 173,...
    243, 251, 321, 408, 423, 547, 553, 569, 570, 595, 597, 599, 608, 631];
in_degen = sort(in_degen', 1, 'ascend');
in_not = [245, 279, 312, 397, 462, 498, 542, 609, 645, 664, 730, 737, ...
    738, 771, 793, 116, 506, 507, 708, 719, 148, 194, 169, 206, 221, 233,...
    284, 300, 451, 537, 616, 648, 682, 702, 705, 756, 784, 787, 623, 655,...
    175, 239, 254, 327, 374, 671, 113, 259, 307, 335, 440, 479, 505, 519,...
    535, 539, 604, 698, 518];
in_not = sort(in_not', 1, 'ascend');
i1 = union(in_nbl, in_active);
i2 = union(in_degen, i1);
injury = union(in_not, i2);
% Set the categories of injured people
nbl = ismember(injury, in_nbl);
nbl = [injury nbl];
nblactive = ismember(injury, i1);
nblactive = [injury nblactive];
nblactivedegen = ismember(injury, i2);
nblactivedegen = [injury nblactivedegen];
% Previously injured
previnj = [245, 279, 312, 397, 462, 498, 542, 609, 645, 664, 730, 737,...
    738, 771, 793, 158, 212, 215, 218, 474, 527, 149, 161, 314, 494,150,...
    200, 329, 410, 469, 534, 591, 635, 746, 790, 427, 112, 117, 253, 448, 774, 518];
previnj = sort(previnj', 1, 'ascend');
pinj = ismember(injury, previnj);
pinj = [injury pinj];

% Export for use in Systat
% All subjects in all 3 data sets
c1 = intersect(tvar(:,1), anthro(:,1));
fullsub = intersect(c1, injury);
% Extra subjects who we have anthro and training info for, but never
% reported a shoulder incident
extrasub = ismember(c1,fullsub);
count = 1;
for hh = 1: length(c1)
    if extrasub(hh,1) == 0
        es(count,1) = c1(hh);
        count = count + 1;
    end
end
% All the subjects combined
fullsubnum = union(fullsub,es);
[g,h] = size(anthkeep);
for l = 1:length(fullsubnum)
    var = fullsubnum(l);
    ii = find(tvar(:,1) == var);
    % subject number
    data(l,1) = var;
    % training variables
    data(l,2:f) = tvar(ii,2:f);
    jj = find(anthkeep(:,1) == var);
    % anthropometry
    data(l,f+1:f+h-1) = anthkeep(jj,2:h);
    % previous injury
    mm = find(pinj(:,1) == var);
    if isempty(mm)
        data(l,f+h) = 0;
    else
        data(l,f+h) = pinj(mm,2);
    end
end
% injured subjects
kk = find(nbl(:,1)== var);
if isempty(kk)
    data(l,f+h+1) = 0;
else

```

```

        data(1,f+h+1) = nbl(kk,2);
    end
end
[rr,ss] = size(data);
includerows = (1:rr);%[1:8,10:21, 23:31,33:98, 100:142, 144:150, 152:rr]; % Remove the rows with
the largest leverage
% Removing the rows with really high leverage makes the p value of the
% overall model fit drop by 2/3, but it makes the p value for bi-deltoid
% breadth jump up really high to .42
data = data(includerows,:);
% Stratification of subjects
[rr,ss] = size(data);
nocount = 1;
yescount = 1;
for tt = 1:rr
    if data(tt,ss) == 0
        data_no(nocount,:) = data(tt,:);
        nocount = nocount + 1;
    else
        data_yes(yescount,:) = data(tt,:);
        yescount = yescount + 1;
    end
end
[tt,uu] = size(data_yes);
[vv,ww] = size(data_no);
% % 50/50 ratio
% whichvars = zeros(1,uu);
% for c = 1:100
%     rno = randi(vv, tt, 1);
%     dataset_no = data_no(rno,:);
%     dataprint = [data_yes; dataset_no];
%     [a,b] = size(dataprint);
%     mdl1 = stepwiseglm(dataprint(:,1:(b-1)), dataprint(:,b), 'constant',...
%     'Distribution', 'binomial', 'link', 'logit', 'CategoricalVars', b-1,...
%     'Criterion', 'aic','Upper', 'linear', 'PredictorVars', [2,4:b-1])
%     whichvars = [whichvars; mdl1.Formula.Terms];
% end
%
% varcount = sum(whichvars)

% Build final model with chosen variables % in planar, frequency,
% longevity, expanded chest depth, interacromium distance, bi-deltoid
% breadth, and previous injury

includevars = [4,6,7,15,18,24]; % Potentially remove Inter-AC distance (var 16)
% highest leverage. No effect noticed in model/residuals
% xlswrite('april14_nblmodel.xlsx', data(:,[1,includevars,ss]))
[c,d] = size(includevars);
mdl = GeneralizedLinearModel.fit(data(:,includevars), data(:,ss),...
'Distribution','binomial','link', 'logit', 'CategoricalVars', d)

%
%     mdl2 = stepwiseglm(data(includerows,includevars), data(includerows,uu), 'constant',...
%     'Distribution', 'binomial', 'link', 'logit', 'CategoricalVars', d,...
%     'Criterion', 'aic','Upper', 'linear')
% %
%     yhat = predict(mdl,data(:,1:24))
% % [cor, corp] = corrcoef(data(:,[includevars(1:5),23]), 'rows', 'pairwise')
% % corrplot(data(:,[includevars(1:5),23]), 'rows', 'pairwise') % Example colinearity plots
% % figure
% % plotSlice(mdl)
% figure
% plotDiagnostics(mdl2)
% % figure
% % plotDiagnostics(mdl, 'contour')
% figure
% plotResiduals(mdl2, 'histogram','ResidualType', 'Raw')
% figure
% plotResiduals(mdl2,'probability','ResidualType', 'Raw')
% figure
% plotResiduals(mdl2, 'fitted','ResidualType', 'Raw')
figure
subplot(3,1,1)

```

```

hist(data_yes(:,15))
h = findobj(gca,'Type','patch');
set(h,'FaceColor','w','LineWidth',1.5)
xlabel('Standard Deviation from Mean')
ylabel('Injured Subjects')
title('Expanded Chest Depth')
xlim([-3 3])
subplot(3,1,2)
hist(data_yes(:,18))
h = findobj(gca,'Type','patch');
set(h,'FaceColor','w','LineWidth',1.5)
xlabel('Standard Deviation from Mean')
ylabel('Injured Subjects')
title('Bi-Deltoid Breadth')
xlim([-3 3])
subplot(3,1,3)
hist(data_yes(:,23))
h = findobj(gca,'Type','patch');
set(h,'FaceColor','w','LineWidth',1.5)
xlabel('Standard Deviation from Mean')
ylabel('Injured Subjects')
title('Shoulder Circumference')
xlim([-3 3])

%% find funny subjects
%% rowfind = [133, 114, 86, 180, 75, 91, 14, 157, 161, 101, 63, 109, 26, 48, 23, 49, 38, 118, 12,
167,162, 28, 83, 112,90, 78,15, 132, 35,27, 53,127, 102, 110]
%% rowfind = [129,110,83, 174, 151, 72]
%% % length(includerows)
%% figure
%% zz = [9, 22, 32, 99, 143, 151];
%% hist(data(rowfind, 25))
%%
%% Run prediction
%% Generate the CV train and test sets
% sampno = randperm(vv);
% rno_train = sampno(1:floor(.8*vv));
% rno_test = sampno((floor(.8*vv)+1):vv);
% train_no = data_no(rno_train,:);
% test_no = data_no(rno_test,:);
%
% sampyes = randperm(tt);
% ryes_train = sampyes(1:floor(.8*tt));
% ryes_test = sampyes((floor(.8*tt)+1):tt);
% train_yes = data_yes(ryes_train,:);
% test_yes = data_yes(ryes_test,:);
%
% train = [train_yes; train_no];
% test = [test_yes; test_no];
%
% for l = 1:50
% sampno = randperm(vv);
% rangeno = 1:floor(.2*vv);
% sampyes = randperm(tt);
% rangeyes = 1:floor(.2*tt);
% for k = 1:5
% train_no = data_no(:,:);
% train_no(sampno(k*rangeno),:) = [];
% test_no = data_no(sampno(k*rangeno),:);
% train_yes = data_yes(:,:);
% train_yes(sampyes(k*rangeyes),:) = [];
% test_yes = data_yes(sampyes(k*rangeyes),:);
%
% train = [train_yes; train_no];
% test = [test_yes; test_no];
%
% Fit the model to the train data
% includevars2 = [4,7,6,15,18,24];
% mdlcv = GeneralizedLinearModel.fit(train(:,includevars2), train(:,ss),...
% 'Distribution','binomial','link','logit');%, 'CategoricalVars', d);
% %

```



```

% Test the newly fit model on the unseen data
yhat = predict(md1cv,test(:,includevars2));
for j = 1:length(yhat)
    if yhat(j,1) < .3
        yhat2(j,1) = 0;
    elseif yhat(j,1) > .3
        yhat2(j,1) = 1;
    else
        yhat2(j,1) = NaN;
        disp('yhat nan')
    end
end
[c,cm] = confusion(test(:,ss)',yhat');
[c2,cm2] = confusion(test(:,ss)',yhat2');

correct(k+5*(1-1),1) = c;
specificity(k+5*(1-1),1) = cm(1,1)/(cm(1,1) + cm(1,2));
sensitivity(k+5*(1-1),1) = cm(2,2)/(cm(2,1) + cm(2,2));
precision(k+5*(1-1),1) = cm(2,2)/(cm(1,2) + cm(2,2));
if isnan(precision(k+5*(1-1),1))
    precision(k+5*(1-1),1) = 0;
end
negpred(k+5*(1-1),1) = cm(1,1)/(cm(1,1) + cm(2,1));

correct(k+5*(1-1),2) = c2;
specificity(k+5*(1-1),2) = cm2(1,1)/(cm2(1,1) + cm2(1,2));
sensitivity(k+5*(1-1),2) = cm2(2,2)/(cm2(2,1) + cm2(2,2));
precision(k+5*(1-1),2) = cm2(2,2)/(cm2(1,2) + cm2(2,2));
if isnan(precision(k+5*(1-1),2))
    precision(k+5*(1-1),2) = 0;
end
negpred(k+5*(1-1),2) = cm2(1,1)/(cm2(1,1) + cm2(2,1));
end
end

%
% perccorrect = [1-mean(correct); std(correct)]
% trueneg = [mean(specificity); std(specificity)]
% truepos = [mean(sensitivity); std(sensitivity)]
% prec = [mean(precision); std(precision)]
% negpre = [mean(negpred); std(negpred)]
%

```

B.2 Sizing Descriptive Statistics

```

% subplot(3,1,1)
% hist(data_yes(:,12))
% title('Medium')
% subplot(3,1,2)
% hist(data_yes(:,13))
% title('Large')
% subplot(3,1,3)
% hist(data_yes(:,14))
% title('Extra Large')

% mu_y = mean(data_yes(:,2))
% tot_y = sum(data_yes(:,2))
% std_y = std(data_yes(:,2))
% mu_n = mean(data_no(:,2))
% tot_n = sum(data_no(:,2))
% std_n = std(data_no(:,2))

mdn_y = median(data_yes(:,2))
mad_y = mad(data_yes(:,2),1)

```

```

mdn_n = median(data_no(:,2))
mad_n = mad(data_no(:,2),1)
md = [mdn_n mdn_y];
ma = [mad_n mad_y ];
bar([0 1], md, .75, 'w', 'LineWidth', 1.5)
hold on
errorbar([0 1],md,ma, '.k', 'LineWidth', 1)
ylabel('Training Runs')

zyesno = ranksum(data_yes(:,2),data_no(:,2))

% mi = sum(data_yes(:,12))/tot_y
% li = sum(data_yes(:,13))/tot_y
% xli = sum(data_yes(:,14))/tot_y
% medu = sum(data_no(:,12))/tot_n
% lu = sum(data_no(:,13))/tot_n
% xlu = sum(data_no(:,14))/tot_n
%
f = find(data_yes(:,12)>0);
med_y = data_yes(f,12)./mdn_y;
g = find(data_yes(:,13)>0);
lar_y = data_yes(g,13)./mdn_y;
h = find(data_yes(:,14)>0);
xl_y = data_yes(h,14)./mdn_y;
fn = find(data_no(:,12)>0);
med_n = data_no(fn,12)./mdn_n;
gn = find(data_no(:,13)>0);
lar_n = data_no(gn,13)./mdn_n;
hn = find(data_no(:,14)>0);
xl_n = data_no(hn,14)./mdn_n;

mmi = median(med_y)
mli = median(lar_y)
mxli = median(xl_y)
mmu = median(med_n)
mlu = median(lar_n)
mxlu = median(xl_n)
smi = mad(med_y,1)
sli = mad(lar_y,1)
sxli = mad(xl_y,1)
smmu = mad(med_n,1)
slu = mad(lar_n,1)
sxlu = mad(xl_n,1)

figure
subplot(3,2,1)
hist(med_y)
xlabel('Runs in Size/Group Median')
ylabel('Subject Count')
xlim([0 3])
subplot(3,2,3)
hist(lar_y, 0:.5:5)
xlabel('Runs in Size/Group Median')
ylabel('Subject Count')
xlim([0 5])
subplot(3,2,5)

```

```

hist(xl_y, 0:.1:1)
xlabel('Runs in Size/Group Median')
ylabel('Subject Count')
xlim([0 1])
subplot(3,2,2)
hist(med_n)
xlim([0 3])
xlabel('Runs in Size/Group Median')
ylabel('Subject Count')
subplot(3,2,4)
hist(lar_n, 0:.5:5)
xlabel('Runs in Size/Group Median')
ylabel('Subject Count')
xlim([0 5])
subplot(3,2,6)
hist(xl_n, 0:.1:1)
xlabel('Runs in Size/Group Median')
ylabel('Subject Count')
xlim([0 1])

figure
y = [mmi mmu;
     mli mlu;
     mxli mxlu];
bar(y)

zm = ranksum(med_y,med_n)
zl = ranksum(lar_y,lar_n)
zx1 = ranksum(xl_y,xl_n)

```

B.3 Descriptive HUT Statistics

```

% Hut size information
mpivcount = 0;
mplcount = 0;
lpivcount = 0;
lplcount = 0;
xlpivcount = 0;
xlplcount = 0;
for mm = 1:n
    if sub(mm,6) == 1
        if sub(mm,5)==1
            mplcount = mplcount+1;
        elseif sub(mm,5) == 0
            mpivcount = mpivcount + 1;
        else
            disp('Hut style not recorded')
            disp(tvar(count,1))
        end
    elseif sub(mm,6) ==2
        if sub(mm,5)==1
            lplcount = lplcount+1;
        elseif sub(mm,5) == 0
            lpivcount = lpivcount + 1;
        else
            disp('Hut style not recorded')
            disp(tvar(count,1))
        end
    elseif sub(mm,6) == 3
        if sub(mm,5)==1

```

```

        xlpcount = xlpcount+1;
    elseif sub(mm,5) == 0
        xlpivcount = xlpivcount + 1;
    else
        disp('Hut style not recorded')
        disp(tvar(count,1))
    end
else
    disp('error in HUT size')
    tvar(count,1)
end
end
% percent time in m planar (percent chosen so that it won't be a confound
% with total number of training incidences
tvar(count, 8) = mplcount;%/tvar(count,2);
% percent time in m pivoted
tvar(count, 9) = mpivcount;%/tvar(count,2);
% percent time in l planar
tvar(count, 10) = lplcount;%/tvar(count,2);
% percent time in l pivoted
tvar(count, 11) = lpivcount;%/tvar(count,2);
% percent time in xl planar
tvar(count, 12) = xlpcount;%/tvar(count,2);
% percent time in xl pivoted
tvar(count, 13) = xlpivcount;%/tvar(count,2);
hsize(count,1) = tvar(count,1);
h = [1 mplcount; 2 mpivcount; 3 lplcount; 4 lpivcount; 5 xlpcount; 6 xlpivcount];
hh = [1 (mplcount + mpivcount); 2 (lplcount+lpivcount); 3 (xlpcount+xpivcount)];
hhh = [1 (mplcount+lplcount+xlpcount); 2 (mpivcount+lpivcount+xlpivcount)];
[aa bb] = (max(h(:,:)));
[cc dd] = (max(hh(:,:)));
[ee ff] = (max(hhh(:,:)));
if isempty(aa)
    hsize(count,2) = NaN;
else
    hsize(count,2) = bb(1,2);
end
if isempty(cc)
    hsize(count,3) = NaN;
else
    hsize(count,3) = dd(1,2);
end
if isempty(ee)
    hsize(count,4) = NaN;
else
    hsize(count,4) = ff(1,2);
end
totalsize(count,1) = tvar(count,1);
totalsize(count,2:7) = [mplcount mpivcount lplcount lpivcount xlpcount xlpivcount];

count = count+1;
else
    continue
end
end
end

[rr,ss] = size(data);
nocount = 1;
yescount = 1;
for tt = 1:rr
    if data(tt,ss) == 0
        data_no(nocount,:) = data(tt,:);
        vv = find(hsize(:,1)==data_no(nocount,1))
        hs_no(nocount,:) = hsize(vv,:);
        totalsize_no(nocount,:) = totalsize(vv,:);
        nocount = nocount + 1;
    else
        data_yes(yescount,:) = data(tt,:);
        ww = find(hsize(:,1)==data_yes(yescount,1))
        hs_yes(yescount,:) = hsize(ww,:);
        totalsize_yes(yescount,:) = totalsize(ww,:);
    end
end

```

```

        yescount = yescount + 1;
    end
end
[tt,uu] = size(data_yes);
[vv,ww] = size(data_no);

% The tvars I care about for sizes piv and plan are 8-13 where it's planar
% then pivoted

ff = find(hs_no(:,3) == 1);
nmeds = size(ff)
gg = find(hs_no(:,3) == 2);
nlrgs = size(gg)
hh = find(hs_no(:,3) == 3);
nxlgs = size(hh)

ii = find(hs_no(:,4) == 1);
nplans = size(ii)
jj = find(hs_no(:,4) == 2);
npivs = size(jj)

ff = find(hs_yes(:,3) == 1);
ymeds = size(ff)
gg = find(hs_yes(:,3) == 2);
ylrgs = size(gg)
hh = find(hs_yes(:,3) == 3);
yxlgs = size(hh)

ii = find(hs_yes(:,4) == 1);
yplans = length(ii)
jj = find(hs_yes(:,4) == 2);
ypivs = length(jj)

mpl = 0;
mpiv = 0;
lpl = 0;
lpiv = 0;
xlp1 = 0;
xlpiv = 0;
for kk = 1:length(hs_yes)
    if hs_yes(kk,2) == 1
        mpl = mpl + 1;
    elseif hs_yes(kk,2) == 2
        mpiv = mpiv + 1;
    elseif hs_yes(kk,2) == 3
        lpl = lpl + 1;
    elseif hs_yes(kk,2) == 4
        lpiv = lpiv + 1;
    elseif hs_yes(kk,2) == 5
        xlp1 = xlp1 + 1;
    elseif hs_yes(kk,2) == 6
        xlpiv = xlpiv + 1;
    else
        disp('error')
    end
end
end
s = 35
mpl/s
mpiv/s
lpl/s
lpiv/s
xlp1/s
xlpiv/s

% mpl = 0;
% mpiv = 0;
% lpl = 0;
% lpiv = 0;
% xlp1 = 0;
% xlpiv = 0;
% for kk = 1:length(hs_no)

```

```

%     if hs_no(kk,2) == 1
%         mpl = mpl + 1;
%     elseif hs_no(kk,2) == 2
%         mpiv = mpiv + 1;
%     elseif hs_no(kk,2) == 3
%         lpl = lpl + 1;
%     elseif hs_no(kk,2) == 4
%         lpiv = lpiv + 1;
%     elseif hs_no(kk,2) == 5
%         xlpiv = xlpiv + 1;
%     elseif hs_no(kk,2) == 6
%         xlpiv = xlpiv + 1;
%     else
%         disp('wtf')
%     end
% end
% s = 145
% mpl/s
% mpiv/s
% lpl/s
% lpiv/s
% xlpiv/s
% xlpiv/s

ts_yes = sum(totalsize_yes)/2785
sum(ts_yes(:,2:7))
ts_no = sum(totalsize_no)/7638
sum(ts_no(:,2:7))

% subplot(3,2,1)
% hist(totalsize_yes(:,2), 10)
% subplot(3,2,2)
% hist(totalsize_yes(:,3), 10)
% subplot(3,2,3)
% hist(totalsize_yes(:,4), 10)
% subplot(3,2,4)
% hist(totalsize_yes(:,5), 10)
% subplot(3,2,5)
% hist(totalsize_yes(:,6), 10)
% subplot(3,2,6)
% hist(totalsize_yes(:,7), 10)

% mdn_y = median(data_yes(:,2))
% mdn_n = median(data_no(:,2))
%
% for mm = 1:length(totalsize_yes)
%     ts_yes_pl(mm,1) =
(totalsize_yes(mm,1)+totalsize_yes(mm,3)+totalsize_yes(mm,5))/(sum(totalsize_yes(mm,1)));
% end
% mdn_pli = median(ts_yes_pl)
% mad_pli = mad(ts_yes_pl, 1)
% for nn = 1:length(totalsize_no)
%     ts_no_pl(nn,1) =
(totalsize_no(nn,1)+totalsize_no(nn,3)+totalsize_no(nn,5))/(sum(totalsize_no(nn,1)));
% end
% mdn_plu = median(ts_no_pl)
% mad_plu = mad(ts_no_pl, 1)
% zpl = ranksum(ts_no_pl, ts_yes_pl)
%
% % fp = find(data_yes(:,8)>0);
% % med_yp = data_yes(fp,8);%./mdn_y;
% % f = find(data_yes(:,9)>0);
% % med_y = data_yes(f,9);%./mdn_y;
% % gp = find(data_yes(:,10)>0);
% % lar_yp = data_yes(gp,10);%./mdn_y;
% % g = find(data_yes(:,11)>0);
% % lar_y = data_yes(g,11);%./mdn_y;
% % hp = find(data_yes(:,12)>0);
% % xl_yp = data_yes(h,12);%./mdn_y;

```

```

%% h = find(data_yes(:,13)>0);
%% xl_y = data_yes(h,13);%./mdn_y;
%%
%% fpn = find(data_no(:,8)>0);
%% med_np = data_no(fpn,8);%./mdn_y;
%% fn = find(data_no(:,9)>0);
%% med_n = data_no(fn,9);%./mdn_y;
%% gpn = find(data_no(:,10)>0);
%% lar_np = data_no(gpn,10);%./mdn_y;
%% gn = find(data_no(:,11)>0);
%% lar_n = data_no(gn,11);%./mdn_y;
%% hpn = find(data_no(:,12)>0);
%% xl_np = data_no(hpn,12);%./mdn_y;
%% hn = find(data_no(:,13)>0);
%% xl_n = data_no(hn,13);%./mdn_y;
%%
%% mmip = median(med_yp)
%% mlip = median(lar_yp)
%% mxlip = median(xl_yp)
%% mmi = median(med_y)
%% mli = median(lar_y)
%% mxli = median(xl_y)
%%
%% mmup = median(med_np)
%% mlup = median(lar_np)
%% mxlup = median(xl_np)
%% mmu = median(med_n)
%% mlu = median(lar_n)
%% mxlu = median(xl_n)
%%
%% smi = mad(med_y,1)
%% sli = mad(lar_y,1)
%% sxli = mad(xl_y,1)
%% smmu = mad(med_n,1)
%% slmu = mad(lar_n,1)
%% sxlu = mad(xl_n,1)

```

APPENDIX C: REQUIREMENTS JUSTIFICATION

The following is a description of how the requirements were created and a description of the validation techniques (if necessary).

Utility:

- 1.1 Dynamic loading is more important than static loading for EVA. A response time of .25 seconds would sample portions of normal human movements without overly constraining the sensor technology choice. This should be taken as an upper bound with faster response times being much more desirable.
- 1.2 The range of pressures applied for keyboard typing is 0-10 kPa (Park, Majidi et al. 2010). The median was taken as a reasonable threshold for discrimination.
- 1.3 The upper pressure range under the soft goods was estimated from elbow joint torque measured by (Schmidt). This was extrapolated into a force, and therefore pressure requirement for the anticipated pressure.
- 1.4 This size was taken from the literature as a reasonable sensor size for other applications (Meyer, Lukowicz et al. 2006).

- 1.5 Targeted “hot spots” will be based on literature review and conversations with subject matter experts. The maximum distances in placement are based on the fact that readings are not expected to vary a great deal over certain areas, such as the torso, since the body’s radius of curvature (and therefore impact location) is large.
- 2.1 Hysteresis will not occur equivalently over different loading profiles. The value of 10% is reasonable over an extreme loading profile, but lower hysteresis is desirable, especially over the anticipated range of loading.
- 2.2 A value of 10% kept error within the sensor resolution over the anticipated range of pressures.
- 2.3 Static loads are not as important as dynamic response for EVA motion, however shifting body positions may lead to high static loading. Drift is a known problem for many pressure-sensing technologies, so 10% was taken as an acceptable error without being prohibitively restrictive.
- 3.1 This requirement ensures that data processing will not further limit the response of the system to movement such that injury information can be accurately monitored.
- 3.2 This requirement ensures that the system is operationally feasible and not overly burdensome. It also encourages simpler solutions, which will enhance robustness.
- 3.3 Wireless data transfer will be necessary for the EMU, where wired data collection is not possible. Alternatively, onboard data storage could be explored. The requirement of a single processing and data transfer unit will decrease system complexity and prevent potential interference.

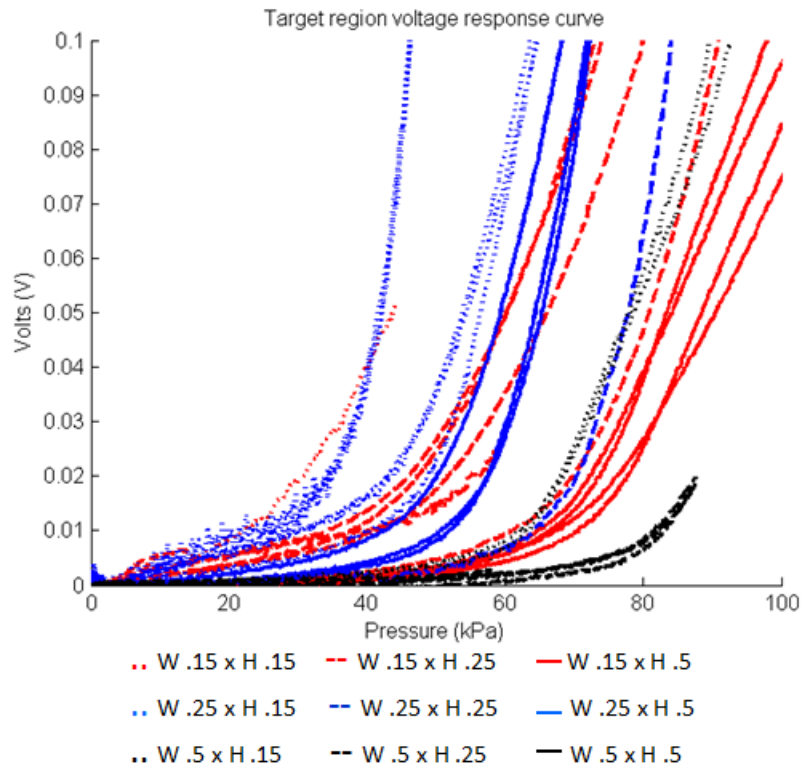
Wearability:

- 1.1 It is very important that the sensors match the person’s body contours for accurate readings. This requirement eliminates rigid sensor technologies.
- 1.2 The NASA requirement for operational hardware was found to be too restrictive for developmental research. In anticipation of its use at the Advanced Suit Lab at JSC, the accommodation range was narrowed in favor of larger subjects since many advanced concepts suits are skewed in this direction as well.
- 1.3 In previous pressure sensing capabilities, external wires and integration points has been a common source of failure (Inaba, Hoshino et al. 1996, Alirezai, Nagakubo et al. 2007). System durability will be improved by this requirement.
- 1.4 This requirement is critical for accurate body mapping. The value of 1cm was taken as an acceptable threshold since readings are not expected to vary a great deal over an area since the body’s radius of curvature (and therefore impact location) is sufficiently large. Additionally, this value is smaller than the maximum sensor size of 2x2 cm.
- 2.1 This will be tested in a suited environment, be that at David Clark, JSC, or Dainese, where a spacesuit environment can be replicated.
- 2.2 Critical requirement to ensure crew health and safety.
- 2.3 Critical requirement to ensure crew health and safety.
- 2.4 Fifty uses was selected because the developmental nature of the system meant anticipating failure beyond this point would be infeasible. Fewer than 30 uses not provide enough value for the end users.

- 3.1 This requirement was added in anticipation of being used in the EMU where a wire pass through is more complicated.
- 3.2 Typical NBL runs last between 3-5 hours. The lower bound was taken as acceptable.

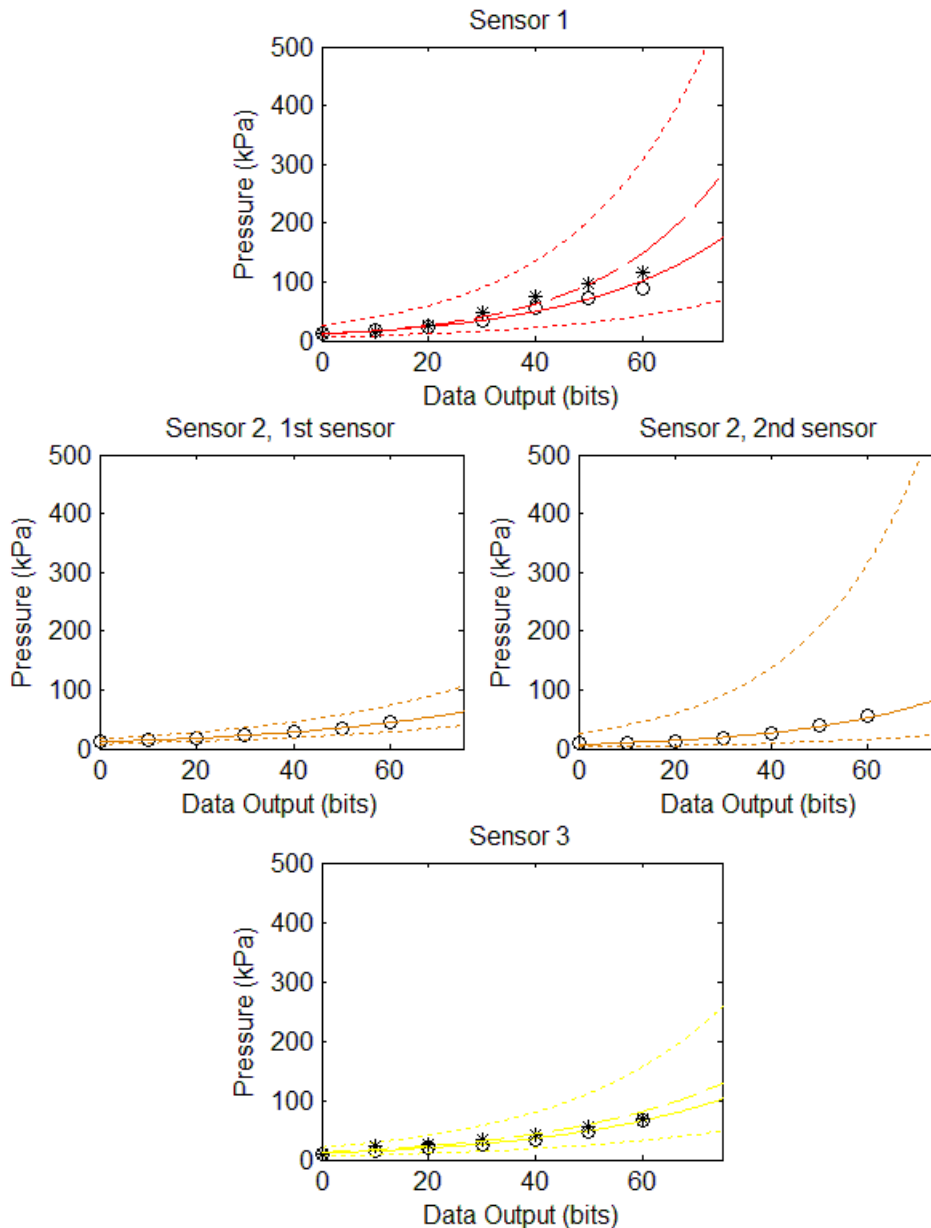
APPENDIX D: CHANNEL CROSS SECTION OPTIMIZATION

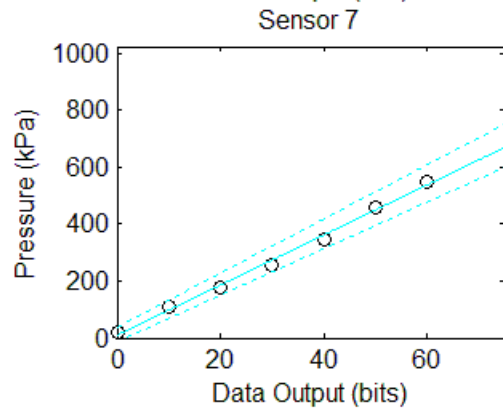
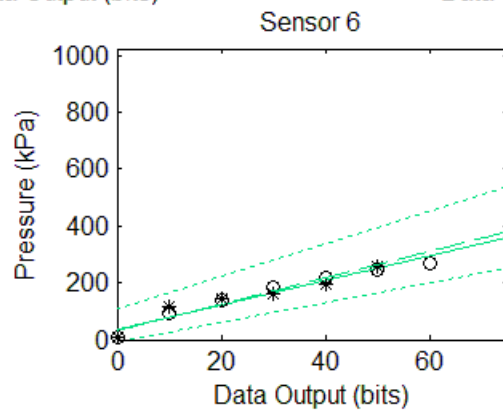
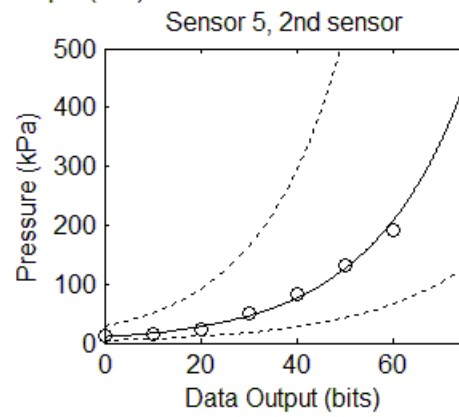
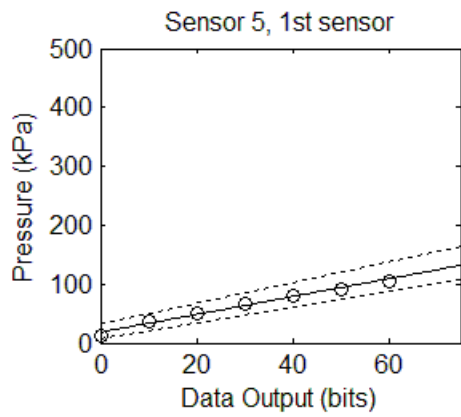
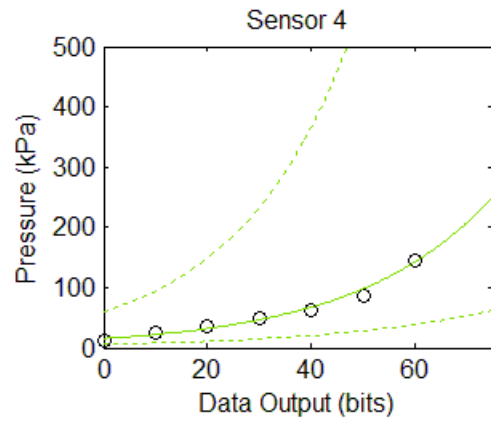
Data used to optimize channel cross section design. Dimensions are given in millimeters by width and height. Designs with the greatest sensitivity were chosen, w.15xh.15 and 1.25xh.15. Due to failure during testing and difficulty in construction, there is an unequal number of plotted profiles per configuration. However, trends in consistency can be seen, and therefore used to determine the most promising designs going forward.

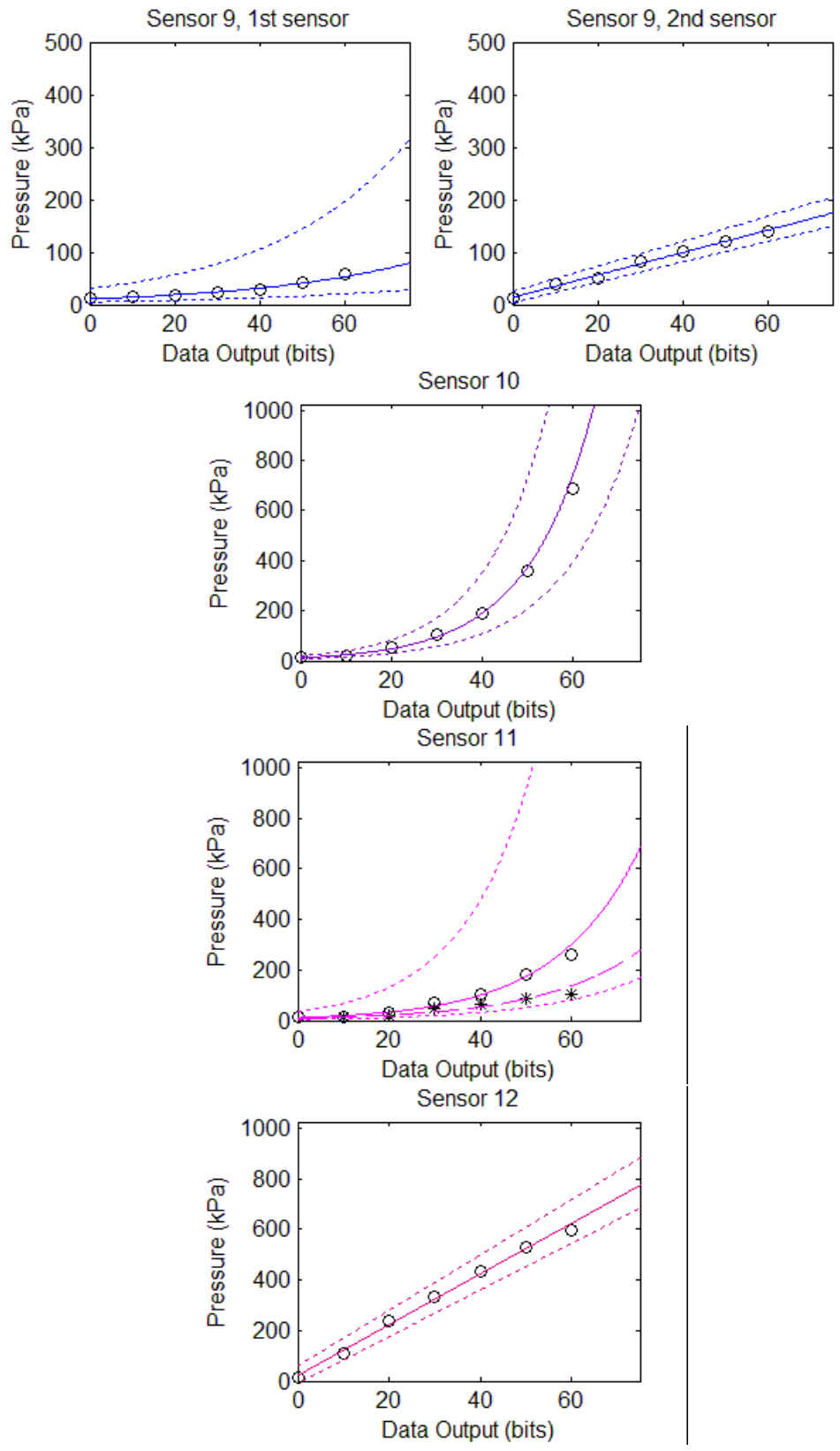


APPENDIX E: CALIBRATION CURVES

Calibration curves for each sensor are given below. They are plotted by raw data in circles, fit curve in solid line, and 95% confidence bounds in dashed lines. When two different sensors were used, both curves are plotted side by side. When the sensor survived the entire duration of the human subject experiments, they were calibrated after the experiment to evaluate their consistency in response. The secondary calibration is plotted in asterisk and its fit curve in a dash line. Note that sensors 6, 9, 11, and 12 are plotted on the y-axis over the full range of sensor response. These sensors were the most sensitive.







APPENDIX F: DERIVATION OF EQUATION GOVERNING SENSOR DISCRIMINATION

The calibrated response of a sensor is given by:

$$y_i = \alpha_1 \ln x_i + \alpha_0 \quad (\text{F.1})$$

where y is the pressure response, β_1 and β_0 are the coefficients fit to the response, and x is the output from the sensor, read in bits of voltage from 0-1024. The difference between each change in bit response corresponds to the minimal detectable change in pressure, or the discrimination of the system. Thereby:

$$D = y_{i+1} - y_i = (\alpha_1 \ln(x_i + 1) + \alpha_0) - (\alpha_1 \ln(x_i) + \alpha_0) \quad (\text{F.2})$$

Simplifying equation F.2 yields:

$$D = \alpha_1 \ln \left(\frac{x_i + 1}{x_i} \right) \quad (\text{F.3})$$

Rearranging F.3 to solve for the bit at which D will equal 1 kPa gives the equation found in Chapter 4:

$$\begin{aligned} \frac{D}{\alpha_1} &= \ln \left(\frac{x_i + 1}{x_i} \right) \\ e^{D/\alpha_1} &= \left(\frac{x_i + 1}{x_i} \right) \\ x \left(e^{D/\alpha_1} - 1 \right) &= 1 \\ x &= \frac{1}{\left(e^{D/\alpha_1} - 1 \right)} \end{aligned} \quad (\text{F.4})$$

Using the fit coefficient for each curve and setting D equal to 1 will give the bit response x , and the corresponding pressure at which resolution of the sensor is equal to 1kPa.

APPENDIX G: POLIPO MATERIALS, MANUFACTURERS, AND CHARACTERISTICS

MATERIALS LIST MIT Pressure Sensing Garment Platform Mark III - 4.3 psid - Breathing Air - Ground based (B34)				
ITEM	MATERIAL	THICKNESS/SPEC	MANUFACTURER	PART NUMBER
Sensor Garment				
Fabric	Tess Carezza Soft Garzato - Nylon lycra blend	130 g/m2	Sitip	
	Veluntino Bielastico - Polyester lycra blend	235 g/m2	Acc. Asolana	

Cover Shirt	Piave - 9300 PA (nylon) 71% EA (elastomer) 29%	Anti-catch weave	Sitip	
Thread	Nylon and lycra blend	60	Coats	
Cuff and Sensor backing	Silicon	.4mm	Bernis	
Zipper	Cotton	-	Opti	
	Plastic	-	Opti	
Targets	Vinyl Heat Transfer	.1mm	Loris Sport	
Neck pad	Neoprene	2mm	Res	
Polipo Sensor System				
Sensor				
> Silicon	Ecoflex 0030 - Silicone Elastomer	MSDS 844	Smooth-On	
> Conductive metal	Gallinstan - Gallium Indium Tin Eutectic	HMIS rating: 1, 0, 1	Alfa Aesar	
> Flex circuit	Copper coated Kapton	.1mm	-	
Sensor Housing				
> Claw fabric	3 Storm 3 Layer (Gortex) - Polyurethane and Polyester	250 Microns	Gore	
> Claw velcro rim	Nylon	.7mm	Velcro	
> Claw velco back	Nylon	.8mm	Velcro	
> Hot glue	Hot Melt Glue	Softens at 80C	FPC Corporation	
> Wire	Copper and Polyester	.68 ohms/met er	Technospir	
> Wire cover	Polyolefin	1.2-.6 mm diameter	Elematic	
> Wire fabric	Tess 0917 Charmeus - Nylon lycra blend	150 g/m2	Spac	
	Tess Carezza Soft Garzato - Nylon lycra blend	130 g/m2	Sitip	
> Fabric glue	Web 35 - Polyurethane	35 g/cm2	Spac	
> Claw velco back	Nylon	.8mm	Velcro	
> Numbers	Vynl Heat Transfer	.1mm	Loris Sport	

Electronics				
> Plastic box and clips	ABS thermoplastic polymer, Terluran GP 35	Custom built	Dainese	
> Sealing Foam	Memory 15	3mm	Astrotech	
> Screws	Steel	3/4"		
> Elastic	Latex and Cotton			
> Header pin metal	Copper alloy with gold flash	2.54 mm spacing	SparkFun	
> Header pin plastic	ABS electrical grade	2.54 mm spacing	SparkFun	
> Electronics board	PCB, fiberglass epoxy laminant with copper leads	Custom built	Screaming Circuits	
> Solder	Copper, Tin, Silver	MSDS 4900	MG Chemicals	
> Connectors pins metal	Brass alloy with gold plated leads	2.54 mm spacing	Digi-Key, Mill-Max Manufacturing Corp.	
> Connectors pins plastic	PCT Polyester	2.54 mm spacing	Digi-Key, Mill-Max Manufacturing Corp.	CG933 Thermx
> 9V battery	Alkaline	9V	Duracell	

APPENDIX H: HAZARD ANALYSIS

The following is the list of Hazards identified for testing inside the confined environment of the space suit. All Hazards were mitigated to an acceptable level prior to the experiment.

1.1 Hazard Summary

This Hazard Analysis addresses potential hazards associated with the integrated test setup for the Human-Suit Pressure Evaluation Test. Hazards generically associated with the manned use of the Mark III Suit itself are addressed in CTSD-ADV-590, "Hazard Analysis for the Mark III Suit Space Suit Assembly (SSA) Used in One-g Operations." Below is the hazard summary list for this test.

POTENTIAL HAZARDS
SEVERITY/PROBABILITY/RAC

BEFORE CONTROLS AFTER

CONTROLS

- | | | | |
|----|-------------------------------|---------|---------|
| 1. | Subject Overheating | IV/B/4 | IV/D/6 |
| 2. | General Personnel Injury | II/C/3 | II/D/4 |
| 3. | Electrical Shock | II/D/4 | II/E/5 |
| 4. | Battery Failure | IV/D/6 | IV/E/7 |
| 5. | Subject-Borne Bulk | I/D/3 | I/E/4 |
| 6. | Hammering | III/B/3 | III/D/5 |
| 7. | Loss of Habitable Environment | II/D/4 | IV/D/6 |

Hazard Analysis – Subject Overheating

Nr.	HAZARD	CAUSE	EFFECT	Sev./Prob./RAC (before controls)	CONTROLS	VERIFICATION	DISPOSITION Sev./Prob./RAC (after controls)
1.	Subject Overheating	Inhibited cooling due to addition of sensing garment underneath the LCVG Overexertion	Personnel Injury	IV/B/4	<p>Minimum five minutes of rest is enforced between each group of functional tasks</p> <p>Subject can rest for additional time beyond the scheduled time if required</p> <p>Subject will be queried for subjective feedback at the completion of each task</p> <p>Subjects are experienced with recognizing need for increased cooling or additional rest</p> <p>Pilot testing conducted in pressurized suit at non-NASA facility demonstrated adequate cooling without use of any LCG</p>	<p>CTSD-ADV-1093, Section 6.2, "Detailed Test Procedures (Suited Run)"</p> <p>CTSD-ADV-1093, Section 6.2, "Detailed Test Procedures (Suited Run)"</p> <p>CTSD-ADV-1093, Section 6.2, "Detailed Test Procedures (Suited Run)"</p> <p>CTSD-ADV_1093, Section 5.5 "Subject Selection"</p> <p>CTSD-ADV_1093, Section 1.3 "Experiment Pilot Study"</p>	Controlled IV/D/6

Hazard Analysis - General Personnel Injury

Nr.	HAZARD	CAUSE	EFFECT	<u>Sev./Prob</u> <u>/RAC</u> (before controls)	CONTROLS	VERIFICATION	<u>Sev./Prob./RA</u> <u>C</u> (after controls)
2.	Slips, trips, falls	Subject performing tasks for which they do not have extensive previous experience Props used in functional tasks not normally in B34 posing trip hazards	Personnel injury Equipment damage	II/C/3	Test personnel will be reminded to monitor tubes, cords and task props at all times Tasks have been designed for similarity to existing common suited tasks when possible Test equipment will be arranged to minimize trip hazards and maximize suit technician access to suited test subjects at all times Only subjects with extensive experience in suits will be selected for this testing Subjects will participate in unsuited task familiarization session and practice each task (suited) before every suited test run	CTSD-ADV-1093, Section 6.1, "Test-Specific Pre-Test Safety Briefing" CTSD-ADV-1093, Section 5.3, "Functional Tasks and Supporting Equipment" CTSD-ADV-1093, Section 5.3, "Functional Tasks and Supporting Equipment" CTSD-ADV-1093, Section 5.5, "Subject Selection" CTSD-ADV-1093, Section 6.2, "Detailed Test Procedures (Suited Run)"	Controlled II/D/4

Hazard Analysis – Battery Failure

Nr.	HAZARD	CAUSE	EFFECT	<u>Sev./Prob</u> <u>/RAC</u> (before controls)	CONTROLS	VERIFICATION	<u>Sev./Prob./RA</u> <u>C</u> (after controls)
3.	Battery failure	Novel pressure sensor batteries Polipo pressure sensor batteries APDM Opal IMU sensor batteries	Personnel Injury Equipment Damage	II/D/4	Unlikely water or sweat will come into contact with the electronics board of the battery pack The <u>pedar</u> NiMH 2000mAh battery pack is internally secured with an overheating and an overcurrent protection (<u>Polyswitch</u>) <u>Polipo</u> battery is a standard 9V commercially available single-use battery contained within sealed case APDM Opal safety precautions include aluminum base to protect the subject, battery protection circuit, safe charging features. Minimum of TCU and substrate sensing garment are between battery case and subject's skin Minimum of sensing garment cover and LCVG are between battery case and suit hardware	Technical documentation submitted in associated TRR package "Human-Suit Pressure Evaluation" Technical documentation submitted in associated TRR package "Human-Suit Pressure Evaluation" CTSD-ADV-1093, Section 4.0 "Suit and Test Configurations" Technical documentation submitted in associated TRR package "Human-Suit Pressure Evaluation" CTSD-ADV-1093, Section 4.0 "Suit and Test Configurations" CTSD-ADV-1093, Section 4.0 "Suit and Test Configurations"	Controlled II/E/5

Hazard Analysis – Low Voltage Shock

Nr.	HAZARD	CAUSE	EFFECT	Sev./Prob / RAC (before controls)	CONTROLS	VERIFICATION	DISPOSITION Sev./Prob./RAC (after controls)
4.	Low voltage	<p>Novel pressure sensor batteries and electronics</p> <p>Polipo pressure sensor batteries and electronics</p> <p>APDM Opal IMU sensor batteries and electronics</p> <p>Moisture entering an electronic component</p> <p>Inadvertent disconnect or breakage</p>	Electrical shock	IV/D/6	<p>All electronic components are separated from the body by at least two layers of fabric.</p> <p>A worst case scenario for Novel pressure sensor is a pad puncture exposing the subject to AC voltage and current of 20 Vpp @ 100 mA.</p> <p>Shorting the Polipo sensor wires of one circuit will result in ~.5mA through the short. Max current ~1.1mA if a sensor is shorted through another's sink wire. A worst case scenario shorting all 12 circuits gives ~6mA and is highly unlikely.</p> <p>Electrical schematics reviewed for safety by NASA personnel.</p> <p>The APDM Opal battery is 3.7V with a nominal current draw estimated at 56mA.</p> <p>Two commercially purchased sensor</p>	<p>CTSD-ADV-1093, Section 6.2, "Detailed Test Procedures (Suited Run)"</p> <p>Calculations and NASA review thereof submitted in associated TRR package "Human-Suit Pressure Evaluation"</p> <p>Calculations and NASA review thereof submitted in associated TRR package "Human-Suit Pressure Evaluation"</p> <p>Email correspondence submitted in associated TRR package "Human-Suit Pressure Evaluation"</p> <p>Calculations and NASA review thereof submitted in associated TRR package</p> <p>Supporting photos and</p>	IV/E/7

Nr.	HAZARD	CAUSE	EFFECT	Sev./Prob / RAC (before controls)	CONTROLS	VERIFICATION	DISPOSITION Sev./Prob./RAC (after controls)
					<p>systems are in closed cases. Polipo electronics and battery cases are closed. Incidental water entry into any electronics is unlikely. Shock due to all systems is covered in this hazard.</p> <p>Polipo and Novel cords have long length to accommodate movement. APDM system requires no cords.</p> <p>Wire leads at Polipo sensor connect held rigidly in place to prevent short. If contact occurs, wires provide sufficient resistance to prevent full short.</p>	<p>documentation provided in the associated TRR package</p> <p>CTSD-ADV-1093, Section 4.0, "Suit and Test Configuration"</p> <p>Supporting photos provided in the associated TRR package</p>	

Hazard Analysis – Subject-Borne Bulk

Nr.	HAZARD	CAUSE	EFFECT	Sev./Prob / RAC (before controls)	CONTROLS	VERIFICATION	DISPOSITION Sev./Prob./RAC (after controls)
5.	Subject-borne bulk	Increased subject-borne hardware above that of normal testing	Bruising or other repetitive injuries Decreased ability for emergency extraction and prompt medical attention in event of an emergency	I/D/3	Pilot testing conducted in pressurized suit at non-NASA facility demonstrated sufficient space and no significant issues associated with subject-bom hardware Subjects are experienced with suit hardware and will be more likely to recognize hardware impingement/comfort issues STE and suit techs briefed to cut through sensing garment components if necessary in an emergency Data acquisition systems and battery packs for pressing sensing components mounted at the base of the back, within reach of open rear hatch of the Mark III	Memo provided in associated TRR package CTSD-ADV-1093, Section 5.5 "Subject Selection" CTSD-ADV-1093, Section 6.1 "Test-Specific Pre-Test Safety Briefing" CTSD-ADV-1093, Section 4.0 "Suit and Test Configurations"	IE/4

Hazard Analysis – Hammering

Nr.	HAZARD	CAUSE	EFFECT	Sev./Prob / RAC (before controls)	CONTROLS	VERIFICATION	DISPOSITION Sev./Prob./RAC (after controls)
6.	Hammering	Suited subject swinging hammer repeatedly during testing	Personnel injury Property damage	III/B/3	Hammer used in testing will be rubber mallet provided by ASL Hammer will employ use of wrist strap for safety during testing	CTSD-ADV-1093, Section 4.0 "Suit and Test Configurations" CTSD-ADV-1093, Section 4.0 "Suit and Test Configurations"	III/D/5

Hazard Analysis – Loss of Habitable Environment

Nr.	HAZARD	CAUSE	EFFECT	Sev./Prob / RAC (before controls)	CONTROLS	VERIFICATION	DISPOSITION Sev./Prob./RAC (after controls)
7.	Loss of Habitable Environment	Use of unsafe materials inside suit pressure envelope Rupture of low pressure sensor liquid	Personnel injury Property damage	II/D/4	All materials placed inside the suit submitted and approved by NASA Personnel <u>Polipo</u> sensor material replaced by similar liquid, <u>Gallinstan</u> . Not a hazardous material	Supporting materials provided in the associated TRR package MSDS sheet provided in the associated TRR package	IV/D/6

APPENDIX I: EXPERIMENTAL PROCEDURES

To ensure each subject was given the same instructions for performing the experiment, the following script was used as a guide to explain the experimental tasks and procedures.

Thank you for participating in our study. We are studying how the human and space suit interact. Currently there are no metrics by which to measure the space suit internally. We will use a series of three sensor systems: One pressure mat placed over the shoulder, a network of 12 sensors distributed over the arm, and a series of inertial measurement units (IMU’s) mounted both on your body and on the space suit. In addition to the sensor measurements, we will also be taking video data from two cameras and audio recordings. In this experiment you will perform a series of 5 motions. Three of those motions are isolated joint movements, meaning you only move one joint in the directed way to perform the movement. The other two are functional tasks, meaning we will give you a task to perform, some basic instructions, but you may complete the movement in the way that is best for you. After the tasks we will ask you for subjective feedback to assess your fatigue, areas of pressure discomfort, and how consistent you felt you were with your movements. You may stop the test at any point for any reason. We will have test personnel to assist you in moving and in making sure the floor is clear for you as you move. Please read this informed consent carefully. Let me know if you have any questions before signing on the back.

TEST SPECIFIC SAFETY BRIEFING

EXPLAIN IMU CALIBRATION MOVEMENTS

After you have completed the IMU calibration, you will begin the experiment. I’ll now explain the 5 tasks and allow you to practice.

Elbow Flexion/Extension

The subject stands away from the donning stand supported by their own effort. Beginning with both arms relaxed at their side, palms facing anterior, the subject bends the arms at the elbow through their maximum range of motion. The subject then releases to the relaxed position.

Shoulder Flexion/Extension

The subject stands away from the donning stand supported by their own effort. Beginning with both arms relaxed at their side, the subject bends the arms at the shoulder through the sagittal plane. The subjects move through their maximum range of motion. The subject then releases to the relaxed position.

Shoulder Abduction/Adduction

The subject stands away from the donning stand supported by their own effort. Beginning with both arms relaxed at their side, the subject bends the arms at the shoulder through the coronal plane. The subject moves through his or her maximum range of motion. The subject then releases to the relaxed position.

Cross Body Reach

The subject stands away from the donning stand supported by their own effort. Beginning with both arms relaxed at their side, the subject will reach across their body in an attempt to touch their hip on the opposite side. The subject will then move their arm up to chest level and sweep their arm in front of their body in the horizontal plane. When the arm is extended straight in front of the shoulder, the subject will then attempt to touch the helmet at the position of their ear on the same side. The movement is then repeated with the opposite arm.

Overhead Hammering

The subject stands away from the donning stand supported by their own effort. Subjects will be given a rubber mallet to be grasped with both hands. The subject will be instructed to hammer flat 7" rubberized square pads, which are fixed to a repurposed ergometer stand, using the mallet. The pads will be fixed in a horizontal orientation at 39" height and the subject will hammer with both hands beginning the movement overhead and ending at the height of the stand (approximately waist level).

I will give you a random order in which to perform these tasks. You will repeat the movement 4 times. Try to be consistent each time in your movement. For the isolated joint movements, try to move through your full range of motion. After you have done each task 4 times, you will move back to the donning stand and rest for 5 minutes. This is when we will ask you for subjective feedback. You may also provide subjective feedback between each task. After your rest, you will perform each of the 5 motions with 4 repetitions, this time in a new order. Again, you will rest for 5 minutes and give subjective feedback. The entire process is repeated again for a 3rd time, or a total of 12 repetitions of the movement. If you need additional rest at any point, just let me know. The total test time is estimated at 80 minutes.

After the pressurized test is done, we will ask you to do the movement series again, unsuited. This will allow us to take "baseline data" so we can know the effect of movement on any sensor readings. We will ask you to attempt to perform the movement in the same way you did suited. We will provide you with feedback as to how quickly or slowly you did the movement on average.

Do you have any questions about the experiment?

The full checklist of experimental procedures is as follows:

6.0 DETAILED TEST PROCEDURES

6.1 Test-Specific Pre-Test Safety Briefing

1. Anyone can stop this test at any time for any reason
2. Test personnel: Manage video camera, extension cords and functional task props at all times.
3. Test personnel: You may remove the internal sensor systems by any means necessary in an emergency situation, including cutting or destroying the pressure sensing hardware.
4. Suited Subject: We will ask you how you're feeling between each task, absent any other reports from you. After each series of 5 tasks, which will last approximately 2 minutes each for a total of 10 minutes, you will rest for at least 5 minutes.

6.2 Detailed Test Procedure (Suited Run)

1. _____ Review summary of test with subject
2. _____ Conduct test-specific pre-test safety briefing, including electrical hazards awareness and test termination if any electrical sensation is experienced
3. _____ Explain IMU calibration movements to the subject
4. _____ Explain functional task movements to the subject and allow them to practice
5. _____ Turn on video cameras
6. _____ Test personnel places IMUs on the subject's arm and body and notes location on the body. IMU 1: Chest _____ IMU 2: Upper Arm _____ IMU 3: Lower Arm _____
7. _____ Subject dons pressure sensing systems
8. _____ Pressure sensing systems are turned on and data collection is initiated
9. _____ Subject dons cover shirt
10. _____ Subject dons LCG
11. _____ Subject performs IMU calibration movements (4 repetitions)
 - a. _____ Wrist pronation/supination to 180 degrees
 - b. _____ Elbow flexion/extension to 90 degrees
 - c. _____ Shoulder flexion/extension to 90 degrees

- d. ___ Shoulder abduction/adduction to 90 degrees
- 12. ___ Data is collected for 30 seconds to obtain baseline resting values for sensors
- 13. ___ Subject dons suit per CTSD-ADV-197 (Mark III)
- 14. ___ ASL technicians pressurize suit to 4.3 psi at 6 ACFM (gauge indicated: 10 SCFM) flow rate per CTSD-ADV-197. Instruct suited subject to rest during this time as much as possible
- 15. ___ Test personnel places IMUs on the suit's arm and body and notes location on the body. IMU 4: Torso ___ IMU 5: Suit Upper Arm ___ IMU 6: Suit Lower Arm ___
- 16. ___ Subject performs IMU calibration movements (5 repetitions)
 - a. ___ Wrist pronation/supination to 180 degrees
 - b. ___ Elbow flexion/extension to 90 degrees
 - c. ___ Shoulder flexion/extension to 90 degrees
 - d. ___ Shoulder abduction/adduction to 90 degrees

Resting Data Collection

- 1. ___ ASL technicians assist subject in moving from donning stand to functional task area
- 2. ___ Call out global time
- 3. ___ Data is collected for 30 seconds to obtain baseline resting values for sensors

NOTE: Instruct subject to complete these tasks at what they consider to be a natural pace

NOTE: Request a report of any symptoms from suited subject after each task and ask qualitative questions from Appendix B during the 5-minute rest periods.

Suited Familiarization Session

- 1. ___ Call out global time
- 2. ___ Subject practices elbow flexion/extension
- 3. ___ Subject practices shoulder flexion/extension
- 4. ___ Subject practices shoulder abduction/adduction

5. ____ Subject practices hammering task
6. ____ Subject practices cross body reach task
7. ____ Call out global time

NOTE: Subject may return to donning stand for rest if necessary at any point

8. ____ Subject returns to donning stand for rest (at least two minutes)
9. ____ Subjective comfort and fatigue data collected from Appendix B.

Suited Data Collection Run

NOTE: The subject completes 4 repetitions of the task. Time is not limited, but the task may be terminated if the subject is unable to complete 4 repetitions.

NOTE: Five minute break (minimum) is enforced between each group of movement tasks. Allow suited subject to take additional rest time as needed.

NOTE: Subject task order is counterbalanced for each subject and each movement run. The task order is provided in Appendix A.

10. ____ ASL technicians assist subject in moving from donning stand to functional task area
11. ____ Call out global time
12. ____ Subject performs elbow flexion/extension task
 - a. Time to completion: 1) _____ 2) _____ 3) _____
 - b. ____ Prompt for subjective feedback
13. ____ Call out global time
14. ____ Subject performs shoulder flexion/extension task
 - a. Time to completion: 1) _____ 2) _____ 3) _____
 - b. ____ Prompt for subjective feedback
15. ____ Call out global time
16. ____ Subject performs shoulder abduction/adduction task
 - a. Time to completion: 1) _____ 2) _____ 3) _____
 - b. ____ Prompt for subjective feedback
17. ____ Call out global time
18. ____ Subject performs cross body reach task

- a. Time to completion: 1) _____ 2) _____ 3) _____
 - b. _____ Prompt for subjective feedback
19. _____ Call out global time
20. _____ Subject performs overhead hammering task
- a. Time to completion: 1) _____ 2) _____ 3) _____
 - b. _____ Prompt for subjective feedback
21. _____ ASL technicians assist subject in returning to the donning stand
22. _____ Subjective comfort and fatigue data collected from Appendix B
23. _____ Data collection is repeated twice
24. _____ Return to CTSD-ADV-197 (Mark III) for suit depressurization and doffing
25. _____ External IMUs removed from suit
26. _____ Subject remains in LCVG with pressure sensors and IMUs in place

6.3 Detailed Test Procedure (Unsuited Run)

1. _____ Review summary of test with subject
2. _____ Conduct test-specific pre-test safety briefing
3. _____ Test personnel confirms by feel the IMU placement on the subject's arm and body and notes any changes
 - a. IMU 1: Chest _____
 - b. IMU 2: Upper Arm _____
 - c. IMU 3: Lower Arm _____
4. _____ Subject performs IMU calibration movements (4 repetitions)
 - a. ___ Wrist pronation/supination to 180 degrees
 - b. ___ Elbow flexion/extension to 90 degrees
 - c. ___ Shoulder flexion/extension to 90 degrees
 - d. ___ Shoulder abduction/adduction to 90 degrees
5. _____ Call out global time

6. ____ Data is collected for 30 seconds to obtain baseline resting values for sensors

NOTE: Request a report of any symptoms from suited subject during the 2-minute rest periods if subject does not provide comments

Unsuited Familiarization Session

NOTE: Instruct the subject to try and recreate the movements they performed inside the pressurized space suit. Provide subject with aids such as task repetition interval (“You completed this task in approximately X seconds per repetition”) to help them best match suited Mark III run cadence.

1. ____ Call out global time
2. ____ Subject practices elbow flexion/extension
3. ____ Subject practices shoulder flexion/extension
4. ____ Subject practices shoulder abduction/adduction
5. ____ Subject practices hammering task
6. ____ Subject practices cross body reach task
7. ____ Subject returns to resting area (at least two minutes)
8. ____ Subjective comfort and fatigue data collected from Appendix B

Unsuited Data Collection Run

7. ____ Subject is moved in line with both GoPro cameras
8. ____ Call out global time
9. ____ Subject performs elbow flexion/extension task
 - a. Time to completion: 1) _____
 - b. ____ Prompt for subjective feedback
10. ____ Call out global time
11. ____ Subject performs shoulder flexion/extension task
 - a. Time to completion: 1) _____
 - b. ____ Prompt for subjective feedback
12. ____ Call out global time
13. ____ Subject performs shoulder abduction/adduction task

- a. Time to completion: 1) _____
- b. _____ Prompt for subjective feedback
- 14. _____ Call out global time
- 15. _____ Subject performs cross body reach task
 - a. Time to completion: 1) _____
 - b. _____ Prompt for subjective feedback
- 16. _____ Call out global time
- 17. _____ Subject performs overhead hammering task
 - a. Time to completion: 1) _____
 - b. _____ Prompt for subjective feedback
- 18. _____ Subjective comfort and fatigue data collected from Appendix B
- 19. _____ Subject returns to non-testing area for sensing system doffing and debrief

APPENDIX J: INFORMED CONSENT

The following form was approved by the MIT Committee on the Use of Humans as Subjects and was signed by each subject prior to the experiment.

CONSENT TO PARTICIPATE IN BIOMEDICAL RESEARCH

Advanced Spacesuit Design

You are asked to participate in a research study conducted by Prof Dava Newman, and her associated investigators from the Department of Aeronautics and Astronautics at the Massachusetts Institute of Technology (M.I.T.). You have been asked to participate in this study because of your interest in spacesuit design, your willingness to try on garment prototypes, no known history of cardiovascular, neurovestibular or pulmonary abnormalities, nor any allergies to latex/silicone-based medical-grade skin adhesives. You

should read the information below, and ask questions about anything you do not understand, before deciding whether or not to participate.

- **PARTICIPATION AND WITHDRAWAL**

Your participation in this research is completely VOLUNTARY. If you choose to participate you may subsequently withdraw from the study at any time without penalty or consequences of any kind. If you choose not to participate, that will not affect your relationship with M.I.T. or your right to health care or other services to which you are otherwise entitled.

- **PURPOSE OF THE STUDY**

The purpose of this research is to assess the effectiveness of advanced space suit designs. In order to quantify this accurately, it is necessary to test suit pieces by reducing the pressure around the garment enclosed areas of the limb, or to test in positively pressurized full body space suits.

- **PROCEDURES**

If you volunteer to participate in this study, we would ask you to do the following things:

Vacuum Chamber Tests:

- ⇒ We will place your limb in a low-pressure chamber with or without a compression garment.
- ⇒ If a compression garment is worn, pressure sensors will be located between the garment and skin in multiple places along the limb so as to measure the pressure distribution in static positions as well as throughout a range of motion. This data will be captured as a function of time so as to find any variations throughout the depressurizing process or range of motion.
- ⇒ The chamber will be slowly depressurized, and compression data recorded by sensors.
- ⇒ You will notify the test director if any discomfort or pain is experienced, in which case the chamber will be brought back to 1 atm and/or the compression garment will be removed. The low-pressure chamber is equipped with a pressure relief valve that can be activated manually by the subject or test director. Pressure measurements will also be monitored real time in order to locate any high or low pressure points.
- ⇒ You will be asked to make a series of movements, which will be repeated 10 times. After each session, assuming the successful completion of the previous session, either the time of exposure to vacuum will be increased, until a period of four or more hours is reached, or you will be asked to perform a new series of movements. At all times the test director will always have as first priority in watching over the subject and seeing to their safety.
- ⇒ You are free to terminate the experiment immediately, at any time, for any reason.

Suit loading tests:

- ⇒ You will don a space suit or space suit component. Prior to the test, you will be fully briefed on the suit, it's function, safety procedures, and given a fit check to ensure maximum comfort.

- ⇒ Pressure sensors will be located between the garment and skin in multiple places along the limb so as to measure the pressure distribution in static positions as well as throughout a range of motion. This data will be captured as a function of time so as to find any variations throughout the depressurizing process or range of motion.
- ⇒ The space suit will be slowly pressurized, and compression data recorded by sensors.
- ⇒ You will notify the test director if any discomfort or pain is experienced, in which case the space suit will be brought back to 1 atm and/or the space suit will be removed. Pressure measurements will also be monitored real time in order to locate any high or low pressure points.
- ⇒ You will be asked to make a series of movements, which will be repeated 10 times. After each session, assuming the successful completion of the previous session, you will be asked to perform a new series of movements. At all times the test director will always have as first priority in watching over the subject and seeing to their safety.
- ⇒ You are free to terminate the experiment immediately, at any time, for any reason.

- **POTENTIAL RISKS AND DISCOMFORTS**

There are no known benefits to the individual subject for participation in this study.

There is a minimal risk from participation in this experiment. Safety precautions will always be the primary consideration. Exposure to underpressure can lead to minor swelling, pain, or edema if prolonged for a considerable period of time. Typically these effects wear off with time (a few hours). Should you experience pain, the chamber can be rapidly repressurized manually via a pressure relieve valve operated by either the subject or the test director. There are no negative effects associated with over pressurization at the level of this study.

If you have any history of cardiovascular, neurovestibular, or pulmonary abnormalities, or any allergies to latex/silicone-based medical-grade skin adhesives, you must notify the test director.

Your exposed limbs will be inspected immediately before and after test sessions. As the possible negative effects of underpressure are immediately evident, these inspections should be adequate in determining any side effects of the experiment. You will contact the MIT Medical Department as well as the test director immediately if any prolonged pain occurs.

The treatment or procedure may involve risks that are currently unforeseeable.

- **ANTICIPATED BENEFITS TO SUBJECTS**

There are no known benefits to the subject for participation in this study.

- **ANTICIPATED BENEFITS TO SOCIETY**

Society may benefit from the development of a spacesuit that will enable humans enough mobility to explore the surface of Mars or the Moon.

- **ALTERNATIVES TO PARTICIPATION**

You may choose not to participate in this research experiment.

- **PAYMENT FOR PARTICIPATION**

You will not receive payment for participation in this study.

- **FINANCIAL OBLIGATION**

Neither you nor your insurance company will be billed for your participation in this research.

- **PRIVACY AND CONFIDENTIALITY**

The only people who will know that you are a research subject are members of the research team and, if appropriate, your physicians and nurses. No information about you, or provided by you during the research will be disclosed to others without your written permission, except: if necessary to protect your rights or welfare, or if required by law.

When the results of the research are published or discussed in conferences, no information will be included that would reveal your identity. If photographs, videos, or audio-tape recordings of you will be used for educational purposes, your identity will be protected or disguised. The results from your participation will be identified by a randomly generated numerical code. These results will be stored on a laptop computer and a back-up hard drive and secured in a locked office of the Man Vehicle Lab. When the data analysis and study are complete, the results will be moved to CD or DVD and filed in the office of the Principle Investigator. The results will always remain anonymous, and always referred to by the numerical code.

- **WITHDRAWAL OF PARTICIPATION BY THE INVESTIGATOR**

The investigator may withdraw you from participating in this research if circumstances arise which warrant doing so. If you experience any severe pain, skin reaction or circulation reduction, or if you become ill during the research, you may have to drop out, even if you would like to continue. The principal investigator will make the decision and let you know if it is not possible for you to continue. The decision may be made either to protect your health and safety, or because it is part of the research plan that people who develop certain conditions may not continue to participate.

- **NEW FINDINGS**

During the course of the study, you will be informed of any significant new findings (either good or bad), such as changes in the risks or benefits resulting from participation in the research or new alternatives to participation, that might cause you to change your mind about continuing in the study. If new information is provided to you, your consent to continue participating in this study will be re-obtained.

- **EMERGENCY CARE AND COMPENSATION FOR INJURY**

If you feel you have suffered an injury, which may include emotional trauma, as a result of participating in this study, please contact the person in charge of the study as soon as possible.

In the event you suffer such an injury, M.I.T. may provide itself, or arrange for the provision of, emergency transport or medical treatment, including emergency treatment and follow-up care, as needed, or reimbursement for such medical services. M.I.T. does not provide any other form of compensation for injury. In any case, neither the offer to provide medical assistance, nor the actual provision of medical services shall be considered an admission of fault or acceptance of liability. Questions regarding this policy may be directed to MIT's Insurance Office, (617) 253-2823. Your insurance carrier may be billed for the cost of emergency transport or medical treatment, if such services are determined not to be directly related to your participation in this study.

• **IDENTIFICATION OF INVESTIGATORS**

In the event of a research related injury or if you experience an adverse reaction, please immediately contact one of the investigators listed below. If you have any questions about the research, please feel free to contact:

Study Role	Name	Daytime Phone #	Address
Principle Investigator	Prof. Dava Newman	617-258-8799	Rm 33-307, 77 Massachusetts Ave, Cambridge, 02139.
Co-Investigator	Prof. Jeff Hoffman	617-252-2253	Rm 37-227, 77 Massachusetts Ave, Cambridge, 021

• **RIGHTS OF RESEARCH SUBJECTS**

You are not waiving any legal claims, rights or remedies because of your participation in this research study. If you feel you have been treated unfairly, or you have questions regarding your rights as a research subject, you may contact the Chairman of the Committee on the Use of Humans as Experimental Subjects, M.I.T., Room E25-143B, 77 Massachusetts Ave, Cambridge, MA 02139, phone 1-617-253 6787.

SIGNATURE OF RESEARCH SUBJECT OR LEGAL REPRESENTATIVE

I have read (or someone has read to me) the information provided above. I have been given an opportunity to ask questions and all of my questions have been answered to my satisfaction. I have been given a copy of this form.

BY SIGNING THIS FORM, I WILLINGLY AGREE TO PARTICIPATE IN THE RESEARCH IT DESCRIBES.

Name of Subject

Name of Legal Representative (if applicable)

Signature of Subject or Legal Representative

Date

SIGNATURE OF INVESTIGATOR

I have explained the research to the subject or his/her legal representative, and answered all of his/her questions. I believe that he/she understands the information described in this document and freely consents to participate.

Name of Investigator

Signature of Investigator

Date (must be the same as subject's)

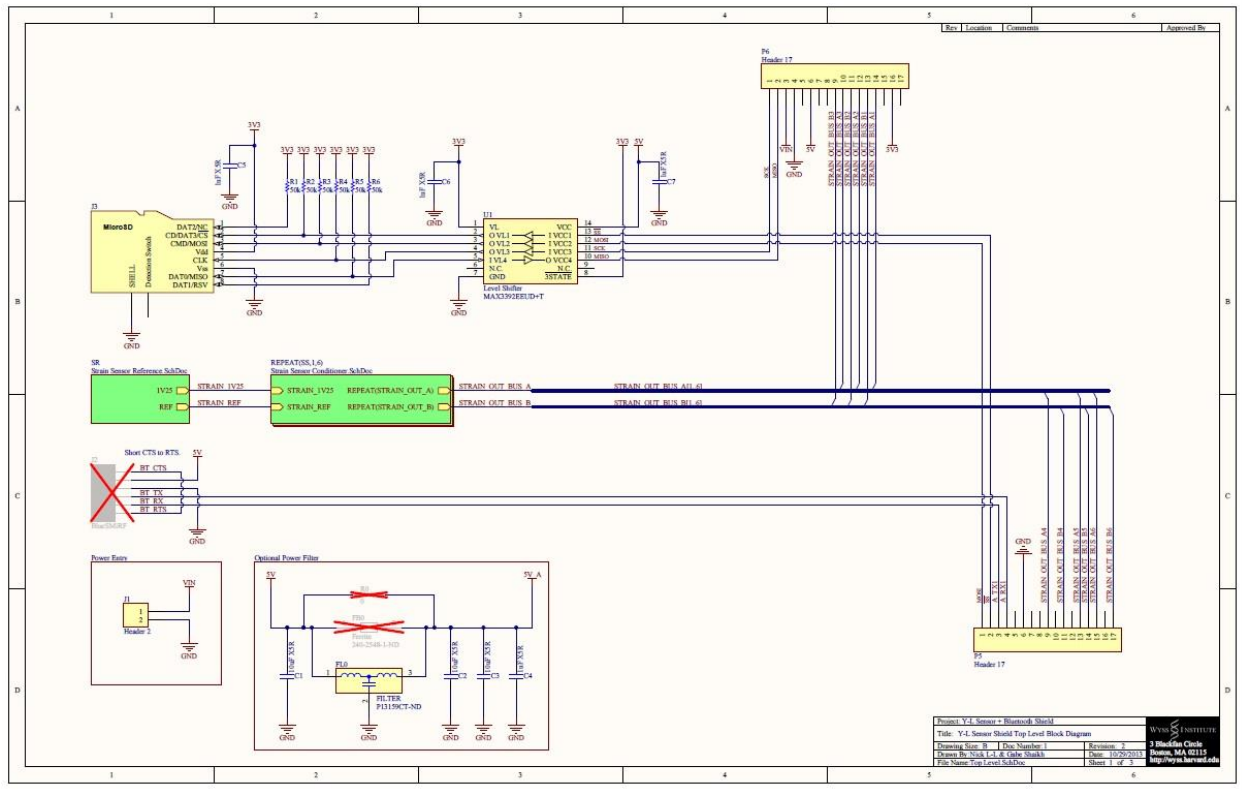
SIGNATURE OF WITNESS (If required by COUHES)

My signature as witness certified that the subject or his/her legal representative signed this consent form in my presence as his/her voluntary act and deed.

Name of Witness

APPENDIX K: CIRCUIT DIAGRAM FOR CUSTOM POLIPO BOARD

Electrical schematic for the custom made electronics board for the Polipo. The board was designed by researchers at the Wyss Institute for Biologically Inspired Engineering. The board is commanded and powered by an Arduino Micro. Data is logged on a micro SD card. Twelve sensors are set up in a constant current circuit and voltage response is compared to a reference voltage.



APPENDIX L: MATLAB CODE FOR HUMAN SUBJECT EXPERIMENT

L.1 Data Separation, Subject 1

```

close all
clc
%
% % Load the data
% data = importdata('JSC s1 Full test.txt');
% s = size(data);
% time = data(:,s(2))/1000;
% experiment = data(:,1:s(2)-1);
% s2 = size(experiment);
%
% % MOVEMENT GROUPS
%
mg1=[];mg2=[];mg3=[];unsuit=[];t1=[];t2=[];t3=[];t0=[];tups=[];tps=[];teups=[];upstat=[];pstat=[];
eupstat=[];
% for i=1:length(time)
%     if (time(i,1)>202 && time(i,1)<220)
%         upstat=[upstat;experiment(i,:)];
%         tups=[tups;time(i)];

```

```

% elseif(time(i,1)>1292 && time(i,1)<1317)
%   pstat=[pstat;experiment(i,:)];
%   tps=[tps;time(i)];
% elseif (time(i,1)>2035 && time(i,1)<2695)
%   mg1=[mg1;experiment(i,:)];
%   t1=[t1;time(i)];
% elseif (time(i,1)>3275 && time(i,1)<3560)
%   mg2=[mg2;experiment(i,:)];
%   t2=[t2;time(i)];
% elseif (time(i,1)>4075 && time(i,1)<4320)
%   mg3=[mg3;experiment(i,:)];
%   t3=[t3;time(i)];
% elseif (time(i,1)>5167 && time(i,1)<5191)
%   eupstat=[eupstat;experiment(i,:)];
%   teups=[teups;time(i)];
% elseif (time(i,1)>5400 && time(i,1)<5740)
%   unsuit=[unsuit;experiment(i,:)];
%   t0=[t0;time(i)];
% elseif (time(i,1)>5750)
%   break;
% end
% end
%
% %% Individual Motions
% %% 2 seconds on either side
%
% load p_mg_workspace
% elb1=[];elb2=[];elb3=[];elb0=[];elb_t1=[];elb_t2=[];elb_t3=[];elb_t0=[];
% sflex1=[];sflex2=[];sflex3=[];sflex0=[];sflex_t1=[];sflex_t2=[];sflex_t3=[];sflex_t0=[];
% sab1=[];sab2=[];sab3=[];sab0=[];sab_t1=[];sab_t2=[];sab_t3=[];sab_t0=[];
% cbr1=[];cbr2=[];cbr3=[];cbr0=[];cbr_t1=[];cbr_t2=[];cbr_t3=[];cbr_t0=[];
% oh1=[];oh2=[];oh3=[];oh0=[];oh_t1=[];oh_t2=[];oh_t3=[];oh_t0=[];
%
% % MG 1
% for i=1:length(t1)
%   if (t1(i,1)>2664 && t1(i,1)<2685)
%     elb1=[elb1;mg1(i,:)];
%     elb_t1=[elb_t1;t1(i)];
%   elseif (t1(i,1)>2307 && t1(i,1)<2330)
%     sflex1=[sflex1;mg1(i,:)];
%     sflex_t1=[sflex_t1;t1(i)];
%   elseif (t1(i,1)>2522 && t1(i,1)<2550)
%     sab1=[sab1;mg1(i,:)];
%     sab_t1=[sab_t1;t1(i)];
%   elseif (t1(i,1)>2227 && t1(i,1)<2259)
%     cbr1=[cbr1;mg1(i,:)];
%     cbr_t1=[cbr_t1;t1(i)];
%   elseif (t1(i,1)>2036 && t1(i,1)<2053)
%     oh1=[oh1;mg1(i,:)];
%     oh_t1=[oh_t1;t1(i)];
%   end
% end
%
% % MG 2
% for i=1:length(t2)
%   if (t2(i,1)>3341 && t2(i,1)<3364)
%     elb2=[elb2;mg2(i,:)];
%     elb_t2=[elb_t2;t2(i)];
%   elseif (t2(i,1)>3481 && t2(i,1)<3508)
%     sflex2=[sflex2;mg2(i,:)];
%     sflex_t2=[sflex_t2;t2(i)];
%   elseif (t2(i,1)>3521 && t2(i,1)<3549)
%     sab2=[sab2;mg2(i,:)];
%     sab_t2=[sab_t2;t2(i)];
%   elseif (t2(i,1)>3275 && t2(i,1)<3302)
%     cbr2=[cbr2;mg2(i,:)];
%     cbr_t2=[cbr_t2;t2(i)];
%   elseif (t2(i,1)>3422 && t2(i,1)<3441)
%     oh2=[oh2;mg2(i,:)];
%     oh_t2=[oh_t2;t2(i)];
%   end
% end

```

```

% end
%
% % MG 3
% for i=1:length(t3)
%     if (t3(i,1)>4238 && t3(i,1)<4260)
%         elb3=[elb3;mg3(i,:)];
%         elb_t3=[elb_t3;t3(i)];
%     elseif (t3(i,1)>4076 && t3(i,1)<4101)
%         sflex3=[sflex3;mg3(i,:)];
%         sflex_t3=[sflex_t3;t3(i)];
%     elseif (t3(i,1)>4193 && t3(i,1)<4222)
%         sab3=[sab3;mg3(i,:)];
%         sab_t3=[sab_t3;t3(i)];
%     elseif (t3(i,1)>4112 && t3(i,1)<4141)
%         cbr3=[cbr3;mg3(i,:)];
%         cbr_t3=[cbr_t3;t3(i)];
%     elseif (t3(i,1)>4295 && t3(i,1)<4312)
%         oh3=[oh3;mg3(i,:)];
%         oh_t3=[oh_t3;t3(i)];
%     end
% end
% end
%
% % MG 0 - Unsuitd
% for i=1:length(t0)
%     if (t0(i,1)>5403 && t0(i,1)<5423)
%         elb0=[elb0;unsuit(i,:)];
%         elb_t0=[elb_t0;t0(i)];
%     elseif (t0(i,1)>5449 && t0(i,1)<5478)
%         sflex0=[sflex0;unsuit(i,:)];
%         sflex_t0=[sflex_t0;t0(i)];
%     elseif (t0(i,1)>5508 && t0(i,1)<5546)
%         sab0=[sab0;unsuit(i,:)];
%         sab_t0=[sab_t0;t0(i)];
%     elseif (t0(i,1)>5596 && t0(i,1)<5631)
%         cbr0=[cbr0;unsuit(i,:)];
%         cbr_t0=[cbr_t0;t0(i)];
%     elseif (t0(i,1)>5709 && t0(i,1)<5727)
%         oh0=[oh0;unsuit(i,:)];
%         oh_t0=[oh_t0;t0(i)];
%     end
% end
% end

%% Plot each sensor pressure load against time
load p_complete_workspace

figure
subplot(2,2,1)
plot (elb_t1, elb1)
xlabel('Time(s)')
ylabel('Pressure (kPa)')
title('MG1: Elbow Flexion')
subplot(2,2,2)
plot (elb_t2, elb2)
xlabel('Time(s)')
ylabel('Pressure (kPa)')
title('MG2: Elbow Flexion')
subplot(2,2,3)
plot (elb_t3, elb3)
xlabel('Time(s)')
ylabel('Pressure (kPa)')
title('MG3: Elbow Flexion')
subplot(2,2,4)
plot (elb_t0, elb0)
xlabel('Time(s)')
ylabel('Pressure (kPa)')
title('Unsuided Elbow Flexion')

figure
subplot(2,2,1)
plot (sflex_t1, sflex1)
xlabel('Time(s)')

```

```

ylabel('Pressure (kPa)')
title('MG1: Shoulder Flexion')
subplot(2,2,2)
plot (sflex_t2, sflex2)
xlabel('Time(s)')
ylabel('Pressure (kPa)')
title('MG2: Shoulder Flexion')
subplot(2,2,3)
plot (sflex_t3, sflex3)
xlabel('Time(s)')
ylabel('Pressure (kPa)')
title('MG3: Shoulder Flexion')
subplot(2,2,4)
plot (sflex_t0, sflex0)
xlabel('Time(s)')
ylabel('Pressure (kPa)')
title('Unsuited Shoulder Flexion')

```

```

figure
subplot(2,2,1)
plot (sab_t1, sab1)
xlabel('Time(s)')
ylabel('Pressure (kPa)')
title('MG1: Shoulder Abduction')
subplot(2,2,2)
plot (sab_t2, sab2)
xlabel('Time(s)')
ylabel('Pressure (kPa)')
title('MG2: Shoulder Abduction')
subplot(2,2,3)
plot (sab_t3, sab3)
xlabel('Time(s)')
ylabel('Pressure (kPa)')
title('MG3: Shoulder Abduction')
subplot(2,2,4)
plot (sab_t0, sab0)
xlabel('Time(s)')
ylabel('Pressure (kPa)')
title('Unsuited Shoulder Abduction')

```

```

figure
subplot(2,2,1)
plot (cbr_t1, cbr1)
xlabel('Time(s)')
ylabel('Pressure (kPa)')
title('MG1: Crossbody Reach')
subplot(2,2,2)
plot (cbr_t2, cbr2)
xlabel('Time(s)')
ylabel('Pressure (kPa)')
title('MG2: Crossbody Reach')
subplot(2,2,3)
plot (cbr_t3, cbr3)
xlabel('Time(s)')
ylabel('Pressure (kPa)')
title('MG3: Crossbody Reach')
subplot(2,2,4)
plot (cbr_t0, cbr0)
xlabel('Time(s)')
ylabel('Pressure (kPa)')
title('Unsuited Crossbody Reach')

```

```

figure
subplot(2,2,1)
plot (oh_t1, oh1)
xlabel('Time(s)')
ylabel('Pressure (kPa)')
title('MG1: Overhead Hammering')
subplot(2,2,2)
plot (oh_t2, oh2)
xlabel('Time(s)')

```

```

ylabel('Pressure (kPa)')
title('MG2: Overhead Hammering')
subplot(2,2,3)
plot (oh_t3, oh3)
xlabel('Time(s)')
ylabel('Pressure (kPa)')
title('MG3: Overhead Hammering')
subplot(2,2,4)
plot (oh_t0, oh0)
xlabel('Time(s)')
ylabel('Pressure (kPa)')
title('Unsuited Overhead Hammering')

figure
subplot(2,2,1)
plot (tups, upstat)
xlabel('Time(s)')
ylabel('Pressure (kPa)')
title('Unpressurized Static')
subplot(2,2,2)
plot (tps, pstat)
xlabel('Time(s)')
ylabel('Pressure (kPa)')
title('Pressurized Static')
subplot(2,2,3)
plot (teups, eupstat)
xlabel('Time(s)')
ylabel('Pressure (kPa)')
title('End of Test Unpressurized Static')
legend('1', '2', '3', '4', '5', '6', '7', '8', '9', '10', '11', '12')

```

L.2 Data Analysis, Subject 1

```

clear all
close all
clc

load p_complete_workspace
load cal_combined_loglin
lin = [5 6 12];

% average static voltage values
base = mean(upstat, 1);

% subtract out the calibrated zero pressure and this will determine the
% offset to subtract from the normal readings from the polipo
dif = base - zp1';
offset(1,:) = call(:,1)'.*(log(zp1))+call(:,2)';
offset(1,lin) = call(lin,1)'.*(zp1(lin, 1))+call(lin,2)';

color = hsv(12);
color(5,:) = [0 0 0];
color(6,:) = [.75 .75 .75];

figure
subplot(2,2,1)
for i = 1:length(elb1)
    c_elb1(i,:) = call(:,1)'.*(log(elb1(i,:)-dif))+call(:,2)'-offset;
    c_elb1(i,lin) = call(lin,1)'.*(elb1(i,lin)-dif(:,lin))+call(lin,2)'-offset(:,lin);
end
for jj = 1:12
    plot (elb_t1, c_elb1(:,jj), 'Color', color(jj,:))
    hold on
end
xlabel('Time(s)')
ylabel('Pressure (kPa)')
title('MG1: Elbow Flexion')
legend('1', '2', '3', '4', '5', '6', '7', '8', '9', '10', '11', '12')
subplot(2,2,2)

```

```

for i = 1:length(elb2)
    c_elb2(i,:) = call(:,1)'.*(log(elb2(i,:)-dif))+call(:,2)''-offset;
    c_elb2(i,lin) = call(lin,1)'.*(elb2(i,lin)-dif(:,lin))+call(lin,2)''-offset(:,lin);
end
for jj = 1:12
    plot (elb_t2, c_elb2(:,jj), 'Color', color(jj,:))
    hold on
end
xlabel('Time(s)')
ylabel('Pressure (kPa)')
title('MG2: Elbow Flexion')
subplot(2,2,3)
for i = 1:length(elb3)
    c_elb3(i,:) = call(:,1)'.*(log(elb3(i,:)-dif))+call(:,2)''-offset;
    c_elb3(i,lin) = call(lin,1)'.*(elb3(i,lin)-dif(:,lin))+call(lin,2)''-offset(:,lin);
end
for jj = 1:12
    plot (elb_t3, c_elb3(:,jj), 'Color', color(jj,:))
    hold on
end
xlabel('Time(s)')
ylabel('Pressure (kPa)')
title('MG3: Elbow Flexion')
subplot(2,2,4)
for i = 1:length(elb0)
    c_elb0(i,:) = call(:,1)'.*(log(elb0(i,:)-dif))+call(:,2)''-offset;
    c_elb0(i,lin) = call(lin,1)'.*(elb0(i,lin)-dif(:,lin))+call(lin,2)''-offset(:,lin);
end
for jj = 1:12
    plot (elb_t0, c_elb0(:,jj), 'Color', color(jj,:))
    hold on
end
xlabel('Time(s)')
ylabel('Pressure (kPa)')
title('Unsuited Elbow Flexion')

figure
subplot(2,2,1)
for i = 1:length(sflext1)
    c_sflext1(i,:) = call(:,1)'.*(log(sflext1(i,:)-dif))+call(:,2)''-offset;
    c_sflext1(i,lin) = call(lin,1)'.*(sflext1(i,lin)-dif(:,lin))+call(lin,2)''-offset(:,lin);
end
for jj = 1:12
    plot (sflext_t1, c_sflext1(:,jj), 'Color', color(jj,:))
    hold on
end
xlabel('Time(s)')
ylabel('Pressure (kPa)')
title('MG1: Shoulder Flexion')
subplot(2,2,2)
for i = 1:length(sflext2)
    c_sflext2(i,:) = call(:,1)'.*(log(sflext2(i,:)-dif))+call(:,2)''-offset;
    c_sflext2(i,lin) = call(lin,1)'.*(sflext2(i,lin)-dif(:,lin))+call(lin,2)''-offset(:,lin);
end
for jj = 1:12
    plot (sflext_t2, c_sflext2(:,jj), 'Color', color(jj,:))
    hold on
end
xlabel('Time(s)')
ylabel('Pressure (kPa)')
title('MG2: Shoulder Flexion')
subplot(2,2,3)
for i = 1:length(sflext3)
    c_sflext3(i,:) = call(:,1)'.*(log(sflext3(i,:)-dif))+call(:,2)''-offset;
    c_sflext3(i,lin) = call(lin,1)'.*(sflext3(i,lin)-dif(:,lin))+call(lin,2)''-offset(:,lin);
end
for jj = 1:12
    plot (sflext_t3, c_sflext3(:,jj), 'Color', color(jj,:))
    hold on
end
end

```

```

xlabel('Time(s)')
ylabel('Pressure (kPa)')
title('MG3: Shoulder Flexion')
subplot(2,2,4)
for i = 1:length(sflex0)
    c_sflex0(i,:) = call(:,1)'.*(log(sflex0(i,:)-dif))+call(:,2)'-offset;
    c_sflex0(i,lin) = call(lin,1)'.*(sflex0(i,lin)-dif(:,lin))+call(lin,2)'-offset(:,lin);
end
for jj = 1:12
    plot (sflex_t0, c_sflex0(:,jj), 'Color', color(jj,:))
    hold on
end
xlabel('Time(s)')
ylabel('Pressure (kPa)')
title('Unsuited Shoulder Flexion')

figure
subplot(2,2,1)
for i = 1:length(sab1)
    c_sab1(i,:) = call(:,1)'.*(log(sab1(i,:)-dif))+call(:,2)'-offset;
    c_sab1(i,lin) = call(lin,1)'.*(sab1(i,lin)-dif(:,lin))+call(lin,2)'-offset(:,lin);
end
for jj = 1:12
    plot (sab_t1, c_sab1(:,jj), 'Color', color(jj,:))
    hold on
end
xlabel('Time(s)')
ylabel('Pressure (kPa)')
title('MG1: Shoulder Abduction')
subplot(2,2,2)
for i = 1:length(sab2)
    c_sab2(i,:) = call(:,1)'.*(log(sab2(i,:)-dif))+call(:,2)'-offset;
    c_sab2(i,lin) = call(lin,1)'.*(sab2(i,lin)-dif(:,lin))+call(lin,2)'-offset(:,lin);
end
for jj = 1:12
    plot (sab_t2, c_sab2(:,jj), 'Color', color(jj,:))
    hold on
end
xlabel('Time(s)')
ylabel('Pressure (kPa)')
title('MG2: Shoulder Abduction')
subplot(2,2,3)
for i = 1:length(sab3)
    c_sab3(i,:) = call(:,1)'.*(log(sab3(i,:)-dif))+call(:,2)'-offset;
    c_sab3(i,lin) = call(lin,1)'.*(sab3(i,lin)-dif(:,lin))+call(lin,2)'-offset(:,lin);
end
for jj = 1:12
    plot (sab_t3, c_sab3(:,jj), 'Color', color(jj,:))
    hold on
end
xlabel('Time(s)')
ylabel('Pressure (kPa)')
title('MG3: Shoulder Abduction')
subplot(2,2,4)
for i = 1:length(sab0)
    c_sab0(i,:) = call(:,1)'.*(log(sab0(i,:)-dif))+call(:,2)'-offset;
    c_sab0(i,lin) = call(lin,1)'.*(sab0(i,lin)-dif(:,lin))+call(lin,2)'-offset(:,lin);
end
for jj = 1:12
    plot (sab_t0, c_sab0(:,jj), 'Color', color(jj,:))
    hold on
end
xlabel('Time(s)')
ylabel('Pressure (kPa)')
title('Unsuited Shoulder Abduction')

figure
subplot(2,2,1)
for i = 1:length(cbr1)
    c_cbr1(i,:) = call(:,1)'.*(log(cbr1(i,:)-dif))+call(:,2)'-offset;
    c_cbr1(i,lin) = call(lin,1)'.*(cbr1(i,lin)-dif(:,lin))+call(lin,2)'-offset(:,lin);

```

```

end
for jj = 1:12
    plot (cbr_t1, c_cbr1(:,jj), 'Color', color(jj,:))
    hold on
end
xlabel('Time(s)')
ylabel('Pressure (kPa)')
title('MG1: Crossbody Reach')
subplot(2,2,2)
for i = 1:length(cbr2)
    c_cbr2(i,:) = call(:,1)'.*(log(cbr2(i,:)-dif))+call(:,2)'-offset;
    c_cbr2(i,lin) = call(lin,1)'.*(cbr2(i,lin)-dif(:,lin))+call(lin,2)'-offset(:,lin);
end
for jj = 1:12
    plot (cbr_t2, c_cbr2(:,jj), 'Color', color(jj,:))
    hold on
end
xlabel('Time(s)')
ylabel('Pressure (kPa)')
title('MG2: Crossbody Reach')
subplot(2,2,3)
for i = 1:length(cbr3)
    c_cbr3(i,:) = call(:,1)'.*(log(cbr3(i,:)-dif))+call(:,2)'-offset;
    c_cbr3(i,lin) = call(lin,1)'.*(cbr3(i,lin)-dif(:,lin))+call(lin,2)'-offset(:,lin);
end
for jj = 1:12
    plot (cbr_t1, c_cbr1(:,jj), 'Color', color(jj,:))
    hold on
end
xlabel('Time(s)')
ylabel('Pressure (kPa)')
title('MG3: Crossbody Reach')
subplot(2,2,4)
for i = 1:length(cbr0)
    c_cbr0(i,:) = call(:,1)'.*(log(cbr0(i,:)-dif))+call(:,2)'-offset;
    c_cbr0(i,lin) = call(lin,1)'.*(cbr0(i,lin)-dif(:,lin))+call(lin,2)'-offset(:,lin);
end
for jj = 1:12
    plot (cbr_t0, c_cbr0(:,jj), 'Color', color(jj,:))
    hold on
end
xlabel('Time(s)')
ylabel('Pressure (kPa)')
title('Unsuited Crossbody Reach')

figure
subplot(2,2,1)
for i = 1:length(oh1)
    c_oh1(i,:) = call(:,1)'.*(log(oh1(i,:)-dif))+call(:,2)'-offset;
    c_oh1(i,lin) = call(lin,1)'.*(oh1(i,lin)-dif(:,lin))+call(lin,2)'-offset(:,lin);
end
for jj = 1:12
    plot (oh_t1, c_oh1(:,jj), 'Color', color(jj,:))
    hold on
end
xlabel('Time(s)')
ylabel('Pressure (kPa)')
title('MG1: Overhead Hammering')
subplot(2,2,2)
for i = 1:length(oh2)
    c_oh2(i,:) = call(:,1)'.*(log(oh2(i,:)-dif))+call(:,2)'-offset;
    c_oh2(i,lin) = call(lin,1)'.*(oh2(i,lin)-dif(:,lin))+call(lin,2)'-offset(:,lin);
end
for jj = 1:12
    plot (oh_t2, c_oh2(:,jj), 'Color', color(jj,:))
    hold on
end
xlabel('Time(s)')
ylabel('Pressure (kPa)')
title('MG2: Overhead Hammering')
subplot(2,2,3)

```



```

for i = 1:length(oh3)
    c_oh3(i,:) = call(:,1)'.*(log(oh3(i,:)-dif))+call(:,2) '-offset;
    c_oh3(i,lin) = call(lin,1)'.*(oh3(i,lin)-dif(:,lin))+call(lin,2) '-offset(:,lin);
end
for jj = 1:12
    plot (oh_t3, c_oh3(:,jj), 'Color', color(jj,:))
    hold on
end
xlabel('Time(s)')
ylabel('Pressure (kPa)')
title('MG3: Overhead Hammering')
subplot(2,2,4)
for i = 1:length(oh0)
    c_oh0(i,:) = call(:,1)'.*(log(oh0(i,:)-dif))+call(:,2) '-offset;
    c_oh0(i,lin) = call(lin,1)'.*(oh0(i,lin)-dif(:,lin))+call(lin,2) '-offset(:,lin);
end
for jj = 1:12
    plot (oh_t0, c_oh0(:,jj), 'Color', color(jj,:))
    hold on
end
xlabel('Time(s)')
ylabel('Pressure (kPa)')
title('Unsuited Overhead Hammering')

figure
subplot(2,2,1)
for i = 1:length(upstat)
    c_upstat(i,:) = call(:,1)'.*(log(upstat(i,:)-dif))+call(:,2) '-offset;
    c_upstat(i,lin) = call(lin,1)'.*(upstat(i,lin)-dif(:,lin))+call(lin,2) '-offset(:,lin);
end
for jj = 1:12
    plot (tups, c_upstat(:,jj), 'Color', color(jj,:))
    hold on
end
xlabel('Time(s)')
ylabel('Pressure (kPa)')
title('Unpressurized Static')
legend('1', '2', '3', '4', '5', '6', '7', '8', '9', '10', '11', '12')
subplot(2,2,2)
for i = 1:length(pstat)
    c_pstat(i,:) = call(:,1)'.*(log(pstat(i,:)-dif))+call(:,2) '-offset;
    c_pstat(i,lin) = call(lin,1)'.*(pstat(i,lin)-dif(:,lin))+call(lin,2) '-offset(:,lin);
end
for jj = 1:12
    plot (tps, c_pstat(:,jj), 'Color', color(jj,:))
    hold on
end
xlabel('Time(s)')
ylabel('Pressure (kPa)')
title('Pressurized Static')
subplot(2,2,3)
for i = 1:length(eupstat)
    c_eupstat(i,:) = call(:,1)'.*(log(eupstat(i,:)-dif))+call(:,2) '-offset;
    c_eupstat(i,lin) = call(lin,1)'.*(eupstat(i,lin)-dif(:,lin))+call(lin,2) '-offset(:,lin);
end
for jj = 1:12
    plot (teups, c_eupstat(:,jj), 'Color', color(jj,:))
    hold on
end
xlabel('Time(s)')
ylabel('Pressure (kPa)')
title('End of Test Unpressurized Static')

figure
nelb_t1 = (elb_t1-elb_t1(1))./(max(elb_t1)-elb_t1(1));
nelb_t2 = (elb_t2-elb_t2(1))./(max(elb_t2)-elb_t2(1));
nelb_t3 = (elb_t3-elb_t3(1))./(max(elb_t3)-elb_t3(1));
nelb_t0 = (elb_t0-elb_t0(1))./(max(elb_t0)-elb_t0(1));

subplot(4, 3, 1)
hold on

```

```

plot(nelb_t1, c_elb1(:,1), 'r')
plot(nelb_t2, c_elb2(:,1), 'g')
plot(nelb_t3, c_elb3(:,1), 'b')
plot(nelb_t0, c_elb0(:,1), 'k')
legend('mg1', 'mg2', 'mg3', 'unsuit')
title('Elbow Flex/Ex')
subplot(4, 3, 2)
hold on
plot(nelb_t1, c_elb1(:,2), 'r')
plot(nelb_t2, c_elb2(:,2), 'g')
plot(nelb_t3, c_elb3(:,2), 'b')
plot(nelb_t0, c_elb0(:,2), 'k')

subplot(4, 3, 3)
hold on
plot(nelb_t1, c_elb1(:,3), 'r')
plot(nelb_t2, c_elb2(:,3), 'g')
plot(nelb_t3, c_elb3(:,3), 'b')
plot(nelb_t0, c_elb0(:,3), 'k')

subplot(4, 3, 4)
hold on
plot(nelb_t1, c_elb1(:,4), 'r')
plot(nelb_t2, c_elb2(:,4), 'g')
plot(nelb_t3, c_elb3(:,4), 'b')
plot(nelb_t0, c_elb0(:,4), 'k')

subplot(4, 3, 5)
hold on
plot(nelb_t1, c_elb1(:,5), 'r')
plot(nelb_t2, c_elb2(:,5), 'g')
plot(nelb_t3, c_elb3(:,5), 'b')
plot(nelb_t0, c_elb0(:,5), 'k')

subplot(4, 3, 6)
hold on
plot(nelb_t1, c_elb1(:,6), 'r')
plot(nelb_t2, c_elb2(:,6), 'g')
plot(nelb_t3, c_elb3(:,6), 'b')
plot(nelb_t0, c_elb0(:,6), 'k')

subplot(4, 3, 7)
hold on
plot(nelb_t1, c_elb1(:,7), 'r')
plot(nelb_t2, c_elb2(:,7), 'g')
plot(nelb_t3, c_elb3(:,7), 'b')
plot(nelb_t0, c_elb0(:,7), 'k')

subplot(4, 3, 9)
hold on
plot(nelb_t1, c_elb1(:,9), 'r')
plot(nelb_t2, c_elb2(:,9), 'g')
plot(nelb_t3, c_elb3(:,9), 'b')
plot(nelb_t0, c_elb0(:,9), 'k')

subplot(4, 3, 10)
hold on
plot(nelb_t1, c_elb1(:,10), 'r')
plot(nelb_t2, c_elb2(:,10), 'g')
plot(nelb_t3, c_elb3(:,10), 'b')
plot(nelb_t0, c_elb0(:,10), 'k')

subplot(4, 3, 11)
hold on
plot(nelb_t1, c_elb1(:,11), 'r')
plot(nelb_t2, c_elb2(:,11), 'g')
plot(nelb_t3, c_elb3(:,11), 'b')
plot(nelb_t0, c_elb0(:,11), 'k')

subplot(4, 3, 12)
hold on

```

```

plot(nelb_t1, c_elb1(:,12), 'r')
plot(nelb_t2, c_elb2(:,12), 'g')
plot(nelb_t3, c_elb3(:,12), 'b')
plot(nelb_t0, c_elb0(:,12), 'k')

figure
nsflex_t1 = (sflex_t1-sflex_t1(1))./(max(sflex_t1)-sflex_t1(1));
nsflex_t2 = (sflex_t2-sflex_t2(1))./(max(sflex_t2)-sflex_t2(1));
nsflex_t3 = (sflex_t3-sflex_t3(1))./(max(sflex_t3)-sflex_t3(1));
nsflex_t0 = (sflex_t0-sflex_t0(1))./(max(sflex_t0)-sflex_t0(1));

subplot(4, 3, 1)
hold on
plot(nsflex_t1, c_sflect1(:,1), 'r')
plot(nsflex_t2, c_sflect2(:,1), 'g')
plot(nsflex_t3, c_sflect3(:,1), 'b')
plot(nsflex_t0, c_sflect0(:,1), 'k')
legend('mg1', 'mg2', 'mg3', 'unsuit')
title('Shoulder Flex/Ex')
subplot(4, 3, 2)
hold on
plot(nsflex_t1, c_sflect1(:,2), 'r')
plot(nsflex_t2, c_sflect2(:,2), 'g')
plot(nsflex_t3, c_sflect3(:,2), 'b')
plot(nsflex_t0, c_sflect0(:,2), 'k')

subplot(4, 3, 3)
hold on
plot(nsflex_t1, c_sflect1(:,3), 'r')
plot(nsflex_t2, c_sflect2(:,3), 'g')
plot(nsflex_t3, c_sflect3(:,3), 'b')
plot(nsflex_t0, c_sflect0(:,3), 'k')

subplot(4, 3, 4)
hold on
plot(nsflex_t1, c_sflect1(:,4), 'r')
plot(nsflex_t2, c_sflect2(:,4), 'g')
plot(nsflex_t3, c_sflect3(:,4), 'b')
plot(nsflex_t0, c_sflect0(:,4), 'k')

subplot(4, 3, 5)
hold on
plot(nsflex_t1, c_sflect1(:,5), 'r')
plot(nsflex_t2, c_sflect2(:,5), 'g')
plot(nsflex_t3, c_sflect3(:,5), 'b')
plot(nsflex_t0, c_sflect0(:,5), 'k')

subplot(4, 3, 6)
hold on
plot(nsflex_t1, c_sflect1(:,6), 'r')
plot(nsflex_t2, c_sflect2(:,6), 'g')
plot(nsflex_t3, c_sflect3(:,6), 'b')
plot(nsflex_t0, c_sflect0(:,6), 'k')

subplot(4, 3, 7)
hold on
plot(nsflex_t1, c_sflect1(:,7), 'r')
plot(nsflex_t2, c_sflect2(:,7), 'g')
plot(nsflex_t3, c_sflect3(:,7), 'b')
plot(nsflex_t0, c_sflect0(:,7), 'k')

subplot(4, 3, 9)
hold on
plot(nsflex_t1, c_sflect1(:,9), 'r')
plot(nsflex_t2, c_sflect2(:,9), 'g')
plot(nsflex_t3, c_sflect3(:,9), 'b')
plot(nsflex_t0, c_sflect0(:,9), 'k')

subplot(4, 3, 10)
hold on
plot(nsflex_t1, c_sflect1(:,10), 'r')

```

```

plot(nsflex_t2, c_sflext2(:,10), 'g')
plot(nsflex_t3, c_sflext3(:,10), 'b')
plot(nsflex_t0, c_sflext0(:,10), 'k')

subplot(4, 3, 11)
hold on
plot(nsflex_t1, c_sflext1(:,11), 'r')
plot(nsflex_t2, c_sflext2(:,11), 'g')
plot(nsflex_t3, c_sflext3(:,11), 'b')
plot(nsflex_t0, c_sflext0(:,11), 'k')

subplot(4, 3, 12)
hold on
plot(nsflex_t1, c_sflext1(:,12), 'r')
plot(nsflex_t2, c_sflext2(:,12), 'g')
plot(nsflex_t3, c_sflext3(:,12), 'b')
plot(nsflex_t0, c_sflext0(:,12), 'k')

figure
nsab_t1 = (sab_t1-sab_t1(1))./(max(sab_t1)-sab_t1(1));
nsab_t2 = (sab_t2-sab_t2(1))./(max(sab_t2)-sab_t2(1));
nsab_t3 = (sab_t3-sab_t3(1))./(max(sab_t3)-sab_t3(1));
nsab_t0 = (sab_t0-sab_t0(1))./(max(sab_t0)-sab_t0(1));

subplot(4, 3, 1)
hold on
plot(nsab_t1, c_sab1(:,1), 'r')
plot(nsab_t2, c_sab2(:,1), 'g')
plot(nsab_t3, c_sab3(:,1), 'b')
plot(nsab_t0, c_sab0(:,1), 'k')
legend('mg1', 'mg2', 'mg3', 'unsuit')
title('Shoulder Ad/Ab')
subplot(4, 3, 2)
hold on
plot(nsab_t1, c_sab1(:,2), 'r')
plot(nsab_t2, c_sab2(:,2), 'g')
plot(nsab_t3, c_sab3(:,2), 'b')
plot(nsab_t0, c_sab0(:,2), 'k')

subplot(4, 3, 3)
hold on
plot(nsab_t1, c_sab1(:,3), 'r')
plot(nsab_t2, c_sab2(:,3), 'g')
plot(nsab_t3, c_sab3(:,3), 'b')
plot(nsab_t0, c_sab0(:,3), 'k')

subplot(4, 3, 4)
hold on
plot(nsab_t1, c_sab1(:,4), 'r')
plot(nsab_t2, c_sab2(:,4), 'g')
plot(nsab_t3, c_sab3(:,4), 'b')
plot(nsab_t0, c_sab0(:,4), 'k')

subplot(4, 3, 5)
hold on
plot(nsab_t1, c_sab1(:,5), 'r')
plot(nsab_t2, c_sab2(:,5), 'g')
plot(nsab_t3, c_sab3(:,5), 'b')
plot(nsab_t0, c_sab0(:,5), 'k')

subplot(4, 3, 6)
hold on
plot(nsab_t1, c_sab1(:,6), 'r')
plot(nsab_t2, c_sab2(:,6), 'g')
plot(nsab_t3, c_sab3(:,6), 'b')
plot(nsab_t0, c_sab0(:,6), 'k')

subplot(4, 3, 7)
hold on
plot(nsab_t1, c_sab1(:,7), 'r')

```

```

plot(nsab_t2, c_sab2(:,7), 'g')
plot(nsab_t3, c_sab3(:,7), 'b')
plot(nsab_t0, c_sab0(:,7), 'k')

subplot(4, 3, 9)
hold on
plot(nsab_t1, c_sab1(:,9), 'r')
plot(nsab_t2, c_sab2(:,9), 'g')
plot(nsab_t3, c_sab3(:,9), 'b')
plot(nsab_t0, c_sab0(:,9), 'k')

subplot(4, 3, 10)
hold on
plot(nsab_t1, c_sab1(:,10), 'r')
plot(nsab_t2, c_sab2(:,10), 'g')
plot(nsab_t3, c_sab3(:,10), 'b')
plot(nsab_t0, c_sab0(:,10), 'k')

subplot(4, 3, 11)
hold on
plot(nsab_t1, c_sab1(:,11), 'r')
plot(nsab_t2, c_sab2(:,11), 'g')
plot(nsab_t3, c_sab3(:,11), 'b')
plot(nsab_t0, c_sab0(:,11), 'k')

subplot(4, 3, 12)
hold on
plot(nsab_t1, c_sab1(:,12), 'r')
plot(nsab_t2, c_sab2(:,12), 'g')
plot(nsab_t3, c_sab3(:,12), 'b')
plot(nsab_t0, c_sab0(:,12), 'k')

figure
ncbr_t1 = (cbr_t1-cbr_t1(1))./(max(cbr_t1)-cbr_t1(1));
ncbr_t2 = (cbr_t2-cbr_t2(1))./(max(cbr_t2)-cbr_t2(1));
ncbr_t3 = (cbr_t3-cbr_t3(1))./(max(cbr_t3)-cbr_t3(1));
ncbr_t0 = (cbr_t0-cbr_t0(1))./(max(cbr_t0)-cbr_t0(1));

subplot(4, 3, 1)
hold on
plot(ncbr_t1, c_cbr1(:,1), 'r')
plot(ncbr_t2, c_cbr2(:,1), 'g')
plot(ncbr_t3, c_cbr3(:,1), 'b')
plot(ncbr_t0, c_cbr0(:,1), 'k')
title('Cross Body Reach')
legend('mg1', 'mg2', 'mg3', 'unsuit')
subplot(4, 3, 2)
hold on
plot(ncbr_t1, c_cbr1(:,2), 'r')
plot(ncbr_t2, c_cbr2(:,2), 'g')
plot(ncbr_t3, c_cbr3(:,2), 'b')
plot(ncbr_t0, c_cbr0(:,2), 'k')

subplot(4, 3, 3)
hold on
plot(ncbr_t1, c_cbr1(:,3), 'r')
plot(ncbr_t2, c_cbr2(:,3), 'g')
plot(ncbr_t3, c_cbr3(:,3), 'b')
plot(ncbr_t0, c_cbr0(:,3), 'k')

subplot(4, 3, 4)
hold on
plot(ncbr_t1, c_cbr1(:,4), 'r')
plot(ncbr_t2, c_cbr2(:,4), 'g')
plot(ncbr_t3, c_cbr3(:,4), 'b')
plot(ncbr_t0, c_cbr0(:,4), 'k')

subplot(4, 3, 5)
hold on
plot(ncbr_t1, c_cbr1(:,5), 'r')
plot(ncbr_t2, c_cbr2(:,5), 'g')

```

```

plot(ncbr_t3, c_cbr3(:,5), 'b')
plot(ncbr_t0, c_cbr0(:,5), 'k')

subplot(4, 3, 6)
hold on
plot(ncbr_t1, c_cbr1(:,6), 'r')
plot(ncbr_t2, c_cbr2(:,6), 'g')
plot(ncbr_t3, c_cbr3(:,6), 'b')
plot(ncbr_t0, c_cbr0(:,6), 'k')

subplot(4, 3, 7)
hold on
plot(ncbr_t1, c_cbr1(:,7), 'r')
plot(ncbr_t2, c_cbr2(:,7), 'g')
plot(ncbr_t3, c_cbr3(:,7), 'b')
plot(ncbr_t0, c_cbr0(:,7), 'k')

subplot(4, 3, 9)
hold on
plot(ncbr_t1, c_cbr1(:,9), 'r')
plot(ncbr_t2, c_cbr2(:,9), 'g')
plot(ncbr_t3, c_cbr3(:,9), 'b')
plot(ncbr_t0, c_cbr0(:,9), 'k')

subplot(4, 3, 10)
hold on
plot(ncbr_t1, c_cbr1(:,10), 'r')
plot(ncbr_t2, c_cbr2(:,10), 'g')
plot(ncbr_t3, c_cbr3(:,10), 'b')
plot(ncbr_t0, c_cbr0(:,10), 'k')

subplot(4, 3, 11)
hold on
plot(ncbr_t1, c_cbr1(:,11), 'r')
plot(ncbr_t2, c_cbr2(:,11), 'g')
plot(ncbr_t3, c_cbr3(:,11), 'b')
plot(ncbr_t0, c_cbr0(:,11), 'k')

subplot(4, 3, 12)
hold on
plot(ncbr_t1, c_cbr1(:,12), 'r')
plot(ncbr_t2, c_cbr2(:,12), 'g')
plot(ncbr_t3, c_cbr3(:,12), 'b')
plot(ncbr_t0, c_cbr0(:,12), 'k')

figure
noh_t1 = (oh_t1-oh_t1(1))./(max(oh_t1)-oh_t1(1));
noh_t2 = (oh_t2-oh_t2(1))./(max(oh_t2)-oh_t2(1));
noh_t3 = (oh_t3-oh_t3(1))./(max(oh_t3)-oh_t3(1));
noh_t0 = (oh_t0-oh_t0(1))./(max(oh_t0)-oh_t0(1));

subplot(4, 3, 1)
hold on
plot(noh_t1, c_oh1(:,1), 'r')
plot(noh_t2, c_oh2(:,1), 'g')
plot(noh_t3, c_oh3(:,1), 'b')
plot(noh_t0, c_oh0(:,1), 'k')
title('Overhead Hammering')
legend('mg1', 'mg2', 'mg3', 'unsuit')
subplot(4, 3, 2)
hold on
plot(noh_t1, c_oh1(:,2), 'r')
plot(noh_t2, c_oh2(:,2), 'g')
plot(noh_t3, c_oh3(:,2), 'b')
plot(noh_t0, c_oh0(:,2), 'k')

subplot(4, 3, 3)
hold on
plot(noh_t1, c_oh1(:,3), 'r')
plot(noh_t2, c_oh2(:,3), 'g')
plot(noh_t3, c_oh3(:,3), 'b')

```

```

plot(noh_t0, c_oh0(:,3), 'k')

subplot(4, 3, 4)
hold on
plot(noh_t1, c_oh1(:,4), 'r')
plot(noh_t2, c_oh2(:,4), 'g')
plot(noh_t3, c_oh3(:,4), 'b')
plot(noh_t0, c_oh0(:,4), 'k')

subplot(4, 3, 5)
hold on
plot(noh_t1, c_oh1(:,5), 'r')
plot(noh_t2, c_oh2(:,5), 'g')
plot(noh_t3, c_oh3(:,5), 'b')
plot(noh_t0, c_oh0(:,5), 'k')

subplot(4, 3, 6)
hold on
plot(noh_t1, c_oh1(:,6), 'r')
plot(noh_t2, c_oh2(:,6), 'g')
plot(noh_t3, c_oh3(:,6), 'b')
plot(noh_t0, c_oh0(:,6), 'k')

subplot(4, 3, 7)
hold on
plot(noh_t1, c_oh1(:,7), 'r')
plot(noh_t2, c_oh2(:,7), 'g')
plot(noh_t3, c_oh3(:,7), 'b')
plot(noh_t0, c_oh0(:,7), 'k')

subplot(4, 3, 9)
hold on
plot(noh_t1, c_oh1(:,9), 'r')
plot(noh_t2, c_oh2(:,9), 'g')
plot(noh_t3, c_oh3(:,9), 'b')
plot(noh_t0, c_oh0(:,9), 'k')

subplot(4, 3, 10)
hold on
plot(noh_t1, c_oh1(:,10), 'r')
plot(noh_t2, c_oh2(:,10), 'g')
plot(noh_t3, c_oh3(:,10), 'b')
plot(noh_t0, c_oh0(:,10), 'k')

subplot(4, 3, 11)
hold on
plot(noh_t1, c_oh1(:,11), 'r')
plot(noh_t2, c_oh2(:,11), 'g')
plot(noh_t3, c_oh3(:,11), 'b')
plot(noh_t0, c_oh0(:,11), 'k')

subplot(4, 3, 12)
hold on
plot(noh_t1, c_oh1(:,12), 'r')
plot(noh_t2, c_oh2(:,12), 'g')
plot(noh_t3, c_oh3(:,12), 'b')
plot(noh_t0, c_oh0(:,12), 'k')

```

L.3 Calibration Processing

```

clear all
close all
clc

% Load the test file

filename = 'march15 s2 recal and hist.xlsx';
alldata = xlsread(filename);
data = alldata(:,1:12);
time = alldata(:,13);
time = time./1000;

```

```

% plot the data
color = hsv(12);
color(5,:) = [0,0,0];

% for i = 1:12
    hold on
    plot(time,data(:,2), 'Color', color(8,:), 'LineWidth', 1.5)
% end
xlabel('Time (sec)')
ylabel('Data Output (bits)')
% legend('s1', 's2','s3', 's4','s5', 's6','s7', 's8','s9', 's10','s11', 's12')

%% Log responses
% Calculate the calibration curves and plot in terms of pressure

pcal = [0 10 20 30 40 50 60]';
vint = 1:1:1024;
vint = log(vint);
vint2 = 1:1024;

% calibrated as measured and is a very good fit with the second calibration
s1cal = [84 88 99 120 147 171 189]';
s1cal = s1cal - 73;
s1 = log(s1cal);
c1 = fit(s1, pcal, 'poly1');
c1plot = c1.p1*vint+c1.p2;

s1cal_post = [191 198 203 215 235 253 270]';
s1cal_post = s1cal_post - 180;
s1_post = log(s1cal_post);
c1_post = fit(s1_post, pcal, 'poly1');
c1plot_post = c1_post.p1*vint+c1_post.p2;
c1_post_ci = confint(c1_post);
c1plot_post_ciL = c1_post_ci(1,1)*vint+c1_post_ci(1,2);
c1plot_post_ciU = c1_post_ci(2,1)*vint+c1_post_ci(2,2);
figure
plot(pcal, s1cal_post, 'ok')
hold on
plot(c1plot_post,vint2, 'Color', color(1,:))
plot(c1plot_post_ciL,vint2, ':', 'Color', color(1,:))
plot(c1plot_post_ciU, vint2, ':', 'Color', color(1,:))
plot(pcal, s1cal, '*k')
hold on
plot(c1plot, vint2,'--','Color', color(1,:))
xlim([0 75])
ylim([0 500])
title('Sensor 1')
ylabel('Pressure (kPa)')
xlabel('Data Output (bits)')

% Calibrated to 1.2 ohm of resistance. The fit is great though!
s2cal = [65 67 71 75 81 88 99]';
s2cal = s2cal - 53;
s2 = log(s2cal);
c2 = fit(s2, pcal, 'poly1');
c2plot = c2.p1*vint+c2.p2;
c2_ci = confint(c2);
c2plot_ciL = c2_ci(1,1)*vint+c2_ci(1,2);
c2plot_ciU = c2_ci(2,1)*vint+c2_ci(2,2);
figure
subplot(1,2,1)
plot(pcal, s2cal, 'ok')
hold on
plot(c2plot, vint2, 'Color', color(2,:))
plot(c2plot_ciL, vint2, ':', 'Color', color(2,:))
plot(c2plot_ciU, vint2, ':', 'Color', color(2,:))
xlim([0 75])
ylim([0 500])

```



```

title('Sensor 2, 1st sensor')
ylabel('Pressure (kPa)')
xlabel('Data Output (bits)')

%
% Calibrated as measured.
% s2cal_post = [93 95 101 106 116]';
s2cal_post2 = [79 80 82 87 97 109 125]';
s2cal_post2 = s2cal_post2 - 70;
s2_post2 = log(s2cal_post2);
c2_post2 = fit(s2_post2, pcal, 'poly1');
c2plot_post2 = c2_post2.p1*vint+c2_post2.p2;
c2_post2_ci = confint(c2_post2);
c2plot_post2_ciL = c2_post2_ci(1,1)*vint+c2_post2_ci(1,2);
c2plot_post2_ciU = c2_post2_ci(2,1)*vint+c2_post2_ci(2,2);

subplot(1,2,2)
plot(pcal,s2cal_post2, 'ok')
hold on
plot(c2plot_post2, vint2, '-', 'Color', color(2,:))
plot(c2plot_post2_ciL,vint2, ':', 'Color', color(2,:))
plot(c2plot_post2_ciU,vint2, ':', 'Color', color(2,:))
xlim([0 75])
ylim([0 500])
title('Sensor 2, 2nd sensor')
ylabel('Pressure (kPa)')
xlabel('Data Output (bits)')

% Great when compared with below. Calibrated as measured
s3cal = [75 81 86 92 100 112 130]';
s3cal = s3cal - 65;
s3 = log(s3cal);
c3 = fit(s3, pcal, 'poly1');
c3plot = c3.p1*vint+c3.p2;
c3_ci = confint(c3);
c3plot_ciL = c3_ci(1,1)*vint+c3_ci(1,2);
c3plot_ciU = c3_ci(2,1)*vint+c3_ci(2,2);
figure
plot(pcal, s3cal, 'ok')
hold on
plot(c3plot, vint2, 'Color', color(3,:))
plot(c3plot_ciL, vint2, ':', 'Color', color(3,:))
plot(c3plot_ciU, vint2, ':', 'Color', color(3,:))

s3cal_post = [122 134 139 146 155 168 181]';
s3cal_post = s3cal_post - 112;
s3_post = log(s3cal_post);
c3_post = fit(s3_post, pcal, 'poly1');
c3plot_post = c3_post.p1*vint+c3_post.p2;
plot(pcal, s3cal_post, '*k')
hold on
plot(c3plot_post, vint2, '--', 'Color', color(3,:))
xlim([0 75])
ylim([0 500])
title('Sensor 3')
ylabel('Pressure (kPa)')
xlabel('Data Output (bits)')

% Second calibration is a bad one. Calibrated as measured and it is a
% very good fit
s4cal = [72 84 96 108 122 145 204]';
s4cal = s4cal - 59;
s4 = log(s4cal);
c4 = fit(s4, pcal, 'poly1');
c4plot = c4.p1*vint+c4.p2;
c4_ci = confint(c4);
c4plot_ciL = c4_ci(1,1)*vint+c4_ci(1,2);
c4plot_ciU = c4_ci(2,1)*vint+c4_ci(2,2);
figure
plot(pcal,s4cal, 'ok')
hold on

```

```

plot(c4plot, vint2, 'Color', color(4,:))
plot(c4plot_ciL, vint2, ':', 'Color', color(4,:))
plot(c4plot_ciU, vint2, ':', 'Color', color(4,:))
xlim([0 75])
ylim([0 500])
title('Sensor 4')
ylabel('Pressure (kPa)')
xlabel('Data Output (bits)')

% Very good fit with calibration. Calibrated as measured.
s5cal_post = [107 111 117 144 177 227 286]';
s5cal_post = s5cal_post - 95;
s5_post = log(s5cal_post);
c5_post = fit(s5_post, pcal, 'poly1');
c5plot_post = c5_post.p1*vint+c5_post.p2;
c5_post_ci = confint(c5_post);
c5plot_post_ciL = c5_post_ci(1,1)*vint+c5_post_ci(1,2);
c5plot_post_ciU = c5_post_ci(2,1)*vint+c5_post_ci(2,2);
figure
subplot(1,2,2)
plot(pcal,s5cal_post, 'ok')
hold on
plot(c5plot_post, vint2, 'Color', color(5,:))
plot(c5plot_post_ciL, vint2, ':', 'Color', color(5,:))
plot(c5plot_post_ciU, vint2, ':', 'Color', color(5,:))
xlim([0 75])
ylim([0 500])
title('Sensor 5, 2nd sensor')
ylabel('Pressure (kPa)')
xlabel('Data Output (bits)')
vint = log(vint2);
% Original broke. Calibrated to 1.2
s5cal = [97 122 136 152 165 177 190]';
s5cal = s5cal -85;
s5 = s5cal; %log(s5cal);
c5 = fit(s5, pcal, 'poly1');
c5plot = c5.p1*vint2+c5.p2;
c5_ci = confint(c5);
c5plot_ciL = c5_ci(1,1)*vint2+c5_ci(1,2);
c5plot_ciU = c5_ci(2,1)*vint2+c5_ci(2,2);
subplot(1,2,1)
plot(pcal,s5cal, 'ok')
hold on
plot(c5plot, vint2, 'Color', color(5,:))
plot(c5plot_ciL, vint2, ':', 'Color', color(5,:))
plot(c5plot_ciU, vint2, ':', 'Color', color(5,:))
xlim([0 75])
ylim([0 500])
title('Sensor 5, 1st sensor')
ylabel('Pressure (kPa)')
xlabel('Data Output (bits)')

% Calibration changed to 1.2
s9cal = [44 47 50 54 61 73 90]';
s9cal = s9cal - 32;
s9 = log(s9cal);
c9 = fit(s9, pcal, 'poly1');
c9plot = c9.p1*vint+c9.p2;
c9_ci = confint(c9);
c9plot_ciL = c9_ci(1,1)*vint+c9_ci(1,2);
c9plot_ciU = c9_ci(2,1)*vint+c9_ci(2,2);
figure
subplot(1,2,1)
plot(pcal, s9cal, 'ok')
hold on
plot(c9plot,vint2, 'Color', color(9,:))
plot(c9plot_ciL, vint2, ':', 'Color', color(9,:))
plot(c9plot_ciU, vint2, ':', 'Color', color(9,:))
xlim([0 75])
ylim([0 500])
title('Sensor 9, 1st sensor')

```

```

ylabel('Pressure (kPa)')
xlabel('Data Output (bits)')

vint = 1:1024;
s9cal_post = [69 96 107 140 159 177 196]';
s9cal_post = s9cal_post - 57;
s9_post = s9cal_post;
c9_post = fit(s9_post, pcal, 'poly1');
c9plot_post = c9_post.p1*vint+c9_post.p2;
c9_post_ci = confint(c9_post);
c9plot_post_ciL = c9_post_ci(1,1)*vint+c9_post_ci(1,2);
c9plot_post_ciU = c9_post_ci(2,1)*vint+c9_post_ci(2,2);
subplot(1,2,2)
plot(pcal, s9cal_post, 'ok')
hold on
plot(c9plot_post, vint2, 'Color', color(9,:))
plot(c9plot_post_ciL, vint2, ':', 'Color', color(9,:))
plot(c9plot_post_ciU, vint2, ':', 'Color', color(9,:))
xlim([0 75])
ylim([0 500])
title('Sensor 9, 2nd sensor')
ylabel('Pressure (kPa)')
xlabel('Data Output (bits)')

% Calibration changed to 1.2 ohms and looks perfect
vint = log(vint2);
s10cal = [51 61 90 146 230 397 727]';
s10cal = s10cal - 39;
s10 = log(s10cal);
c10 = fit(s10, pcal, 'poly1');
c10plot = c10.p1*vint+c10.p2;
c10_ci = confint(c10);
c10plot_ciL = c10_ci(1,1)*vint+c10_ci(1,2);
c10plot_ciU = c10_ci(2,1)*vint+c10_ci(2,2);
figure
plot(pcal, s10cal, 'ok')
hold on
plot(c10plot, vint2, 'Color', color(10,:))
plot(c10plot_ciL, vint2, ':', 'Color', color(10,:))
plot(c10plot_ciU, vint2, ':', 'Color', color(10,:))

% figure
% vint2 = 1:1024;
% ex10 = exp(c10.p1)*(vint2) + exp(c10.p2);
% ex10_ciL = exp(c10_ci(1,1))*(vint2)+exp(c10_ci(1,2));
% es10_ciU = exp(c10_ci(2,1))*(vint2)+exp(c10_ci(2,2));
% plot(s10cal, pcal, 'ok')
% hold on
% plot(ex10plot, vint2, 'Color', color(10,:))
% plot(ex10plot_ciL, vint2, ':', 'Color', color(10,:))
% plot(ex10plot_ciU, vint2, ':', 'Color', color(10,:))
xlim([0 75])
ylim([0 1024])
ylabel('Pressure (kPa)')
xlabel('Data Output (bits)')
title('Sensor 10')

% Fits well with the second calibration and is a great fit. calibrated as
% measured
s11cal = [60 63 76 117 151 231 305]';
s11cal = s11cal - 47;
s11 = log(s11cal);
c11 = fit(s11, pcal, 'poly1');
c11plot = c11.p1*vint+c11.p2;
c11_ci = confint(c11);
c11plot_ciL = c11_ci(1,1)*vint+c11_ci(1,2);
c11plot_ciU = c11_ci(2,1)*vint+c11_ci(2,2);
figure
plot(pcal, s11cal, 'ok')

```

```

hold on
plot(c11plot,vint2, 'Color', color(11,:))
plot(c11plot_ciL,vint2, ':', 'Color', color(11,:))
plot(c11plot_ciU,vint2, ':', 'Color', color(11,:))

s11cal_post = [132 137 164 181 205 225]';
s11cal_post = s11cal_post - 119;
s11_post = log(s11cal_post);
c11_post = fit(s11_post, pcal(2:7), 'poly1');
c11plot_post = c11_post.p1*vint+c11_post.p2;
plot(pcal(2:7), s11cal_post, '*k')
hold on
plot(c11plot_post, vint2, '--', 'Color', color(11,:))
xlim([0 75])
ylim([0 1024])
ylabel('Pressure (kPa)')
xlabel('Data Output (bits)')
title('Sensor 11')

%
%% Linear calibration
vint = 1:1024;

% Compare with below. Calibrated as measured
s6cal = [72 153 203 246 278 306 331]';
s6cal = s6cal - 62;
s6 = s6cal;
c6 = fit(s6, pcal, 'poly1');
c6plot = c6.p1*vint+c6.p2;
c6_ci = confint(c6);
c6plot_ciL = c6_ci(1,1)*vint+c6_ci(1,2);
c6plot_ciU = c6_ci(2,1)*vint+c6_ci(2,2);
figure
plot(pcal,s6cal, 'ok')
hold on
plot(c6plot, vint2, 'Color', color(6,:))
plot(c6plot_ciL, vint2, ':', 'Color', color(6,:))
plot(c6plot_ciU, vint2, ':', 'Color', color(6,:))
%
s6cal_post = [74 180 211 225 258 323]';
s6cal_post = s6cal_post - 64;
s6_post = s6cal_post;
c6_post = fit(s6_post(1:6), pcal(1:6), 'poly1');
c6plot_post = c6_post.p1*vint+c6_post.p2;
plot(pcal(1:6), s6cal_post, '*k')
hold on
plot(c6plot_post,vint2, '--', 'Color', color(6,:))
xlim([0 75])
ylim([0 1024])
ylabel('Pressure (kPa)')
xlabel('Data Output (bits)')
title('Sensor 6')

% % Calibrated as measured.
% pcal7_post = [0 10 40 50 60]';
% s7cal_post = [163 222 403 431 486]';
s7cal_post2 = [84, 171 ,240, 322, 410, 522, 611]';
s7cal_post2 = s7cal_post2 - 64;
s7_post2 = s7cal_post2;%log(s7cal_post2);
c7_post2 = fit(s7_post2, pcal, 'poly1');
c7plot_post2 = c7_post2.p1*vint+c7_post2.p2;
c7_post2_ci = confint(c7_post2);
c7plot_post2_ciL = c7_post2_ci(1,1)*vint+c7_post2_ci(1,2);
c7plot_post2_ciU = c7_post2_ci(2,1)*vint+c7_post2_ci(2,2);
figure
plot(pcal,s7_post2, 'ok')
hold on
plot(c7plot_post2, vint2, 'Color', color(7,:))

```

```

plot(c7plot_post2_ciL, vint2, ':', 'Color', color(7,:))
plot(c7plot_post2_ciU,vint2, ':', 'Color', color(7,:))
xlim([0 75])
ylim([0 1024])
ylabel('Pressure (kPa)')
xlabel('Data Output (bits)')
title('Sensor 7')

% Calibrated as measured
s12cal_post = [80 168 256 345 470 563 645]';
s12cal_post = [85 182 311 408 506 603 669]';
s12cal_post = s12cal_post - 73;
s12_post = s12cal_post;%log(s12cal_post);
c12_post = fit(s12_post, pcal, 'poly1');
c12plot_post = c12_post.p1*vint+c12_post.p2;
c12_post_ci = confint(c12_post);
c12plot_post_ciL = c12_post_ci(1,1)*vint+c12_post_ci(1,2);
c12plot_post_ciU = c12_post_ci(2,1)*vint+c12_post_ci(2,2);
figure
plot(pcal,s12_post, 'ok')
hold on
plot(c12plot_post, vint2, 'Color', color(12,:))
plot(c12plot_post_ciL, vint2, ':', 'Color', color(12,:))
plot(c12plot_post_ciU, vint2, ':', 'Color', color(12,:))
xlim([0 75])
ylim([0 1024])
ylabel('Pressure (kPa)')
xlabel('Data Output (bits)')
title('Sensor 12')
%%
%% % Set the calibration data set for each subject
%% % Need to do the calibration curve for sensor 12 and 6
%% % Need to decide what to do with the sensor 10 calibration for both
%% % subjects 2 and 3
%% % Use the calibration curves for pre-experiment for sensors 1,3,11 since
%% % they will probably be more accurate since not tested so long after the
%% % fact.
%% % zp = 50;
call = [c1_post.p1 c1_post.p2; % Sensor 1 never broke but the second calibration is better
        c2.p1 c2.p2;
        c3.p1 c3.p2;
        c4.p1 c4.p2;
        c5.p1 c5.p2;
        c6.p1 c6.p2;
        0 0
        0 0;
        c9.p1 c9.p2;
        c10.p1 c10.p2;
        c11.p1 c11.p2;
        c12_post.p1 c12_post.p2] % Sensor 12 never broke but the original calibration was bad
zp1 = [11; 12; 10; 13; 12; 10; 12; 0; 12; 12; 13; 12];
resbit1 = round(1./(exp(1./call(:,1))-1))
respres1 = call(:,1).*log(resbit1)+call(:,2)

cal2 = [c1_post.p1 c1_post.p2;
        c2.p1 c2.p2;
        c3.p1 c3.p2;
        c4.p1 c4.p2;
        c5.p1 c5.p2;
        c6.p1 c6.p2;
        c7.p1 c7.p2;
        0 0;
        c9.p1 c9.p2;
        c10.p1 c10.p2; % Note that this is not the correct curve
        c11.p1 c11.p2;
        c12_post.p1 c12_post.p2]
zp2 = [11; 12; 10; 13; 12; 10; 12; 0; 12; 12; 13; 12];
resbit2 = round(1./(exp(1./cal2(:,1))-1))
respres2 = cal2(:,1).*log(resbit2)+cal2(:,2)

```

```

cal3 = [c1_post.p1 c1_post.p2;
        c2_post2.p1 c2_post2.p2;
        c3.p1 c3.p2;
        c4.p1 c4.p2;
        c5_post.p1 c5_post.p2;
        c6.p1 c6.p2;
        c7_post2.p1 c7_post2.p2;
        0 0;
        c9_post.p1 c9_post.p2;
        c10.p1 c10.p2; % Note that this is not the correct curve
        c11.p1 c11.p2;
        c12_post.p1 c12_post.p2]
zp3 = [11; 9; 10; 13; 12; 10; 20; 0; 12; 12; 13; 12];
resbit3 = round(1./(exp(1./cal3(:,1))-1))
respres3 = cal3(:,1).*log(resbit3)+cal3(:,2)

```

L.4 Sequential Activation Data processing

```

clear all
close all
clc

% Load the data
load p_plot_sl_calres

%Select the relevant profiles and modify the offset
% % Cross Body Reach
%
cbr1 = [0;0;0; 0];
for y = 1:length(c_cbr1(:,1))
    if c_cbr1(y,1)<0
        c_cbr1(y,1) = NaN;
    end
end
for y = 1:length(c_cbr2(:,1))
    if c_cbr2(y,1)<-5
        c_cbr2(y,1) = NaN;
    end
end
for y = 1:length(c_cbr3(:,1))
    if c_cbr3(y,1)<-5
        c_cbr3(y,1) = NaN;
    end
end
for y = 1:length(c_cbr0(:,1))
    if c_cbr0(y,1)<-5
        c_cbr0(y,1) = NaN;
    end
end
co_cbr1(:,1) = c_cbr1(:,1)+cbr1(1);
co_cbr2(:,1) = c_cbr2(:,1)+cbr1(2);
co_cbr3(:,1) = c_cbr3(:,1)+cbr1(3);
co_cbr0(:,1) = c_cbr0(:,1)+cbr1(4);

cbr2 = [12.4, 12.4, 7.1, 7.1];
co_cbr1(:,2) = c_cbr1(:,2)+cbr2(1);
co_cbr2(:,2) = c_cbr2(:,2)+cbr2(2);
co_cbr3(:,2) = c_cbr3(:,2)+cbr2(3);
co_cbr0(:,2) = c_cbr0(:,2)+cbr2(4);

cbr4 = [3.9, 3.9, 3.9, 3.9];
co_cbr1(:,4) = NaN;
co_cbr2(:,4) = c_cbr2(:,4)+cbr4(2);
co_cbr3(:,4) = NaN;

cbr5 = [2.5, 2.5, 2.5, 2.5];

```

```

co_cbr1(:,5) = c_cbr1(:,5)+cbr5(1);
co_cbr2(:,5) = c_cbr2(:,5)+cbr5(2);
co_cbr3(:,5) = c_cbr3(:,5)+cbr5(3);

cbr6 = [0; 0; 0; 0];
co_cbr1(:,6) = c_cbr1(:,6)+cbr6(1);
co_cbr2(:,6) = c_cbr2(:,6)+cbr6(2);
co_cbr3(:,6) = c_cbr3(:,6)+cbr6(3);
co_cbr0(:,6) = c_cbr0(:,6)+cbr6(4);

cbr10 = [0; 0; 0; 0];
for w = 1:length(c_cbr1(:,10))
    if c_cbr1(w,10)<-6
        c_cbr1(w,10) = NaN;
    end
end
co_cbr1(:,10) = c_cbr1(:,10)+cbr10(1);
co_cbr2(:,10) = NaN;
co_cbr3(:,10) = NaN;

cbr11 = [-1.5, -1.5, -1.5, -1.5];
co_cbr1(:,11) = c_cbr1(:,11)+cbr11(1);
co_cbr2(:,11) = c_cbr2(:,11)+cbr11(2);
co_cbr3(:,11) = c_cbr3(:,11)+cbr11(3);
co_cbr0(:,11) = c_cbr0(:,11)+cbr11(4);

% Aggregate the data
[a,b] = size(co_cbr1);
[c,d] = size(co_cbr2);
[e,f] = size(co_cbr3);

% s = [.146; .35; .58; .83];
% f = [.35; .58; .82; 1];

% s = [.085; .31; .535; .773]; %- .005; % - .055;
% f = [.32; .53; .773; .98]; %- .005;

s = [.055; .29; .51; .75]; %- .005; % - .055;
f = [.29; .51; .75; .97]; %- .005;

col_cbr1(:, :) = co_cbr1(round(a*s(1)):round(a*f(1)), :);
col_cbr1(:,b+1) = (cbr_t1(round(a*s(1)):round(a*f(1)),1) - cbr_t1(round(a*s(1)),1))/
(cbr_t1(round(a*f(1)),1) - cbr_t1(round(a*s(1)),1));
co2_cbr1(:, :) = co_cbr1(round(a*s(2)):round(a*f(2)), :);
co2_cbr1(:,b+1) = (cbr_t1(round(a*s(2)):round(a*f(2)),1) - cbr_t1(round(a*s(2)),1))/
(cbr_t1(round(a*f(2)),1) - cbr_t1(round(a*s(2)),1));
co3_cbr1(:, :) = co_cbr1(round(a*s(3)):round(a*f(3)), :);
co3_cbr1(:,b+1) = (cbr_t1(round(a*s(3)):round(a*f(3)),1) - cbr_t1(round(a*s(3)),1))/
(cbr_t1(round(a*f(3)),1) - cbr_t1(round(a*s(3)),1));
co4_cbr1(:, :) = co_cbr1(round(a*s(4)):round(a*f(4)), :);
co4_cbr1(:,b+1) = (cbr_t1(round(a*s(4)):round(a*f(4)),1) - cbr_t1(round(a*s(4)),1))/
(cbr_t1(round(a*f(4)),1) - cbr_t1(round(a*s(4)),1));
%
% s = [.085; .31; .534; .773] - .003; % - .055;
% f = [.32; .54; .773; .98] + .005;
% col_cbr2(:, :) = co_cbr2(round(c*s(1)):round(c*f(1)), :);
% col_cbr2(:,b+1) = (cbr_t2(round(c*s(1)):round(c*f(1)),1) - cbr_t2(round(c*s(1)),1))/
(cbr_t2(round(c*f(1)),1) - cbr_t2(round(c*s(1)),1));
% co2_cbr2(:, :) = co_cbr2(round(c*s(2)):round(c*f(2)), :);
% co2_cbr2(:,b+1) = (cbr_t2(round(c*s(2)):round(c*f(2)),1) - cbr_t2(round(c*s(2)),1))/
(cbr_t2(round(c*f(2)),1) - cbr_t2(round(c*s(2)),1));
% co3_cbr2(:, :) = co_cbr2(round(c*s(3)):round(c*f(3)), :);
% co3_cbr2(:,b+1) = (cbr_t2(round(c*s(3)):round(c*f(3)),1) - cbr_t2(round(c*s(3)),1))/
(cbr_t2(round(c*f(3)),1) - cbr_t2(round(c*s(3)),1));
% co4_cbr2(:, :) = co_cbr2(round(c*s(4)):round(c*f(4)), :);
% co4_cbr2(:,b+1) = (cbr_t2(round(c*s(4)):round(c*f(4)),1) - cbr_t2(round(c*s(4)),1))/
(cbr_t2(round(c*f(4)),1) - cbr_t2(round(c*s(4)),1));
%

```

```

% s = [.085; .325; .535; .773]-.01; % - .055;
% f = [.32; .54; .77; .98]+.01;
% co1_cbr3(:, :) = co_cbr3(round(e*s(1)):round(e*f(1)), :);
% co1_cbr3(:,b+1) = (cbr_t3(round(e*s(1)):round(e*f(1)),1) - cbr_t3(round(e*s(1)),
1))/(cbr_t3(round(e*f(1)),1) - cbr_t3(round(e*s(1)),1));
% co2_cbr3(:, :) = co_cbr3(round(e*s(2)):round(e*f(2)), :);
% co2_cbr3(:,b+1) = (cbr_t3(round(e*s(2)):round(e*f(2)),1) - cbr_t3(round(e*s(2)),
1))/(cbr_t3(round(e*f(2)),1) - cbr_t3(round(e*s(2)),1));
% co3_cbr3(:, :) = co_cbr3(round(e*s(3)):round(e*f(3)), :);
% co3_cbr3(:,b+1) = (cbr_t3(round(e*s(3)):round(e*f(3)),1) - cbr_t3(round(e*s(3)),
1))/(cbr_t3(round(e*f(3)),1) - cbr_t3(round(e*s(3)),1));
% co4_cbr3(:, :) = co_cbr3(round(e*s(4)):round(e*f(4)), :);
% co4_cbr3(:,b+1) = (cbr_t3(round(e*s(4)):round(e*f(4)),1) - cbr_t3(round(e*s(4)),
1))/(cbr_t3(round(e*f(4)),1) - cbr_t3(round(e*s(4)),1));

```

```

figure
subplot(7,1,1)
hold on
plot(co1_cbr1(:,12), co1_cbr1(:,1), '-r')
plot(co2_cbr1(:,12), co2_cbr1(:,1), '-k')
plot(co3_cbr1(:,12), co3_cbr1(:,1), '-b')
plot(co4_cbr1(:,12), co4_cbr1(:,1), '-g')
% plot(co1_cbr2(:,12), co1_cbr2(:,1), 'r')
% plot(co2_cbr2(:,12), co2_cbr2(:,1), 'k')
% plot(co3_cbr2(:,12), co3_cbr2(:,1), 'b')
% plot(co4_cbr2(:,12), co4_cbr2(:,1), 'g')
% plot(co1_cbr3(:,12), co1_cbr3(:,1), '--r')
% plot(co2_cbr3(:,12), co2_cbr3(:,1), '--k')
% plot(co3_cbr3(:,12), co3_cbr3(:,1), '--b')
% plot(co4_cbr3(:,12), co4_cbr3(:,1), '--g')
title('Sensor 1')
axis tight

```

```

% figure
subplot(7,1,2)
hold on
plot(co1_cbr1(:,12), co1_cbr1(:,2), '-r')
plot(co2_cbr1(:,12), co2_cbr1(:,2), '-k')
plot(co3_cbr1(:,12), co3_cbr1(:,2), '-b')
plot(co4_cbr1(:,12), co4_cbr1(:,2), '-g')
% plot(co1_cbr2(:,12), co1_cbr2(:,2), 'r')
% plot(co2_cbr2(:,12), co2_cbr2(:,2), 'k')
% plot(co3_cbr2(:,12), co3_cbr2(:,2), 'b')
% plot(co4_cbr2(:,12), co4_cbr2(:,2), 'g')
% plot(co1_cbr3(:,12), co1_cbr3(:,2), '--r')
% plot(co2_cbr3(:,12), co2_cbr3(:,2), '--k')
% plot(co3_cbr3(:,12), co3_cbr3(:,2), '--b')
% plot(co4_cbr3(:,12), co4_cbr3(:,2), '--g')
title('Sensor 2')
axis tight

```

```

% figure
subplot(7,1,3)
hold on
plot(co1_cbr1(:,12), co1_cbr1(:,4), '-r')
plot(co2_cbr1(:,12), co2_cbr1(:,4), '-k')
plot(co3_cbr1(:,12), co3_cbr1(:,4), '-b')
plot(co4_cbr1(:,12), co4_cbr1(:,4), '-g')
% plot(co1_cbr2(:,12), co1_cbr2(:,4), 'r')
% plot(co2_cbr2(:,12), co2_cbr2(:,4), 'k')
% plot(co3_cbr2(:,12), co3_cbr2(:,4), 'b')
% plot(co4_cbr2(:,12), co4_cbr2(:,4), 'g')
% plot(co1_cbr3(:,12), co1_cbr3(:,4), '--r')
% plot(co2_cbr3(:,12), co2_cbr3(:,4), '--k')
% plot(co3_cbr3(:,12), co3_cbr3(:,4), '--b')
% plot(co4_cbr3(:,12), co4_cbr3(:,4), '--g')
title('Sensor 4')
axis tight

```

```

% figure

```



```

subplot(7,1,4)
hold on
plot(co1_cbr1(:,12), co1_cbr1(:,5), '-r')
plot(co2_cbr1(:,12), co2_cbr1(:,5), '-k')
plot(co3_cbr1(:,12), co3_cbr1(:,5), '-b')
plot(co4_cbr1(:,12), co4_cbr1(:,5), '-g')
% plot(co1_cbr2(:,12), co1_cbr2(:,5), 'r')
% plot(co2_cbr2(:,12), co2_cbr2(:,5), 'k')
% plot(co3_cbr2(:,12), co3_cbr2(:,5), 'b')
% plot(co4_cbr2(:,12), co4_cbr2(:,5), 'g')
% plot(co1_cbr3(:,12), co1_cbr3(:,5), '--r')
% plot(co2_cbr3(:,12), co2_cbr3(:,5), '--k')
% plot(co3_cbr3(:,12), co3_cbr3(:,5), '--b')
% plot(co4_cbr3(:,12), co4_cbr3(:,5), '--g')
title('Sensor 5')
axis tight

% figure
subplot(7,1,5)
hold on
plot(co1_cbr1(:,12), co1_cbr1(:,6), '-r')
plot(co2_cbr1(:,12), co2_cbr1(:,6), '-k')
plot(co3_cbr1(:,12), co3_cbr1(:,6), '-b')
plot(co4_cbr1(:,12), co4_cbr1(:,6), '-g')
% plot(co1_cbr2(:,12), co1_cbr2(:,6), 'r')
% plot(co2_cbr2(:,12), co2_cbr2(:,6), 'k')
% plot(co3_cbr2(:,12), co3_cbr2(:,6), 'b')
% plot(co4_cbr2(:,12), co4_cbr2(:,6), 'g')
% plot(co1_cbr3(:,12), co1_cbr3(:,6), '--r')
% plot(co2_cbr3(:,12), co2_cbr3(:,6), '--k')
% plot(co3_cbr3(:,12), co3_cbr3(:,6), '--b')
% plot(co4_cbr3(:,12), co4_cbr3(:,6), '--g')
title('Sensor 6')
axis tight

% figure
subplot(7,1,6)
hold on
plot(co1_cbr1(:,12), co1_cbr1(:,10), '-r')
plot(co2_cbr1(:,12), co2_cbr1(:,10), '-k')
plot(co3_cbr1(:,12), co3_cbr1(:,10), '-b')
plot(co4_cbr1(:,12), co4_cbr1(:,10), '-g')
% plot(co1_cbr2(:,12), co1_cbr2(:,10), 'r')
% plot(co2_cbr2(:,12), co2_cbr2(:,10), 'k')
% plot(co3_cbr2(:,12), co3_cbr2(:,10), 'b')
% plot(co4_cbr2(:,12), co4_cbr2(:,10), 'g')
% plot(co1_cbr3(:,12), co1_cbr3(:,10), '--r')
% plot(co2_cbr3(:,12), co2_cbr3(:,10), '--k')
% plot(co3_cbr3(:,12), co3_cbr3(:,10), '--b')
% plot(co4_cbr3(:,12), co4_cbr3(:,10), '--g')
title('Sensor 10')
axis tight

% figure
subplot(7,1,7)
hold on
plot(co1_cbr1(:,12), co1_cbr1(:,11), '-r')
plot(co2_cbr1(:,12), co2_cbr1(:,11), '-k')
plot(co3_cbr1(:,12), co3_cbr1(:,11), '-b')
plot(co4_cbr1(:,12), co4_cbr1(:,11), '-g')
% plot(co1_cbr2(:,12), co1_cbr2(:,11), 'r')
% plot(co2_cbr2(:,12), co2_cbr2(:,11), 'k')
% plot(co3_cbr2(:,12), co3_cbr2(:,11), 'b')
% plot(co4_cbr2(:,12), co4_cbr2(:,11), 'g')
% plot(co1_cbr3(:,12), co1_cbr3(:,11), '--r')
% plot(co2_cbr3(:,12), co2_cbr3(:,11), '--k')
% plot(co3_cbr3(:,12), co3_cbr3(:,11), '--b')
% plot(co4_cbr3(:,12), co4_cbr3(:,11), '--g')
title('Sensor 11')
axis tight

```

```

for j = .01:.01:.99
    x = max(find(co1_cbr1(:,b+1) < j));
    y = min(find(co1_cbr1(:,b+1) > j));
    interp = (co1_cbr1(x,:) + co1_cbr1(y,:))/2;
    per(round(j*100),:,1) = interp(1,:);
    x2 = max(find(co2_cbr1(:,b+1) < j));
    y2 = min(find(co2_cbr1(:,b+1) > j));
    interp2 = (co2_cbr1(x2,:) + co2_cbr1(y2,:))/2;
    per(round(j*100),:,2) = interp2(1,:);
    x3 = max(find(co3_cbr1(:,b+1) < j));
    y3 = min(find(co3_cbr1(:,b+1) > j));
    interp3 = (co3_cbr1(x3,:) + co3_cbr1(y3,:))/2;
    per(round(j*100),:,3) = interp3(1,:);
    x4 = max(find(co4_cbr1(:,b+1) < j));
    y4 = min(find(co4_cbr1(:,b+1) > j));
    interp4 = (co4_cbr1(x4,:) + co4_cbr1(y4,:))/2;
    per(round(j*100),:,4) = interp4(1,:);

%
%     x = max(find(co1_cbr2(:,b+1) < j));
%     y = min(find(co1_cbr2(:,b+1) > j));
%     interp = (co1_cbr2(x,:) + co1_cbr2(y,:))/2;
%     per(round(j*100),:,5) = interp(1,:);
%     x2 = max(find(co2_cbr2(:,b+1) < j));
%     y2 = min(find(co2_cbr2(:,b+1) > j));
%     interp2 = (co2_cbr2(x2,:) + co2_cbr2(y2,:))/2;
%     per(round(j*100),:,6) = interp2(1,:);
%     x3 = max(find(co3_cbr2(:,b+1) < j));
%     y3 = min(find(co3_cbr2(:,b+1) > j));
%     interp3 = (co3_cbr2(x3,:) + co3_cbr2(y3,:))/2;
%     per(round(j*100),:,7) = interp3(1,:);
%     x4 = max(find(co4_cbr2(:,b+1) < j));
%     y4 = min(find(co4_cbr2(:,b+1) > j));
%     interp4 = (co4_cbr2(x4,:) + co4_cbr2(y4,:))/2;
%     per(round(j*100),:,8) = interp4(1,:);
%
%
%     x = max(find(co1_cbr3(:,b+1) < j));
%     y = min(find(co1_cbr3(:,b+1) > j));
%     interp = (co1_cbr3(x,:) + co1_cbr3(y,:))/2;
%     per(round(j*100),:,9) = interp(1,:);
%     x2 = max(find(co2_cbr3(:,b+1) < j));
%     y2 = min(find(co2_cbr3(:,b+1) > j));
%     interp2 = (co2_cbr3(x2,:) + co2_cbr3(y2,:))/2;
%     per(round(j*100),:,10) = interp2(1,:);
%     x3 = max(find(co3_cbr3(:,b+1) < j));
%     y3 = min(find(co3_cbr3(:,b+1) > j));
%     interp3 = (co3_cbr3(x3,:) + co3_cbr3(y3,:))/2;
%     per(round(j*100),:,11) = interp3(1,:);
%     x4 = max(find(co4_cbr3(:,b+1) < j));
%     y4 = min(find(co4_cbr3(:,b+1) > j));
%     interp4 = (co4_cbr3(x4,:) + co4_cbr3(y4,:))/2;
%     per(round(j*100),:,12) = interp4(1,:);
end
for k = 1:length(per)
    for l = 1:b+1
        mu(k,l) = nanmean(per(k,l,:));
        stdev(k,l) = nanstd(per(k,l,:));
    end
end
figure
hold on
xx = .01:.01:.99;
color = hsv(12);
xpatch = [xx, fliplr(xx)];
for n = 1:12
    top(n,:) = (stdev(:,n)+mu(:,n))';
    bottom(n,:) = (mu(:,n)-stdev(:,n))';
    ypatch(n,:) = [top(n,:), fliplr(bottom(n,:))]
    for o = 1:length(ypatch)
        if isnan(ypatch(1,o))
            ypatch(n,o) = 0;
        end
    end
end

```

```

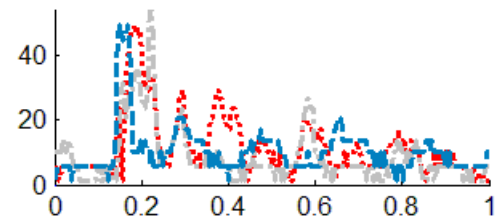
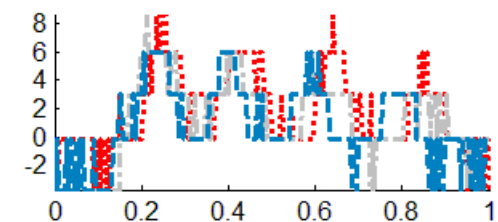
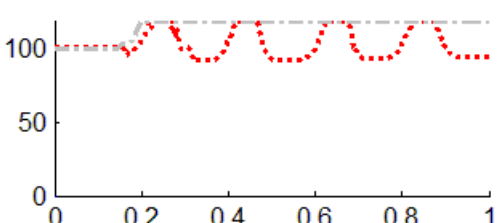
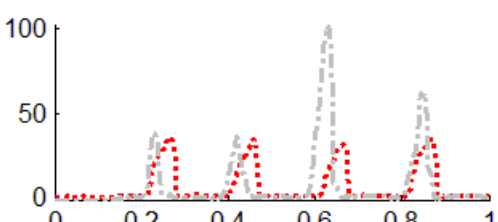
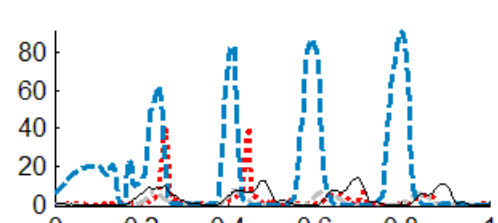
        end
    end
    patch(xpatch,ypatch(n,:),1,'FaceColor', color(n,:), 'EdgeColor','none')
    alpha(.2); % make patch transparent
    plot(xx, mu(:,n), 'Color', color(n,:))
end

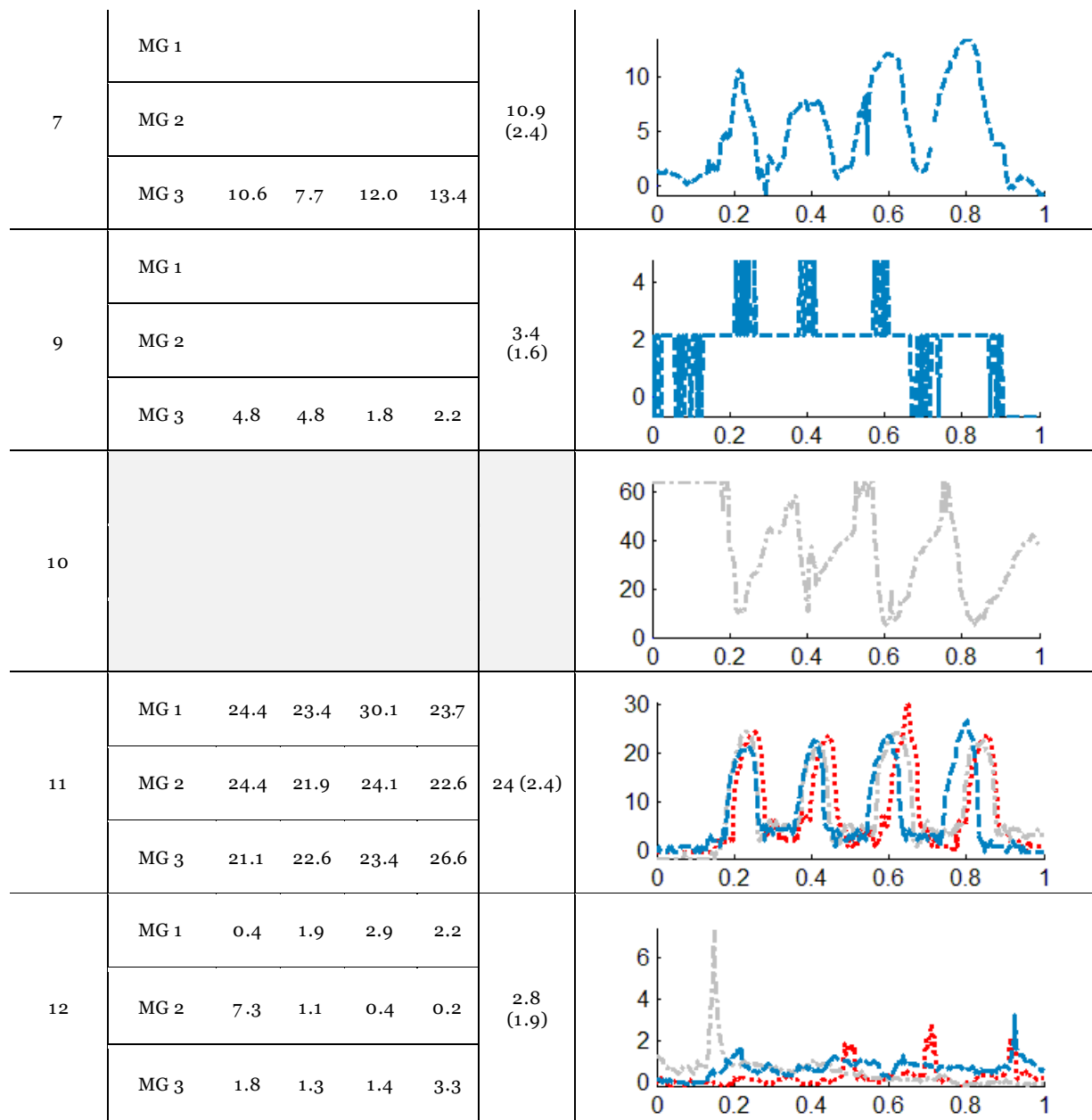
color2 = [64 232 154; 1 169 177; 241 34 72; 249 116 38; 255 205 1; 150 150 150]/256;
s2plot = [1, 2, 5, 6, 10, 11];
figure('Position', [100, 100, 1260, 900])
for p = 1:length(s2plot)
    subplot(6,1, p)
    hold on
    patch(xpatch,ypatch(s2plot(p),:),1,'FaceColor', color2(p,:), 'EdgeColor','none')
    alpha(.3); % make patch transparent
    plot(xx, mu(:,s2plot(p)), 'Color', color2(p,:), 'LineWidth', 1.5)
    ylim([-1 65])
    xlabel(sprintf('Sensor %i', s2plot(p)))
    ylabel('Pressure (kPa)')
end

```

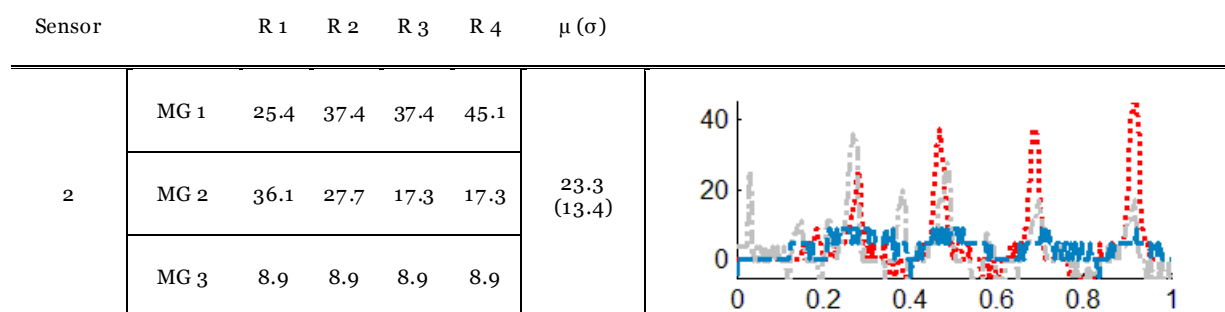
APPENDIX M: ALL USABLE PRESSURE SENSING PROFILES
Subject 1

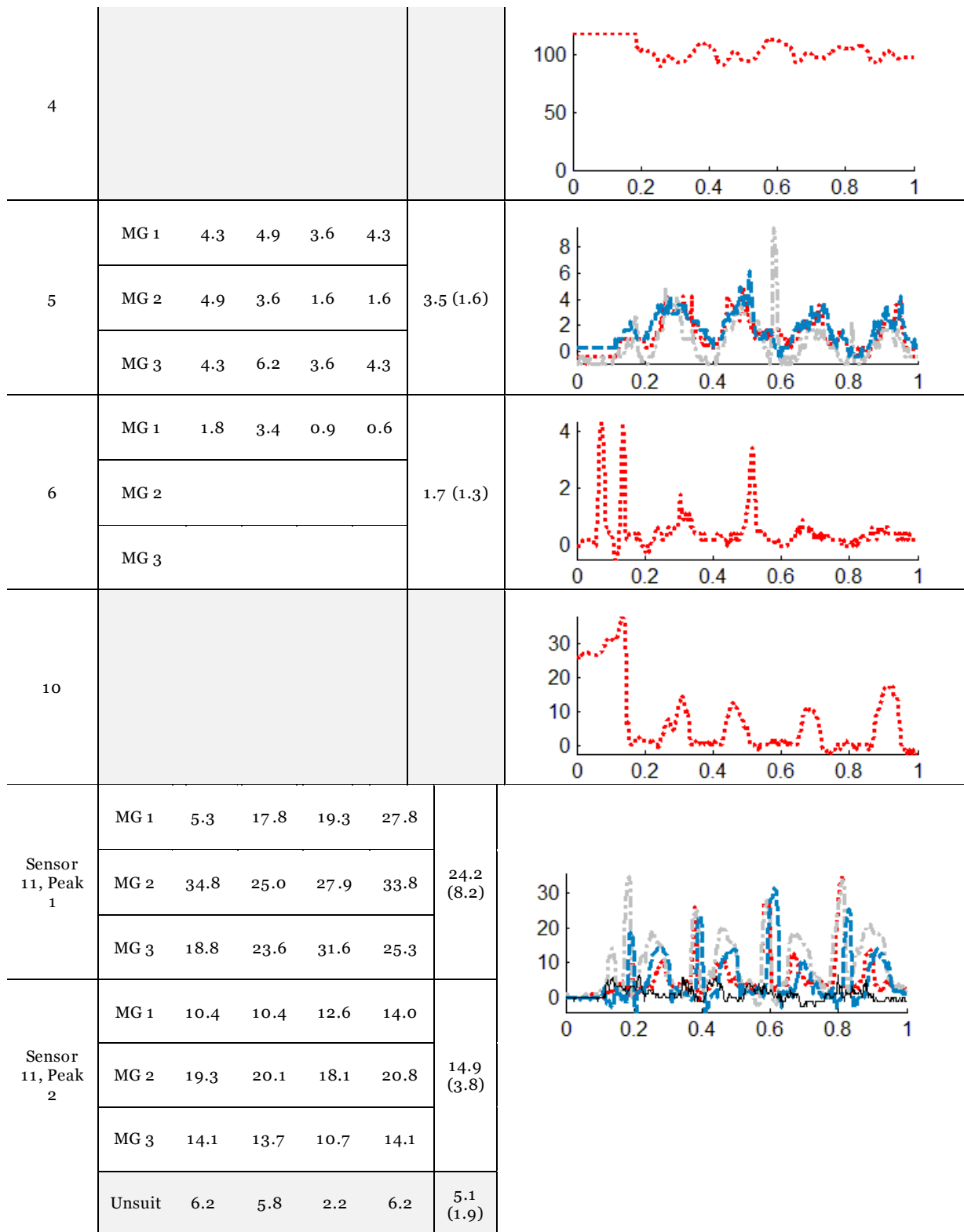
Elbow Flexion/Extension

Sensor		R 1	R 2	R 3	R 4	μ (σ)	
2	MG 1	49.4	29.1	20.5	17.3	28.2 (14.5)	
	MG 2	54.1	23.6	26.4	13.8		
	MG 3	49.4	20.5	20.5	13.8		
3	MG 1	8.7	6.0	8.7	6.0	6.2 (1.9)	
	MG 2	8.7	6.0	6.0	3.0		
	MG 3	6.0	6.0	6.0	3.0		
4							
5	MG 1	36.0	34.6	30.7	34.6	46.7 (24.3)	
	MG 2	37.9	36.0	102.0	61.7		
	MG 3						
6	MG 1	39.2	39.2	6.9	5.2	36.9 (35.4)	
	MG 2	6.8	7.8	7.8	5.7		
	MG 3	62.3	83.4	86.6	91.5		
	Unsuit	9.6	12.6	14.3	11.0	11.9 (2)	

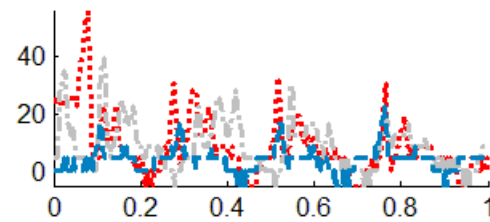
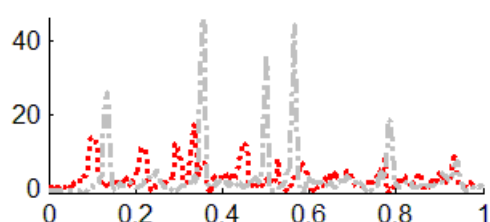

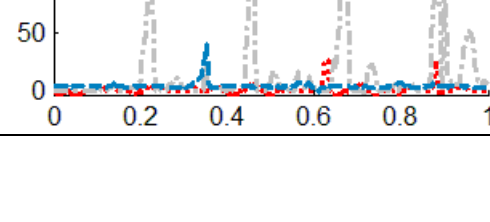


Shoulder Flexion/Extension





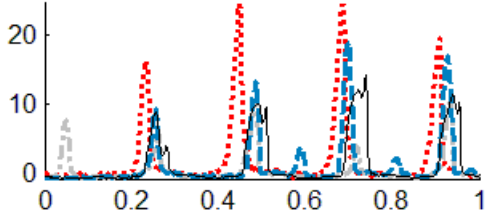
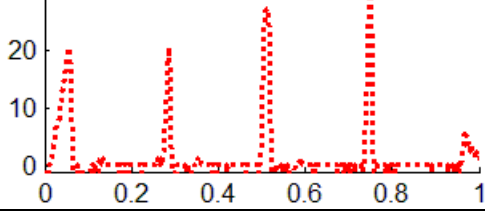
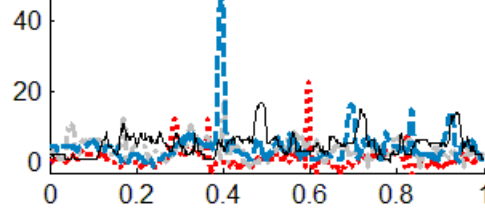
Shoulder Abduction/Adduction

Sensor		R 1	R 2	R 3	R 4	μ (σ)	
2	MG 1	55.9	30.6	33.0	30.6	28.3 (11.5)	
	MG 2	39.4	28.1	30.6	19.5		
	MG 3	16.3	16.3	16.3	22.6		
4							
Sensor 5 Peak 1	MG 1	14.2	17.5	8.2	7.6	22.9 (15.1)	
	MG 2	26.0	46.5	44.5	18.8		
	MG 3						
Sensor 5 Peak 2	MG 1	11.5	12.8	6.8	8.9	11.7 (10.5)	
	MG 2	5.6	36.6	3.6	7.6		
	MG 3						
6	MG 1	2.9	5.7	5.4	6.6	19.7 (17.5)	
	MG 2	8.3	70.0	30.4	86.6		
	MG 3	5.0	7.1	3.2	5.7		
9	MG 1	5.8	5.8	27.9	26.4	52.2 (55.5)	
	MG 2	99.9	123.5	148.8	125.7		
	MG 3	7.3	40.3	7.3	7.3		

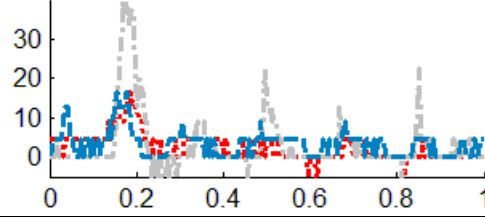
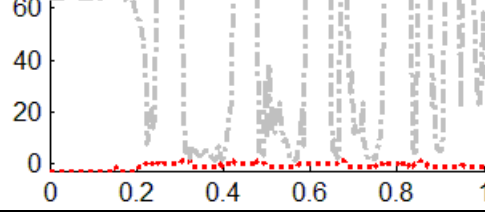
11	MG1	9.6	8.1	8.1	8.1	12.6 (10.3)	
	MG 2	6.3	6.3	6.3	6.3		
	MG 3	6.3	22.3	37.9	25.1		
	Unsuit	17.0	19.0	17.0	14.3	16.8 (1.9)	

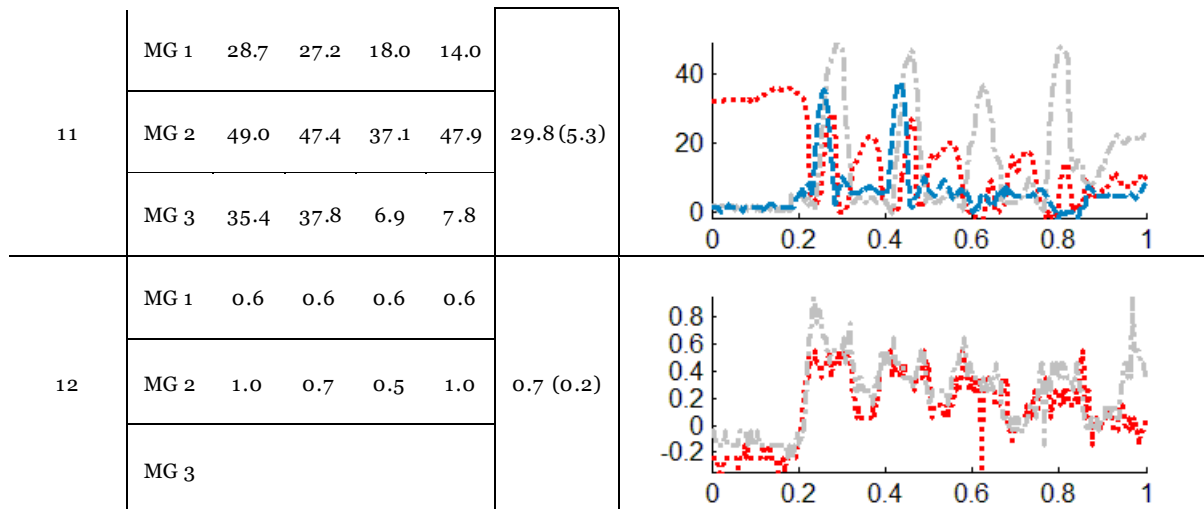
Cross Body Reach

Sensor		R 1	R 2	R 3	R 4	μ (σ)	
1	MG 1	62.6	71.4	71.1	55.3	44.6 (16.9)	
	MG 2	31.1	41.0	26.8	25.2		
	MG 3	34.8	34.8	49.8	31.1		
2	MG 1	6.2	6.2	6.2	8.2	7.5(2.3)	
	MG 2	4.2	6.2	8.2	12.0		
	MG 3	10.1	6.2	6.2	10.1		
4							
5	MG 1	23.5	11.6	7.7	4.4	38.4 (28.6)	
	MG 2	40.7	50.6	77.7	73.0		
	MG 3	5.0	46.0	38.7	81.6		

6	MG 1	16.3	24.4	24.4	19.6	14.5 (6.7)	
	MG 2	5.7	10.6	4.1	9.9		
	MG 3	9.4	13.3	18.9	17.0		
	Unsuit	8.9	10.1	14.4	11.5	11.2 (2.4)	
10							
11	MG 1	4.4	12.5	22.6	8.1	14.9 (11.3)	
	MG 2	12.5	18.0	8.9	6.3		
	MG 3	8.1	46.7	16.5	14.3		
	Unsuit	8.9	10.1	14.4	11.5	9.0 (1.0)	

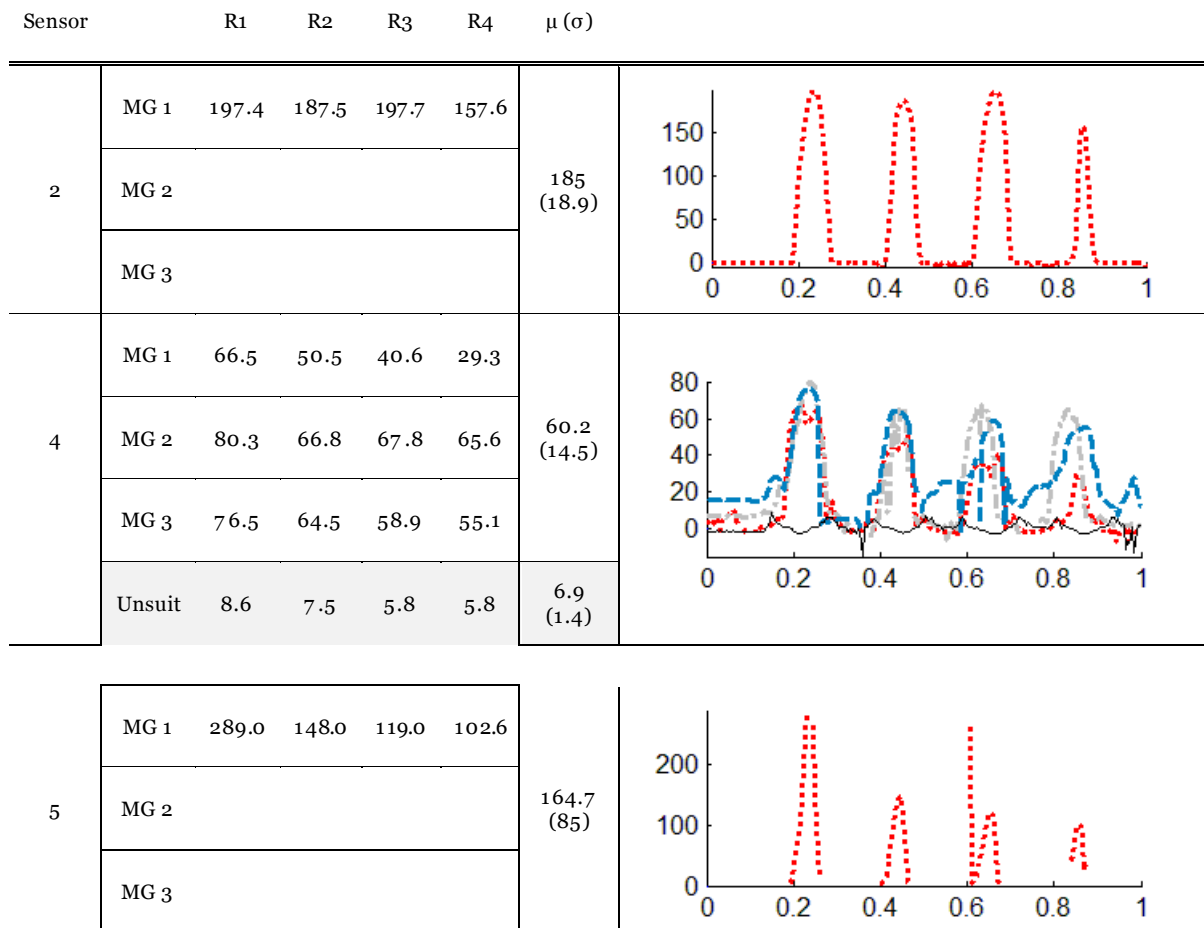
Overhead Hammering

Sensor		R 1	R 2	R 3	R 4	μ (σ)	
2	MG 1	16.3	4.8	4.8	4.8	13.9 (10.4)	
	MG 2	39.4	22.6	12.8	22.6		
	MG 3	16.3	8.9	8.9	4.8		
10							



Subject 2

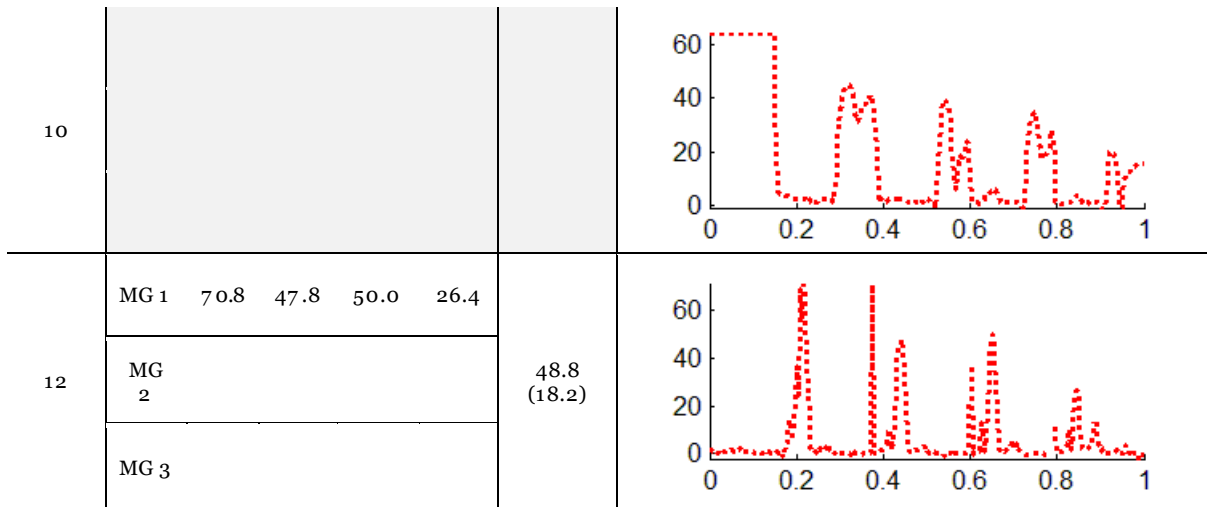
Elbow Flexion/Extension



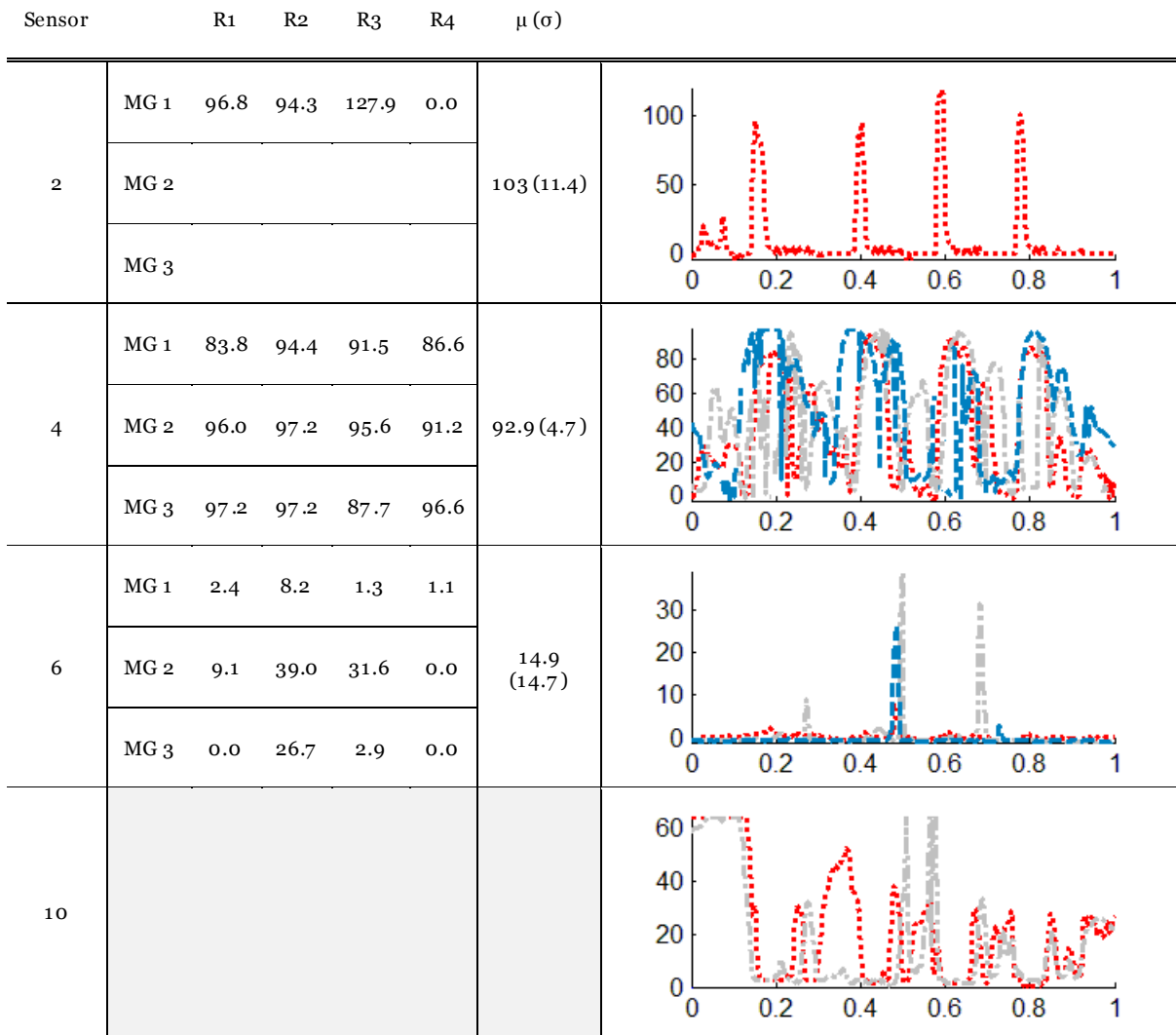
6	MG 1	2.0	3.1	4.1	2.7	5.3 (2.5)	
	MG 2	4.8	4.5	5.7	4.3		
	MG 3	7.1	6.6	6.6	11.5		
	Unsuit	18.2	8.7	10.8	9.4	11.8 (4.4)	
10							

Shoulder Flexion/Extension

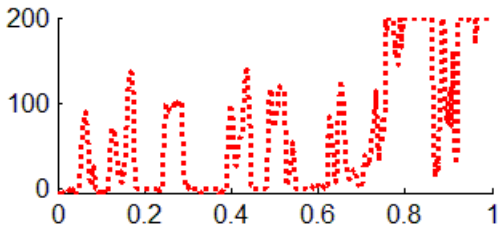
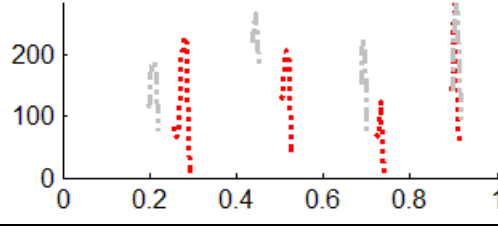
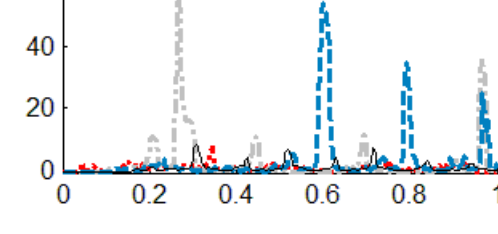
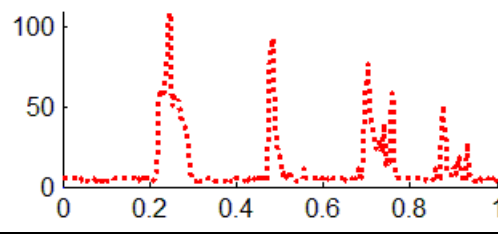
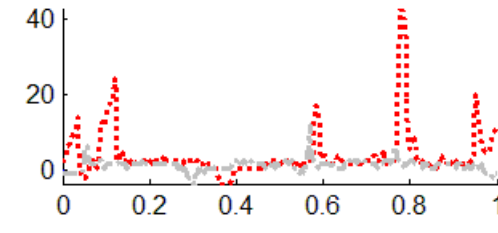
Sensor		R1	R2	R3	R4	μ (σ)	
2	MG 1	98.2	135.5	126.8	122.8	120.8 (16)	
	MG 2						
	MG 3						
4	MG 1	66.7	68.6	67.3	70.4	73.7 (6.4)	
	MG 2	80.2	75.1	77.5	83.6		
	MG 3						
6	MG 1	1.5	2.0	1.1	5.7	24.5 (27.3)	
	MG 2	0.4	5.9	13.1	29.0		
	MG 3	61.4	65.5	41.5	67.4		



Shoulder Abduction/Adduction



Cross Body Reach

Sensor		R1	R2	R3	R4	μ (σ)	
2	MG 1	137.1	137.6	165.3		146.7 (16.1)	
	MG 2						
	MG 3						
5	MG 1	226.8	207.6	122.4	279.0	224.5 (52.9)	
	MG 2	189.1	265.7	226.1	279		
	MG 3						
6	MG 1	8.0	1.5	2.2	2.0	20.5 (20.3)	
	MG 2	56.1	10.8	11.5	36.4		
	MG 3	3.6	54.2	35.0	24.9		
	Unsuit	8.0	6.4	7.3	2.0	5.9 (2.7)	
9	MG 1	109.1	92.7	76.8	50.1	82.2 (25.1)	
	MG 2						
	MG 3						
10							

Overhead Hammering

Sensor		R1	R2	R3	R4	μ (σ)	
1	MG 1	20.5	21.9	20.5	17.4	16.9 (4.1)	
	MG 2	17.4	17.4	19.0	7.8		
	MG 3	10.0	15.7	17.4	17.4		
	Unsuit	10.4	6.7	8.7	8.7	8.6 (1.5)	
2	MG 1	139.3	111.9	139.3	120.7	127.8 (13.8)	
	MG 2						
	MG 3						
4	MG 1	78.3	78.8	75.4	65.5	75.9 (5.7)	
	MG 2	78.5	76.0	77.0	78.0		
	MG 3	89.0	79.8	83.2	84.2		
6	MG 1	5.9	4.3	2.9	4.1	2.3 (1.9)	
	MG 2	0.4	0.6	1.7	0.4		
	MG 3	0.6	2.0	0.4	0.8		
	Unsuit	3.1	2.9	4.7	2.2	3.2 (1.0)	
10							

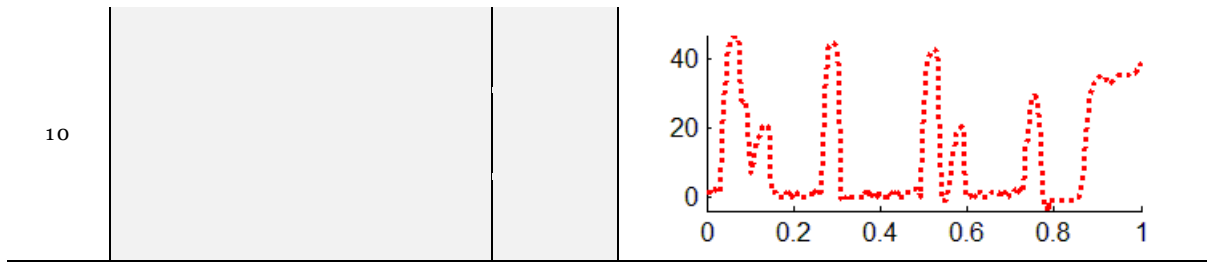
Subject 3

Elbow Flexion/Extension

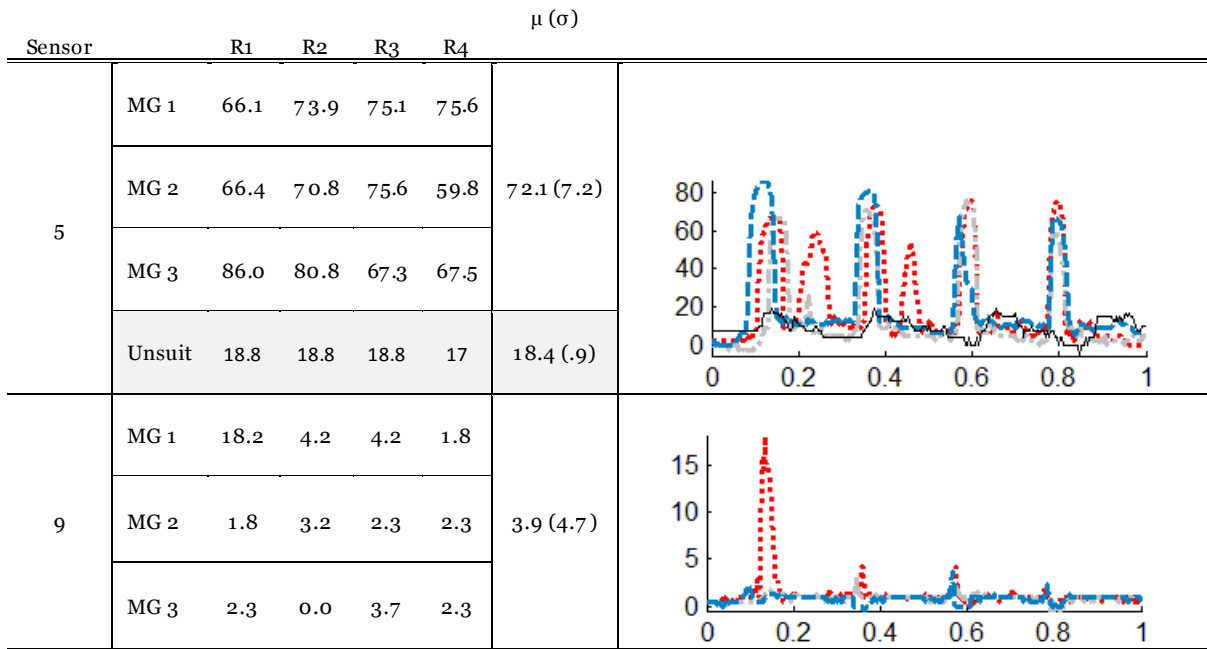
Sensor		R1	R2	R3	R4	μ (σ)	
2	MG 1	7.6	7.6	7.6	10.8	9.3 (9.8)	
	MG 2	4.0	4.0	4.0	4.0		
	MG 3	39.7	7.6	7.6	7.6		
5	MG 1	53.6	54.4	58.4	53.8	55.8 (3.0)	
	MG 2	60.1	55.3	58.1	60.6		
	MG 3	52.1	52.0	54.0	57.7		
6	MG 1	21.2	19.6	25.6	26.5	30.5 (8.3)	
	MG 2	35.1	37.8	35.8	42.0		
	MG 3						

Shoulder Flexion/Extension

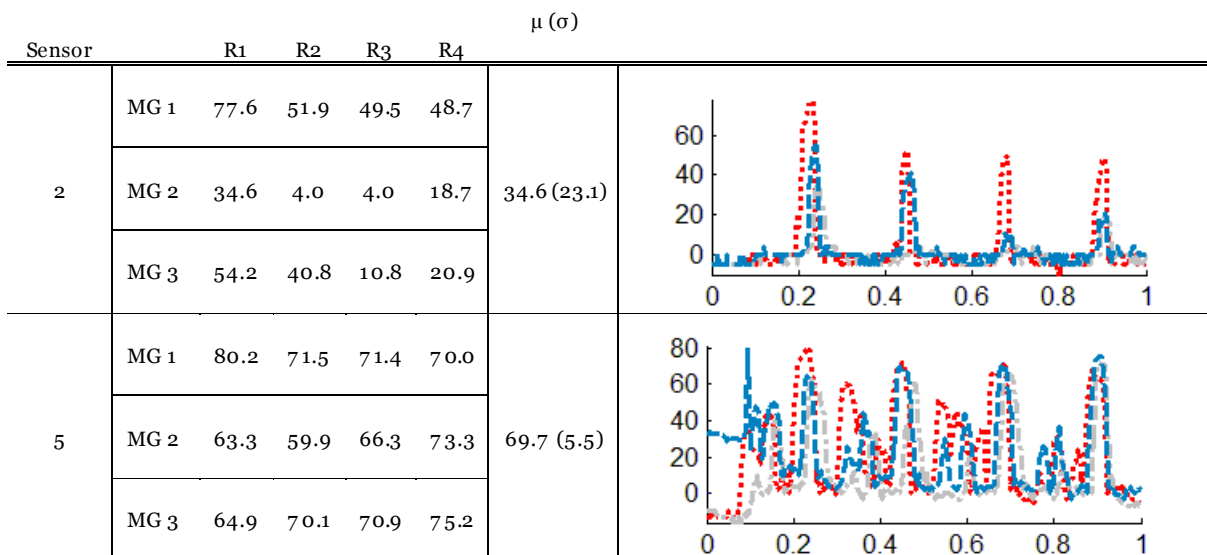
Sensor		R1	R2	R3	R4	μ (σ)	
5	MG 1	58.9	77.6	80.9	0.0	68.3 (23.5)	
	MG 2	54.4	76.1	76.5	80.8		
	MG 3	70.0	87.4	81.4	75.4		
	Unsuit	20.4	20.4	20.4	18.7	20 (0.9)	
6	MG 1	2.2	2.7	4.1	3.6	2.6 (1.0)	
	MG 2	2.9	2.5	1.1	1.3		
	MG 3						



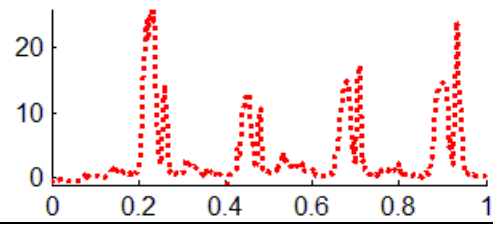
Shoulder Abduction/Adduction



Cross Body Reach

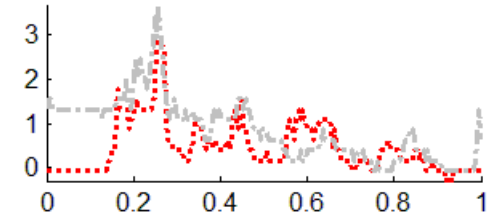
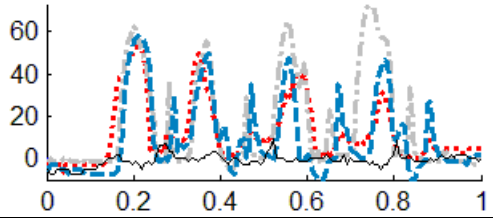


6	MG 1	25.8	12.9	17.0	24.0	19.9 (6.0)
	MG 2					
	MG 3					



Overhead Hammering

Sensor		R1	R2	R3	R4	μ (σ)
5	MG 1	52.5	49.6	39.7	31.5	52.5 (11.2)
	MG 2	62.5	55.7	64.6	72.7	
	MG 3	58.0	49.4	47.4	46.6	
	Unsuit	7.3	9.5	2.1	8.4	6.8 (3.3)
6	MG 1	2.9	1.6	1.3	0.6	1.7 (1.0)
	MG 2	3.6	1.6	1.3	0.8	
	MG 3					



APPENDIX N: HUMAN-SUIT INTERACTION SUBJECTIVE FEEDBACK

Subjects provided subjective feedback by answering the following questions regarding fatigue, comfort, contact, and consistency of movement. In addition to the materials below, a large print out of the body graphic was provided to allow the subject to better demonstrate where contact was felt. Subjects were asked these questions before the experiment, between each movement group, and after the experiment was completed.

Subject number _____ Movement group: Pre 1 2 3 Unsuit

Fatigue

Rate of Perceived Exertion: 1 2 3 4 5 6 7 8 9 10

How long would you be able to perform these tasks (minutes): 0 15 30 60 >60

Rate your level of effort for each task on a scale from 1-5:

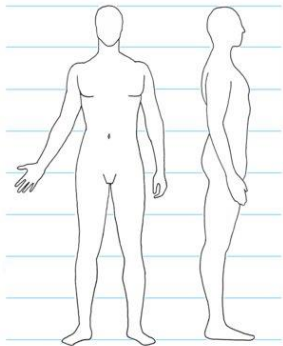
Task	Minimal Effort	Small Effort	Reasonable Effort	Large Effort	Maximum Effort
Elbow F/E	1	2	3	4	5
Shoulder F/E	1	2	3	4	5
Shoulder A/A	1	2	3	4	5
Cross-Body Reach	1	2	3	4	5
Overhead Hammer	1	2	3	4	5

Which task was the most fatiguing? Why?

Pressure and Comfort

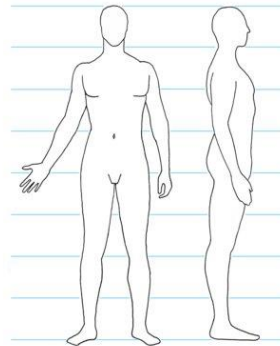
Identify the location and nature of the contact you feel between your body and the suit for each task. Rate your discomfort on a scale from 1 to 10 for each contact area:

Elbow F/E



Noticeable changes over time?

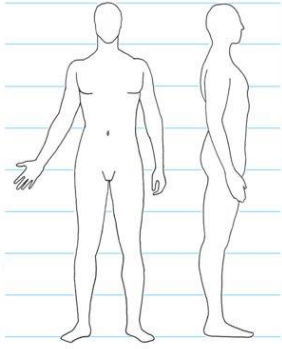
Shoulder F/E



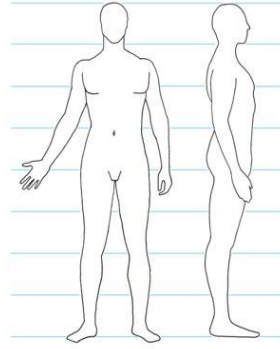
Noticeable changes over time?

Shoulder A/A

Cross-Body Reach

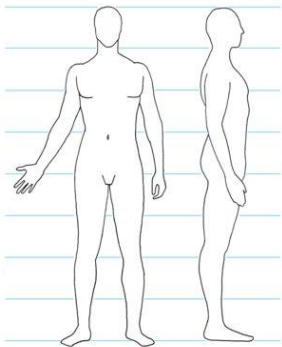


Noticeable changes over time?



Noticeable changes over time?

Overhead Hammer



Noticeable changes over time?

Biomechanics

Rate your perceived consistency of movement for each task on a scale from 1-5:

<i>Task</i>	<i>Not Consistent</i>	<i>Somewhat Consistent</i>	<i>Consistent</i>	<i>Very Consistent</i>	<i>Extremely Consistent</i>
Elbow F/E	1	2	3	4	5
Shoulder F/E	1	2	3	4	5
Shoulder A/A	1	2	3	4	5
Cross-Body Reach	1	2	3	4	5
Overhead Hammer	1	2	3	4	5

Did you alter your movement strategy at any point in the test? Why?

APPENDIX O: SUBJECT ORDERED TEST CONDITIONS

Tasks per subject were randomized and counterbalanced prior to the experiment. Each subject performed the tasks in the following order:

Tests numbers:

1. Elbow Flexion/Extension
2. Shoulder Flexion/Extension
3. Shoulder Abduction/Adduction
4. Cross Body Reach
5. Overhead Hammering

Subject 1:

1. Movement group 1: 5, 4, 2, 3, 1
2. Movement group 2: 4, 1, 5, 2, 3
3. Movement group 3: 2, 4, 3, 1, 5

Subject 2:

1. Movement group 1: 3, 5, 1, 2, 4
2. Movement group 2: 5, 4, 1, 2, 3
3. Movement group 3: 3, 1, 5, 4, 2

Subject 3:

1. Movement group 1: 2, 4, 3, 5, 1
2. Movement group 2: 1, 5, 2, 3, 4
3. Movement group 3: 2, 1, 4, 3, 5